

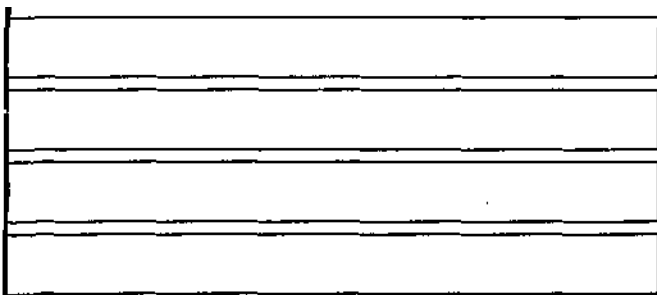
Contract Report 523

Applications of Statistical Methods to the Study of Climate and Flooding Fluctuations in the Central United States

by Kenneth E. Kunkel, Stanley A. Changnon, and Robin T. Shealy
Office of Applied Climatology

Prepared for the
U.S. Geological Survey

March 1992



Illinois State Water Survey
Atmospheric Sciences Division
Champaign, Illinois

A Division of the Illinois Department of Energy and Natural Resources

**APPLICATIONS OF STATISTICAL METHODS
TO THE STUDY OF CLIMATE AND FLOODING
FLUCTUATIONS IN THE CENTRAL UNITED STATES**

by

**Kenneth E. Kunkel
Stanley A. Changnon
and
Robin T. Shealy**

**Division of Atmospheric Sciences
Office of Applied Climatology**

**Illinois State Water Survey
2204 Griffith Drive
Champaign, Illinois 61820-7495**

**FINAL REPORT
USGS Grant 14-08-0001-G1731**

March 1992

FOREWORD

This research was partially supported by the U.S. Geological Survey, Department of the Interior under USGS award number 14-08-001-G1731. The views and conclusions contained in this document are those of the authors and should not be interpreted as necessarily representing the official policies, either expressed or implied, of the U.S. Government.

TABLE OF CONTENTS

	Page
FOREWORD	ii
1. INTRODUCTION	1
2. DATA AND ANALYSIS	1
A. Sources	1
B. Reasons for Potential Errors in Interpretation	4
C. Analytical Methods	6
Definitions	6
Flood Partial Duration Series	7
Precipitation Partial Duration Series	8
Comparison of Water Surplus Events to Peak Row Events: A Pilot Study	9
Statistical Methods	11
3. PRECIPITATION ANALYSIS	15
A. Relationship to Long-Term Climate Anomalies	16
Results	16
Relevance to Assessing Hydrologic Effects from GCMs	26
B. Temporal Variations	32
4. FLOOD ANALYSIS	39
A. Temporal Trends in Floods	39
B. Periods of Maximum Flood Conditions	65
C. Investigation of Relatively Small-Scale Areal Variations in Temporal Trends of Floods	77
Conclusions	83
5. FLOOD AND PRECIPITATION RELATIONSHIPS	85
A. Associations	85
B. Temporal Fluctuations	94

6. SUMMARY AND CONCLUSIONS.	95
ACKNOWLEDGMENTS.	99
REFERENCES.	99
PUBLICATIONS.	100
APPENDIX A - STREAMGAGING STATIONS.	91
APPENDIX B - STREAM BASINS.	94
APPENDIX C - PRECIPITATION STATIONS.	105
APPENDIX D - STREAMGAGING-PRECIPITATION STATION ASSOCIATIONS.	112
APPENDIX E - LOCATIONS OF PRECIPITATION STATIONS.	119
APPENDIX F - LOCATIONS OF ASSOCIATED PRECIPITATION STATIONS.	120
APPENDIX G - PENTADAL FREQUENCIES OF FLOOD AND PRECIPITATION EVENTS (WARM SEASON).	131
APPENDIX H - PENTADAL FREQUENCIES OF FLOOD AND PRECIPITATION EVENTS (COLD SEASON).	146

ISSN 0733-3927

The body of this report was printed on recycled and recyclable paper

1. INTRODUCTION

This report presents the findings of a two-year study to employ statistical techniques to analyze the historical temporal and spatial patterns of flooding and precipitation events in the midwestern United States. The results have implications for understanding global climate change since an understanding of how climatic fluctuations in the past have affected flood characteristics is a necessary prelude to assessing the hydrologic consequences of future climate change. This study expanded on a previous pilot study of Illinois (Changnon, 1983) to a nine-state region of the midwestern United States. Particular objectives of this research were:

- a) To identify whether there have been significant temporal changes in the frequency, duration, and magnitude of floods in the central United States since 1920 (when most streamgage records began).
- b) To identify fluctuations in climate variables that may be related to flooding.
- c) To determine the extent to which these two sets of time series are statistically related.

The nature of the above investigations was exploratory throughout the project. Since the definitions of floods and extreme precipitation events are somewhat arbitrary, various formulations of them were tested during the project and assessed for consistency. In addition, numerous analytical techniques were employed.

2. DATA AND ANALYSIS

A. Sources

The period 1921-1985 was chosen for analysis because most streamgage records began around 1920. The area of analysis encompassed the nine-state region of Illinois, Indiana, Iowa, Kentucky, Michigan, Minnesota, Missouri, Ohio, and Wisconsin. This area has a relatively, homogeneous climate with similar causal mechanisms for heavy precipitation across the region. This area also surrounds Illinois and allowed us to look at the regional applicability of the results of the

previous pilot study. Data from streamgaging stations were chosen based on the following criteria:

- 1) There were no significant control structures upstream of the station.
- 2) Less than 25% of data were missing over the 65-year period of record.

The following steps were undertaken to identify the streamgaging stations used in the study:

- 1) Lists of all streamflow stations were obtained for each state from the EarthInfo Hydrodata CD-ROM.
- 2) These lists were then screened to eliminate those stations with a period of record shorter than from 1921-1985 and with more than 25% missing data within the period of record. However, once this screening was completed, it was noticed that Indiana, Kentucky, and Michigan had very few stations that met the criteria. In order to represent these states' basins, the screening criteria were loosened to allow inclusion of stations with a period of record including 1931-1985.
- 3) Arthur Scott, Head of the U.S. Geological Survey (USGS) Northeast Region, was contacted to identify a knowledgeable person in each USGS District Office in the region who could comment on the quality of each station on the lists compiled in (step 2), particularly with regard to the influence of man-made structures.
- 4) A letter to each of these experts asked for their comments on the quality of their state's stations, with the list generated in (step 2) sent as a general guideline. Comments were received immediately from Ohio and Minnesota, and eventually from Illinois, Indiana, Iowa, Michigan, and Wisconsin, and appropriate stations were chosen based on these comments. Comments from Missouri and Kentucky were never received, so stations from these states were chosen from a list generated by Harry Lins from the national USGS headquarters office and provided to us by Melvin Lew. Two stations from Missouri and two from Kentucky were on the list. No additional stations were chosen because of lack of knowledge of human influence.

- 5) An additional five stations (not in Missouri or Kentucky) did not have a period of record from 1931-1985 and had more than 25% missing data. These stations were deemed of high quality by the state experts, and were included to fill in spatial gaps in the basin distribution.

By this process, 79 basins were chosen. Each basin's boundary was defined with respect to the streamgaging station; it included all tributaries and drainage area upstream from the streamgage location. Appendix A gives a complete list of the streamgaging stations used in this study along with their periods of record. Appendix B contains maps with the basin boundaries.

Our analysis of climate data was restricted to precipitation. Data were obtained from a total of 1500 stations on the Midwestern Climate Information System (MICIS) (Kunkel et al., 1990) from the National Climatic Data Center's Summary-of-the-Day dataset and were available as candidates. The criteria employed to choose stations were as follows: 1) the period of record included 1921-1990; and 2) there was less than 40% missing data in the record. In addition, we required that each basin had at least one precipitation station located within its boundaries in order to study the relationship between streamflow and precipitation. For many basins, the precipitation data from MICIS were adequate.

However, some of the 79 basins did not have sufficient available precipitation data covering the flow period of record. The following process was used to acquire added precipitation data for each basin:

- 1) The counties whose territory was partly or completely in a basin were identified, and a convex polygon containing these counties was constructed. All precipitation stations with data on MICIS within this polygon and with a period of record that included at least 1948-1990 were identified.
- 2) The U.S. Weather Service Climatological Data publications from 1921-1947 of the state (or states) where the basin was located were examined in order to ascertain all the precipitation stations in the above-mentioned map with available data for 1921-1947. The ones found to have such a record formed the final list for acquisition.

- 3) The states containing the precipitation stations found in steps 1 and 2 were contacted to see if these stations were digitized, and all the data were acquired. Data were obtained from several state climatologists including James Zandlo (Minnesota), Fred Nurnberger (Michigan), Kenneth Scheeringa (Indiana), and Pam Naber Knox (Wisconsin). In addition, 20 stations on the acquisition list not previously digitized were digitized by the Illinois State Water Survey for this project.

For each stream basin, precipitation stations located within or near the basin boundaries were identified. These "associated" precipitation basins were used in certain analyses comparing the flood and precipitation event time series.

In total, relatively complete daily precipitation data were available for 240 stations. A list of the precipitation stations is given in Appendix C, and a list of the precipitation stations within or near each basin is given in Appendix D. A map of the locations of the streamgaging and precipitation stations is given in Figure 1.

B. Reasons for Potential Errors in Interpretation

There are several potential conditions that could lead to errors in the interpretation of the results. First, the flow data for the chosen basins could be of questionable quality at various times in the streamgaging station record. Second, the chosen basins, though screened carefully for insulation from in-channel human modification, may have experienced other changes (e.g., changes in runoff characteristics due to increased agricultural use in the basin). Third, in assessing flood-precipitation relationships in a basin, the precipitation stations within this basin may not have been uniformly distributed and may not provide an accurate basin-wide heavy precipitation estimate. Fourth, in some portions of the Midwest, the availability of a "dense" spatial array of basins was not present because of the paucity of nonmodified basins. This affects large-scale analysis of conditions. Because it is very difficult to quantitatively assess the influence of the above factors in any particular basin, it was not done in this study. However, our qualitative interpretation of the results has attempted to account for these sources of "error" or "noise."

Long-term streamgaging and precipitation station locations

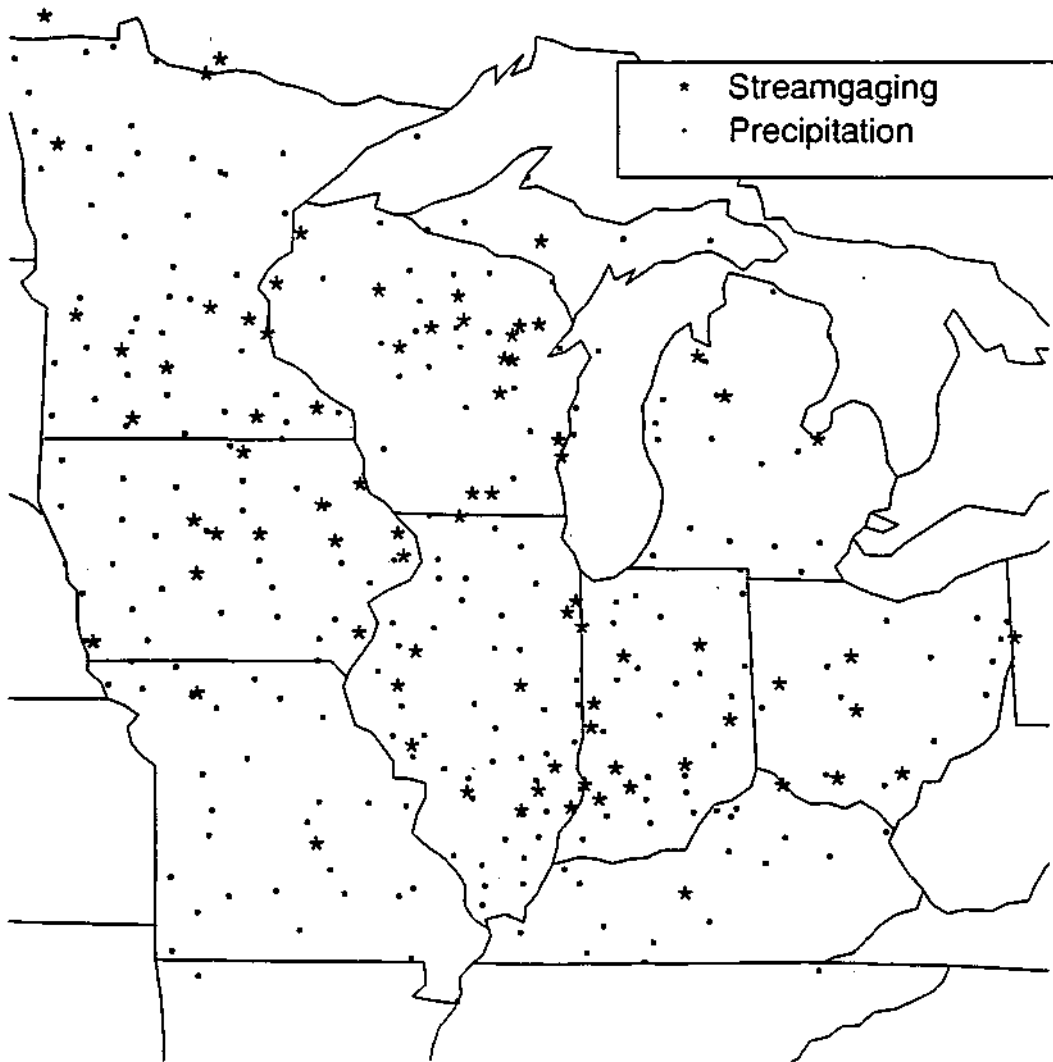


Figure 1. Locations of streamgaging and precipitation data stations.

C. Analytical Methods

Definitions

In order to carry out the outlined analyses, it was necessary to determine the working definitions of flood events and precipitation events. We also wished to analyze precipitation-flood relationships for the cold and warm seasons when precipitation and flow dynamics are different. Floods in the warm season (May 1 - November 30) are primarily the result of intense, short-duration storms, often convective in nature. Floods in the cold season (December 1 - April 30) may reflect the contributions of snowmelt, or prolonged multi-day precipitation. Because of these differences, the analysis of flood and extreme precipitation events was separated into two periods. During the warm season, convective rains dominate as flood-causing events and snowmelt is not an important factor. But during the cold season snowmelt can be a contributing factor.

Three measures associated with a flood event were defined:

- 1) Peak flow time - the date of the peak flow.
- 2) Flood duration - the time from the day the flow first rose above a threshold to the day it fell back below it. The threshold is defined here to be the peak value of the smallest flood in the partial duration series (defined below).
- 3) Peak flow intensity - the flow in cubic feet per second (cfs) on the day of the highest flow of the flood.

A precipitation event was defined as the accumulated precipitation over periods ranging from 1 to 10 days. Examination of the data revealed that most floods in the warm season could be associated with heavy precipitation events lasting a few days.

The causative factors for floods in the cold season are potentially more complicated. The situation is more straightforward in the warm season when precipitation (rain) results immediately in either increases in soil water storage or increases in runoff, which change streamflow. However, in the cold season, some precipitation occurs in the form of snow, which may accumulate and not affect

streamflow for days, weeks, or even months. Conversely, rapid melting of the snowpack can result in flooding in the absence of precipitation. Use of precipitation variables more complex than the 'm'-day liquid precipitation total was subsequently explored for the cold season. A conceptual approach employed was to define a liquid-equivalent precipitation value P_e as

$$P_e = P - \Delta W_e$$

over a specified period of days, where

P = actual liquid precipitation

W_e = change in the water equivalent of the snowpack in the period

Since most of the stations in the National Weather Service's cooperative climate network do not measure snowpack water equivalent, the water equivalent based on snowdepth measurements was estimated using an average value of the water equivalent/snowdepth ratio of 1/3. However, even though a few more stations had snowdepth records (a few more than had snowpack water equivalent), the general poor quality of the snowdepth data precluded this analysis on a regional scale. In the few cases where the snowdepth data were adequate, partial duration series (defined below) using actual liquid precipitation and using liquid-equivalent precipitation were compared and found to be nearly identical. Because of these findings, we decided to simply use the actual liquid precipitation value as the basic climatic variable for both the warm and cold seasons.

Flood Partial Duration Series

A peak flow partial duration series of recurrence Y years over an N -year period of non-missing record is the N/Y largest flows in the daily series, subject to temporal separation criteria, and their times of occurrence. It is adjusted for missing data by reducing the number of events in the series by the amount of missing data, in years (to the nearest integer). The source of the flood separation criteria is the U.S. Water Resources Council Bulletin #17B (1981). Hereafter, a peak flow series is referred to as a "flood partial duration series."

The algorithm used in our study to derive a flood partial duration series is as follows. First, determine the number of flood events = 'n' in the series, based on the recurrence and the amount of missing data. Then,

- 1) Find all local maxima in the series. The largest local maximum is the first flood in the series.
- 2) Until 'n' floods have been found:
 - a) Find the next largest flow value not already in the series. For reference, call this the current "candidate flood."
 - b) For each flood already in the series, determine if the temporal separation criterion holds: if its location is at least $\frac{2n(A)+5}{A}$ days away from the candidate flood (A = basin drainage area in square miles) and there is at least one day between it and the candidate flood where the flow is less than 75% of the maximum of the two flood values, then the candidate flood becomes part of the series. If the above is not true, the candidate flood is rejected.

Partial duration series were defined with respect to seasons; for example, the cold season partial duration series only considers daily flows from December 1 to April 30 in the record. The recurrence is defined in terms of number of seasons. In studying floods separately for the warm and cold seasons, we chose a recurrence interval of one season for each; this was a compromise between the conflicting requirements of identifying enough events to make subsequent statistical analyses meaningful but limiting the analysis to floods of hydrologic and societal significance.

Precipitation Partial Duration Series

Extreme precipitation events of a specified length were defined by a partial duration series of a specified duration. An extreme precipitation partial duration series with event length of 'm' days of recurrence Y years over an N -year period of nonmissing record is the N/Y largest precipitation values accumulated over 'm' days of the daily series and their temporal locations. It is adjusted for missing data by reducing the number of events in the series by the amount of missing data, in years (to the nearest integer). In addition, overlap of events in time is disallowed.

The algorithm used to determine an extreme precipitation partial duration series was as follows. First, we found the number of precipitation events = 'n' in the series, based on the recurrence and the amount of missing data.

- 1) Then we found the highest 'm'-day precipitation value in the daily series. This was the first event in the partial duration series.
- 2) Until 'n' events had been found, we found the highest 'm'-day precipitation value in the part of the daily series not within 'm-1' days of any of the precipitation events currently in the partial duration series. This event was put into the series.

This procedure ensured that there was no overlap of precipitation events in the series. Put more exactly, if an event occurred from day 't' to 't+m-1', then we eliminated from further consideration days 't-m+1' ('m-1' days before start of event) to 't+2m-2' ('m-1' days after the event).

Precipitation partial duration series were defined with respect to seasons similar to the flood series. Again the recurrence was defined in terms of number of seasons.

Comparison of Water Surplus Events to Peak Flow Events: A Pilot Study

It was necessary to decide early in the project whether the flood partial duration series should be relative to peak flow intensities or water surplus (integrated flow above a predefined threshold over a time interval). These alternatives were investigated because floods of different character (lengthy floods of moderately high flow values vs. brief floods of very high flow values) could have markedly different impacts. A study comparing the two series was initiated for a sample of the basins in Minnesota and Ohio.

It was necessary to define a water surplus partial duration series. As in the peak flow series, separation criteria were used to prevent defining events too close to each other. We used the following algorithm:

- 1) Determine the number of events 'n' in the series, based on the recurrence and the amount of missing data. Choose a threshold (in cfs) for consideration.
- 2) Find all time intervals throughout which daily flow levels exceeded this threshold. For each interval, compute the water surplus, which was the accumulated sum of the excess daily flow (daily flow - threshold) for the interval's duration. These intervals are the initially defined events.
- 3) Until the separation criterion was met, for each pair of events derived above, determine if the temporal separation criterion holds: if their centers (midway between start and end date) are at least $2\sqrt{A}+5$ days apart, then these two events are counted as separate events. As before, A is the basin drainage area in square miles. If the two events are within the separation distance, they are merged into one; a new water surplus value and event interval extent were computed.
- 4) Rank the resultant events in decreasing order of water surplus magnitude, and extract the top 'n' events as the partial duration series.

This series was also defined with respect to both seasons. Thresholds were empirically chosen so that approximately 200 events were identified. The reason for having a separation rule to combine water surplus events, is that the flow level may rise over the threshold, subside to slightly below it for a day or two, then rise above the threshold again. It was concluded that the definition approach used best described one water surplus flood.

The pilot study showed that for all of the basins, the identified temporal locations (time of occurrence) of flood events from the peak flow partial duration series and from the water surplus partial duration series were virtually coincident. Therefore, in subsequent analyses, we used only the peak flow partial duration series to define the flood series.

Statistical Methods

Both flood and precipitation partial duration series were examined for temporal nonuniformity over the period of record. It was first decided to test for such nonuniformity independent of the nature of the temporal fluctuations; the fluctuations could be an overall linear trend or of a shorter term fluctuation.

Testing for temporal uniformity in a flood or precipitation series is equivalent to testing if the event locations within the period of record follow a uniform distribution. The Kolmogorov-Smirnov statistic was used for this analysis. This test determines whether the actual cumulative distribution function (cdf) of event occurrence differs significantly from a postulated event cdf. Because the working hypothesis assumes that there is no temporal inhomogeneity, the postulated event cdf is a uniform distribution, which takes the form,

$$F_{un}(d) = (d - d_b)/(d_e - d_b)$$

where

$$\begin{aligned} d &= \text{day number} \\ d_b &= \text{beginning day number of the period of record} \\ d_e &= \text{ending day number of the period of record} \end{aligned}$$

As the first step in the analysis, the actual cdf was calculated from the partial duration series as

$$F_{ac}(d) = k/N$$

where

$$\begin{aligned} k &= \text{number of events occurring on or before day number } d \\ N &= \text{total number of events in the period of record} \end{aligned}$$

The next step in the analysis was to determine the maximum deviation D between $F_{ac}(d)$ and $F_{un}(d)$, i.e.,

$$D = \max_{d_b \leq d \leq d_e} | F_{un}(d) - F_{ac}(d) |$$

In this test, D is the measure of the goodness of fit between the theoretical and actual cdf s.

Probability (p) values were computed based on the algorithm given in Birnbaum (1952). If the p -value is low, this is evidence that the observed distribution of count locations is very probably not uniform, providing evidence of localized temporal grouping of events or a strongly fluctuating return time of these events. A temporally uniform series can be alternatively interpreted as a homogeneous Poisson process with intensity equal to the recurrence of the series.

This analysis was performed on both warm- and cold-season floods and on their precipitation events. The one-year series is therefore, as described above, a one-season series. When considering events restricted to a particular season, the nonseasonal part of the time axis was excised before the test was applied. In addition, missing portions of the record were excised, since the partial duration series was adjusted for these periods.

In addition to a test of general inhomogeneity, we tested if there was a linear trend in flood frequency, duration, and intensity, and in precipitation event frequency. To study flood and precipitation event frequency trends, the number of events were counted in 5-year periods (pentads) for each flow and precipitation station record. The pentads were chosen to be 1921-1925, 1926-1930, . . . , 1981-1985 for the flow records, and additionally 1985-1990 for the precipitation stations. If the amount of data missing in the pentad was at most 40%, the counts were adjusted by the amount of missing data:

$$\text{counts (adjusted)} = \text{counts (unadjusted)} / (1-m)$$

where m = fractional percentage of missing data in the pentad. If more than 40% of the data was missing in the pentad, the pentad was not used in the analysis. The median flood duration and intensity were calculated for each pentad. These measures were then regressed onto each pentad to see if a linear trend could be detected. A robust regression with iterative Huber-weighting of the residuals was used (see Hampel et al., 1986 for details). The final weights were then used in a weighted least-squares regression analysis to obtain standard errors for significance tests on the trend slopes.

To fulfill the third objective of the study, we examined two approaches for assessing relationships between the prevalence and severity of floods and extreme precipitation events: 1) measurement of precipitation conditions before a flood; and 2) assessing the degree of "tracking" of the two time series.

To implement (1), two questions were asked about pre-flood conditions:

- a) How often do extreme precipitation events tend to occur just before floods?
- b) What length of extreme precipitation event is most closely linked to a flood condition? For example, do extreme 1-day events more often precede floods than extreme 3-day events?

With an answer to (b), the extreme precipitation study could then go forward, with this event length. Section 5 discusses (a) in detail.

To answer the above questions, a period of time before each flood peak in each basin was examined; should a large amount of precipitation fall in this period, it was considered at least in part a trigger for the flood event. It is referred to as the "flood influence period." The flood influence period f_i is defined as

$$f_i = \ln(A) + 5 + m$$

where

A = drainage of the basin in square miles

m = precipitation event length (days) being searched for in the period

It was decided to use this length for the flood influence period because $[\ln(A)+5]$ is the minimum distance between flood peaks and hence could be thought of as a representative response time of a basin to precipitation conditions; 'm' was added so that the last day of an m-day precipitation event could fall within $\ln(A)+5$ days of flood peak.

The association of floods and m-day precipitation events in a basin was defined to be the percentage of floods that have an m-day extreme precipitation event in the floods' influence periods. Specifically, if a flood peak was on day 't',

then it had an m -day precipitation event associated with it if one occurred between day $t-(f_i+1)$ and $t+m-1$.

Most basins had more than one associated precipitation station; we wanted all data from each basin's precipitation station to be used to eliminate geographical variation in precipitation conditions. Therefore, an "aggregate" precipitation record, composed of the individual records of precipitation stations in the basin, had to be defined. Three methods of aggregation of the precipitation records of all associated precipitation stations of a basin were explored:

- 1) Average of the daily values. Missing data at any station was not included in the average; if all stations had missing data on a particular day, the day was recorded as having missing data for the aggregate record.
- 2) Harmonic mean of the daily values. The weights were the inverse distances of the precipitation stations from the streamgaging station.
- 3) The maximum of the daily values. The record was divided into ' m '-day periods (' m ' = precipitation event length) and the period with the maximum precipitation was taken as the aggregate record of the period.

In a pilot study of the effect of aggregation method on association, it was found that there was no difference between (1) and (2); this indicated that the influence of a precipitation station in a basin depends little on its location in the basin. In comparing the averaging method (1) and the maximum method (3), it was found that in small basins, there was virtually no difference. However, in large basins with many associated precipitation stations, the averaging method produced a larger association than the maximum method. The averaging method was subsequently used in all analyses.

Cold and warm seasons were studied separately. In computing the association within a season, the season start was defined to be 20 days earlier for the aggregate precipitation record than for the flow record, because the flood influence period length averaged about 20 days for the 79 candidate basins. For example, the cold-season flow record extended from December 1 to April 30, and the cold-season precipitation record extended from November 11 to April 30.

Methods for correlating flood measures with precipitation magnitude were extensively examined. Initially, we attempted to correlate by 5-year periods (pentads) from 1921-1925, 1926-1930, to 1981-1985. The pentadal measures of the three flood variables were 1) the number of events in the pentad, 2) median duration of floods in the pentad, and 3) median peak value for all events in the pentad. There were two possible pentadal precipitation event measurements: the count and the median magnitude of events.

Investigations of these correlations revealed that they did not adequately address the degree of "tracking" of precipitation events with flood events. For example, if each pentad in a one-year flow partial duration series showed five floods, and the same occurred for the precipitation series in the basin, then the flood and extreme precipitation processes tracked each other perfectly at a pentadal time scale; however, both Pearson and Spearman (rank) correlations are undefined. Therefore, it was decided to not consider such correlations.

Three alternative methods showing promise are being investigated: 1) a chi-square test; 2) a modified Kolmogorov-Smirnov test to measure a distance between flood and precipitation event distributions; and 3) a modified Kendall's tau calculation. These methods are being implemented at the time of this report and will appear in articles to be submitted to scientific publications.

3. PRECIPITATION ANALYSIS

Floods occur as the result of the combination of several weather conditions. Flood characteristics are affected by precipitation totals, short-term heavy precipitation rates, and antecedent soil moisture conditions in the basin. For the purposes of this study, we examined only short-term multi-day precipitation totals because they largely control the incidence of floods of the magnitude herein investigated. Long-term records (daily precipitation) were available for many stations. By contrast, soil moisture measurements were not widely available, and short-term precipitation rates requiring at least hourly data were also not available at the time and space scales relevant to floods.

A. Relationship to Long-Term Climate Anomalies

Results

The first step was to identify the precipitation event lengths that were most closely associated with flood events. To this end, an exploratory association analysis was done on the 79 candidate basins to ascertain an optimal precipitation event length (optimal in the sense of finding the best association) that precedes a flood. Extreme events of such length would be those most closely related to floods. Although the statistical analysis of the flood events and the precipitation events was subsequently done independently, we considered it essential to make an intelligent and informed choice of precipitation duration so that the precipitation events were of hydrologic importance.

Precipitation event lengths of 1-, 3-, 5-, 7-, and 10-days were tested. Associations of 1-year and 2-year floods with five different precipitation event recurrences (0.2, 0.3, 0.5, 0.75; 1.0, in seasons) were computed for each season, and an average over all basins was calculated. The results are in Figure 2.

It was found in both the cold and warm seasons that the association level generally increased as precipitation event length increased; also, as expected, the association increased substantially as precipitation recurrence time decreased (more precipitation events are included as candidates to be associated with flood events). The incremental increase in association level was large from 1-day to 3-day events; further increases in event length caused relatively minor increases in association. Therefore, the "7-day" event was chosen for further statistical analyses.

One of the questions raised during the heavy precipitation analysis was: "Do extreme precipitation events occur more frequently during climatic periods of above-average precipitation?" To address this, we aggregated 7-day precipitation events by 5-year periods (pentads) from 1921-1925 through 1986-1990. For each pentad the total precipitation was calculated for each station. A comparison between the total pentad precipitation and the number of extreme precipitation events revealed a general trend toward increasing precipitation amounts as the number of extreme precipitation events increased. Figure 3 summarizes the results for the warm and cold seasons. The points in this figure represent the average precipitation for all station pentads with equal values for the number of precipitation events. Also shown are standard deviation values of +1 and -1. The correlation between the two

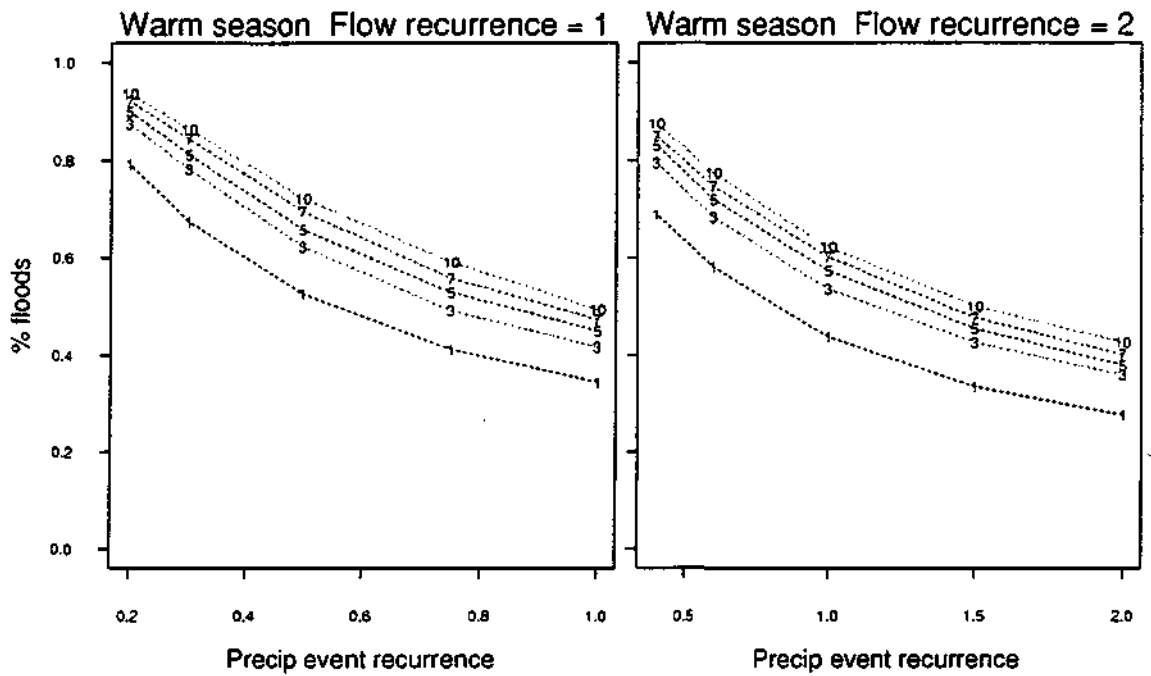


Figure 2a. Association between the occurrences of floods and extreme precipitation events as a function of the precipitation recurrence interval used to select candidate precipitation events for the warm seasons. The floods included exceed the threshold for 1-year and 2-year recurrences. Association curves are given for 1-day, 3-day, 5-day, 7-day, and 10-day precipitation event lengths.

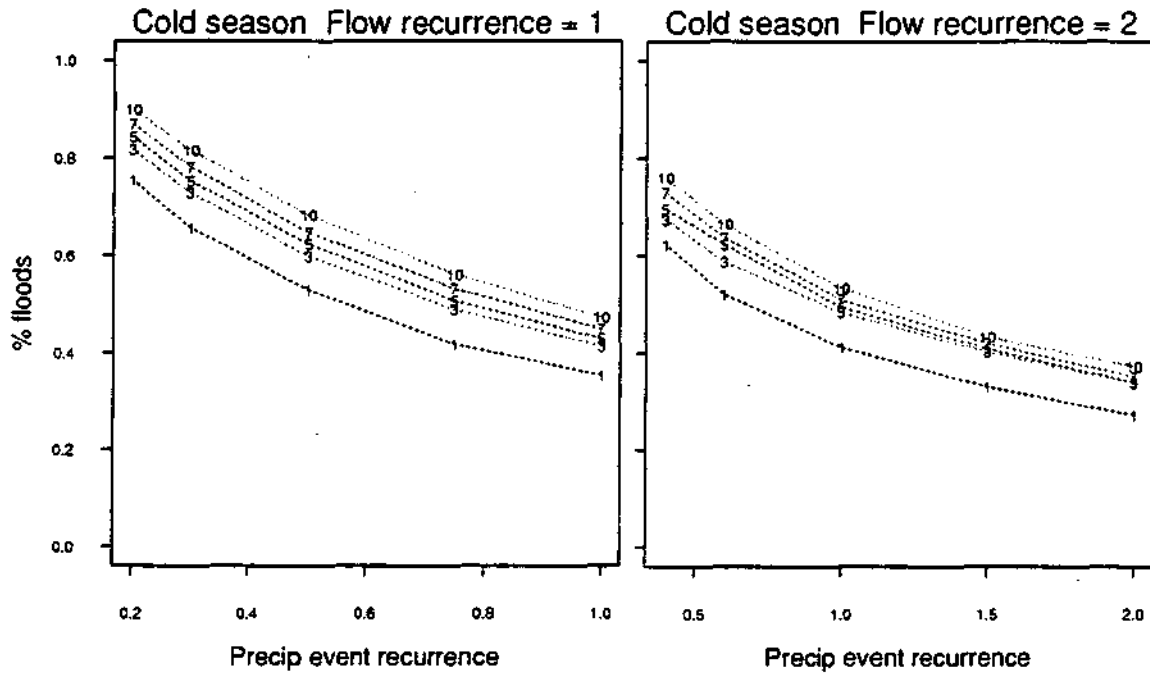


Figure 2b. Association between the occurrences of floods and extreme precipitation events as a function of the precipitation recurrence interval used to select candidate precipitation events for the cold seasons. The floods included exceed the threshold for 1-year and 2-year recurrences. Association curves are given for 1-day, 3-day, 5-day, 7-day, and 10-day precipitation event lengths.

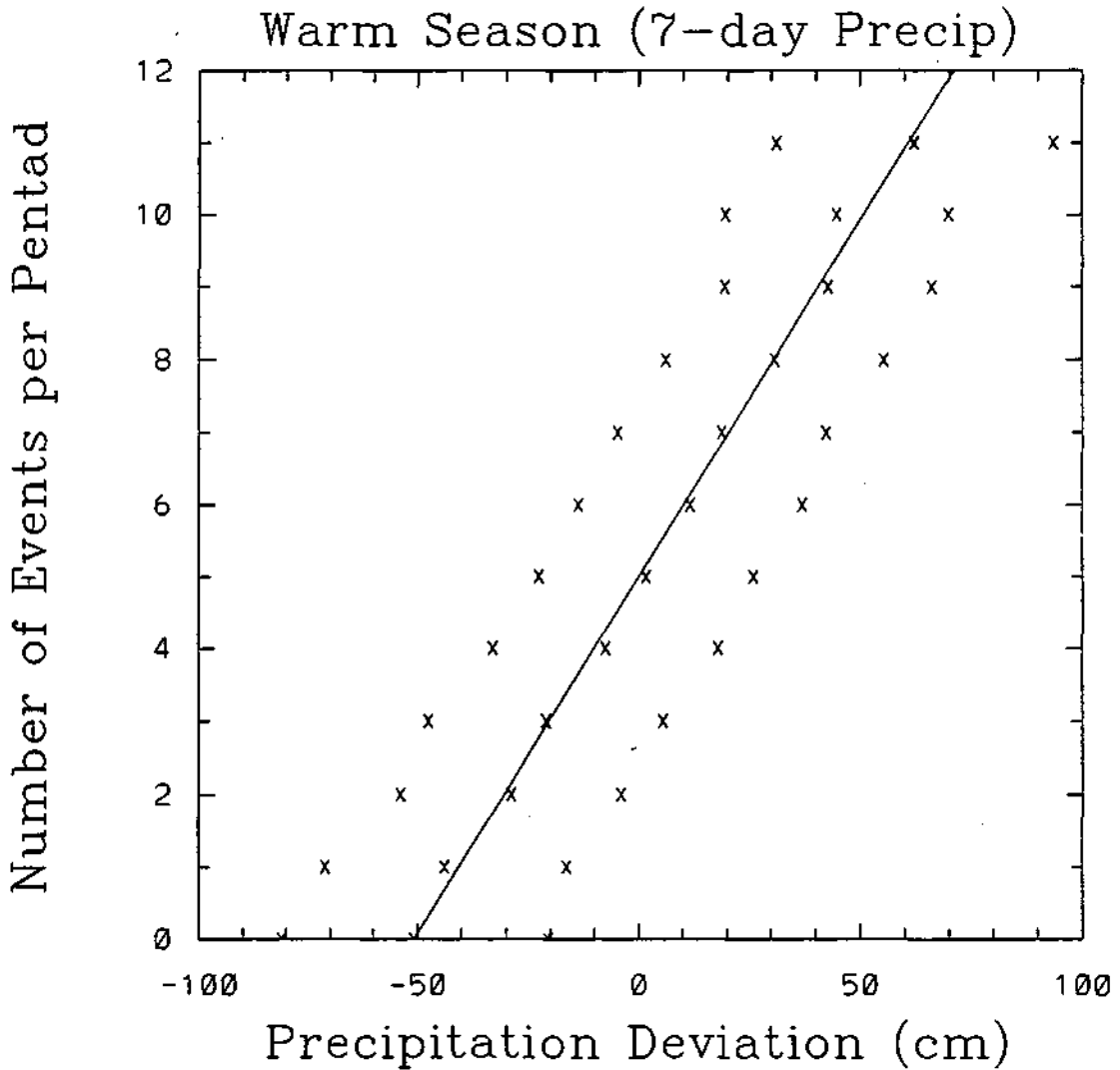


Figure 3a. Number of 7-day extreme precipitation events (magnitude > the threshold for a 1-year recurrence interval) during a pentad as a function of the pentad precipitation deviation for the warm season. Each set of three points at discrete values of the number of events represents the mean and ± 1 standard deviation of the values for all station-pentads with an equal number of events. The solid line is a least-squares fit to the mean values.

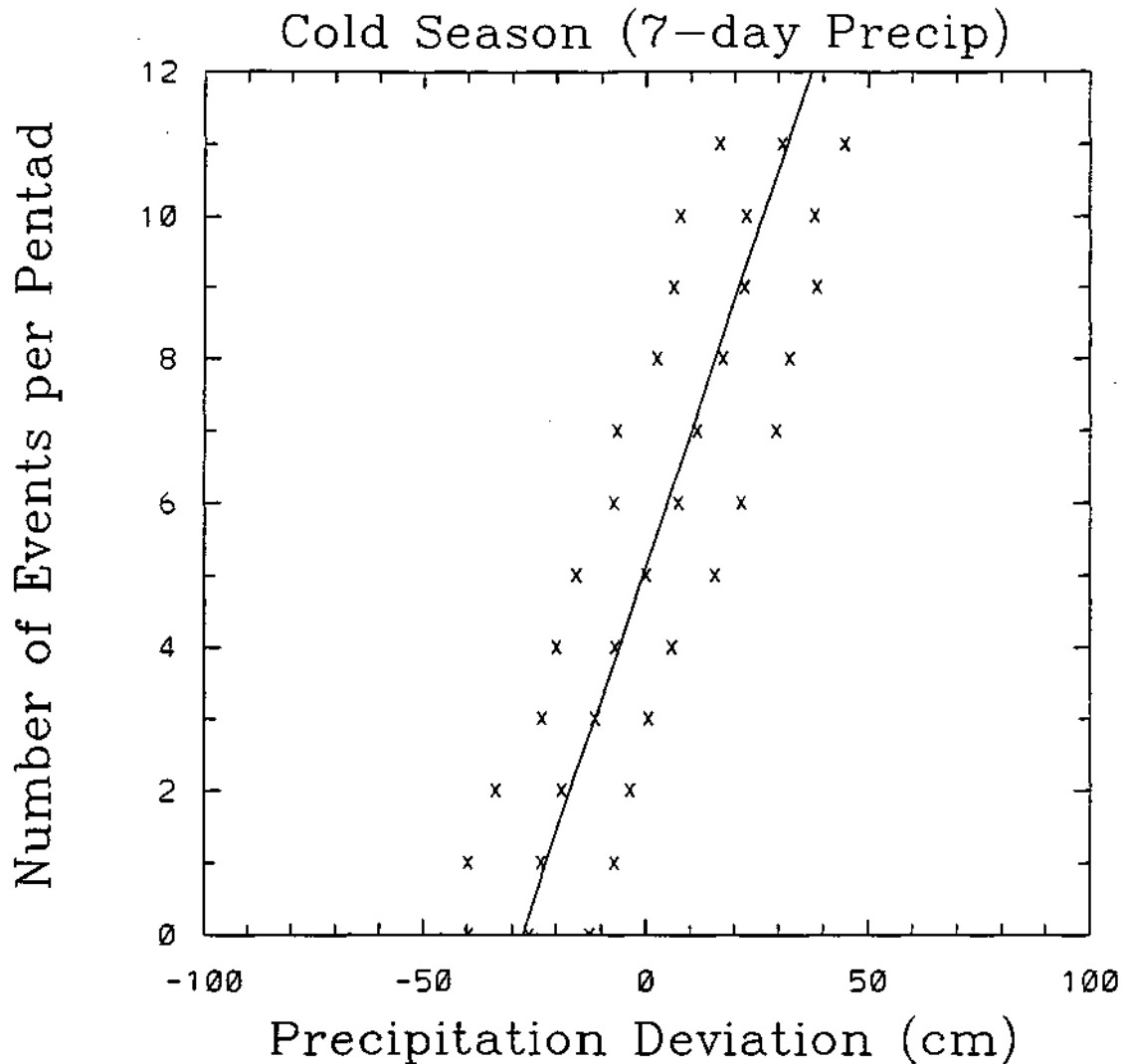


Figure 3b. Number of 7-day extreme precipitation events (magnitude > the threshold for a 1-year recurrence interval) during a pentad as a function of the pentad precipitation deviation for the cold season. Each set of three points at discrete values of the number of events represents the mean and ± 1 standard deviation of the values for all station-pentads with an equal number of events. The solid line is a least-squares fit to the mean values.

variables is quite obvious. The correlation coefficient between the individual values of the number of events and total precipitation is +0.65 for the warm season and +0.69 for the cold season.

These graphs, however, are somewhat misleading since the precipitation events themselves make a significant contribution to the total seasonal precipitation. Figure 4 is similar to Figure 3 except that for each pentad, the total precipitation from the extreme events has been subtracted from the total seasonal precipitation. It is clear that there is now little relationship between the number of extreme precipitation events and the total nonevent precipitation ($r = -0.12$ for the warm season and -0.16 for the cold season).

To shed further light on these findings, weekly precipitation was calculated for each station for its period of record. For each pentad, the frequency of occurrence was calculated for several categories of weekly totals. A summary of the 7-day frequency distributions, averaged over all stations and sorted by the total pentad precipitation for the warm and cold seasons, appears in Figure 5. Positive relationships exist in the warm season (Figure 5a) between the total pentad precipitation and incidences of 51-100 mm and > 100 mm events. For example, when pentad precipitation is below normal, the expected number of 7-day precipitation events in the 51-100 mm category is two in the warm season, but this increases to four events when the precipitation departure from normal is +100 mm. These two top categories probably include most of the extreme events. (Although the average threshold for a 1-year recurrence interval event is about 100 mm, the weekly precipitation totals are calculated over fixed dates. Therefore, events will often be split and distributed over two adjacent weeks, resulting in some effect of the extreme events on the frequencies in categories less than 100 mm.) There is also a significant negative correlation between total pentad precipitation and the frequency of dry weeks. By contrast, the relative changes in the 1-25 mm and 26-50 mm categories are much smaller. These results are similar to those of Changnon and Huff (1971), who found that there was little difference in the number of small and medium rainfall events in the summer between drought and non-drought years. An analysis of variance indicated that the extreme events above account for 42% of the interpentadal variance in total precipitation.

For the cold season (Figure 5b), strong positive correlations also exist between the total pentad precipitation and the 51-100 mm and >100 mm categories. The behavior for the other categories is rather confusing and no definitive conclusions can

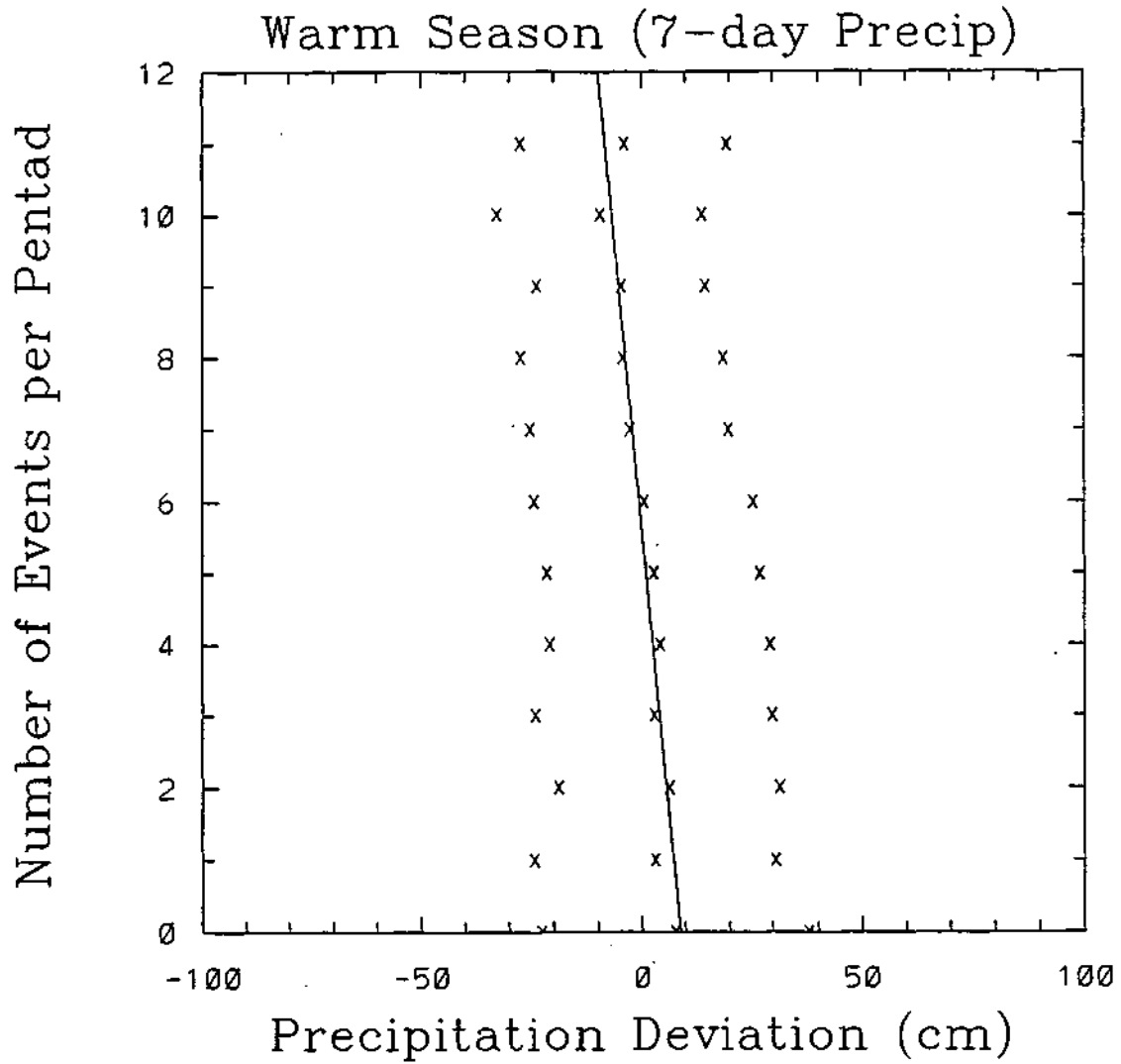


Figure 4a. Same as Figure 3a except that the total event precipitation has been subtracted from the total pentad precipitation.

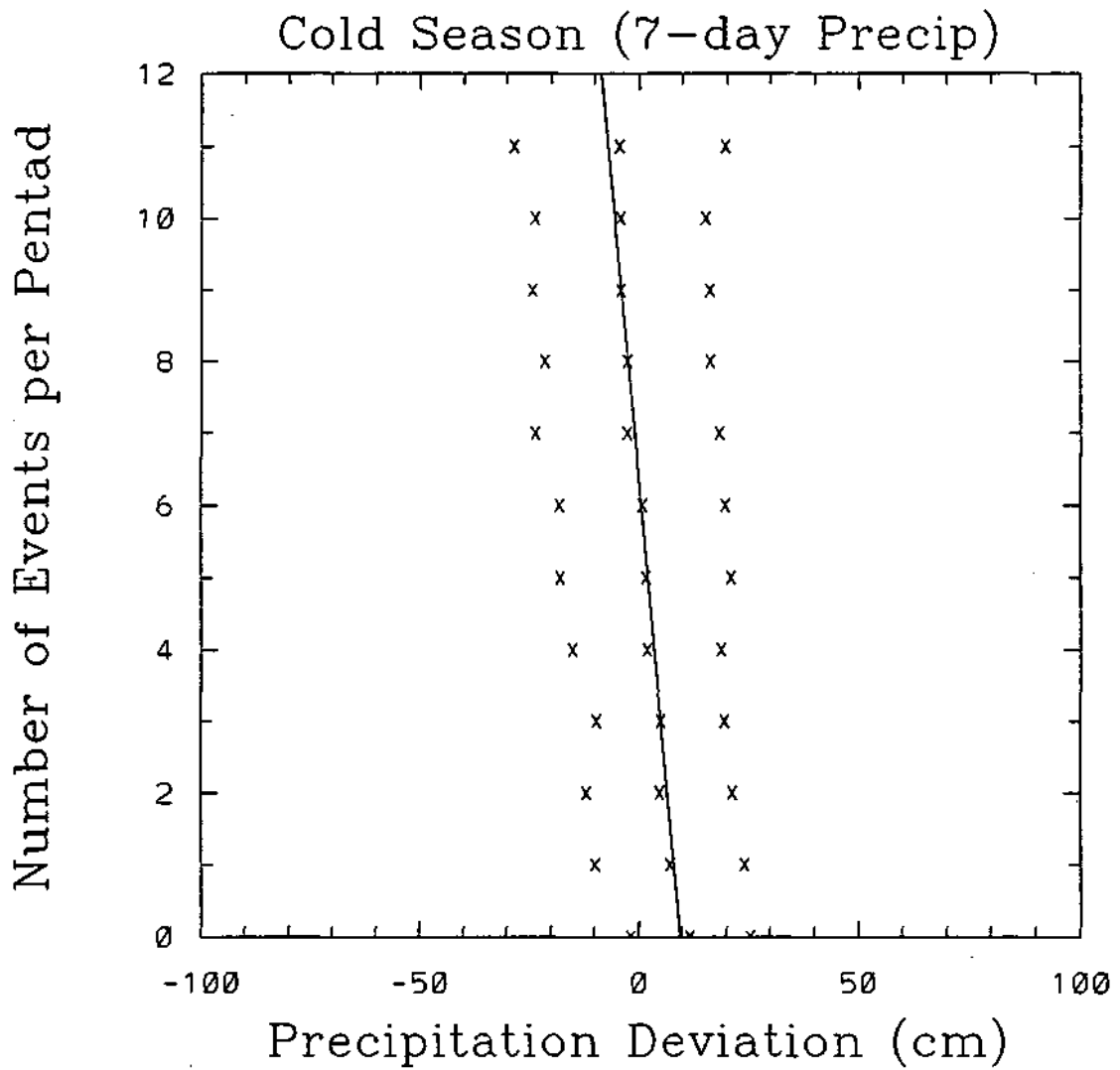


Figure 4b. Same as Figure 3b except that the total event precipitation has been subtracted from the total pentad precipitation.

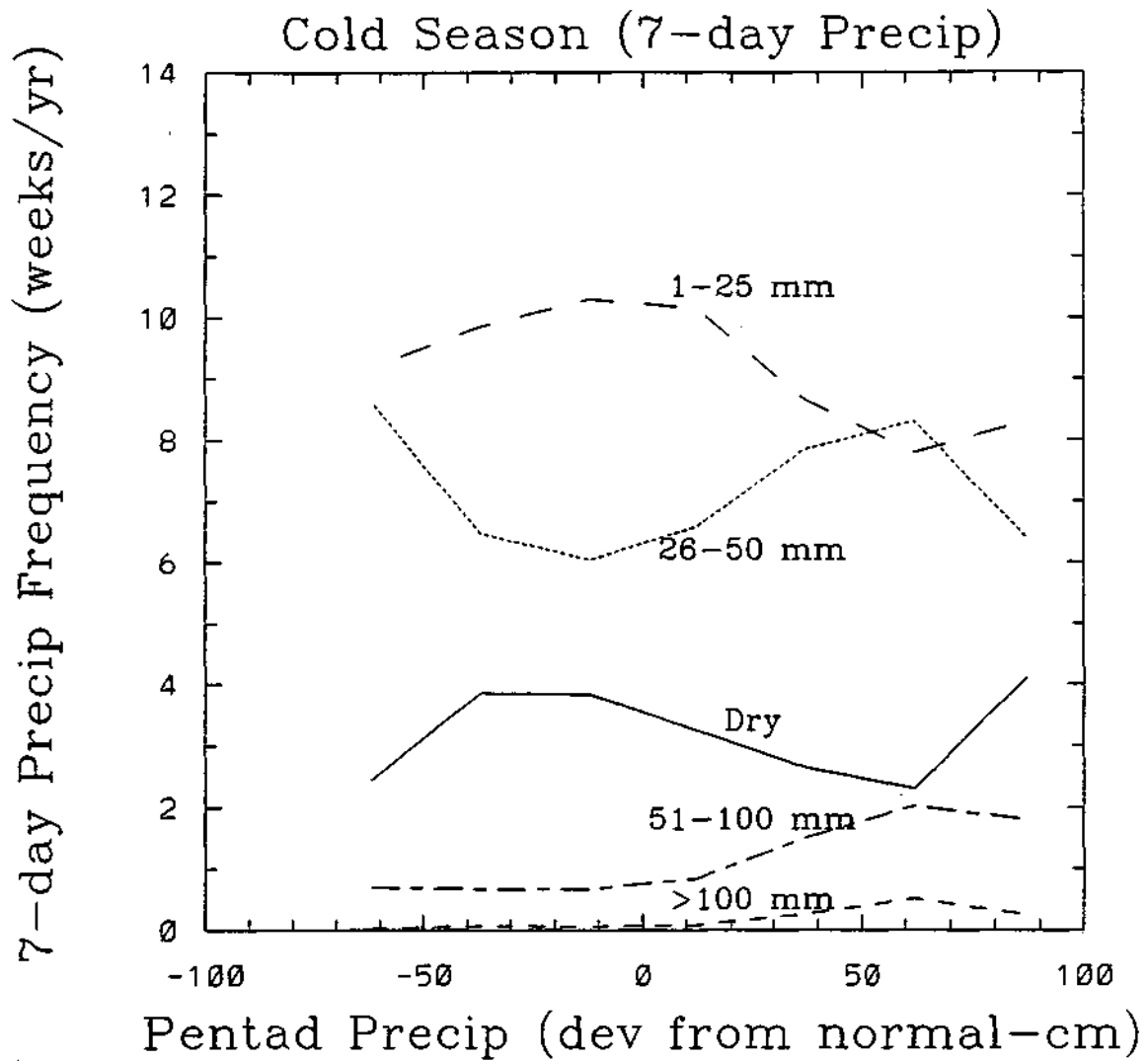


Figure 5a. Frequency of occurrence of weekly precipitation totals in five categories vs. total pentad precipitation for the warm season. These curves are composites for all stations and all pentads.

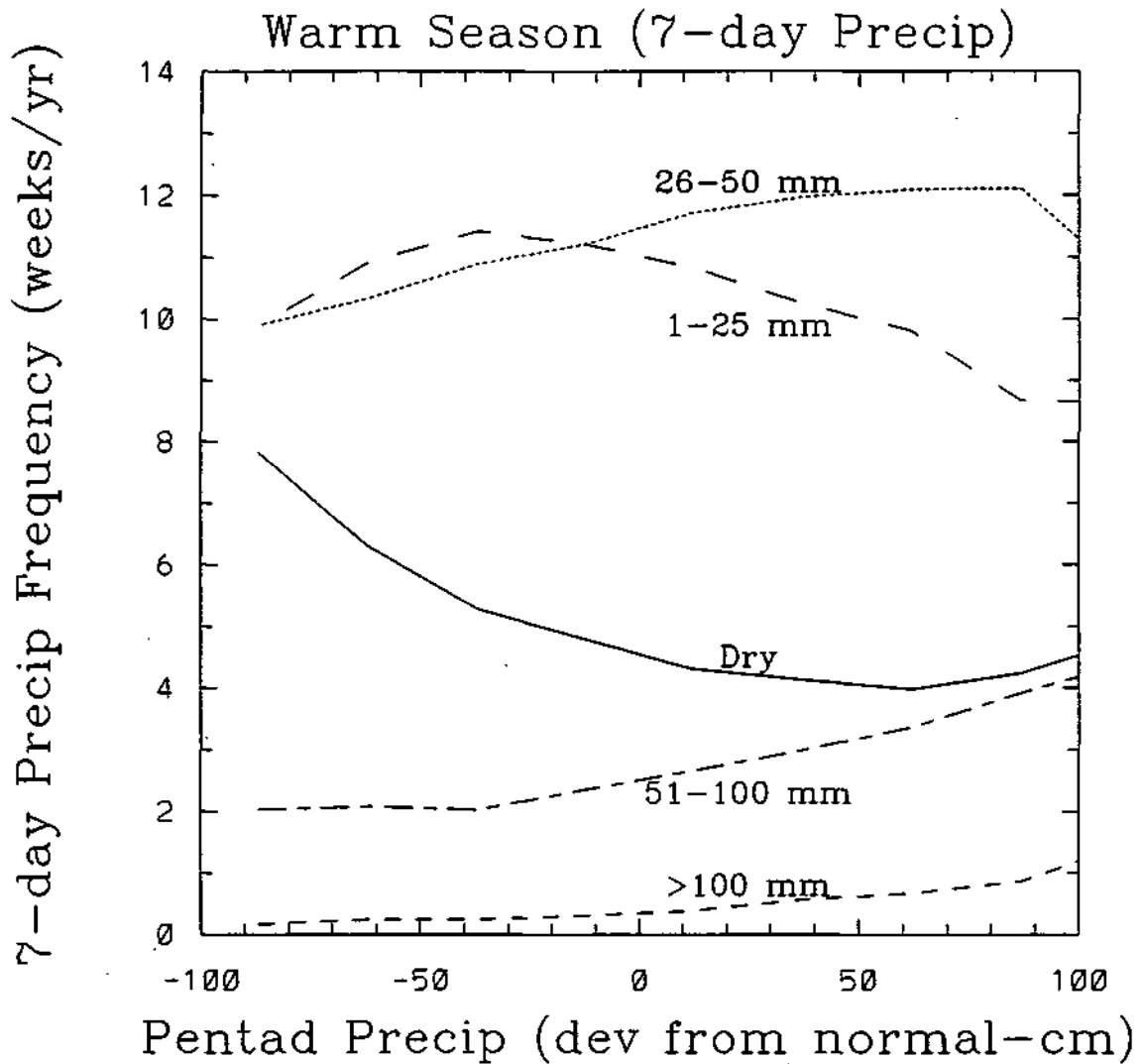


Figure 5b. Frequency of occurrence of weekly precipitation totals in five categories vs: total pentad precipitation for the cold season. These curves are composites for all stations and all pentads.

be made. The extreme events account for 49% of the interpentadal variance, similar to the warm season.

A similar study was done for temperature, comparing the frequency of extreme precipitation events with seasonal temperature anomalies calculated over pentads. In this study, we found no statistically significant relationship between the two; that is, there was no tendency for warmer (colder) than normal seasons to be characterized by a higher or lower frequency of extreme precipitation events. Specifically, the correlation coefficient between this pentadal count of extreme precipitation events and the pentadal temperature deviation was -0.11 for the warm season and -0.02 for the cold season.

Relevance to Assessing Hydrologic Effects from GCMs

Figures 3 and 4 imply that the frequency of occurrence of extreme precipitation events is in fact random and may not be tied to any particular long-term circulation anomalies. From another perspective, these events contribute nearly one-half of the interpentadal precipitation variance.

The implications for global climate change impacts assessment are significant. These results suggest that general circulation model (GCM) estimates of precipitation changes for months or seasons will not be adequate for estimation of hydrologic (flooding) impacts if they do not adequately model the frequency of occurrence of these extreme precipitation events. Since these events are often mesoscale in size, they may not be modeled directly by the current generation of GCMs. The question then arises: "Do the precipitation parameterization schemes used in these models properly represent the frequency of occurrence of extreme events?" These results also may raise concerns about GCM predictions of average precipitation changes, since our study indicates that these extreme events account for almost half of the interpentadal variance. This is clearly a major challenge. Rind et al. (1989) indicate that daily and monthly precipitation variability tends to increase with increases in the mean and suggests that better estimates of future variability are dependent on better model estimates of the mean. These results suggest that the mean and variability are partially interdependent since these extreme events tend to increase both, at least on long multi-year time scales.

These questions led us to look at the relationship between extreme precipitation events at a point and precipitation magnitudes averaged over spatial scales equivalent to current and future GCM resolutions. The following analysis was performed for each extreme precipitation event at each long-term station. For each event, all precipitation reports within a rectangular grid were averaged to produce a grid-scale precipitation value. This was done for two grid sizes: 2° latitude x 2.5° longitude, and 4° latitude x 5° longitude, selected to be comparable to the grids of some current and near-future GCMs. Separate calculations were also done for three different locations of the extreme event with respect to the grid position: center, corner, and halfway between the center and corner. The above analysis was restricted to the period 1948-1990 since digital daily precipitation data are not available for a dense network of stations prior to that time. This analysis was performed on about 10,000 station-events.

Table 1 summarizes of the ratio of grid-to-event precipitation magnitudes for the two seasons, the two grid sizes, and the three positions of the event. This ratio increases with decreasing grid size, as expected. Also, the ratio increases as the position of the event becomes more centrally located with respect to the grid. The ratios are higher in the cold season than the warm season; this is also expected because of the higher spatial variability of convective warm-season precipitation. However, the warm-season ratios are still relatively high, suggesting that these events are usually associated with widespread significant precipitation.

During the above analysis, the precipitation for each station within the grid was recorded. Figure 6 shows the probability distributions of station precipitation expressed as a ratio to grid-average precipitation. Each curve is an average of all events for an event position halfway between the center and corner of the grid. As expected, the distributions during the warm season are wider, indicative of the larger spatial variability of convective precipitation. The variability also becomes greater as the grid size increases. Pitman et al. (1990) have shown that the components of the hydrologic cycle (particularly runoff) are very sensitive not just to the grid-average precipitation, but also to the distribution of precipitation within the grid. These curves could be used to assess the probability of flood-producing localized (sub-grid scale) precipitation extremes from GCM grid-average precipitation.

Another solution to the resolution limitations of GCMs is the coupling of regional models with GCMs (e.g., Giorgi et al., 1989). This has been done in the western part of the United States. This would provide the spatial resolution

necessary to directly model these events. Another approach would involve an exhaustive study of the types of synoptic situations that cause extreme events. The frequency of occurrence of synoptic events can be obtained from GCM data.

Further analysis of the precipitation data produced the probability distributions for all weeks (not just those with extreme events) for fixed grid boxes. These boxes encompassed the area between 35°N to 45°N latitude, and 83°W to 93°W longitude. This included only those grid boxes in the above area that lie on the U.S. side of the border. Figure 7 shows the results of this analysis for the warm and cold seasons for several categories of precipitation events. This shows that the relative (expressed as a ratio to the grid-average precipitation) sub-grid scale variability decreases as the grid-average precipitation increases. These curves could be used along with a threshold value for an extreme event to estimate the areal coverage of extreme events within a grid box from the GCM grid-average precipitation value.

Table 1. Ratio of grid-averaged precipitation to extreme event precipitation (7-day totals)

	Position of Event in Grid		
	Center	Midway Between Center and Corner	Corner
Warm Season 2° lat. x 2.5° long.	0.67 ± 0.21	0.63 ± 0.22	0.56 ± 0.24
Cold Season 2° lat. x 2.5° long.	0.81 ± 0.20	0.79 ± 0.23	0.73 ± 0.27
Warm Season 4° lat. x 5° long.	0.55 ± 0.19	0.51 ± 0.19	0.41 ± 0.19
Cold Season 4° lat. x 5° long.	0.72 ± 0.21	0.68 ± 0.24	0.59 ± 0.27

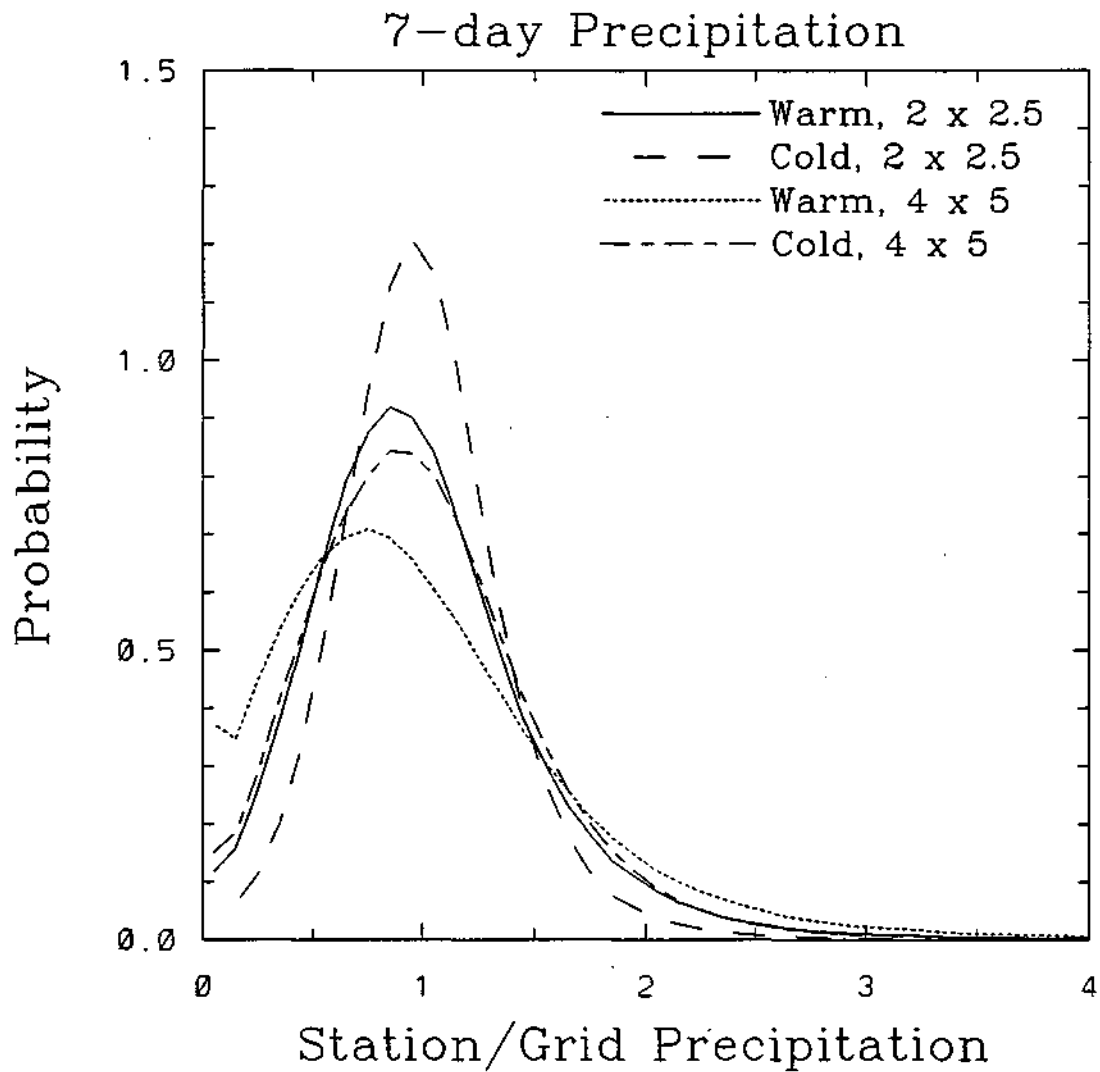


Figure 6. Probability of occurrence of 7-day station precipitation totals expressed as a ratio to grid-average precipitation. The curves represent a composite of all events.

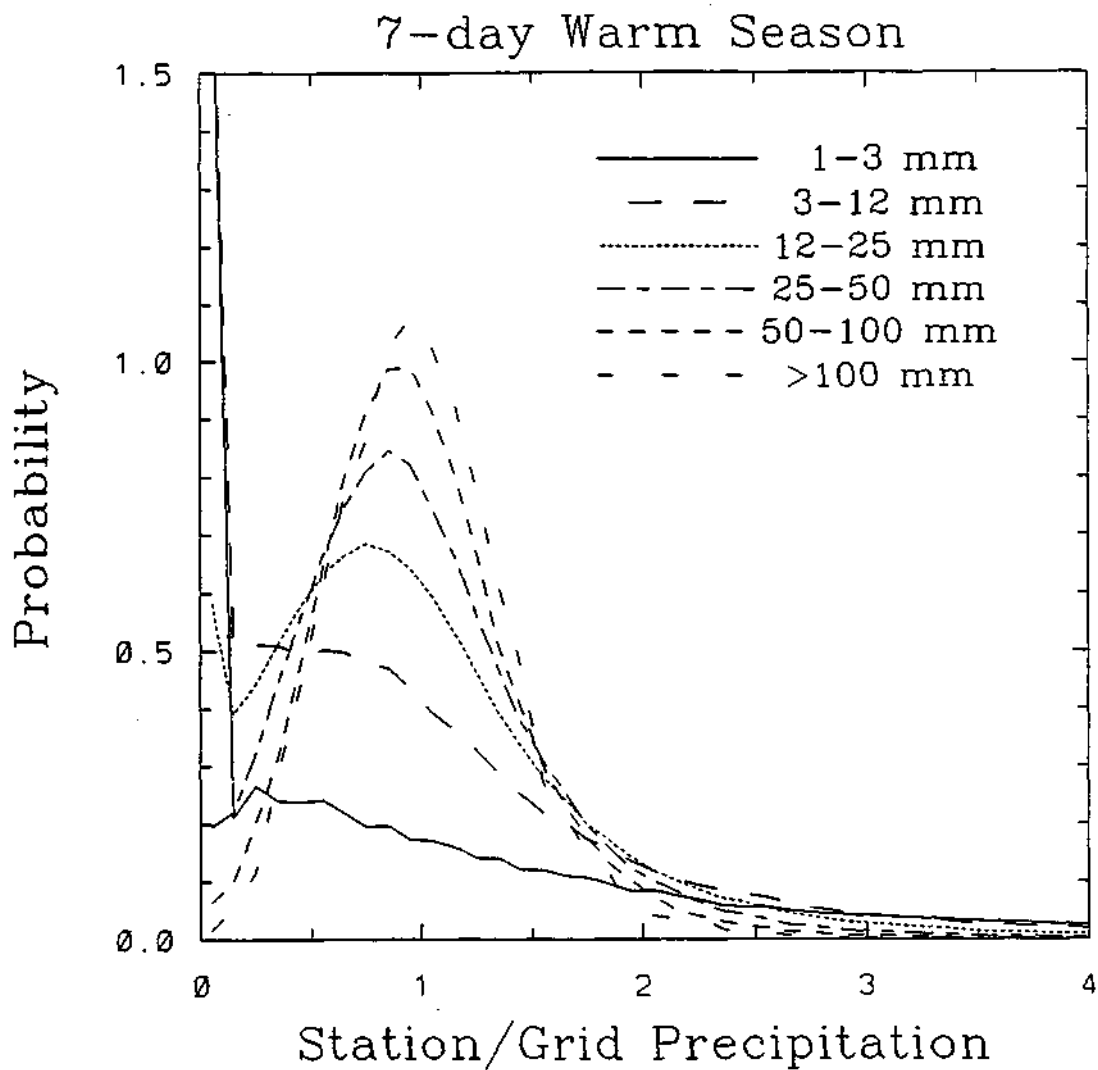


Figure 7a. Probability of occurrence of 7-day station precipitation totals for several categories of grid-average precipitation for the warm season. This analysis covers the time period from 1949-1990 and the spatial area at 35° N-45° N latitude and 83° W-93° W longitude. The grid size is 2.0° latitude by 2.5° longitude.

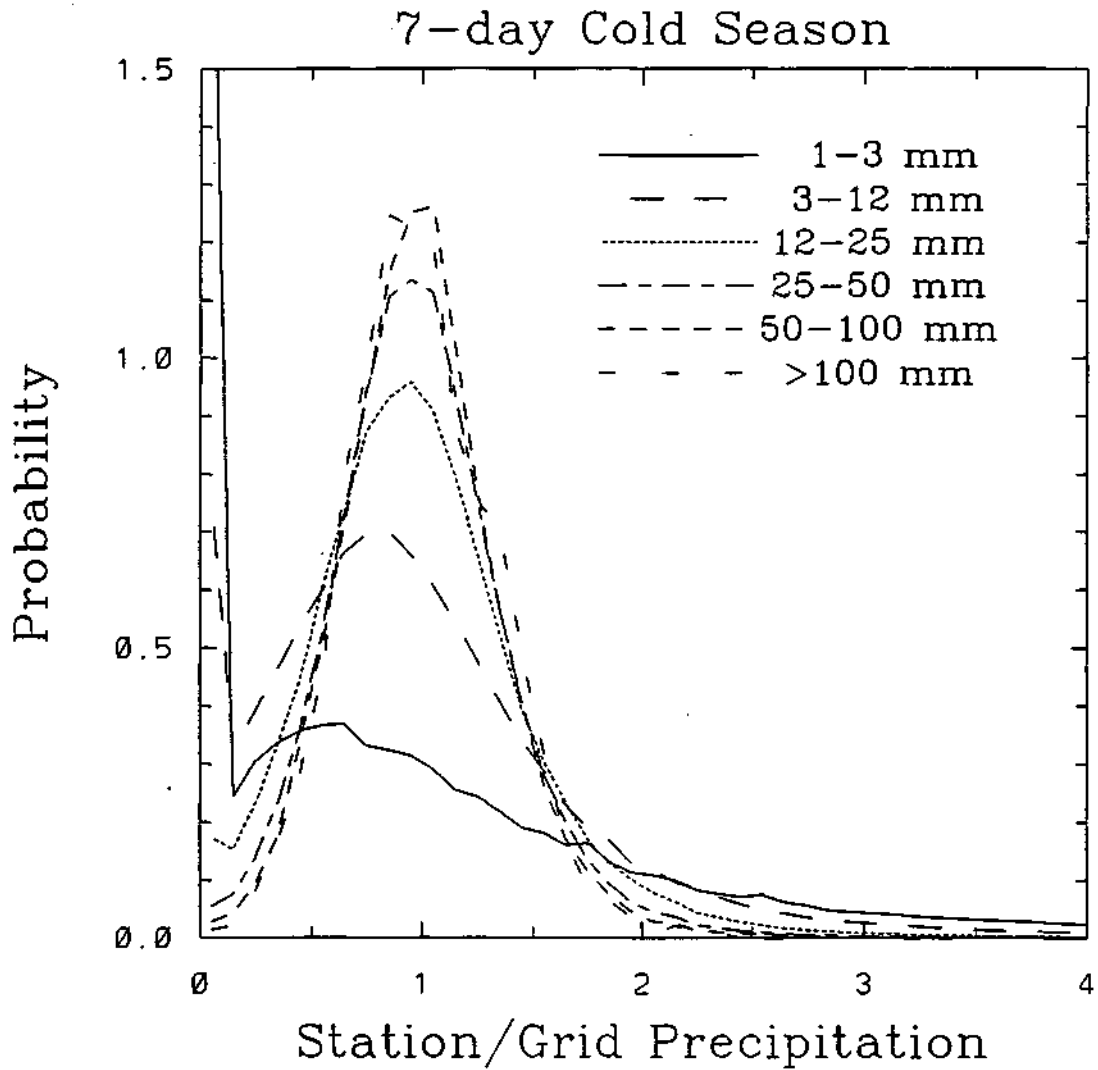


Figure 7b. Probability of occurrence of 7-day station precipitation totals for several categories of grid-average precipitation for the cold season. This analysis covers the time period from 1949-1990 and the spatial area at 35° N-45° N latitude and 83° W-93° W longitude. The grid size is 2.0° latitude by 2.5° longitude.

B. Temporal Variations

The Kolmogorov-Smirnov test was applied to each of the extreme precipitation event time series to identify any significant temporal fluctuations over the period of record. Figures 8 and 9 show the results of this analysis for the warm and cold seasons, respectively. These figures include the p-values (Figures 8a and 9a) for individual stations, a computer-generated contour map outlining p-values of 0.20, 0.10, and 0.05 (Figures 8b and 9b), and identification of those stations where temporal fluctuations are significant at the 10% level (Figures 8c and 9c). For the warm season, relatively few stations exhibit statistically significant temporal fluctuations. Most stations with significant fluctuations are located around Lake Michigan, in central Minnesota, in western Iowa, and eastern Ohio. Only 23 out of the approximately 240 long-term stations exhibit statistically significant fluctuations over this period. For the cold season, 45 stations exhibit significant temporal fluctuations at the 10% level. These are concentrated in western Iowa and southern Minnesota, northern Illinois, and in the vicinity of the Great Lakes.

We conclude from the above data that for the most part the temporal fluctuations in 1921-1990 were consistent with a random process. However, there are a few areas in which statistically significant fluctuations have occurred, as indicated by a clustering of stations with significant deviations in the cold season.

Another aspect of our analysis utilized the pentad values of extreme precipitation event frequencies to examine trends for the 1921-1990 period. The results of this analysis are displayed in Figures 10 and 11 for the warm and cold seasons, respectively. These figures include the slopes of the analyses for individual stations (Figures 10a and 11a), a contour analysis outlining areas with slopes greater than +0.2 events/pentad or less than -0.2 events/pentad (Figures 10b and 11b), and identification of stations with statistically significant trends at the 10% level (Figures 10c and 11c). These analyses indicated relatively small areas of trends for the warm season. Upward trends were prevalent in northern and central Minnesota, western Iowa and in the vicinity of Lake Michigan, and most of Kentucky and eastern Ohio. However, most areas exhibited nearly flat trends over this period. Only 41 of the 240 stations had statistically significant trends. For the cold season, upward trends were observed over an area encompassing most of Iowa and southern Minnesota, northern Illinois, and southern Michigan where the variability increased (Figure 11b). Downward trends were observed in central Indiana and southwestern Ohio. A total of 32 of 240 stations exhibited statistically significant trends.

Warm season Event recurrence = 1 year

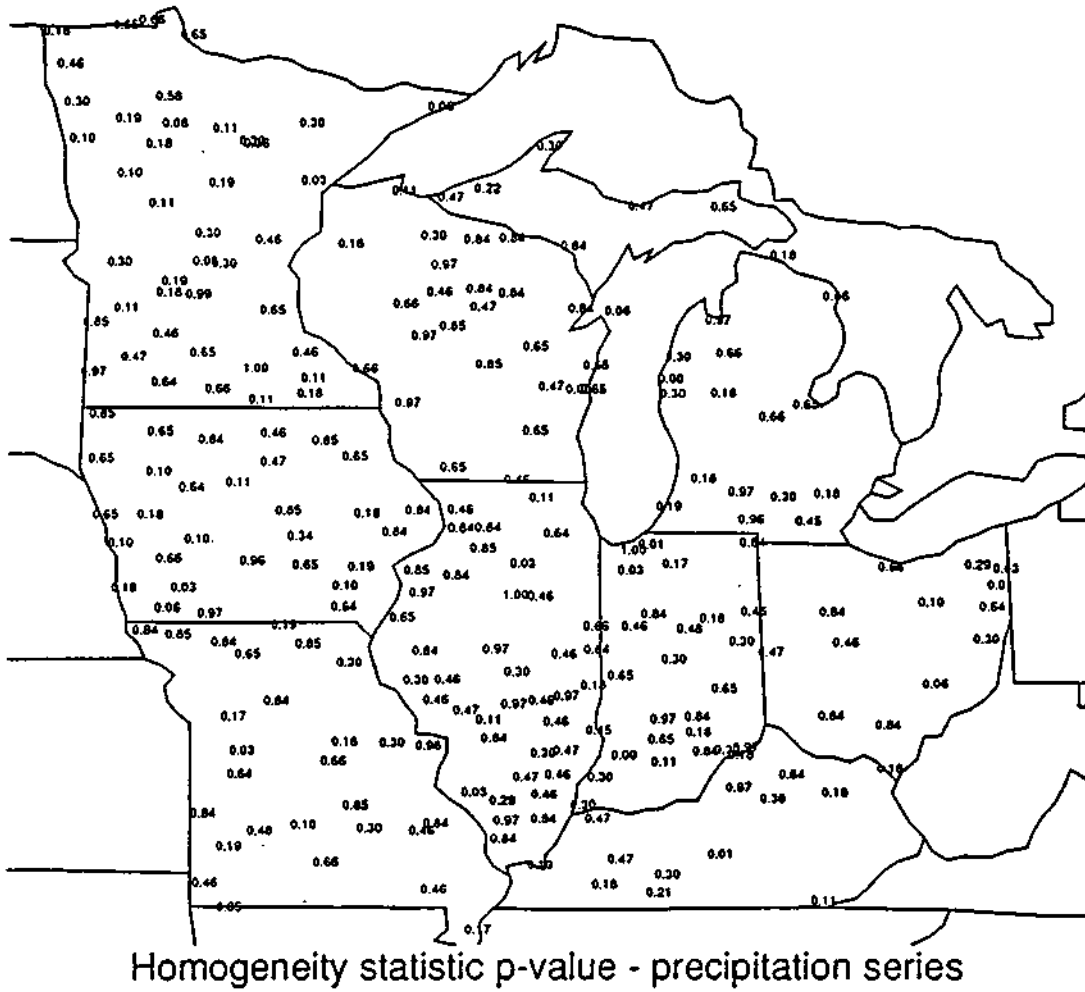


Figure 8a. Results from the Kolmogorov-Smirnov test for temporal fluctuations in the extreme precipitation event time series for the warm season. This shows the p-values for individual precipitation stations.

Warm season Event recurrence = 1 year

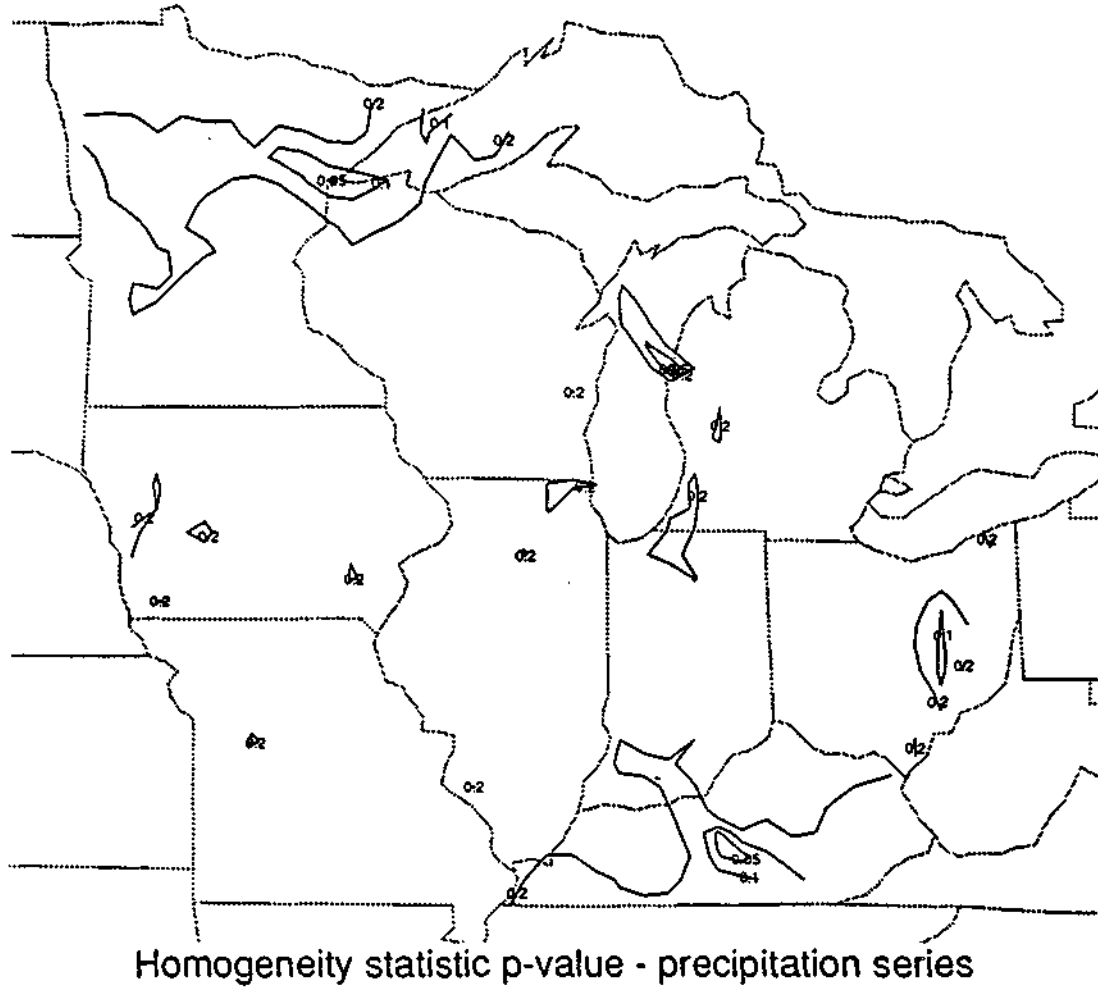
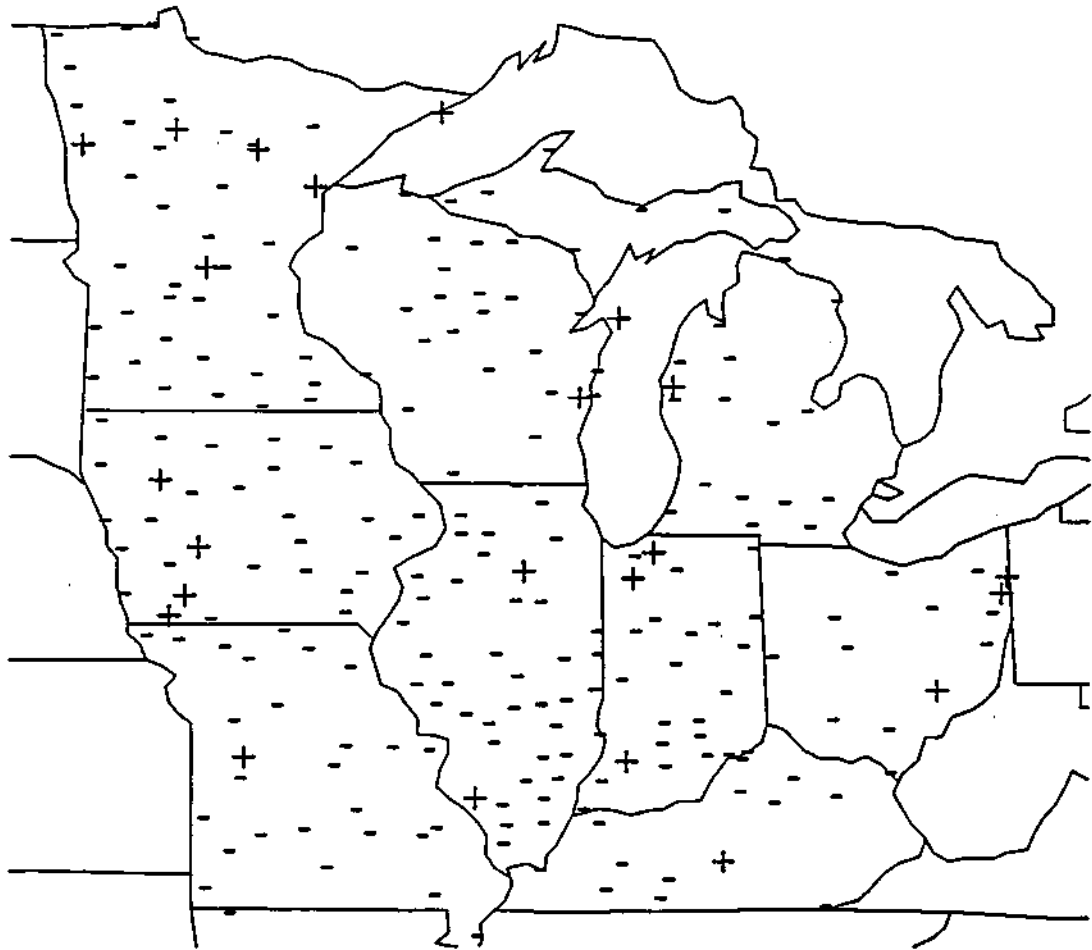


Figure 8b. Computer-generated contour analysis of the p-values in Figure 8a for p-values of 0.20, 0.10, and 0.05, which correspond to significance levels of 20%, 10%, and 5%, respectively.

Warm season Event recurrence = 1 year



Significant values of the homogeneity statistic - precipitation series

Figure 8c. Statistical significance of the Kolmogorov-Smirnov test for temporal fluctuations in the extreme precipitation event time series for the warm season. Plus signs indicate stations where statistically significant temporal fluctuations have occurred at the 10% significance level. Minus signs indicate stations where the temporal fluctuations were not statistically significant.

Cold season Event recurrence = 1 year

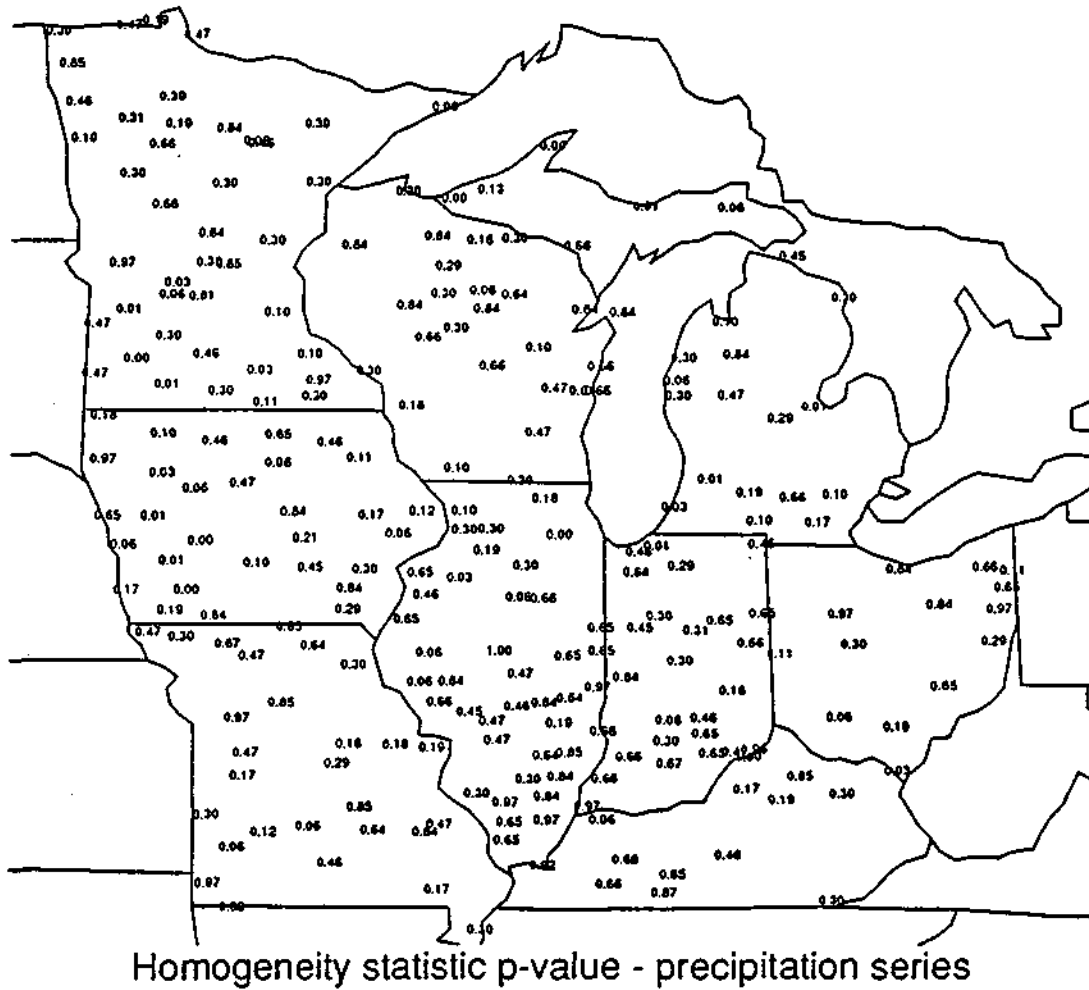


Figure 9a. Results from the Kolmogorov-Smirnov test for temporal fluctuations in the extreme precipitation event time series for the cold season. This shows the p-values for individual precipitation stations.

Cold season Event recurrence = 1 year

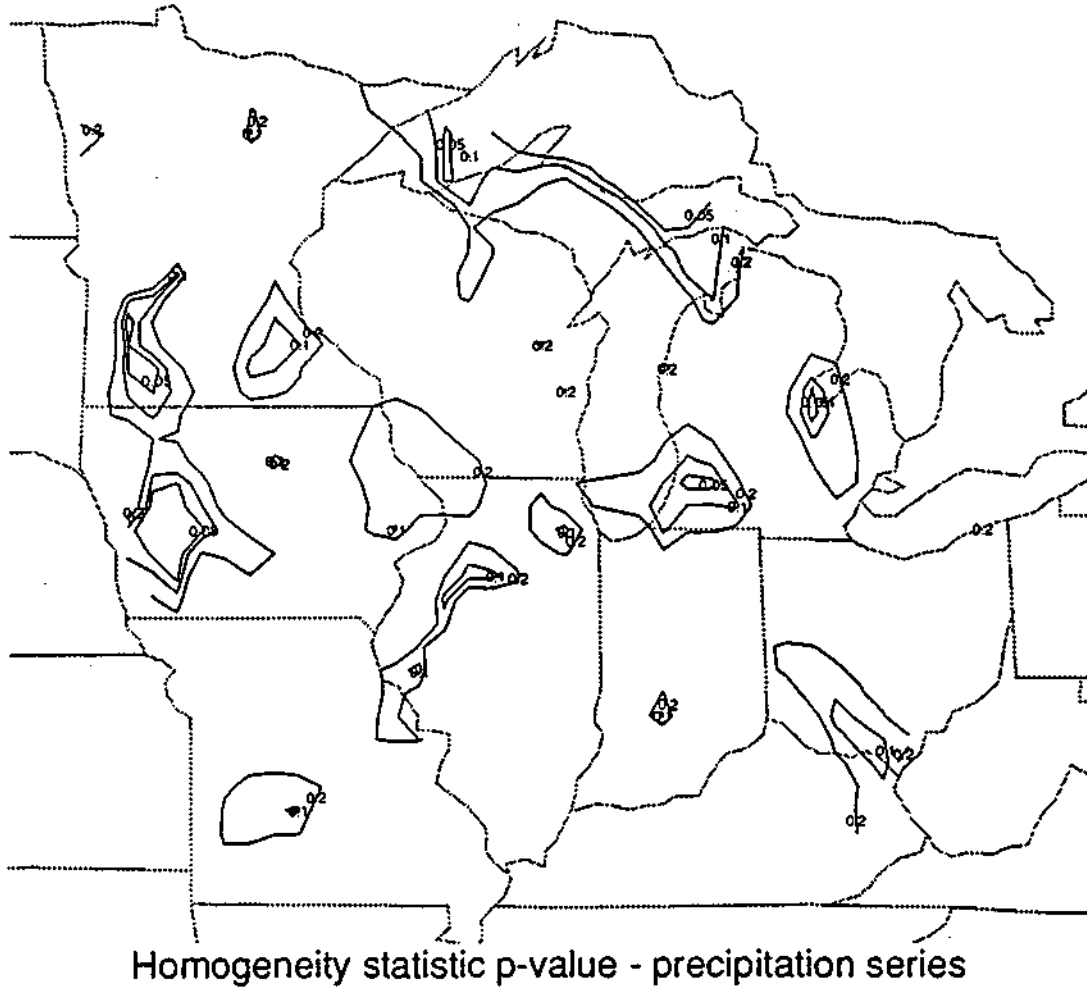
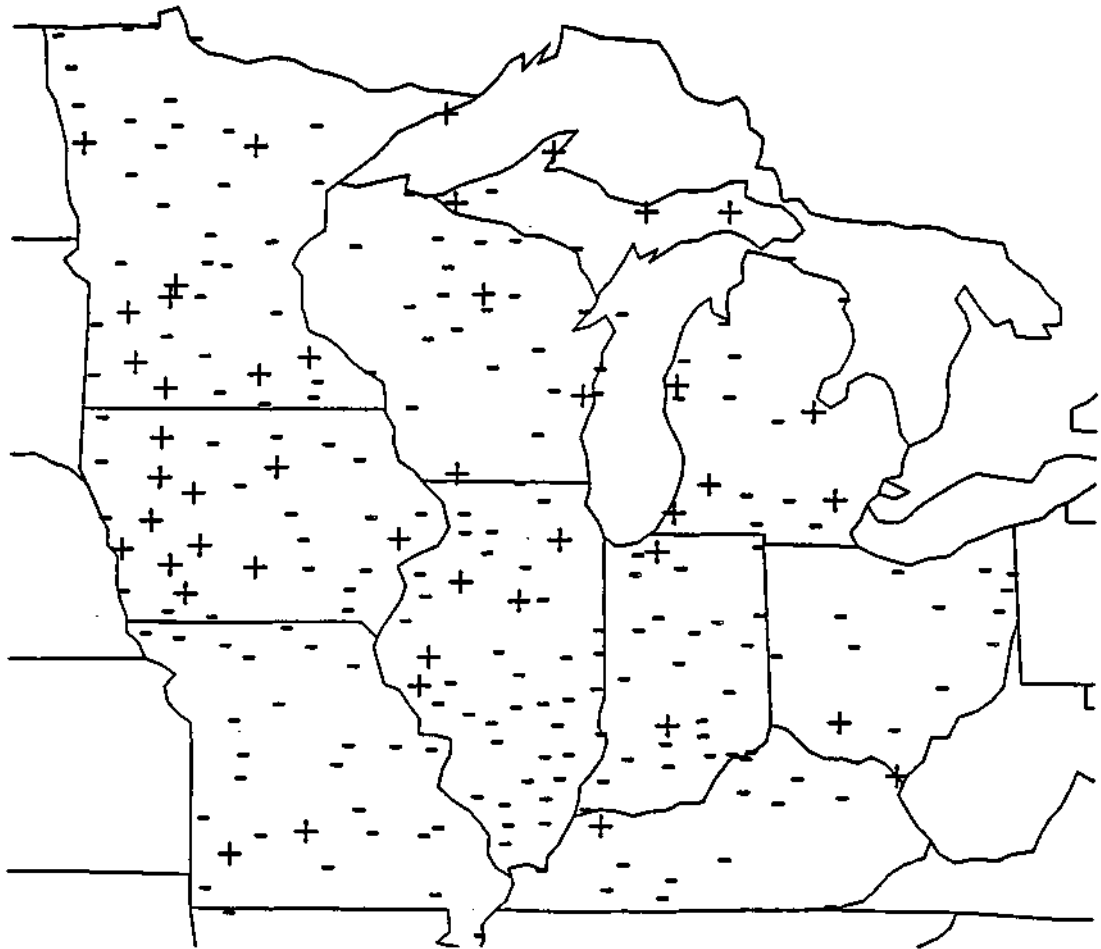


Figure 9b. Computer-generated contour analysis of the p-values in Figure 9a for p-values of 0.20, 0.10, and 0.05, which correspond to significance levels of 20%, 10%, and 5%, respectively.

Cold season Event recurrence = 1 year



Significant values of the homogeneity statistic - precipitation series

Figure 9c. Statistical significance of the Kolmogorov-Smirnov test for temporal fluctuations in the extreme precipitation event time series for the cold season. Plus signs indicate stations where statistically significant temporal fluctuations have occurred at the 10% significance level. Minus signs indicate stations where the temporal fluctuations were not statistically significant.

4. FLOOD ANALYSIS

A. Temporal Trends in Floods

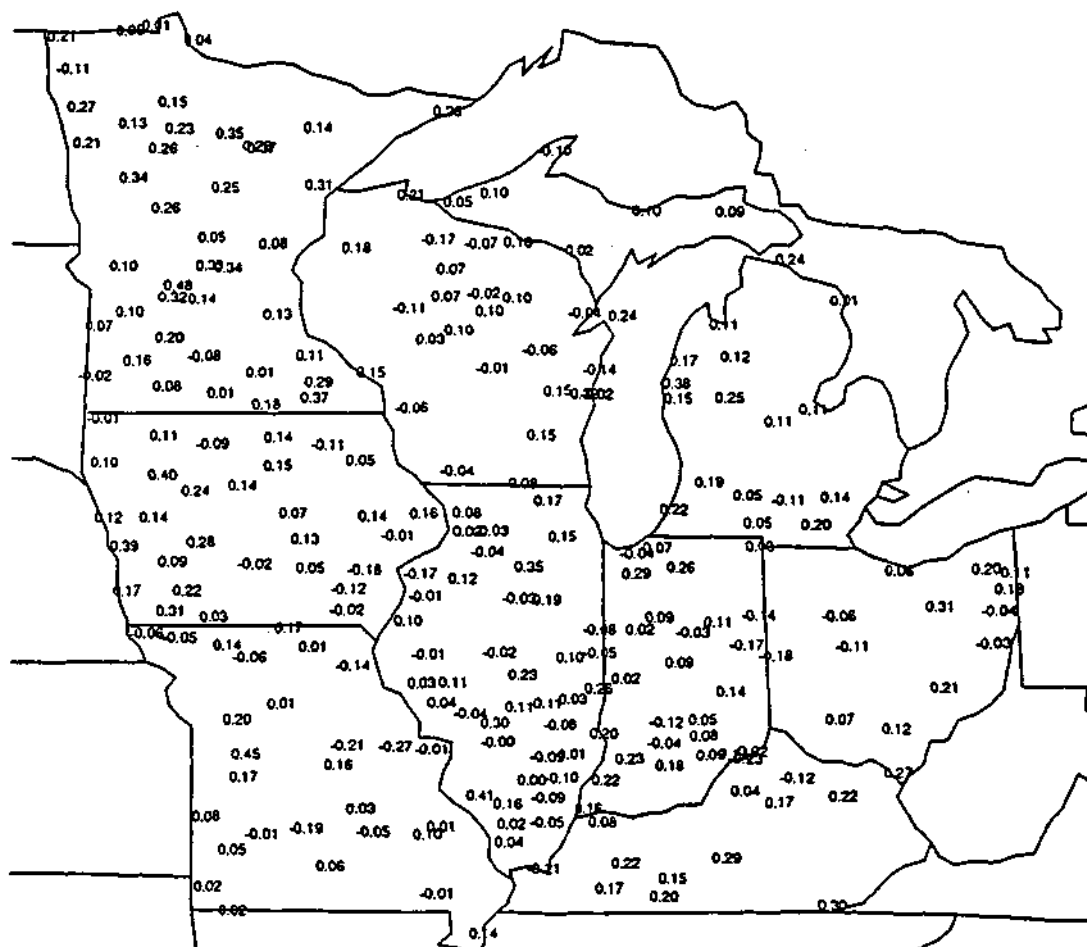
Analysis of various flood conditions was pursued. Three major historical flood conditions were analyzed including 1) frequency of floods, 2) duration of floods, and 3) intensity of floods. Values for the flood conditions have been organized into pentad (5-year) values for several of the temporal analyses.

The Kolmogorov-Smirnov test was used to evaluate the statistical significance of temporal fluctuations in flood occurrences. The results of this analysis are shown in Figures 12 and 13 for the warm and cold seasons, respectively. These figures include the p-values for individual stations (Figures 12a and 13a), contour maps analysis for p-values of 0.20, 0.10, 0.05, and 0.02 (Figures 12b and 13b), and identification of those stations with statistically significant fluctuations at the 10% level. For the warm season, most stations in Iowa, Minnesota, and northern Illinois exhibit statistically significant temporal fluctuations in floods, with p-values of 0.2 or less. This latter area was detected in the earlier Illinois study (Changnon, 1983). By contrast, in the rest of the region the fluctuations in most basins are consistent with a random process. Out of the 79 basins, 27 exhibited significant temporal fluctuations. During the cold season, most basins do not exhibit statistically significant fluctuations. The few stations that do are concentrated in southern Iowa, western Illinois, and southern Ohio. Only 17 of the 79 basins exhibited statistically significant fluctuations.

Another aspect of our trend analysis utilized the pentad values of flood frequency, flood intensity, and flood duration for each basin to calculate trends from 1921-1985. The trend line has been derived with the robust regression method of "M-estimation", using a Huber-weighting function (Hampel et al., 1986) as described in the statistical methods section. Resulting trend values have been plotted on midwestern maps to discern areas with similar trends, including up, down, and no apparent trend, over the 65-year period.

The results of the trend analyses for flood frequency is given in Figures 14 and 15 for the warm and cold seasons, respectively. These include slopes for individual stations (Figures 14a and 15a), a contour analysis outlining areas with slopes greater than 0 in increments of 0.2 events/pentad and less than -0.2 events/pentad (Figures

Warm season Event recurrence = 1 year



Linear trend slope estimates - precipitation count trends

Figure 10a. Results of the regression analysis for trends in precipitation event frequencies versus pentad for the warm season. This shows the slopes for the individual precipitation stations. The units are number of events per pentad.

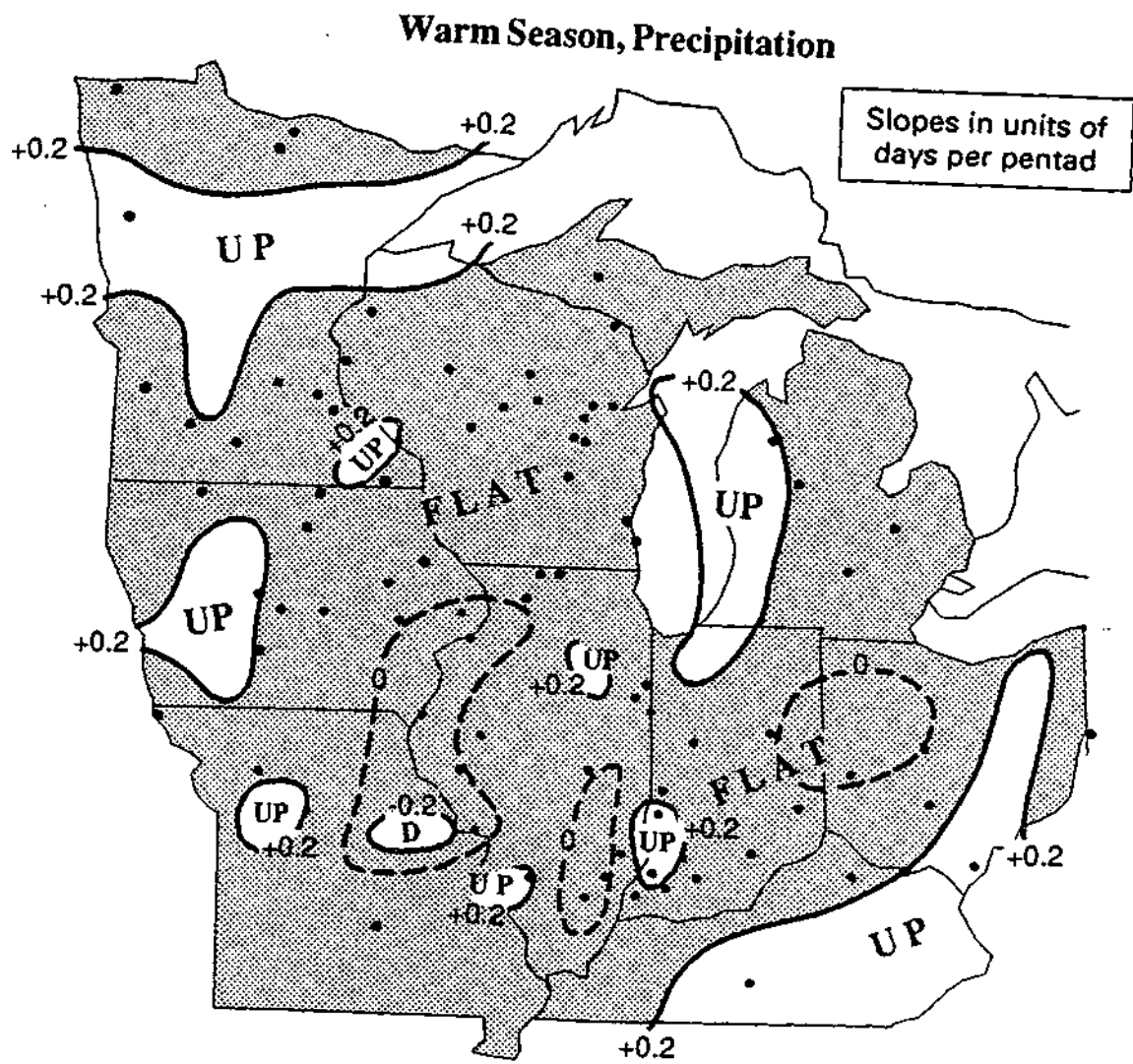


Figure 10b. Contour analysis of the trends in Figure 10a Slopes $> +0.2$ events per pentad and < -0.2 events per pentad are outlined.

Warm season Event recurrence = 1 year

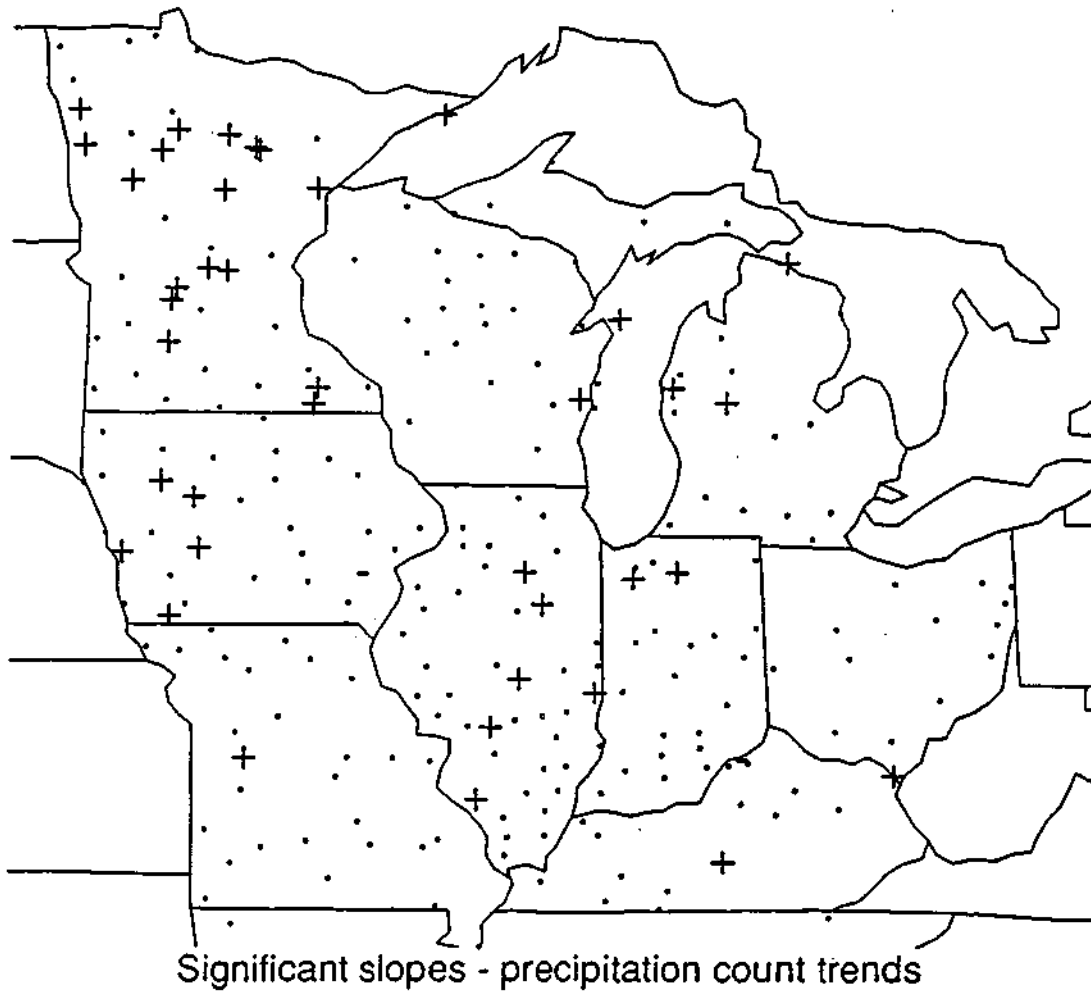


Figure 10c. Statistical significance of the trends of precipitation event frequency vs. pentad for the warm season. Pluses and minuses indicate statistically significant upward and downward trends, respectively, at the 10% level. Periods indicate stations where trends were not significant.

Cold season Event recurrence = 1 year

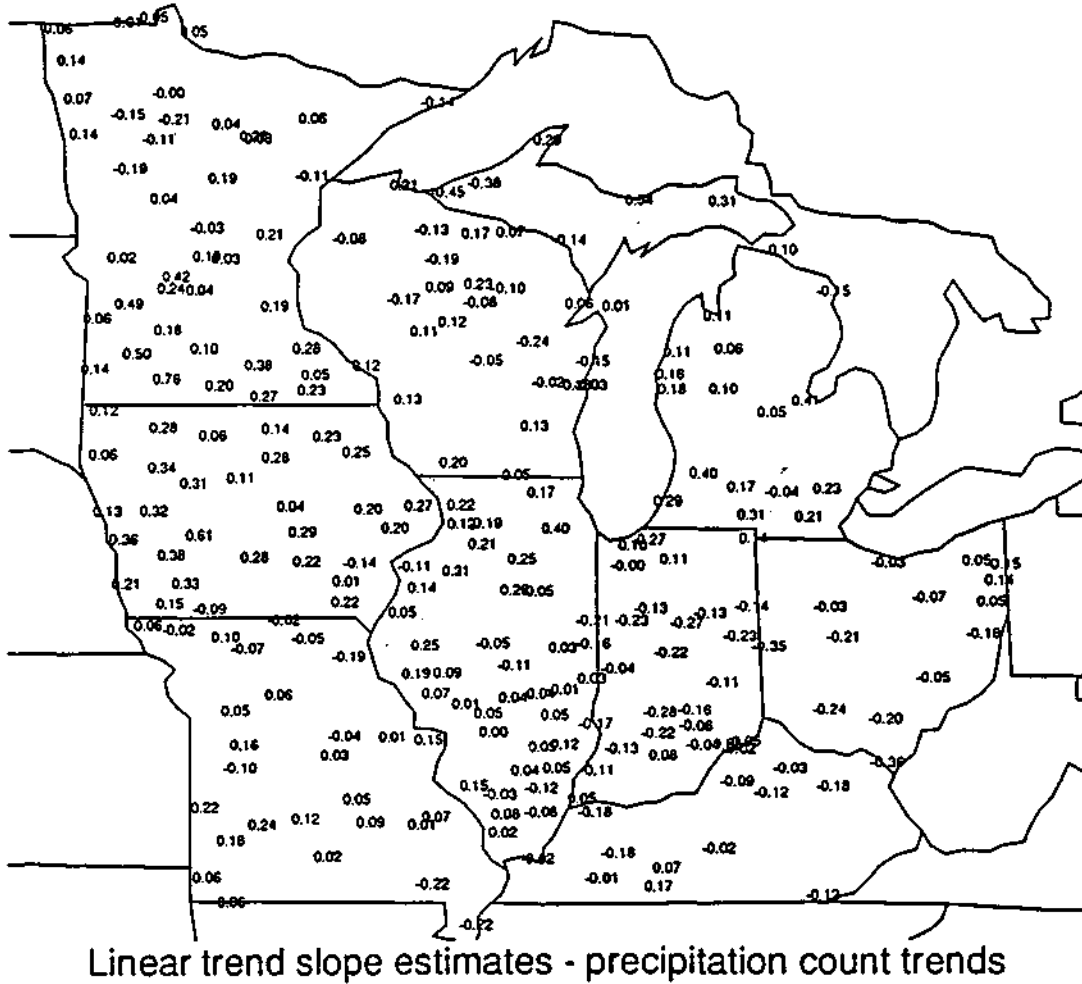


Figure 11a. Results of the regression analysis for trends in the precipitation event frequency versus pentad for the cold season. This shows the slopes for the individual precipitation stations. The units are number of events per pentad.

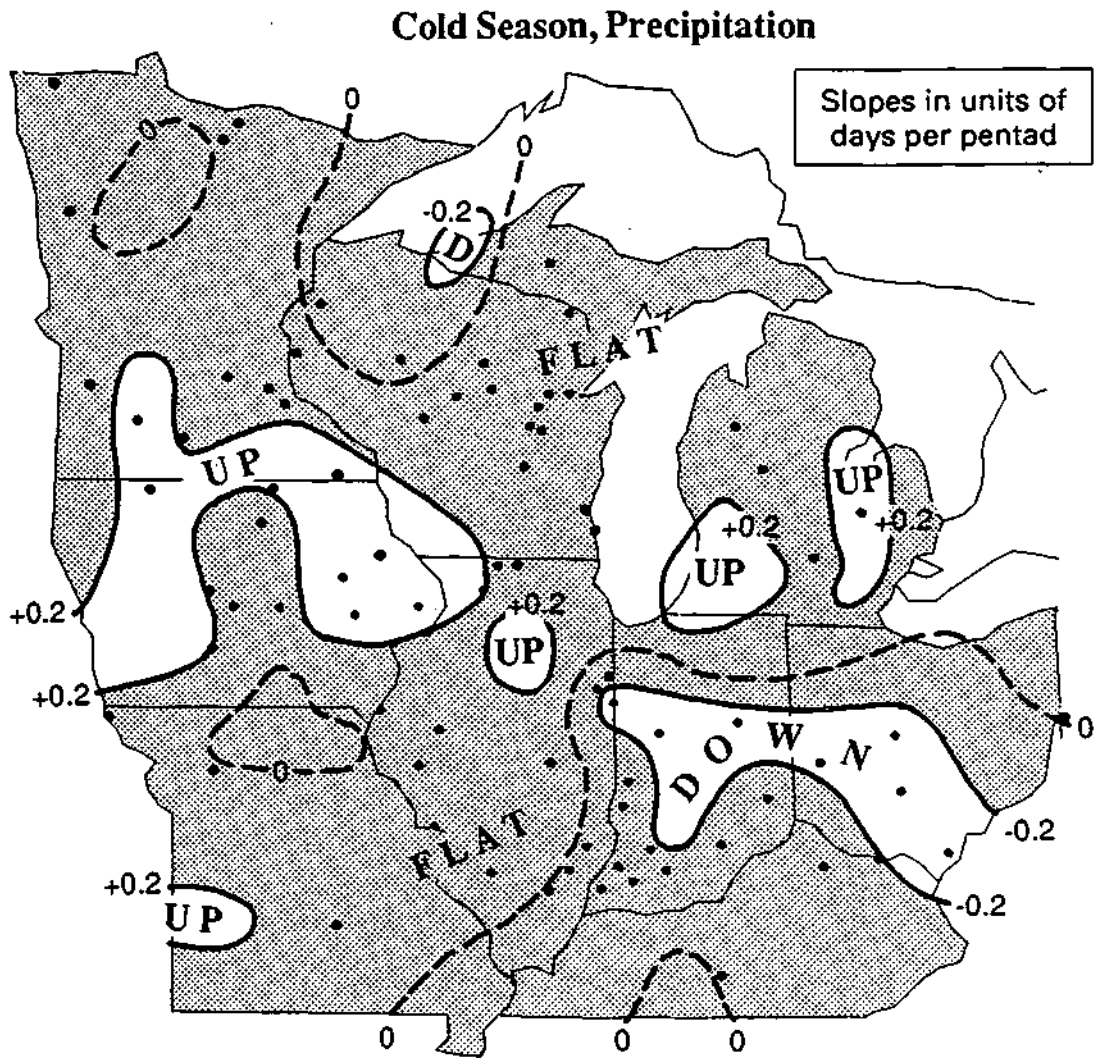


Figure 11b. Contour analysis of the trends in Figure 11a. Slopes $> +0.2$ events per pentad and < -0.2 events per pentad are outlined.

Cold season Event recurrence = 1 year

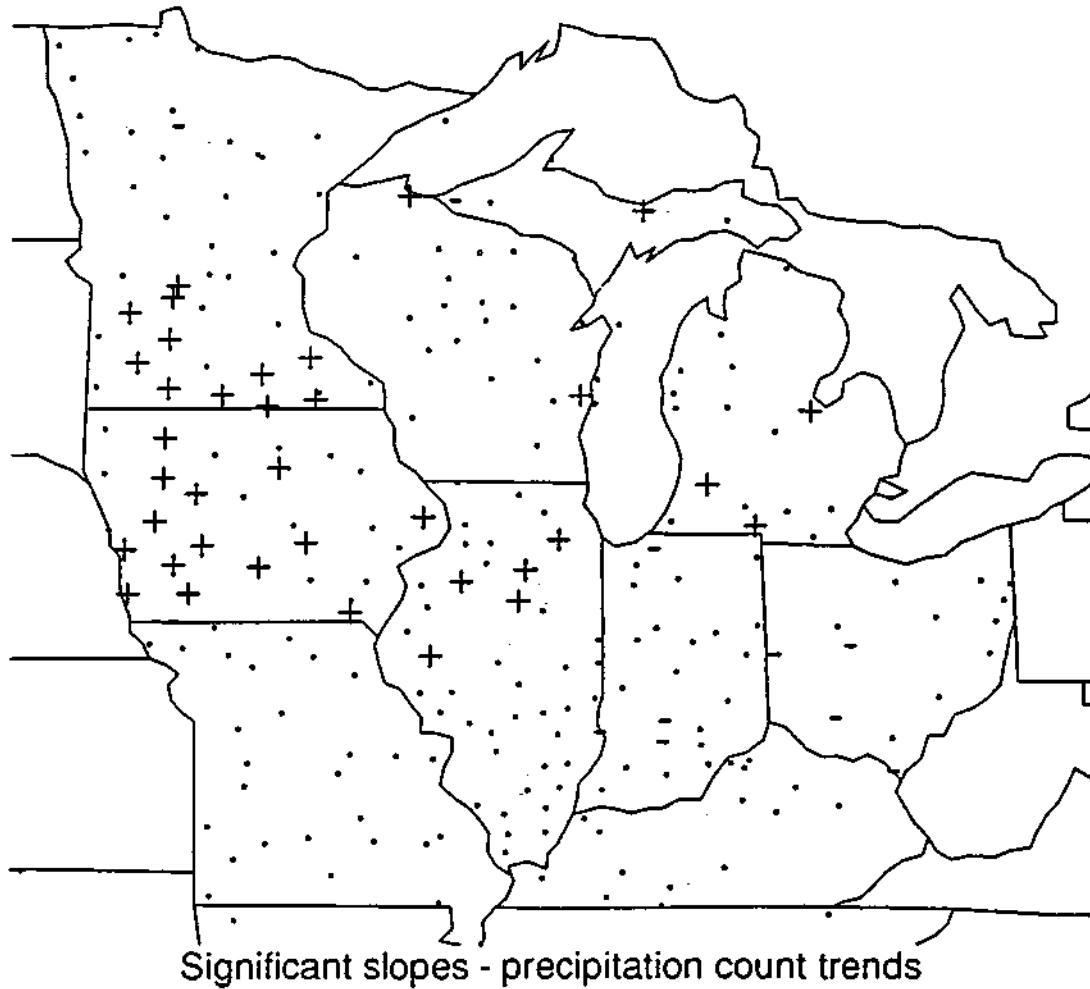


Figure 11c. Statistical significance of the trends of precipitation event frequency vs. pentad for the cold season. Pluses and minuses indicate statistically significant upward and downward trends, respectively, at the 10% level. Periods indicate stations where trends were not significant.

Warm season Flood recurrence = 1 year

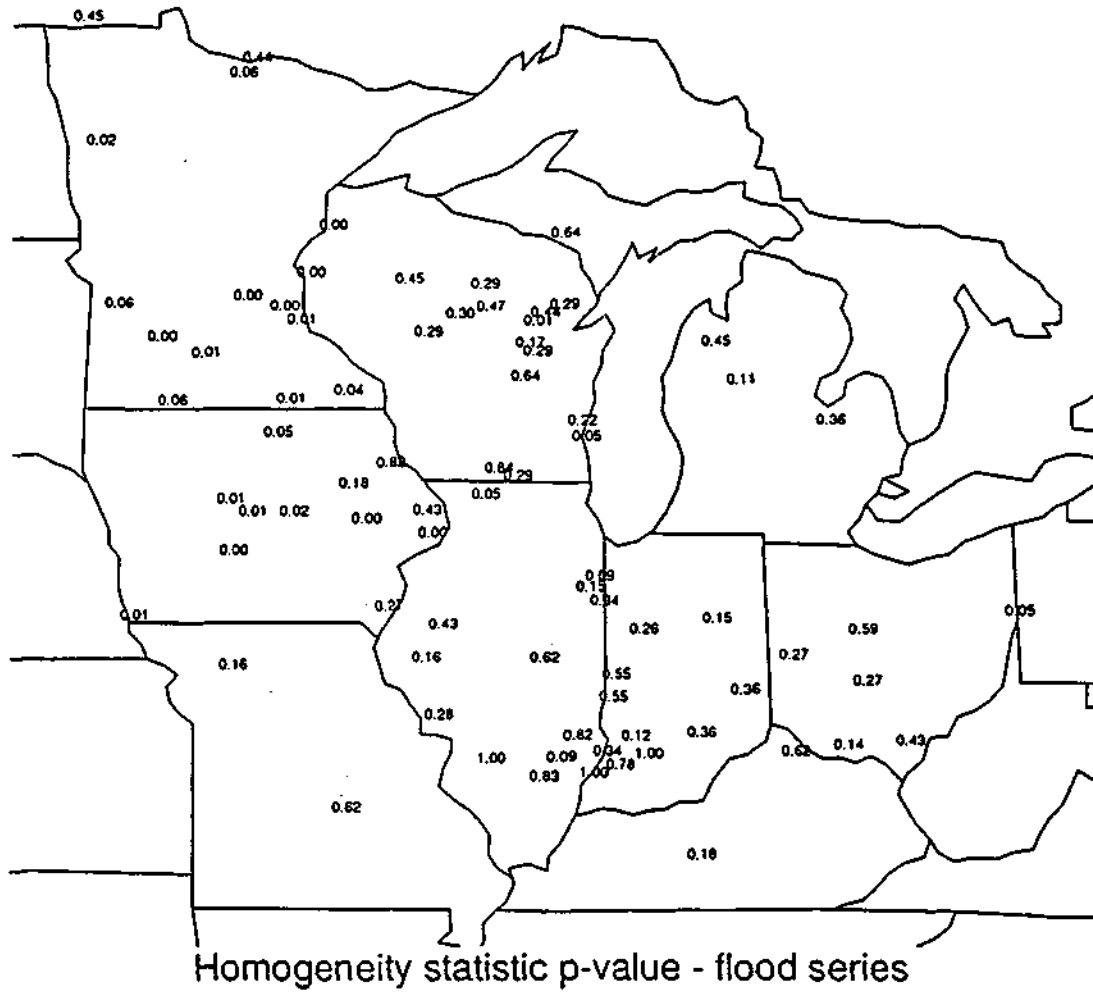


Figure 12a. Results from the Kolmogorov-Smirnov test for temporal fluctuations in the flood event time series for the warm season, which shows the p-values for individual flow stations.

Warm season Flood recurrence = 1 year

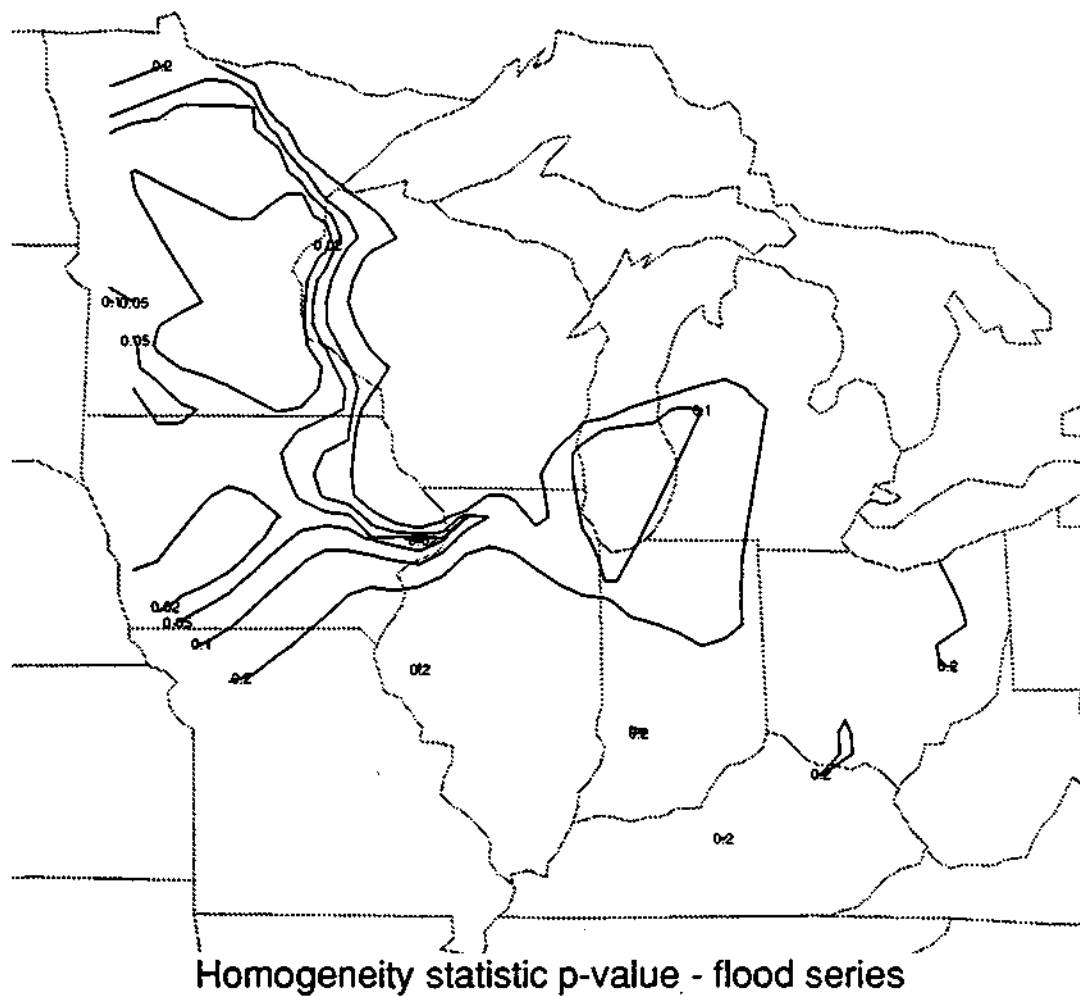


Figure 12b. Computer-generated contour analysis of the p-values in Figure 12a for p-values of 0.20, 0.10, 0.05, and 0.02, which correspond to significance levels of 20%, 10%, 5%, and 2%, respectively.

Warm season Flood recurrence = 1 year

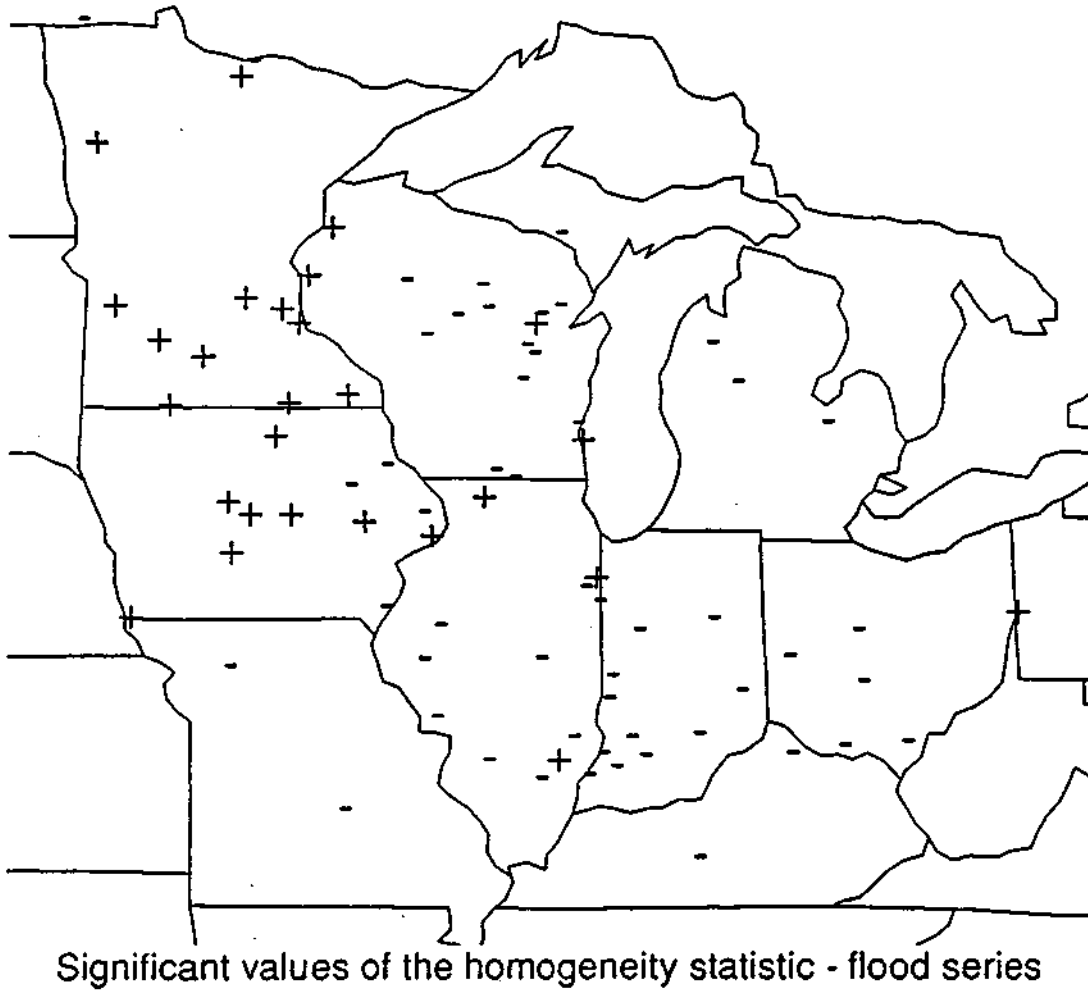


Figure 12c. Statistical significance of the Kolmogorov-Smirnov test for temporal fluctuations in the flood event time series for the warm season. Plus signs indicate stations where statistically significant temporal fluctuations have occurred at the 10% significance level. Minus signs indicate stations where the temporal fluctuations were not statistically significant.

Cold season Flood recurrence = 1 year

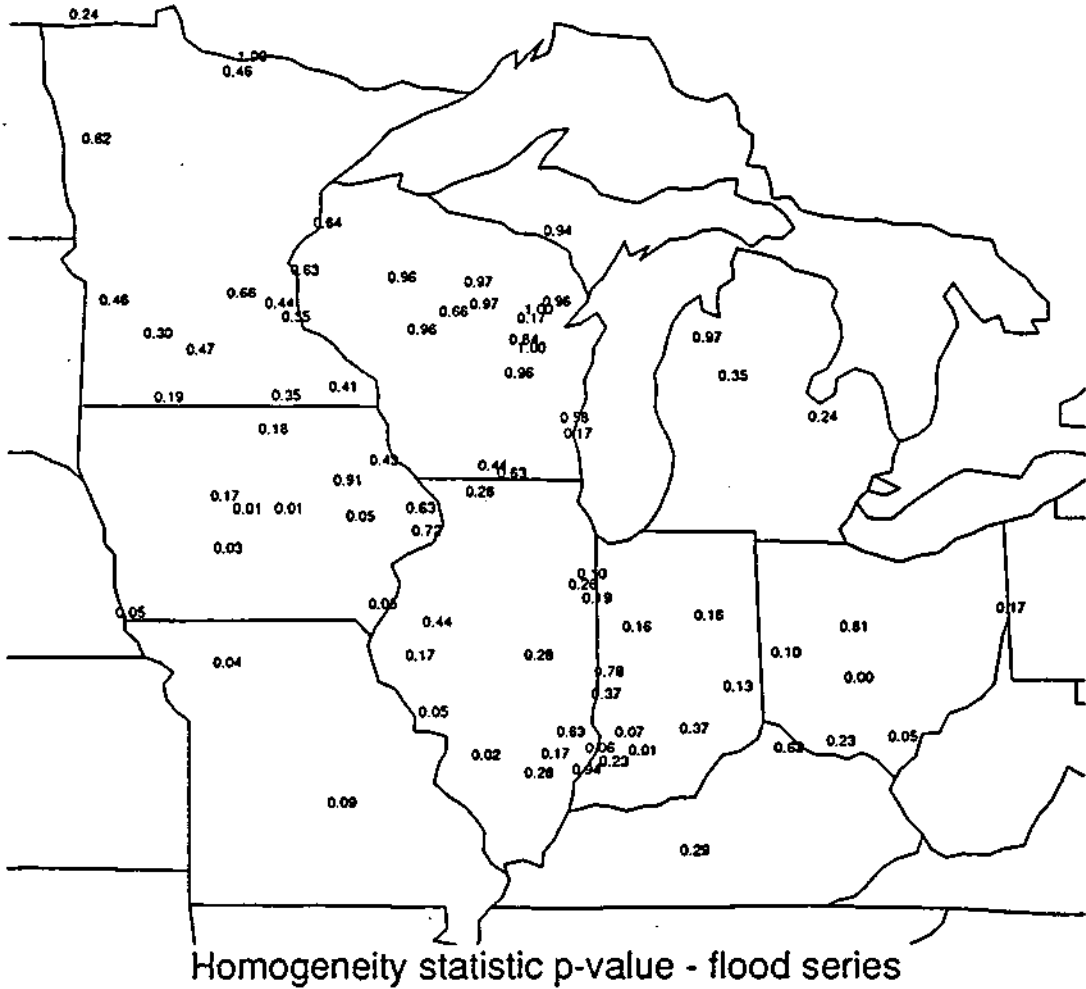


Figure 13a. Results from the Kolmogorov-Smirnov test for temporal fluctuations in the flood event time series for the cold season. This shows the p-values for individual flow stations.

Cold season Flood recurrence = 1 year

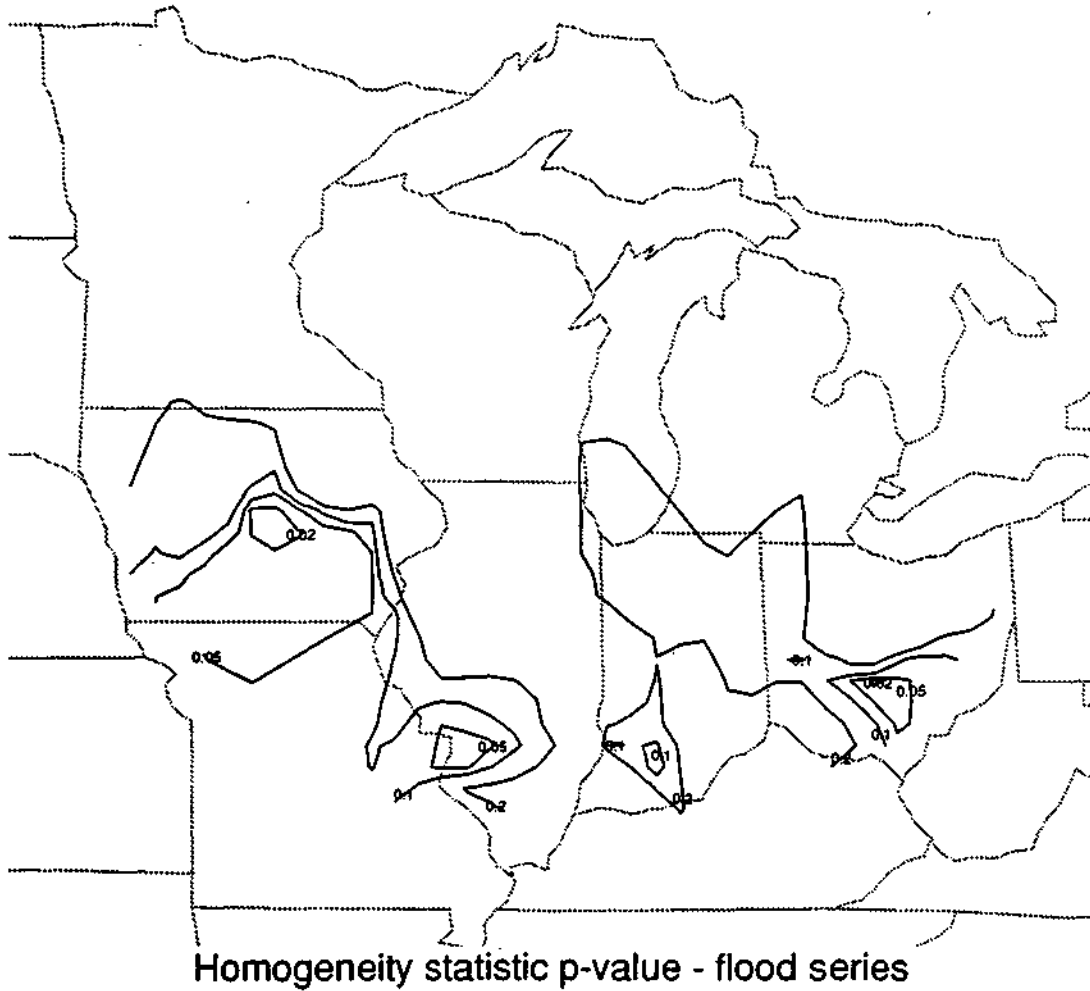
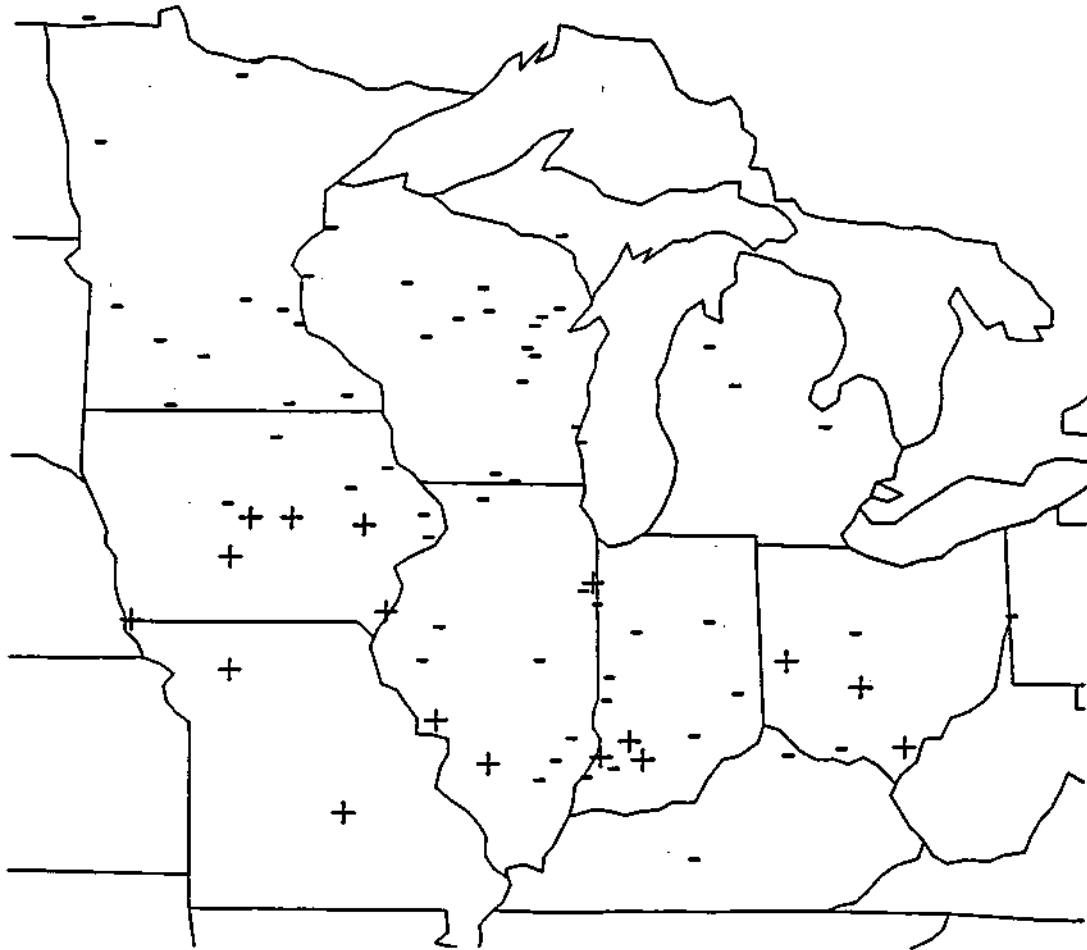


Figure 13b. Computer-generated contour analysis of the p-values in Figure 13a for p-values of 0.20, 0.10, 0.05, and 0.02, which correspond to significance levels of 20%, 10%, 5%, and 2%, respectively.

Cold season Flood recurrence = 1 year



Significant values of the homogeneity statistic - flood series

Figure 13c. Statistical significance of the Kolmogorov-Smirnov test for temporal fluctuations in the flood event time series for the cold season. Plus signs indicate stations where statistically significant temporal fluctuations have occurred at the 10% significance level. Minus signs indicate stations where the temporal fluctuations were not statistically significant.

14b and 15b), and identification of stations with statistical significance at the 10% level (Figures 14c and 15c).

For the warm season this analysis indicated broad areas of increasing flood frequency extending across much of the Midwest for the 1921-1985 period. Regions of greatest increase in flood frequency were found in a broad area including most of Iowa, Minnesota, and northwestern Wisconsin, and in smaller areas in northeastern Illinois, southern Indiana, and central Michigan. An area of slight downward trends was evident in southern Ohio. Much of the area from southern Illinois through north central Indiana and southern lower Michigan essentially had no upward or downward trend in the frequency of floods. There were 25 basins (32% of the total) with statistically significant trends.

For the cold season (Figure 15), upward trends were generally lower in magnitude than for the warm season. They were found in a broad area in the western part of the region from central Minnesota across Iowa, Missouri, and into western Illinois. Another area of upward trends was found in central lower Michigan. Downward trends were found in central and southern Ohio. The area from northeastern Minnesota across Wisconsin, eastern Illinois, Indiana, and into Kentucky had little or no trend. There were 24 basins with statistically significant trends.

Results of the trend analysis for median flood duration are shown in Figures 16 and 17 for the warm and cold seasons, respectively. These include slopes for individual stations (Figures 16a and 17a), a contour analysis of the slopes (Figures 16b and 17b), and identification of stations with statistically significant trends at the 10% level (Figures 16c and 17c). Examination of these results for the warm season showed little similarity to the frequency trend patterns. In general, almost all stations exhibited little or no trends. Only 11 basins showed significant trends.

For the cold season, much of Minnesota and a small part of northern Iowa exhibited upward trends while central Michigan had downward trends. The rest of the region showed little or no trends. The areas of upward trends in duration also were characterized by upward trends in frequencies. However, there were much larger areas with upward trends in frequencies. The area of downward trends in duration was characterized by upward trends in frequencies.

Warm season Flood recurrence = 1 year

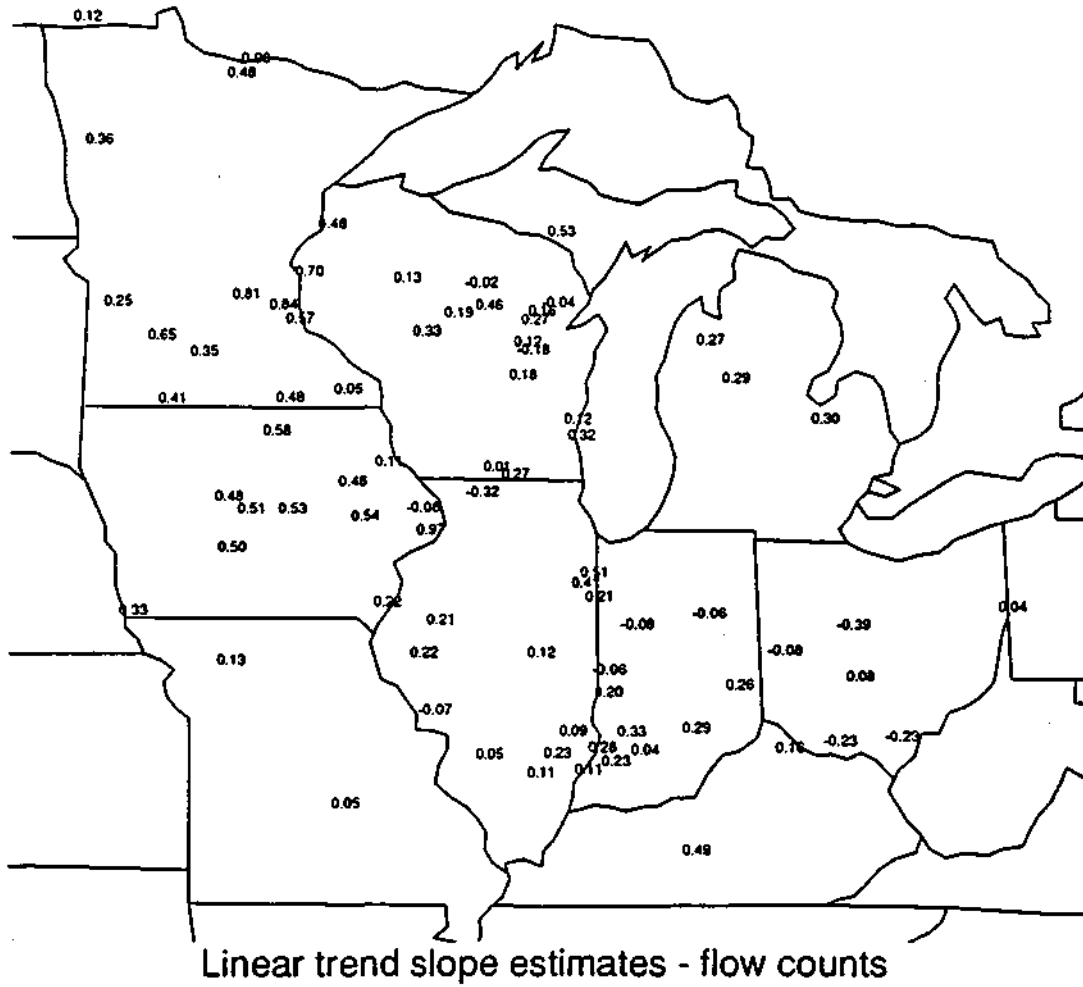


Figure 14a. Results of the regression analysis for trends in flood event frequencies versus pentad for the warm season. This shows the slopes for the individual flow stations. The units are number of events per pentad.

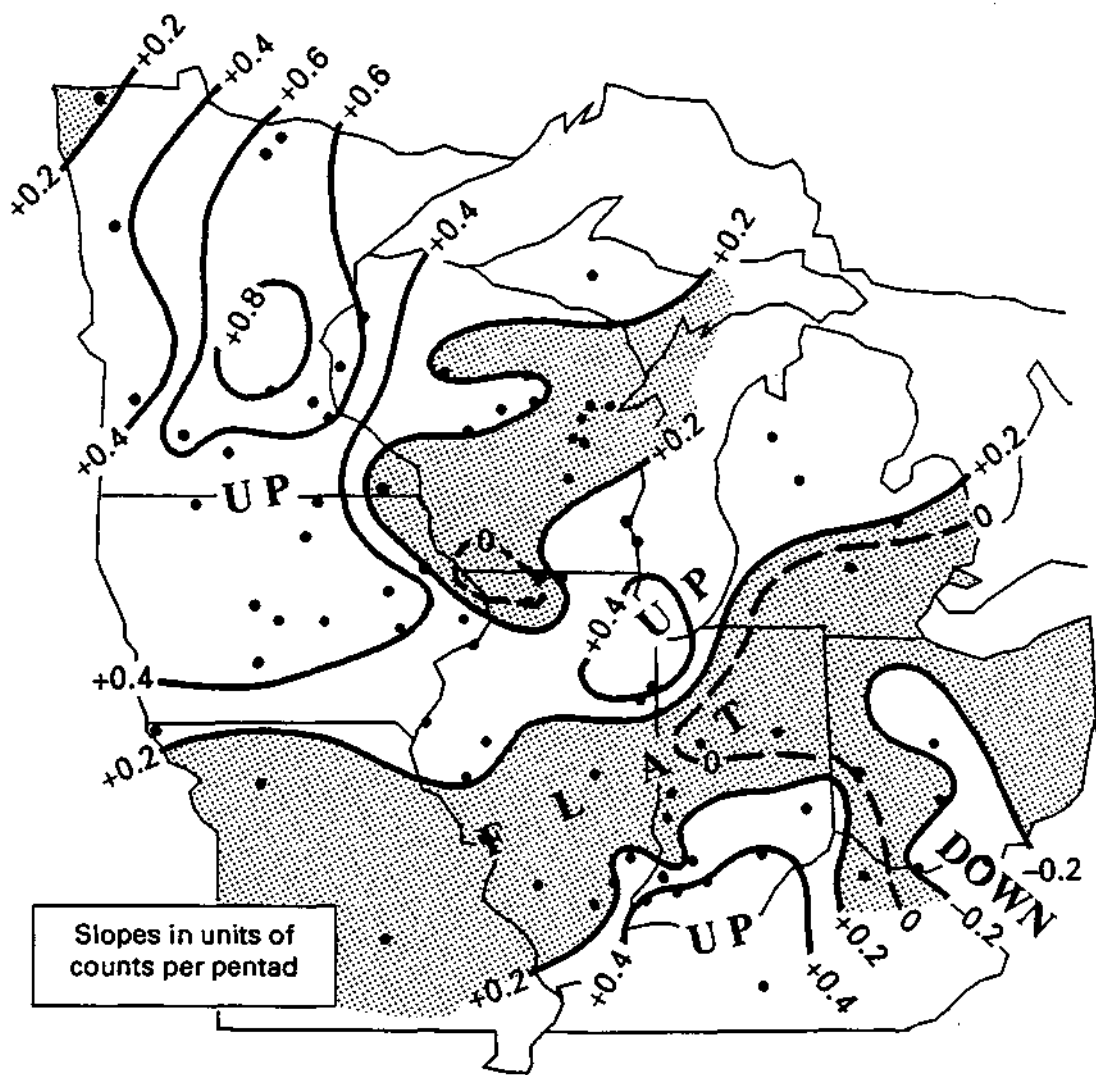


Figure 14b. Contour analysis of the trends in Figure 14a. Slopes $> +0.2$ events per pentad and < -0.2 events per pentad are outlined.

Warm season Flood recurrence = 1 year

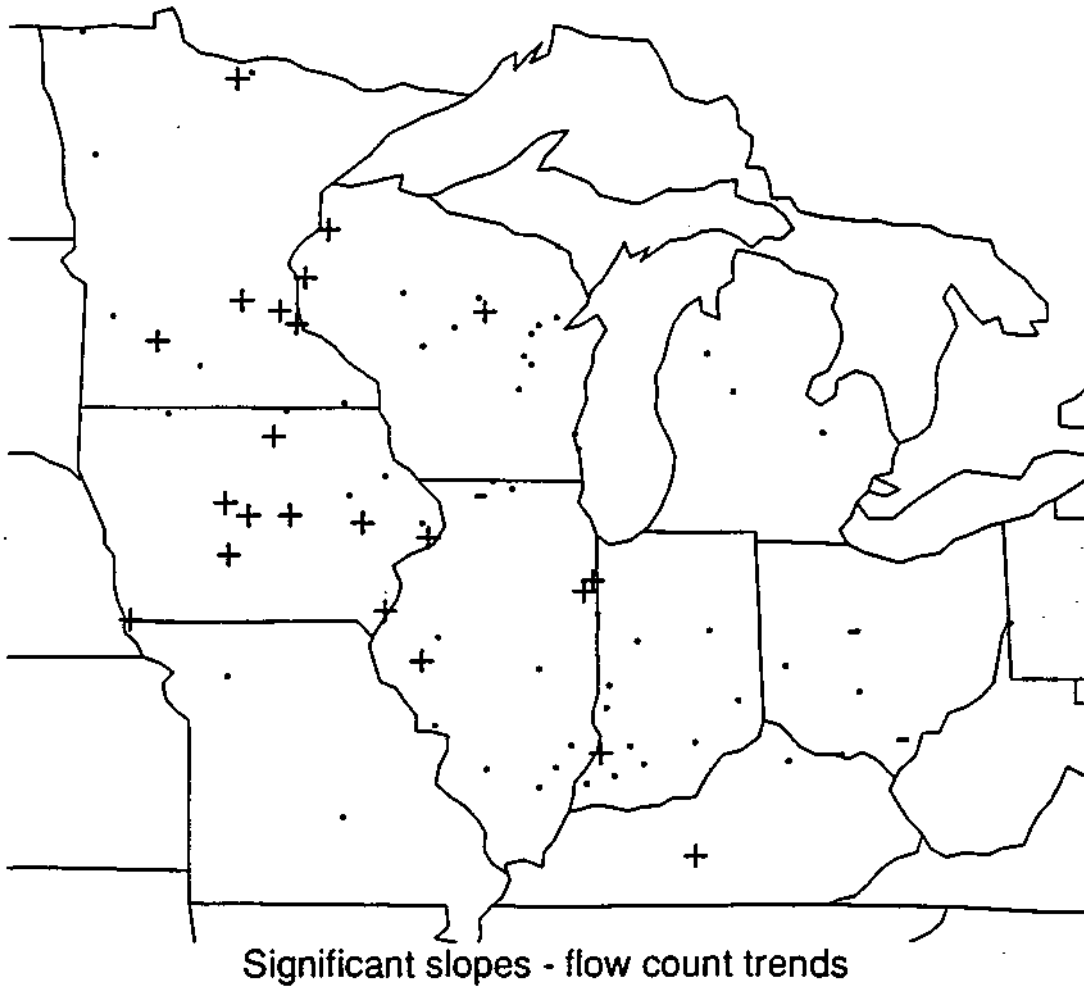


Figure 14c. Statistical significance of the trends of flood event frequencies vs. pentad for the warm season. Pluses and minuses indicate statistically significant upward and downward trends, respectively, at the 10% level. Periods indicate stations where trends were not significant.

Cold season Flood recurrence = 1 year

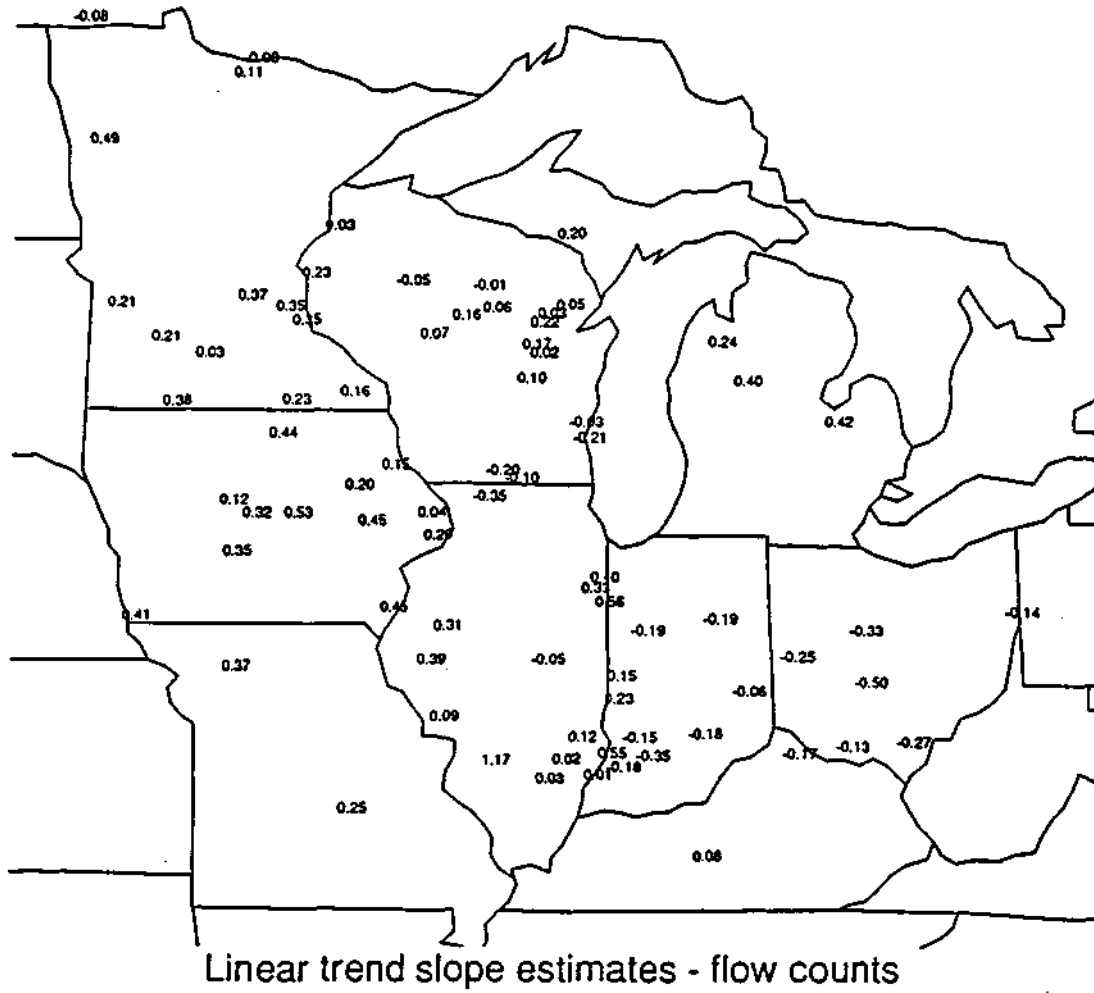


Figure 15a. Results of the regression analysis for trends in the flood event frequencies versus pentad for the cold season. This shows the slopes for the individual flow stations. The units are number of events per pentad.

Cold Season, Flood Frequencies

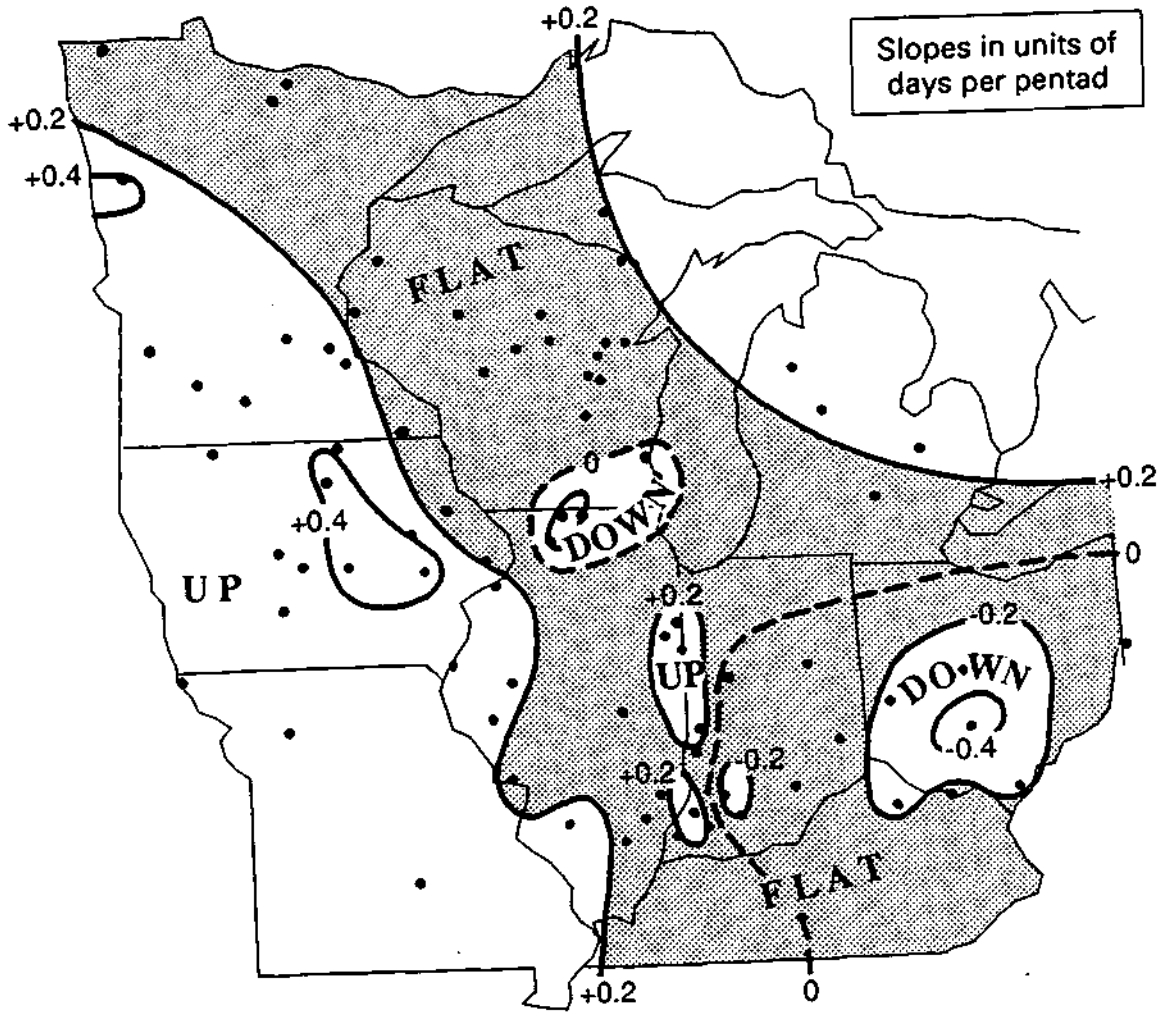


Figure 15b. Contour analysis of the trends in Figure 15a. Slopes $> +0.2$ events per pentad and < -0.2 events per pentad are outlined.

Cold season Flood recurrence = 1 year

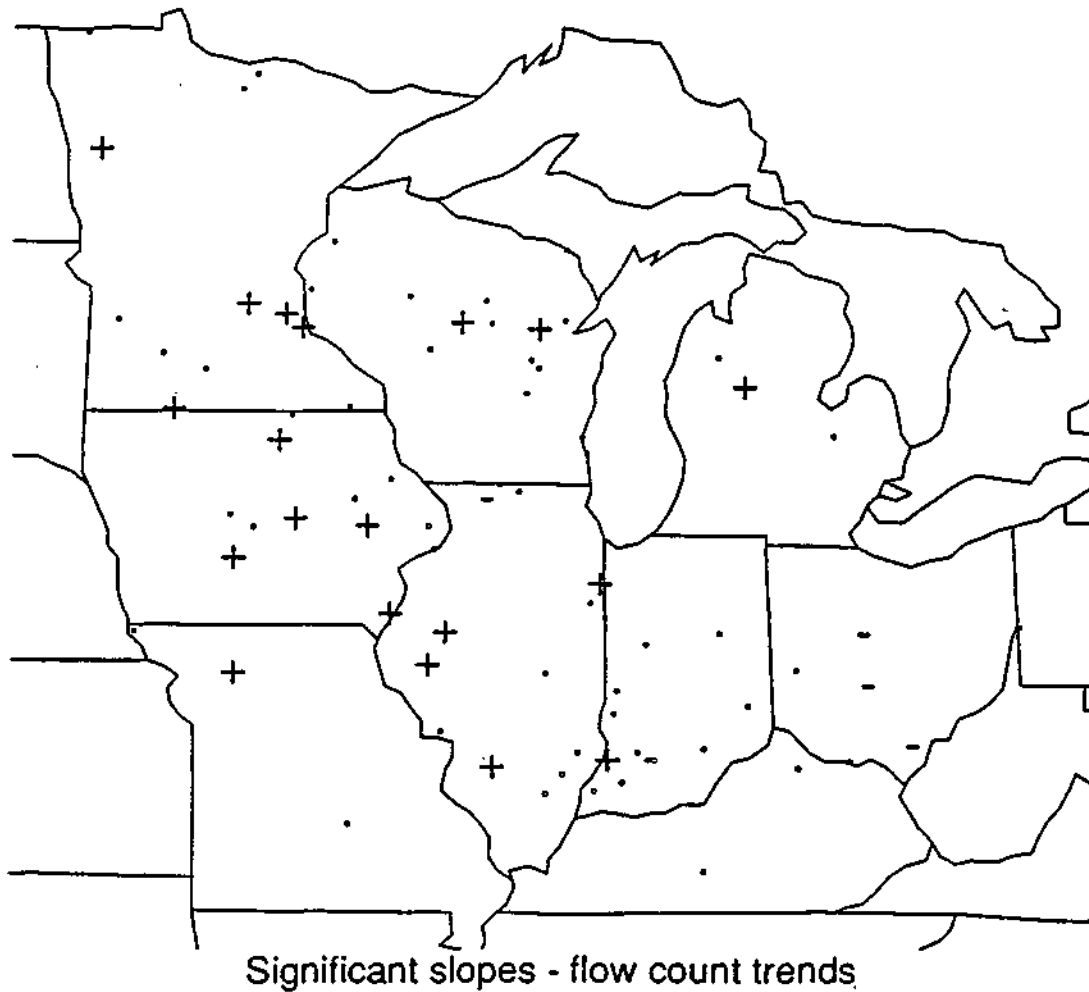


Figure 15c. Statistical significance of the trends of flood event frequencies vs. pentad for the cold season. Pluses and minuses indicate statistically significant upward and downward trends, respectively, at the 10% level. Periods indicate stations where trends were not significant.

Warm season Flood recurrence = 1 year

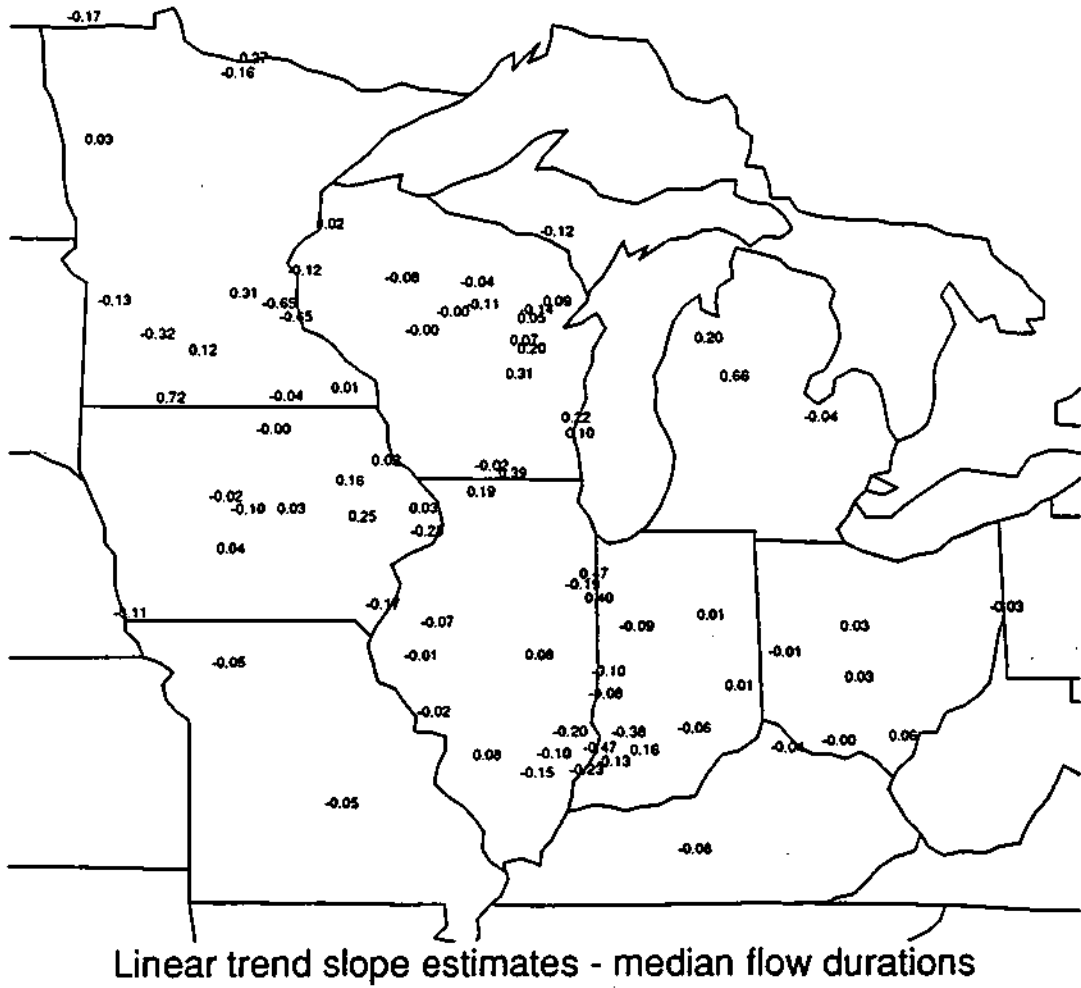


Figure 16a.

Results of the regression analysis for trends in the time series of median flow durations vs. pentad for the warm season. The units are number of days per pentad.

Warm Season, Flood Duration

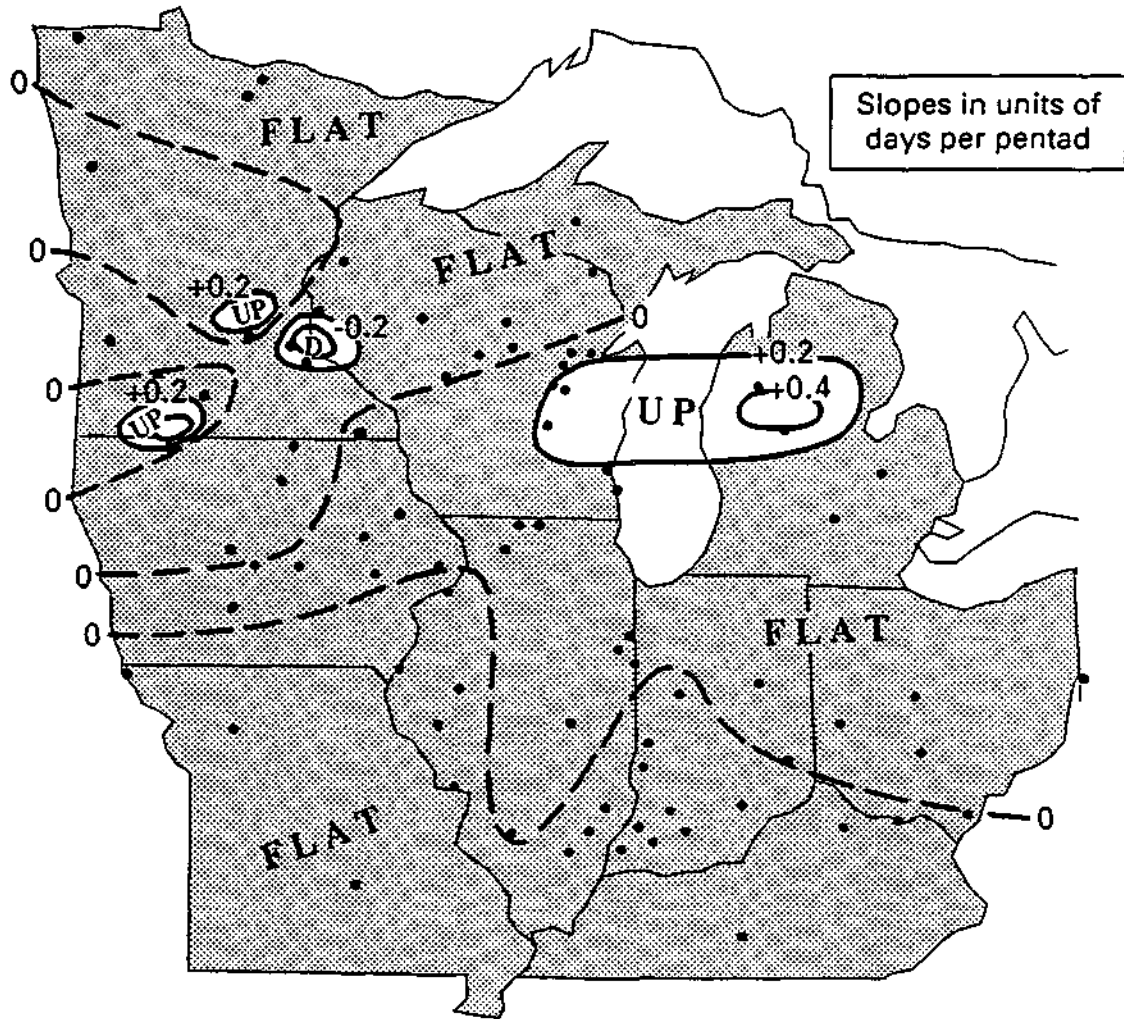


Figure 16b. Contour analysis of the slopes in Figure 16a. Slopes $>+0.2$ days per pentad and >-0.2 days per pentad are outlined.

Warm season Flood recurrence = 1 year

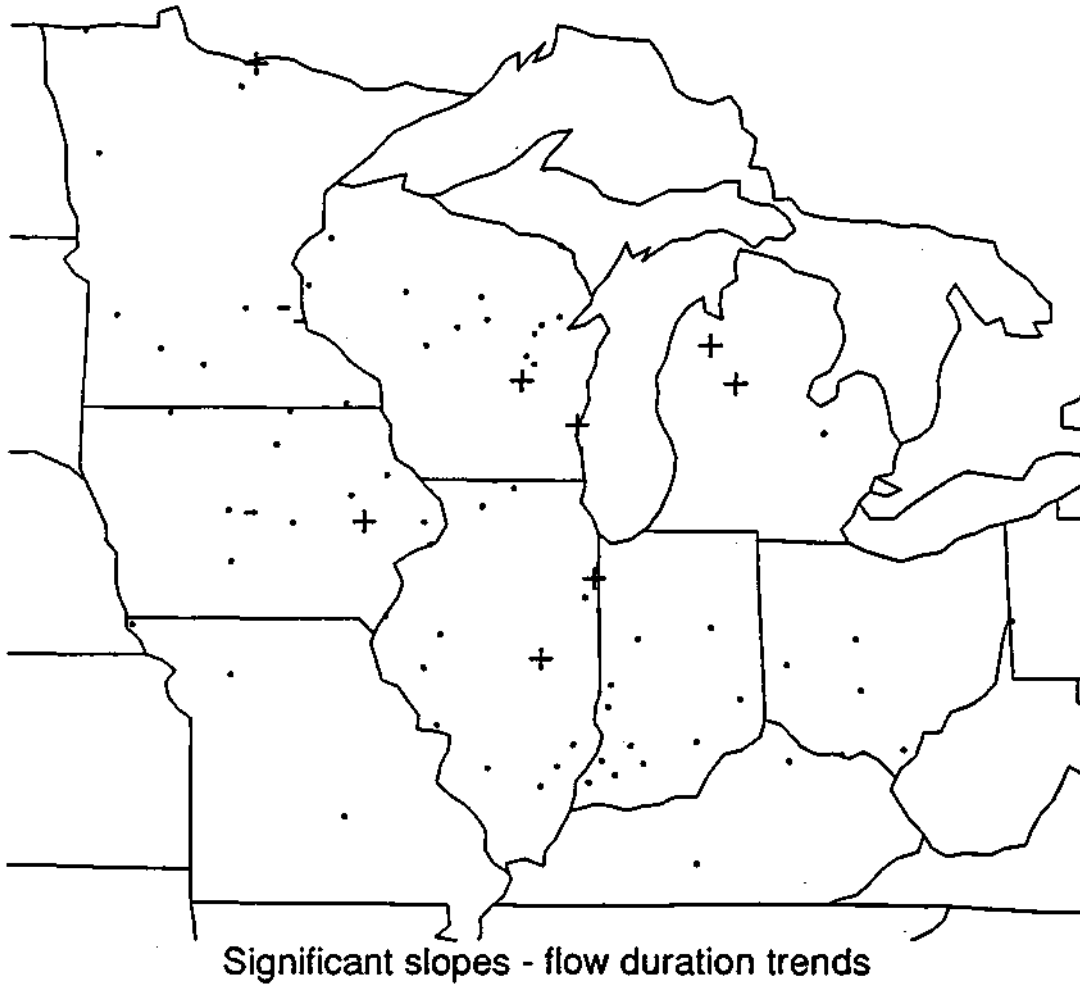


Figure 16c. Statistical significance of the trend analyses of flow duration vs. pentad. Pluses and minuses indicates statistically significant upward and downward trends, respectively, at the 10% level. Periods indicate stations where trends were not significant.

Cold season Flood recurrence = 1 year

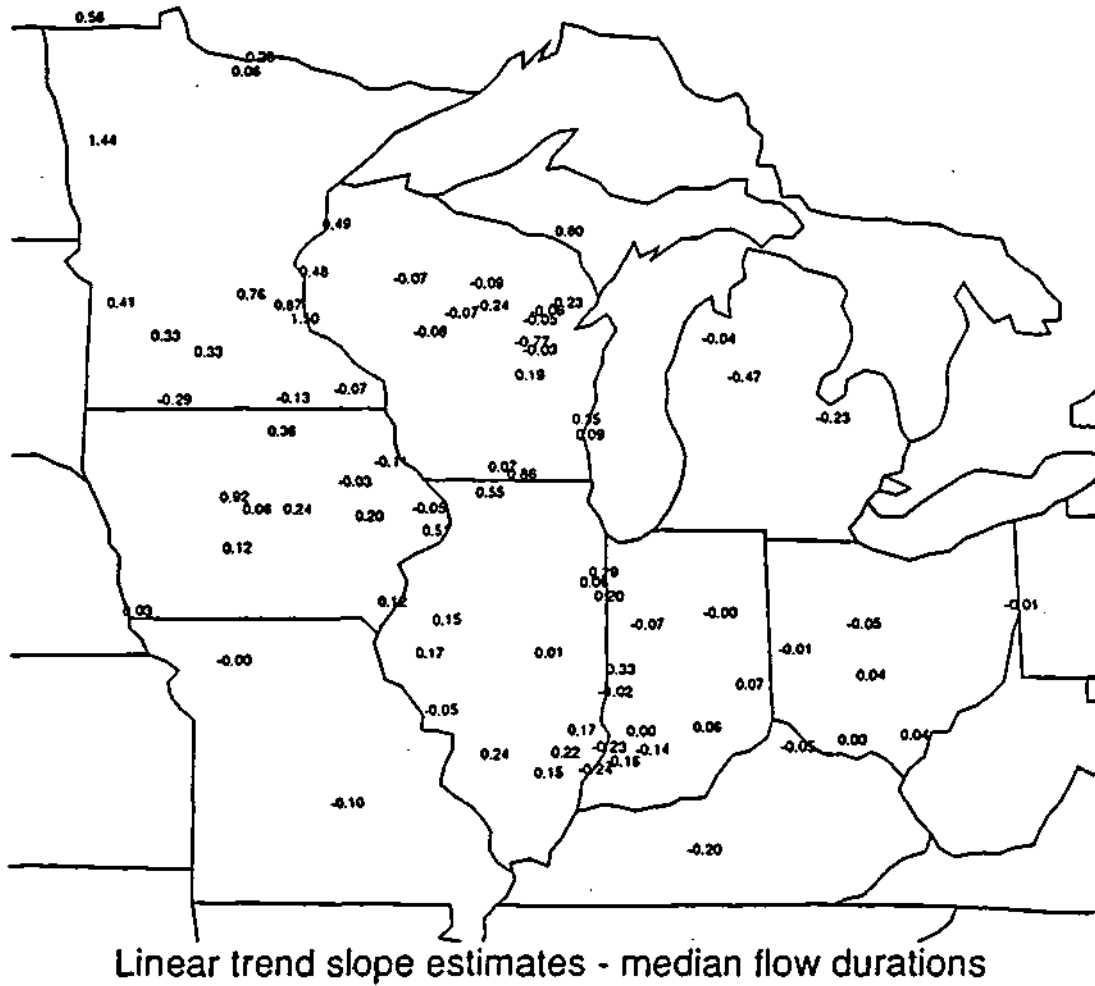


Figure 17a. Results of the regression analysis for trends in the time series of median flow durations vs. pentad for the cold season. The units are number of days per pentad.

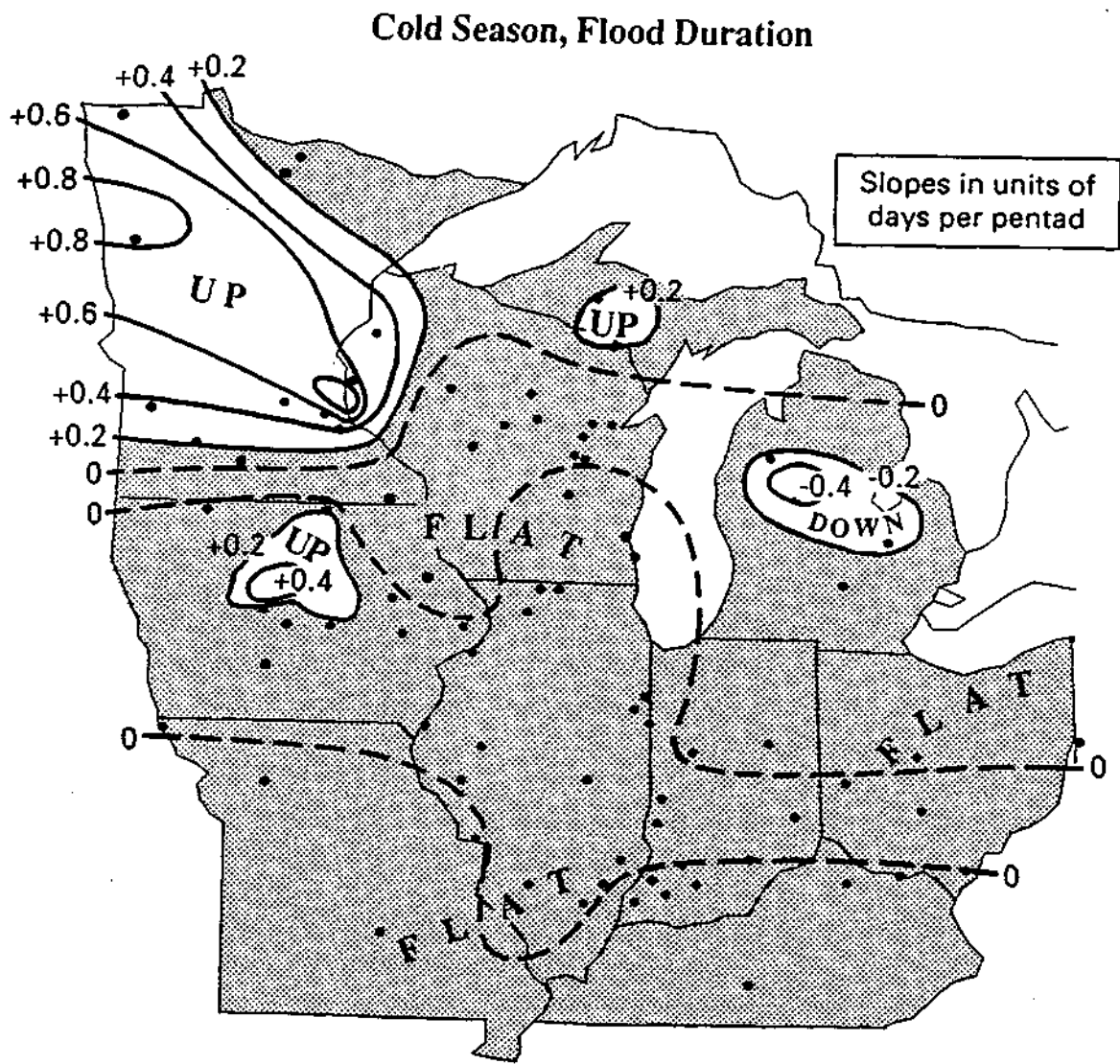


Figure 17b. Contour analysis of the slopes in Figure 17a. Slopes $>+0.2$ days per pentad and >-0.2 days per pentad are outlined.

Cold season Flood recurrence = 1 year

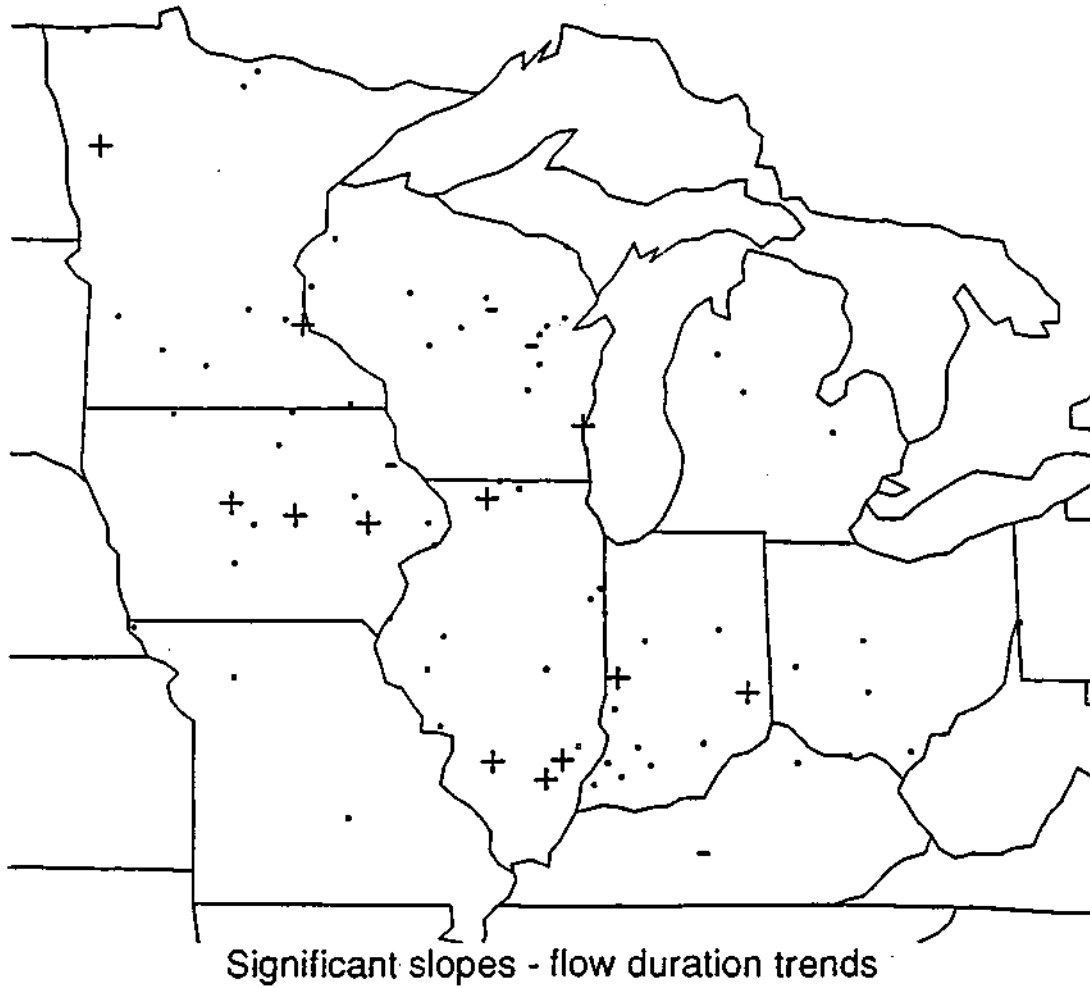


Figure 17c. Statistical significance of the trend analyses of flow duration vs. pentad. Pluses and minuses indicates statistically significant upward and downward trends, respectively, at the 10% level. Periods indicate stations where trends were not significant.

The results of the trend analysis for flood magnitude or intensity are shown in Figures 18 and 19 for the warm and cold seasons, respectively. These include the slope estimates for individual stations (Figures 18a and 19a), nondimensional slope estimates for individual stations (Figures 18b and 19b), a contour analysis of the nondimensional slopes (Figures 18c and 19c), and identification of stations with statistically significant trends at the 10% level (Figures 18d and 19d). The nondimensional slopes are the ratio of the slope in cfs to the peak daily flow of the smallest flood in the partial duration series. There are very few areas which exhibit significant trends in the intensity of warm-season floods. In fact, only 5 of the 79 basins exhibit statistically significant trends, and these are randomly scattered around the region. For the cold season, there is a coherent area of upward trends in flood intensity through central Minnesota. This area coincides with upward trends in both flood frequencies and flood durations. Most basins in the rest of the region do not show significant trends for flood intensity. A total of 12 of the 79 basins show statistically significant trends.

To summarize, the trend analysis indicated spatially coherent areas of significant trends in flood frequency. However, there were few areas with trends in flood durations and intensity. This analysis revealed that for the cold season, flood frequency, intensity, and duration increased simultaneously in much of central Minnesota. Elsewhere, there was less agreement among the flood characteristics. Many basins in the Midwest had an increase in flood frequencies in the warm and cold seasons. By contrast, most basins did not show either upward or downward trends in flood duration and flood intensity.

B. Periods of Maximum Flood Conditions

The specific pentads during which the highest flood value was achieved at each station during the 1921-1985 period were identified. This investigation aimed at determining the degree of regional homogeneity in the incidence of maximum flood activity, seen as an indicator of climatic effects or nonclimatic factors affecting flood data. Analysis of peak period anomalies also might reveal questionable data.

The peak pentad values for flood frequencies in the Midwest were plotted and analyzed. The pentad analysis during the 65-year period was broken down into three periods defined as: 1) early period, 1921-1935; 2) middle period, 1936-1960; and 3) late period, 1961-1985. The resulting pattern for the warm season (figure 20) reveals

Warm season Flood recurrence = 1 year

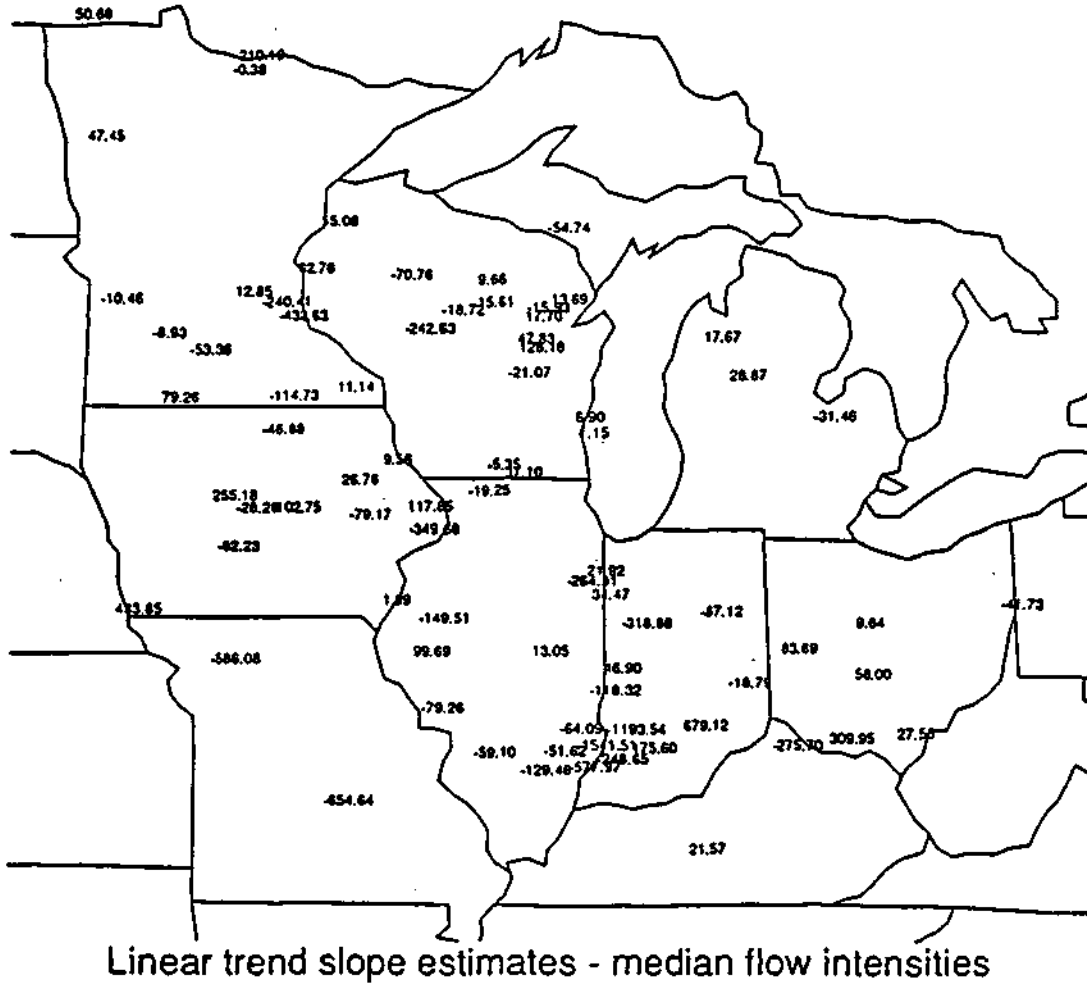


Figure 18a. Results of the regression analysis for trends in the time series of median flow intensities vs. pentad for the warm season. The units are cubic feet per second (cfs) per pentad.

Warm season Flood recurrence = 1 year

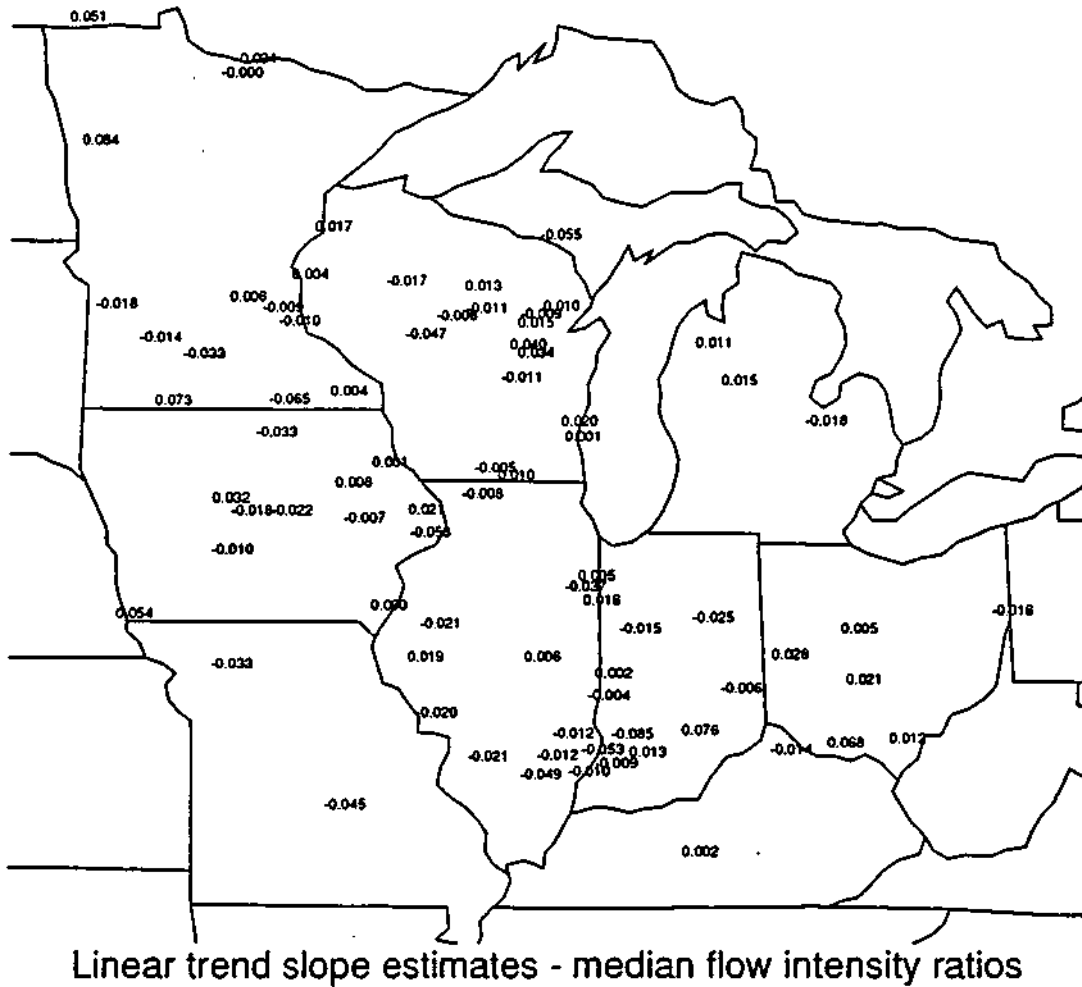


Figure 18b. Same as in Figure 18a except that the median flow intensities have been expressed as a ratio to the threshold for a one-year recurrence event. The resulting values are nondimensional.

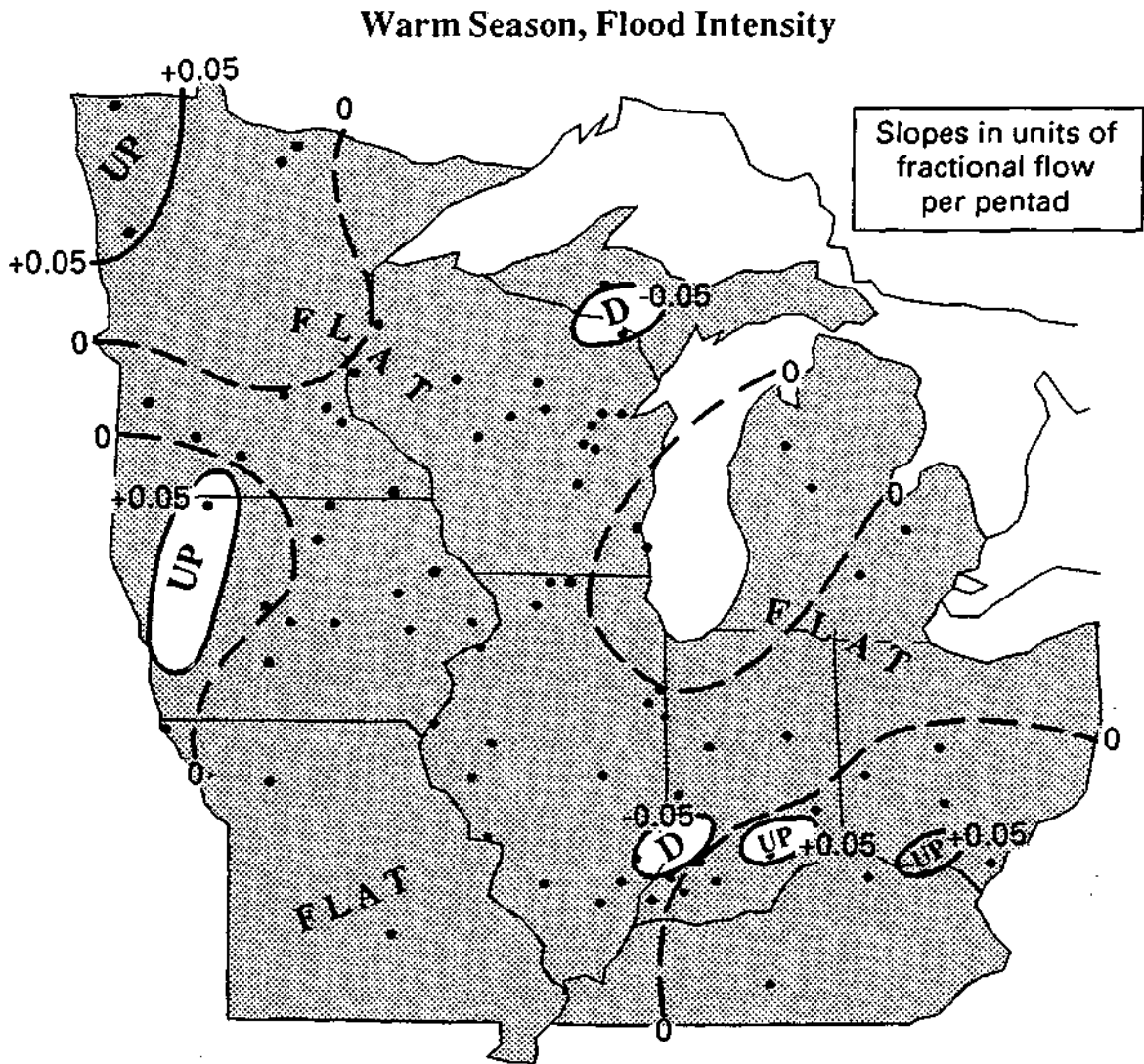


Figure 18c. Contour analysis of the slopes in Figure 18b. Slopes +0.05 fractional flow volume per pentad and -0.05 fractional flow volume per pentad are outlined.

Warm season Flood recurrence = 1 year

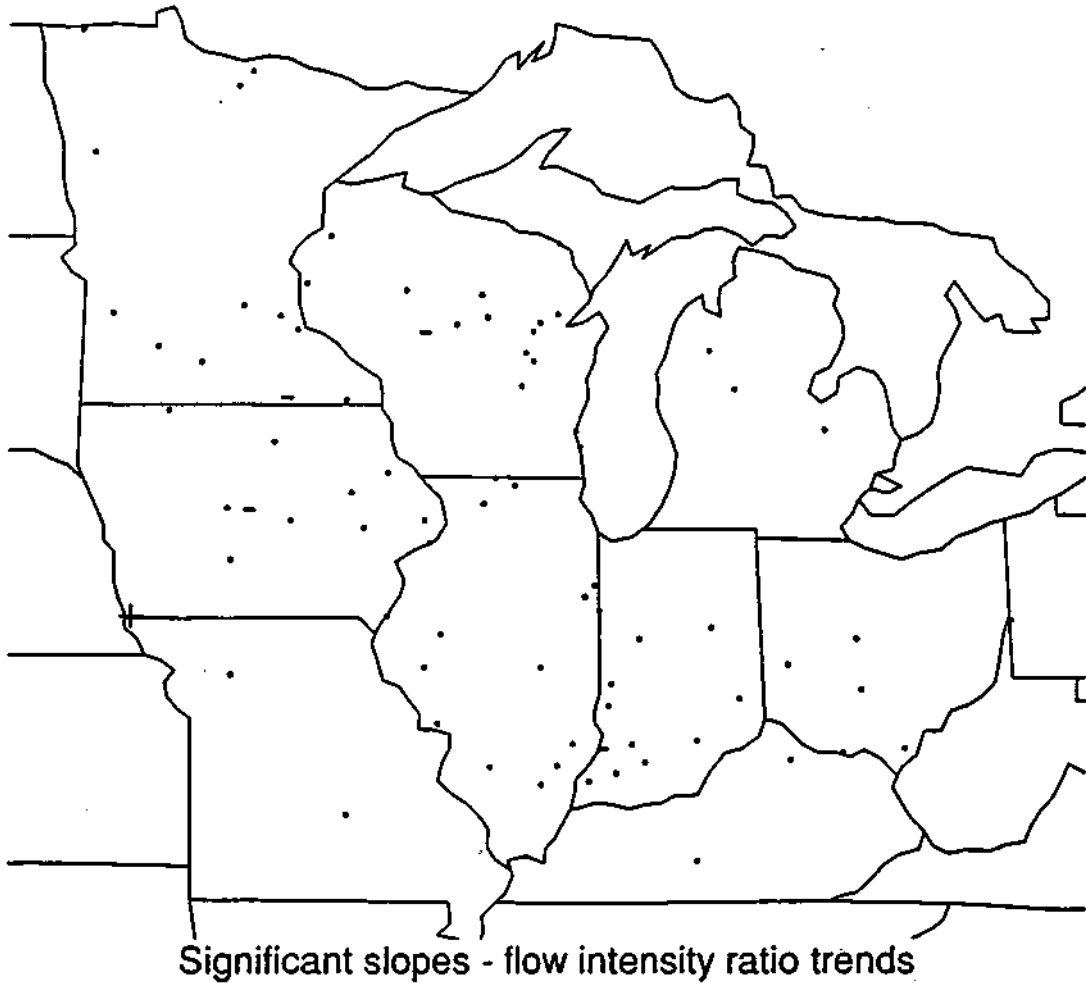


Figure 18d. Statistical significance of the trend analyses of flow intensities vs. pentad. Pluses and minuses indicates statistically significant upward and downward trends, respectively, at the 10% level. Periods indicate stations where trends were not significant.

Cold season Flood recurrence = 1 year

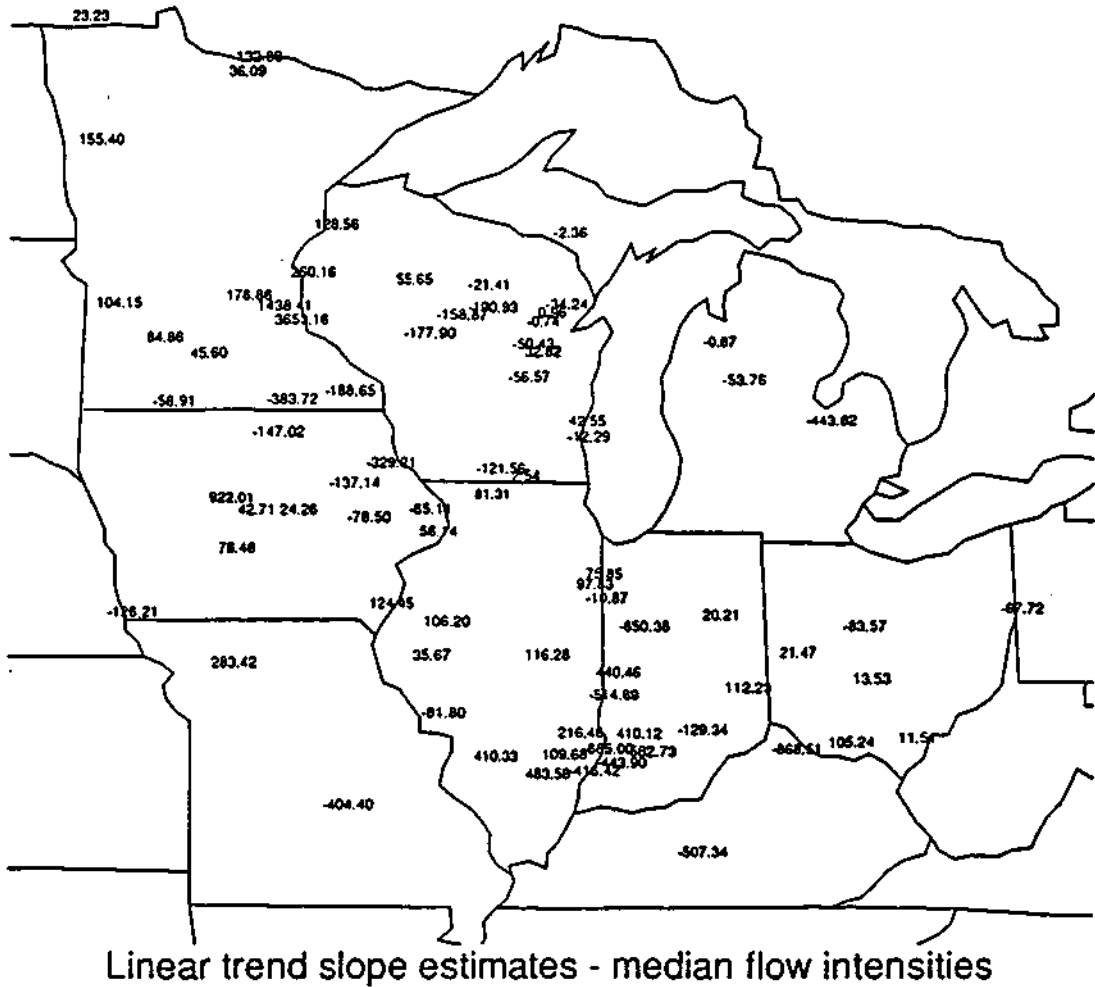
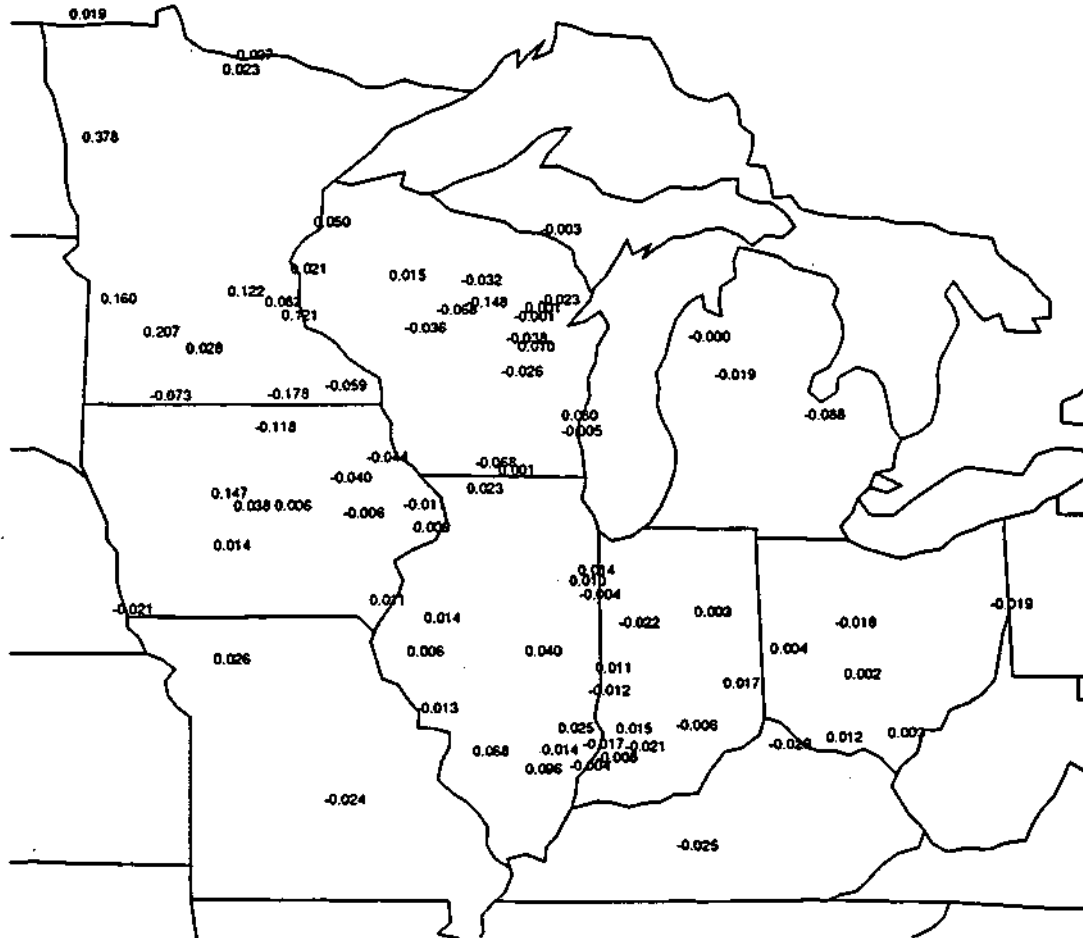


Figure 19a. Results of the regression analysis for trends in the median flow intensities vs. pentad for the cold season. The units are cubic feet per second (cfs) per pentad.

Cold season Flood recurrence = 1 year



Linear trend slope estimates - median flow intensity ratios

Figure 19b. Same as Figure 19a except that the flow intensities have been expressed as a ratio to the intensity threshold for a one-year recurrence interval flood. The resulting values are nondimensional.

Cold Season, Flood Intensity

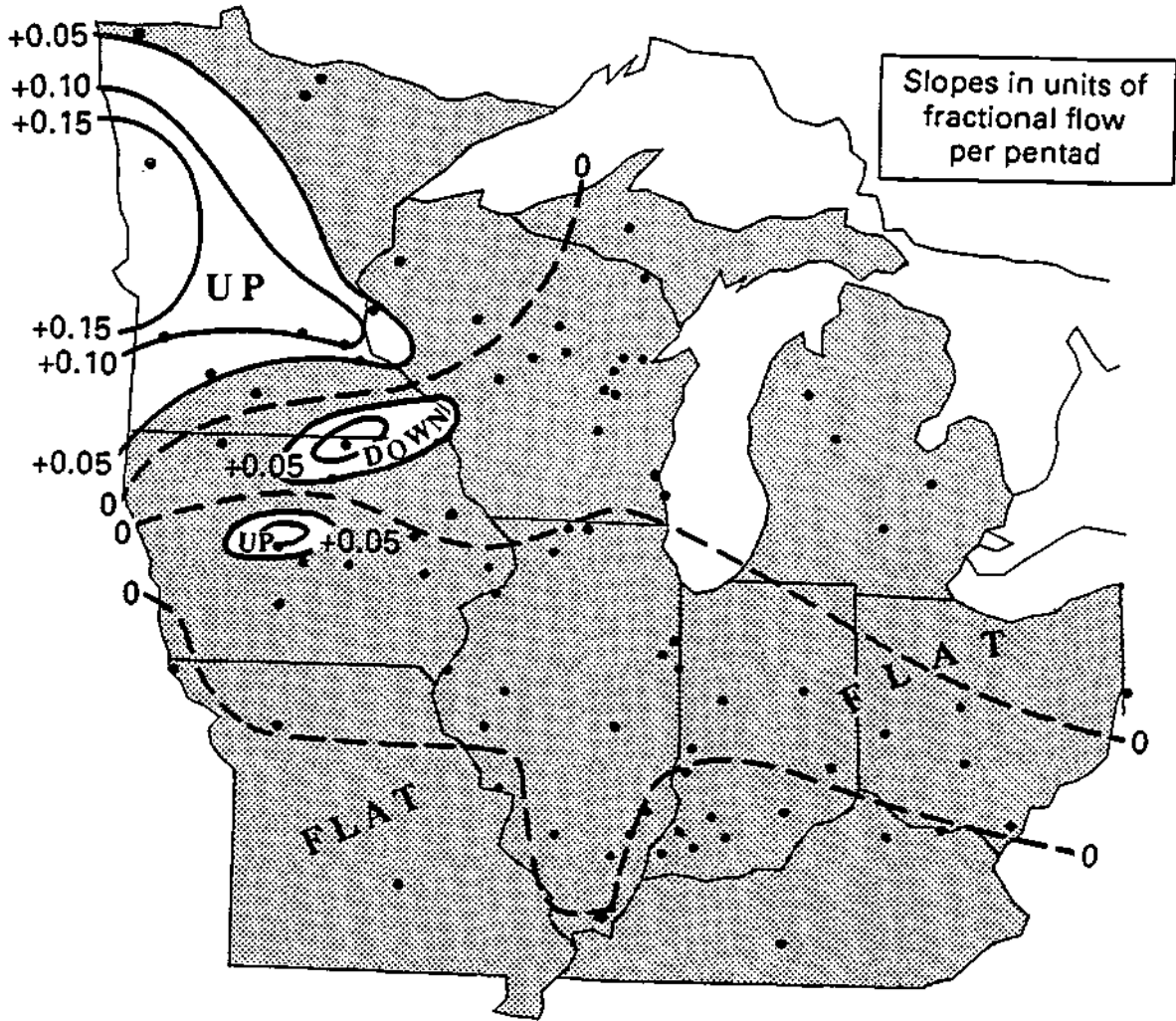


Figure 19c. Contour analysis of the slopes in Figure 19b for the cold season. Slopes +0.05 fractional flow volume per pentad and -0.05 fractional flow volume per pentad are outlined.

Cold season Flood recurrence = 1 year

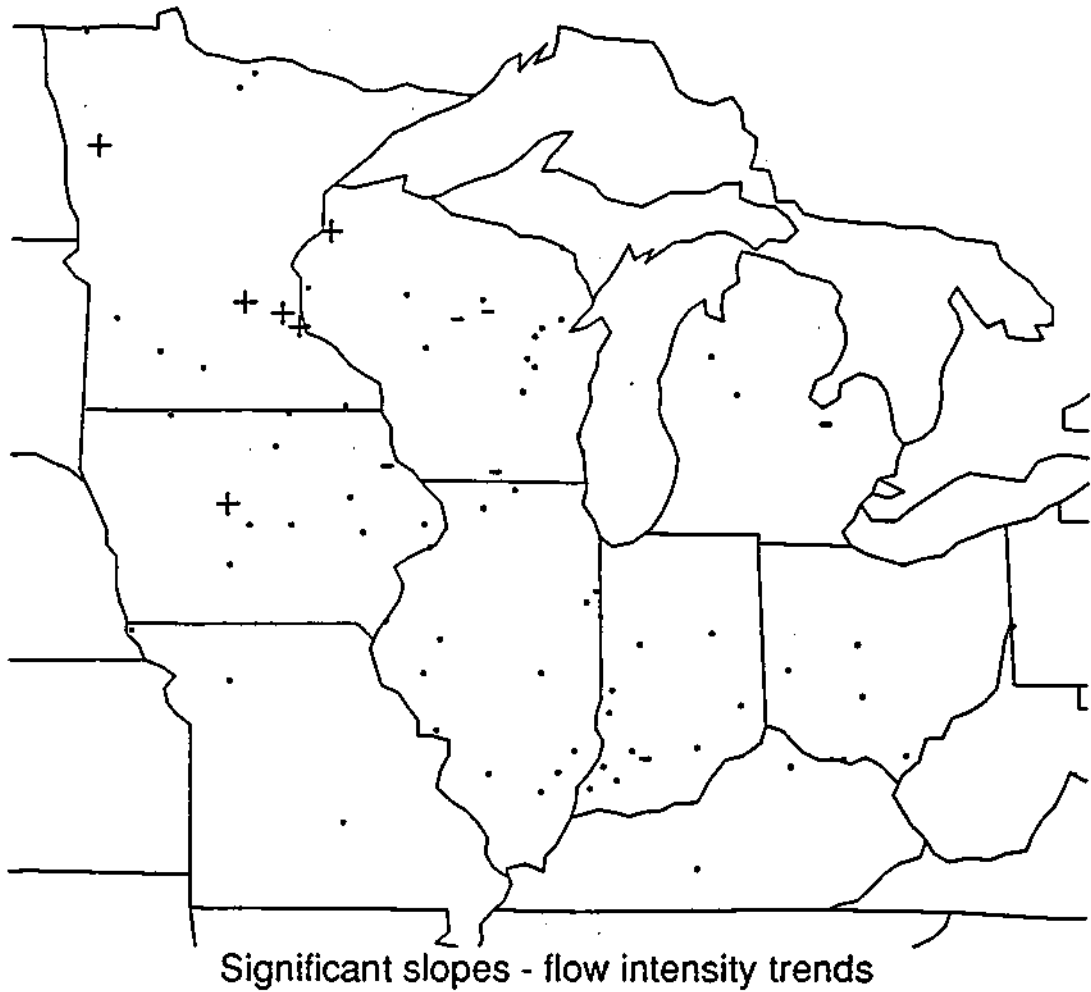


Figure 19d. Statistical significance of the trend analyses of flow intensities vs. pentad. Pluses and minuses indicates statistically significant upward and downward trends, respectively, at the 10% level. Periods indicate stations where trends were not significant.

Warm Season, Flood Frequency Peaks

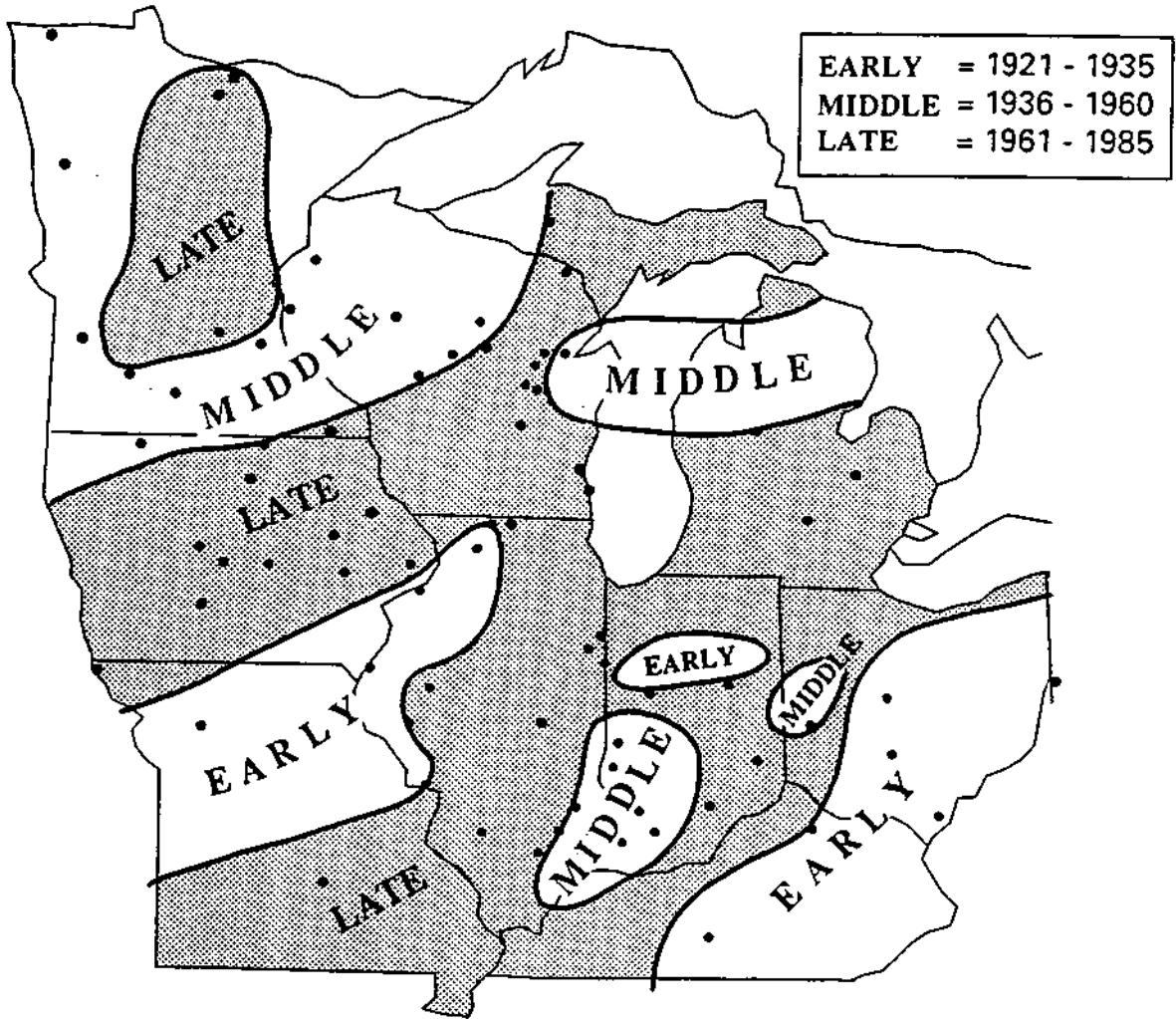


Figure 20a. Spatial analysis of the time periods during which occurred the peak pentad for flood incidence for the warm season. Darkened circles give the locations of stations upon which this analysis was based.

Cold Season, Flood Frequency Peaks

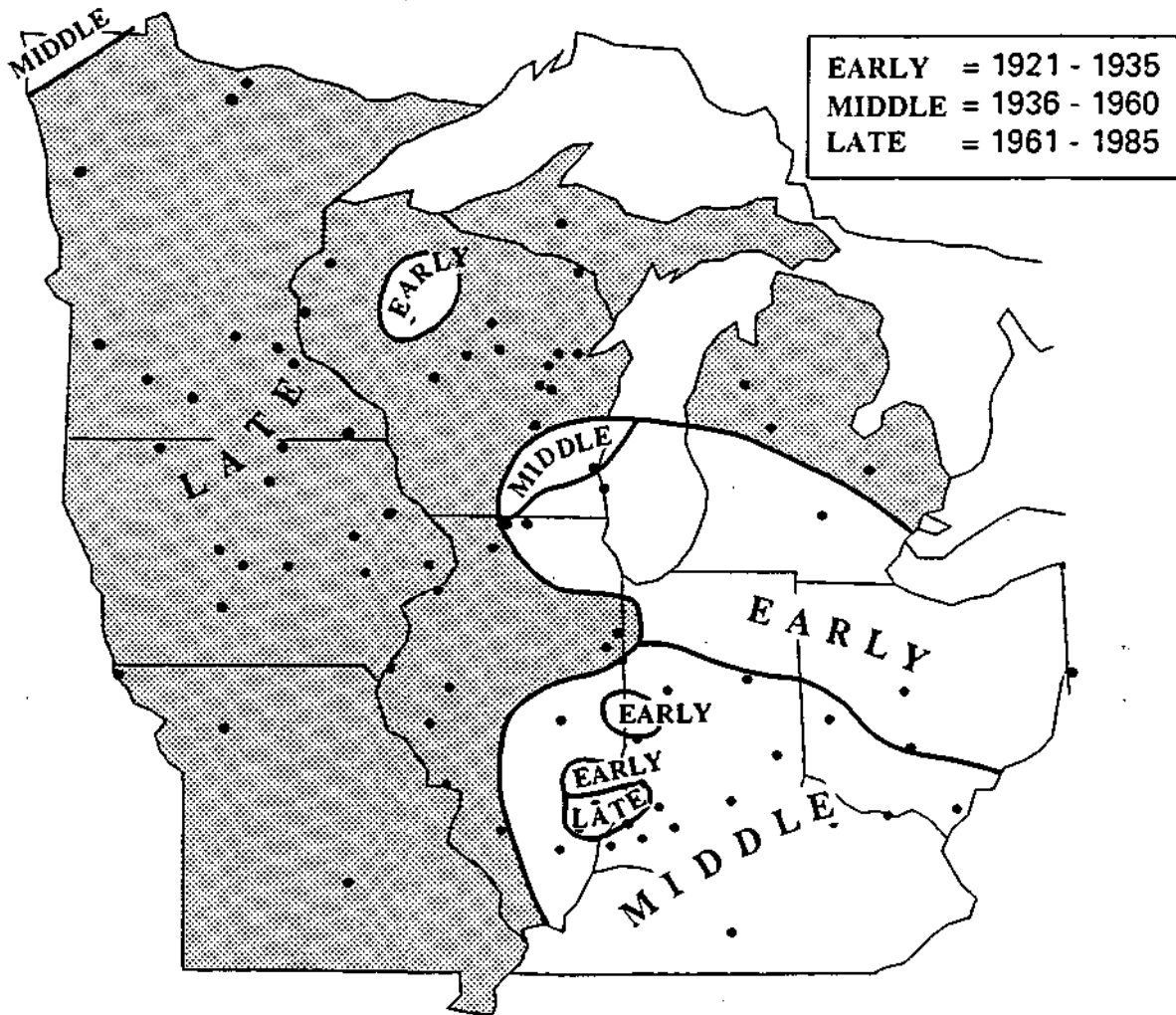


Figure 20b. Spatial analysis of the time periods during which occurred the peak pentad for flood incidence for the cold season. Darkened circles give the locations of stations upon which this analysis was based.

coherent regions of occurrence of the peak pentads. Two large regions, one in the southwest (Missouri and northern Illinois) and one in the east (Ohio and northern Indiana) had their peak pentads during the early 15 years of the 65-year study period. There were 14 basins rated as having an early peak and they occurred in the 1921-1925 or 1926-1930 pentads. The areas defined by basins that achieved their peak pentad in either flood incidence during the middle 25 years, 1936-1960, comprised portions of lower Michigan, eastern Minnesota, western Wisconsin, and southern Indiana. Of the 79 basins, 25 achieved peaks during this middle period. Many of these peaks occurred during the pentad of 1941-1945, particularly in Minnesota and Wisconsin. The primary time of activity in flood frequencies was the late period, 1961-1985. Of the 79 basins, 40 achieved their peak flood incidence in this latest period. The area of late-period peaks embraces southern Illinois, southern Wisconsin, Iowa, and large portions of Minnesota. The primary pentad for peak activity was 1981-1985 with 25 basins out of 79 (32%) achieving their peak in this one pentad. The results on peak pentads do appear to be regionally coherent.

There was somewhat less regional coherence found in the pentads of peak activity based on the flood durations. Approximately half of the basins experienced their peak pentad in the middle period. These were concentrated in an arc-shaped area from eastern Iowa through western and central Wisconsin, into central Minnesota. Approximately one-quarter of the basins experienced their peak pentad in the early and late periods. The most frequently occurring peak pentads were 1931-1936, and 1956-1960 with 17% and 14% of the basins, respectively.

The spatial analysis of pentads of greatest flood intensity revealed a sizable coherent area with peak values occurring in the middle period. This area encompasses most of Minnesota, Wisconsin, and Iowa. In total, 57% of the basins experienced their highest flood intensities in the middle period, 19% in the early period, and 23% in the late period.

For the cold season, the peak pentads for flood frequencies were concentrated in the late period. Fully 50% of the basins recorded their peak frequencies during 1961-1985, of which 32% were in the 1981-1985 pentad. These basins were generally located in the western half of the region including most basins in Minnesota, Iowa, Wisconsin, Michigan, Missouri, and Illinois.

There was somewhat less regional coherence in the peak pentads for flood duration. However, as with flood frequencies, approximately half of the basins

experienced their peak flood intensities in the late period, of which 23% were in the 1976-1980 pentad. These basins were generally located in the western portions of the region. Approximately 10% and 38% of the basins experienced their peak flood durations in the early and middle periods, respectively.

For flood intensity, approximately half of the basins experienced their peaks in the middle period. Forty percent of the basins experienced their peak flood intensities in the late period, with only 10% experiencing peak intensities in the early period. Generally, most basins in the northwestern quadrant experienced their peak intensities in the late period, while basins in the central portion experienced peak intensities during the middle period.

C. Investigation of Relatively Small-Scale Areal Variations in Temporal Trends of Floods

One major objective of this study was to investigate the temporal characteristics of floods across the Midwest. Three flood characteristics (frequency, duration, and intensity) were under investigation. Every effort had been made to secure streamflow records of flood events that exhibited little or no fluctuations over time caused by basin or channel changes. However, in the basin records selected by our criteria and the USGS staff, the potential remained that the data included erroneous temporal characteristics. Thus, all flood analyses performed attempted to assess possible errors.

It was considered important to interpret the temporal behavior of the floods in the 79 basins using regional analyses. For example, a group of adjacent streamgauge basins showing quite different characteristics in their temporal behavior would suggest either questionable flood data or highly varying storm influences on their performance.

We hypothesized that general temporal trends in flooding over the 1921-1985 period could be influenced by changing climate and principally by alterations in heavy rainfall events. If true, the temporal relationship of the incidence of flooding and heavy rainfall should show general spatial agreement. This is particularly true for the incidence of floods, that is, a 5-year period with several heavy rain events would have several floods. Furthermore, during a 5-year period with several flood-producing heavy rain events in one small basin, the same events should extend over basins in

adjacent areas. It seems less likely that the flood durations and intensities should exhibit similar regional-scale homogeneity. Warm-season convective rainstorms capable of producing severe floods may produce heavy rains over large mesoscale areas (3000 to 30,000 km²), but the heaviest and/or longer lasting rains within the storm zone vary considerably over space. That is, two basins 100 km apart may get rains from a given storm sufficient to cause a flood in both, but it is possible that the duration of the two floods or their magnitudes (peaks) would differ considerably.

A specific objective of the regional analysis of trends in the three flood characteristics of the 79 basins addressed the question of regional representativeness in sampling and the potential for small-scale variations. Inspection of Figure 1 reveals that the spatial density/array of the 79 basins was less than uniform across the nine-state region. The development of patterns based on the magnitudes of temporal trends across the region for the 79 basins with an uneven areal distribution raises questions about the representativeness of regions defined by trend characteristics of only a few gage stations. For example, there were only two streamgage stations in the entire state of Missouri, and they are located more than 200 miles apart (Figure 1). If their trends of flood frequencies are alike, how safe is it to infer that basins in the area between them had similar trends?

Regional analysis of trends in flood characteristics also has to consider other factors influencing floods such as different sizes of basins (large vs. small because they represent different capabilities of sampling intense short-duration floods), and "interconnection" when both gages are in the same drainage system. These basins may show the same trends and are not considered independent samples in an areal analysis.

Inspection of the placement of the 79 basins with quality flood data (Figure 1), indicates one region with a relatively dense number of long-term streamgage records. This was centered in Wisconsin, which had 17 stations with quality flood records. The flood characteristics of these 17 stations, plus 3 in adjacent states, were analyzed for trends of frequency, duration, and intensity of floods.

Figure 21 presents the location of the 20 streamgages analyzed in this spatial investigation of trends. Shown for each station is 1) the basin area, 2) the beginning of the record as expressed as the first year in a complete 5-year period (1921-1925; 1926-1930; etc.), 3) an indication of any sizable amounts of missing data during the entire period of quality record, and 4) those stations that were connected by

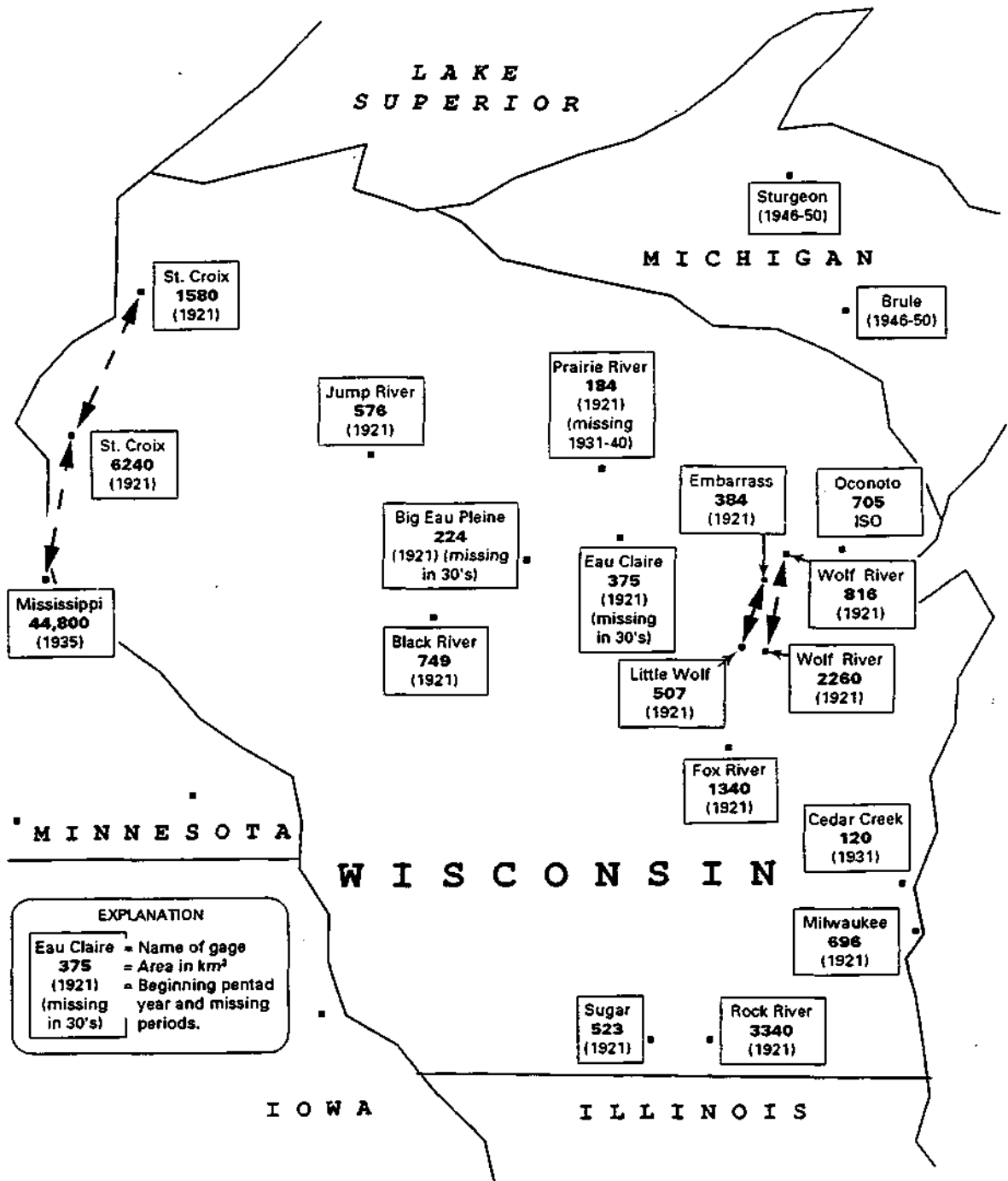


Figure 21. Streamflow stations used in the regional flood analysis.

measuring flow on rivers in the same basin. Most of the basins, except two along the west side of the state on the St. Croix River, which drains into the Mississippi, were small basins with under 1,000 km² areas. Other exceptions were the Rock River and the Fox River in southern Wisconsin. Inspection of Figure 21 further reveals that most stations had complete flow records beginning in the 1921-1925 pentad. Only two stations had partially missing records during the 1930s. Two pairs of streamgage stations in the dense array of basins in east-central Wisconsin were interconnected. Two of these were on the Wolf River, and two on the Little Wolf River, and these are marked by arrows on Figure 21. In general, the data showed good similarities in quality and length of record available for this spatial analysis of temporal trends in flooding.

The linear trend slopes, in number of floods per five years, reveal that most of Wisconsin had upward trends (Figure 22) in floods. The trends greater than +0.4 were statistically significant at the 5% level. Although increased frequencies of floods with time existed over most of Wisconsin, large areas had essentially flat trends ranging from 0 (no trend) to +0.2 floods per pentad.

Of considerable importance is the fact that there was considerable spatial variability in the trends experienced over the 65-year period in east-central Wisconsin. Basins in one area had downward trends of -0.49 floods per pentad, whereas basins 80 km away had upward trends of +0.4 per pentad. These differences are in basins that are not influenced by length of record, quality of record, or by interconnection on the same stream. In this area, two pairs of basins had widely differing values. For example, the Wolf River at New London had an downward trend of -0.18, whereas the Wolf River at Shawano (located 50 km upstream), had an upward trend of +0.16 floods per decade. The spatial differences noted in this area reveal the potential for sharp regional differences in long-term trends in the incidence of floods. This affects the interpretation of the nine-state patterns shown in Figure 14 and 15.

Figure 23 presents the patterns based on the slopes of the linear trends fit to the median pentad flood durations. The values shown are in units of days (duration) per pentad. For example, a value of +0.2, such as found in southern Wisconsin, indicates that an increase of 0.2 days occurred every five years over the 65-year period, indicating floods in 1981-1985 were 2.4 days longer lasting than those in 1921-1925. The pattern is strikingly different from that based on the incidence of floods (Figure 22). Much of northern and western Wisconsin had little or no trend in flood

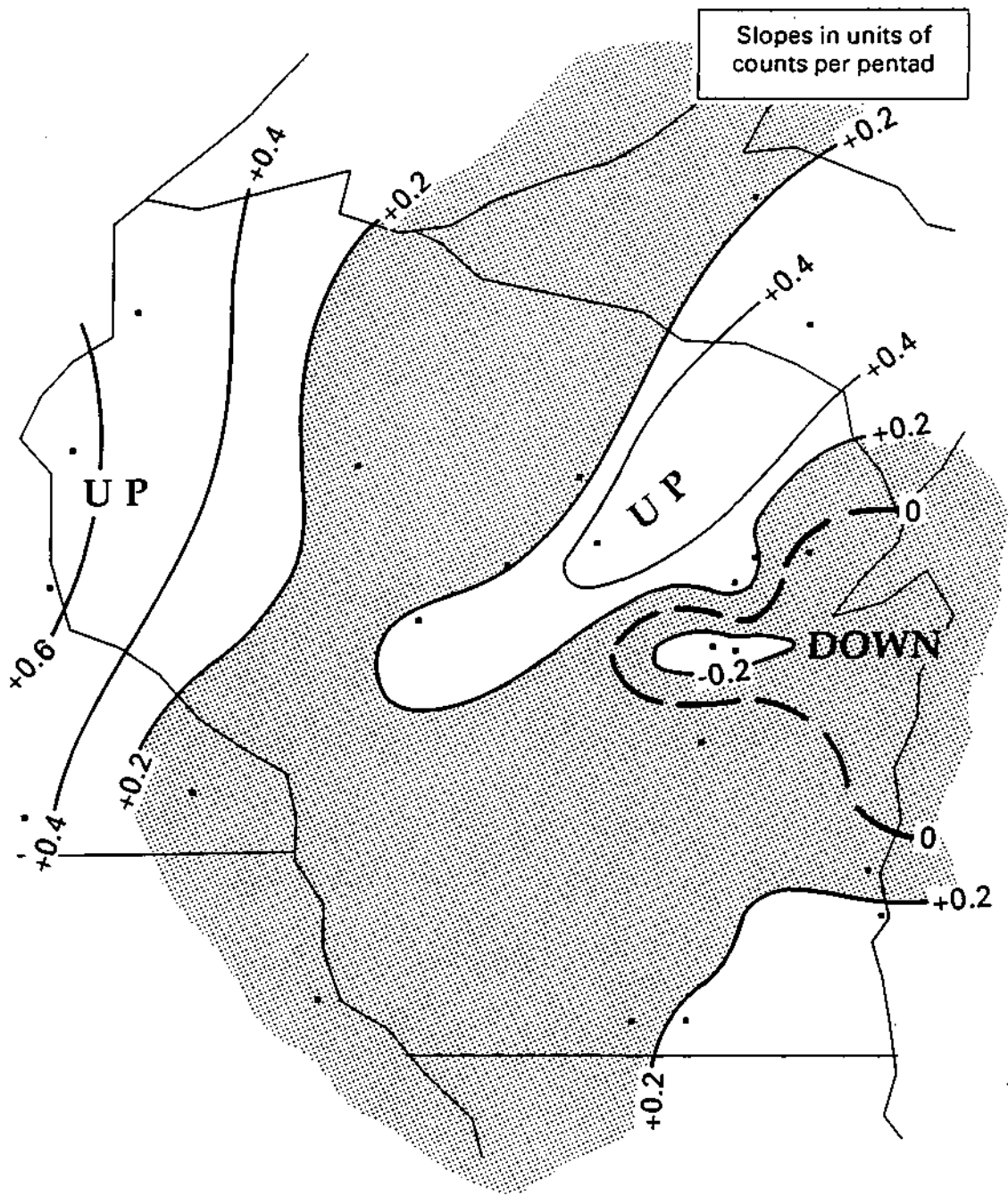


Figure 22. Spatial patterns of the slopes from a regression analysis of number of floods versus pentad for the warm season. Darkened circles give locations of stations upon which this analysis was based.

Warm Season, Flood Duration

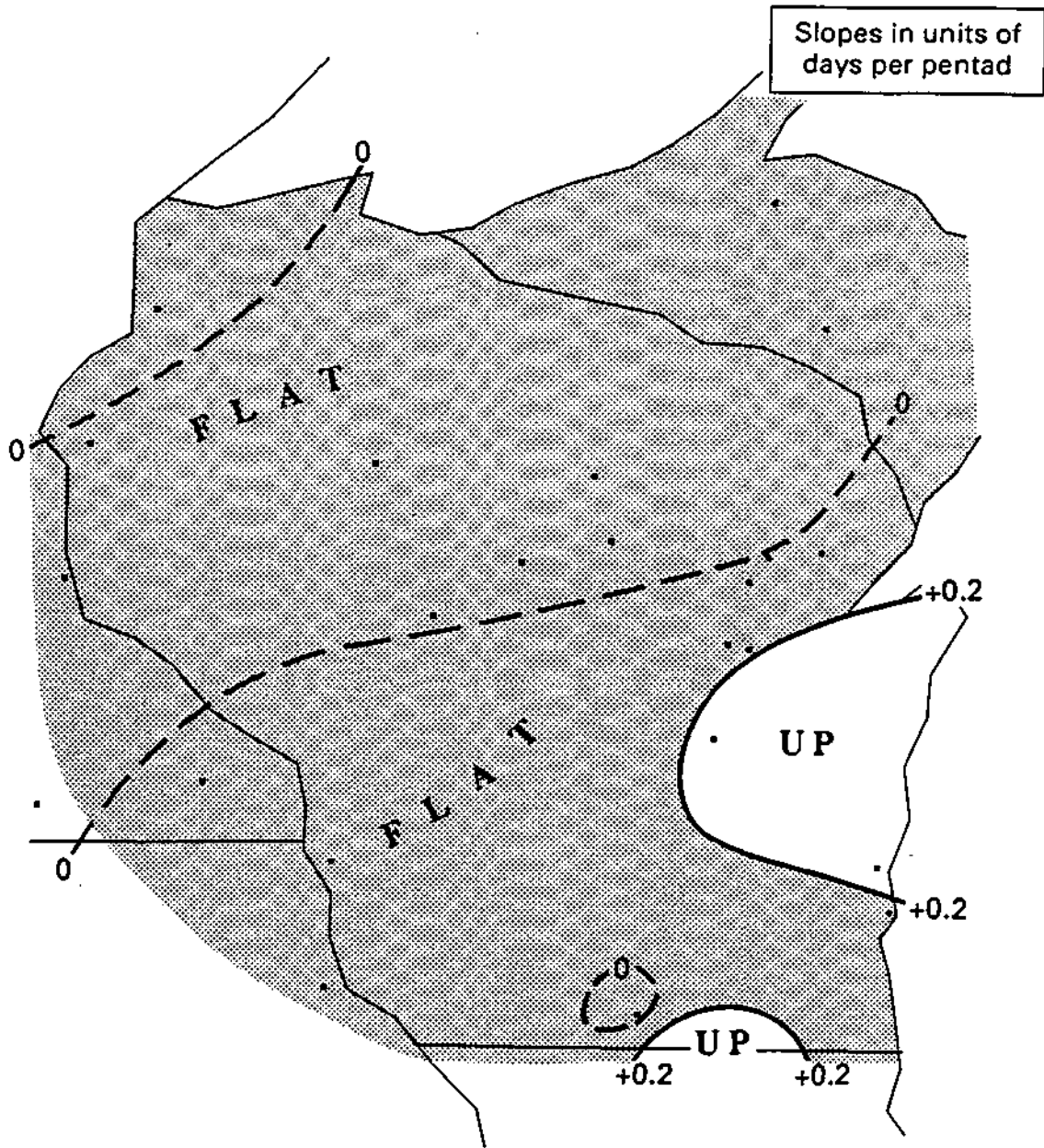


Figure 23. Spatial patterns of the slopes from a regression analysis of flood duration versus pentad for the warm season. Darkened circles give location of stations upon which this analysis was based.

durations. Only two stations, both located in eastern Wisconsin, had significant upward trends at the 10% probability levels.

Figure 24 presents the pattern based on trend slopes for flood intensity. The values are expressed in fractional flow volume per pentad. This pattern, when compared with those for flood frequency (Figure 22) and flood durations (Figure 23), shows very small trends. In general, the eastern and northwestern portions exhibit slight upward trends while the central and western portions showed slight downward trends. Only two stations, one in central Wisconsin and the other in southeast Minnesota, showed significant (downward) trends.

Conclusions

The results for the study of flood incidence trends in the Wisconsin area indicated that of the 22 basins, 4 stations showed a significant upward trend and none showed a significant downward trend.

The duration and intensity trends for most of the 22 basins in the study area showed little upward or downward trend over the 65-year period.

A comparison of the trends of the three flood characteristics showed that areas of significant trends in flood frequencies did not coincide with areas of trends in duration and intensity. Thus, there is little agreement in trends among the three flood characteristics found in this area.

The investigation also focused on spatial variability which was considerable across short distances, based on the patterns developed from the trend values. Portions of east-central Wisconsin, where there are nine basins within a relatively small area, showed sharp demarcation in trends from upward, to flat, or downward. This suggests that small-scale variations in trends can occur due to relatively localized periods (pentads or decades) of increased or decreased storm frequency.

Warm Season, Flood Intensity

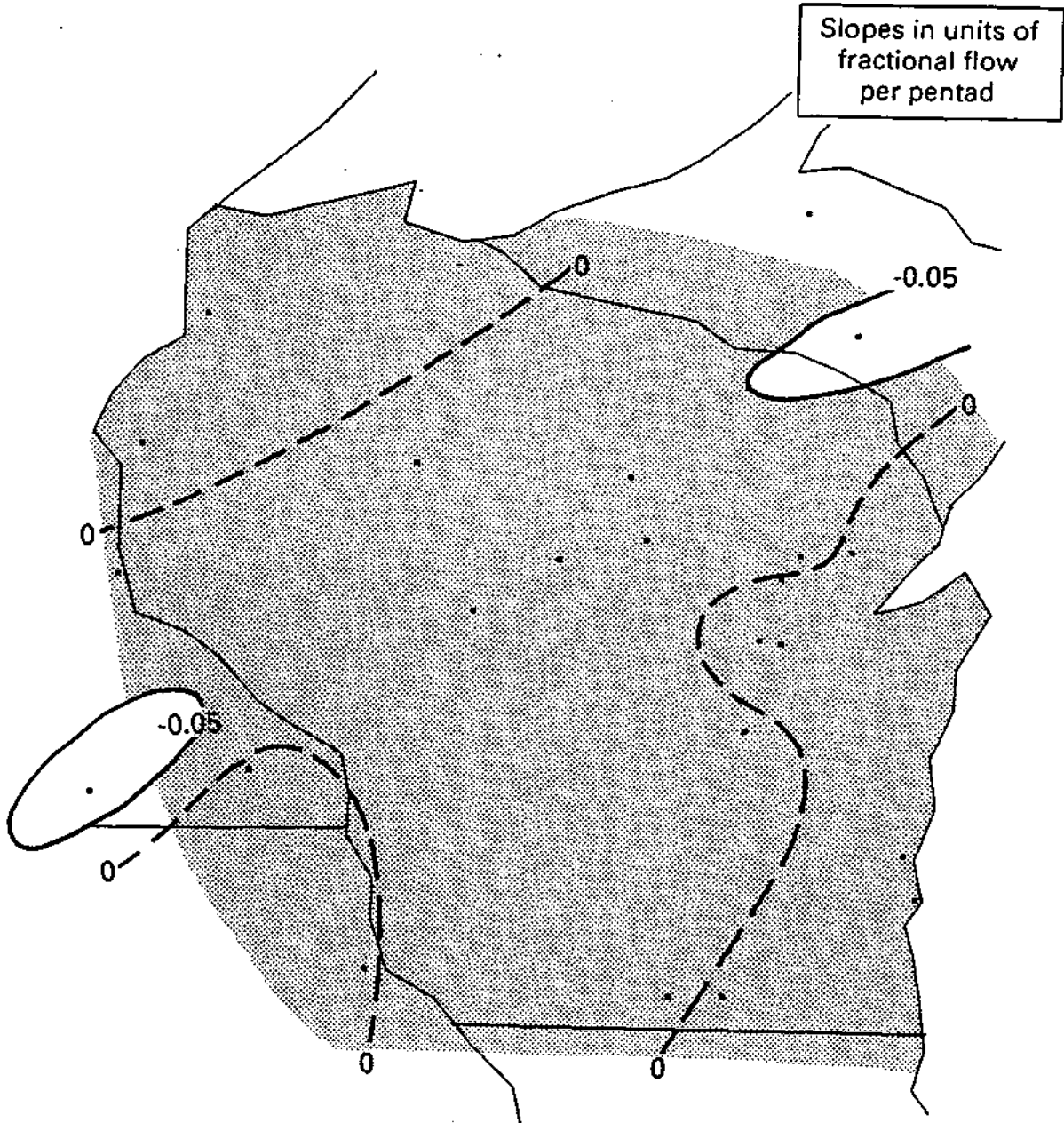


Figure 24. Spatial patterns of the slopes from a regression analysis of flood magnitudes versus pentad for the warm season. Darkened circles give the locations of stations upon which this analysis was based.

5. FLOOD AND PRECIPITATION RELATIONSHIPS

A. Associations

The aggregated temporal associations between the occurrences of flood and precipitation events were shown in Figure 2 for the warm and cold seasons. The behavior is virtually identical for the two seasons. In particular, for flood and precipitation recurrence intervals of one year, the association for the 7-day precipitation event is about 0.5 for a 1-year recurrence interval for the precipitation. In other words, for a 65-year period of record, about half of the 65 flood events can be associated with one of the top 65 precipitation events. As the precipitation recurrence interval is decreased (i.e., more precipitation events are included), the association rises substantially. For instance, for precipitation event recurrence of 0.5 years, the association is 0.7 (i.e., about 70% of the 65 flood events can be associated with one of the top 130 precipitation events). When considering a flood recurrence interval of two years, the basic relationships are similar although the actual association levels are slightly lower.

It is not surprising that the association levels are not perfect. Other factors besides total precipitation affect runoff. In particular, short-term precipitation rates and antecedent soil moisture play important roles. In addition, precipitation patterns may exhibit considerable spatial variability, particularly during the warm season when precipitation is often connectively driven. Since a relatively small number of point measurements of precipitation are used to represent the basin-wide average, there is significant sampling uncertainty in the precipitation values. When these factors are considered, the associations found in this study are not unrealistic and may not be indicative of sampling problems caused by the paucity of precipitation data.

The association values for individual flow stations are displayed in Figures 25 and 26 for the warm season, and Figures 27 and 28 for the cold season. The results are shown for two precipitation recurrence intervals (1 year and 0.5 years). For the warm season the pattern is somewhat complex. There is a slight tendency for association levels to be larger in the south. This is somewhat more evident in the results for the 0.5 precipitation recurrence interval. By contrast, cold-season association shows a distinct latitudinal gradient, particularly for 0.5-year precipitation recurrences. This is consistent with the precipitation characteristics in the cold season. At the more southern latitudes, the associations are higher because large

Warm season Flood recurrence = 1 year Precip recurrence = 1 year

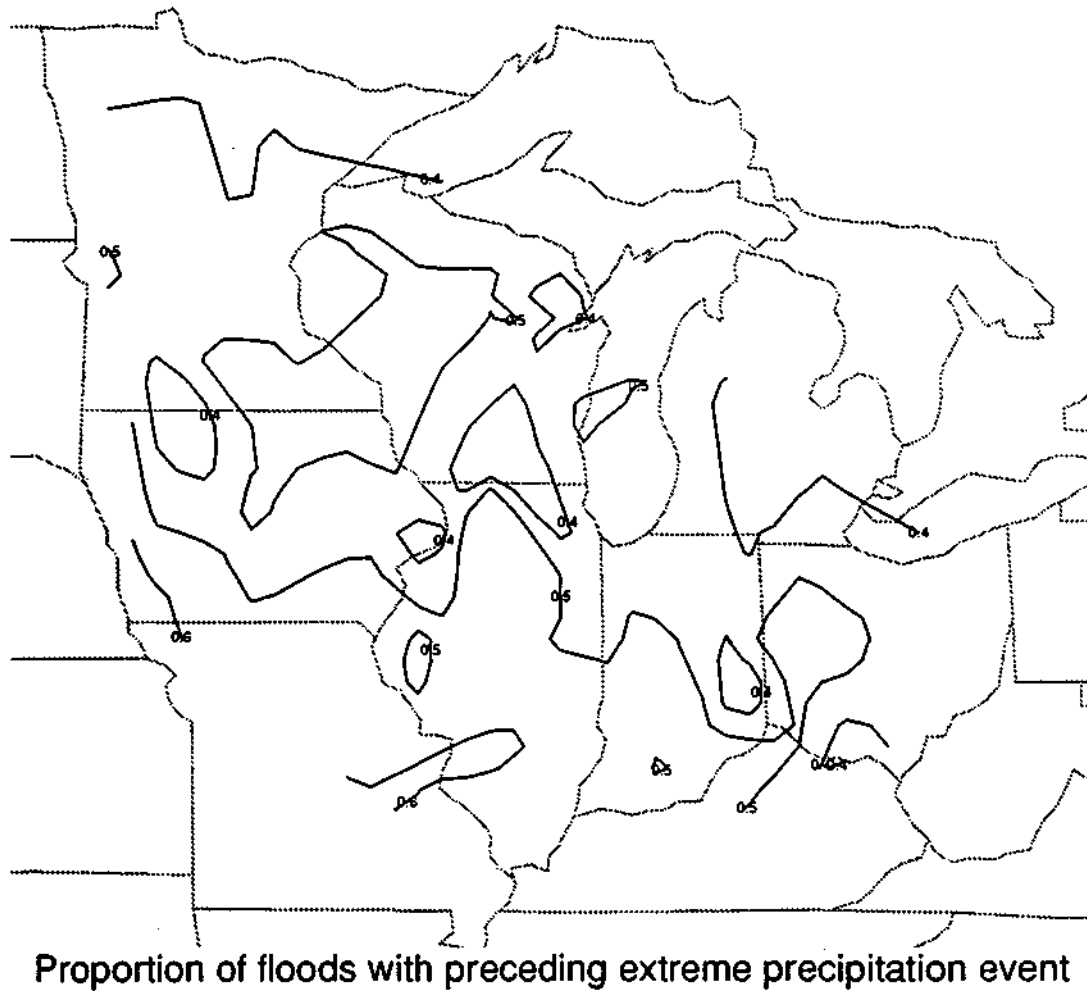


Figure 25b. Computer-generated contour analysis of the association values in Figure 25a.

Warm season Flood recurrence = 1 year Precip recurrence = .5 years

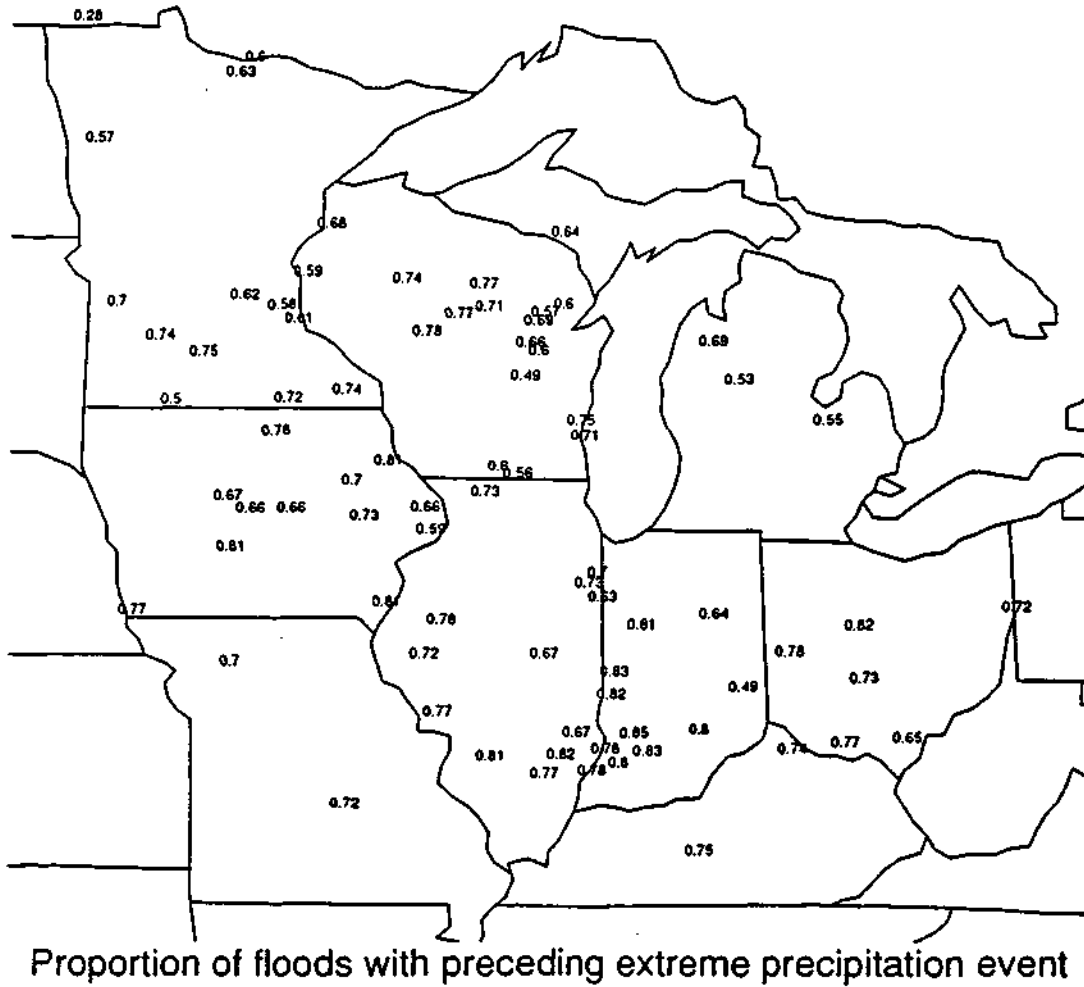


Figure 26a. Values of the temporal associations between flood events and precipitation events for the warm season for 0.5-year precipitation event and 1-year flood recurrences.

Warm season Flood recurrence = 1 year Precip recurrence = .5 years

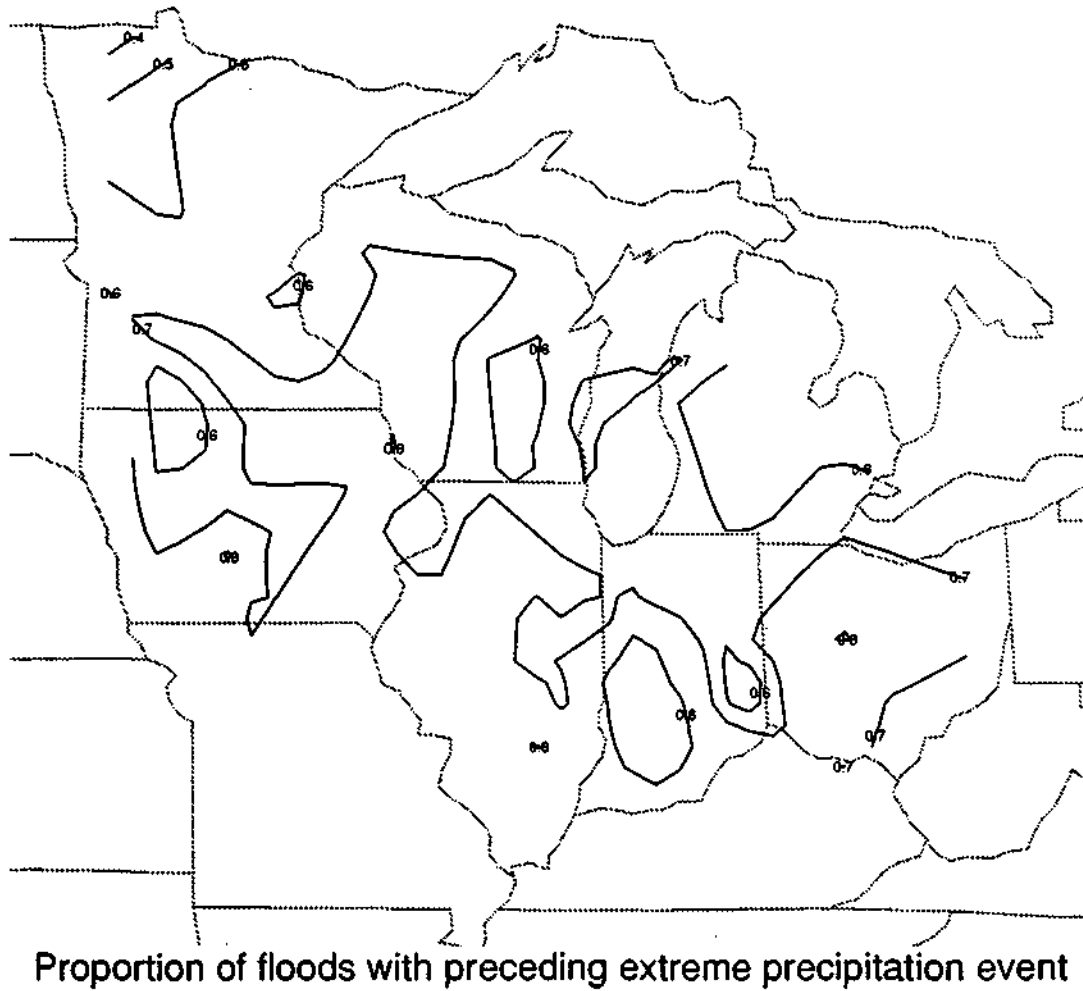
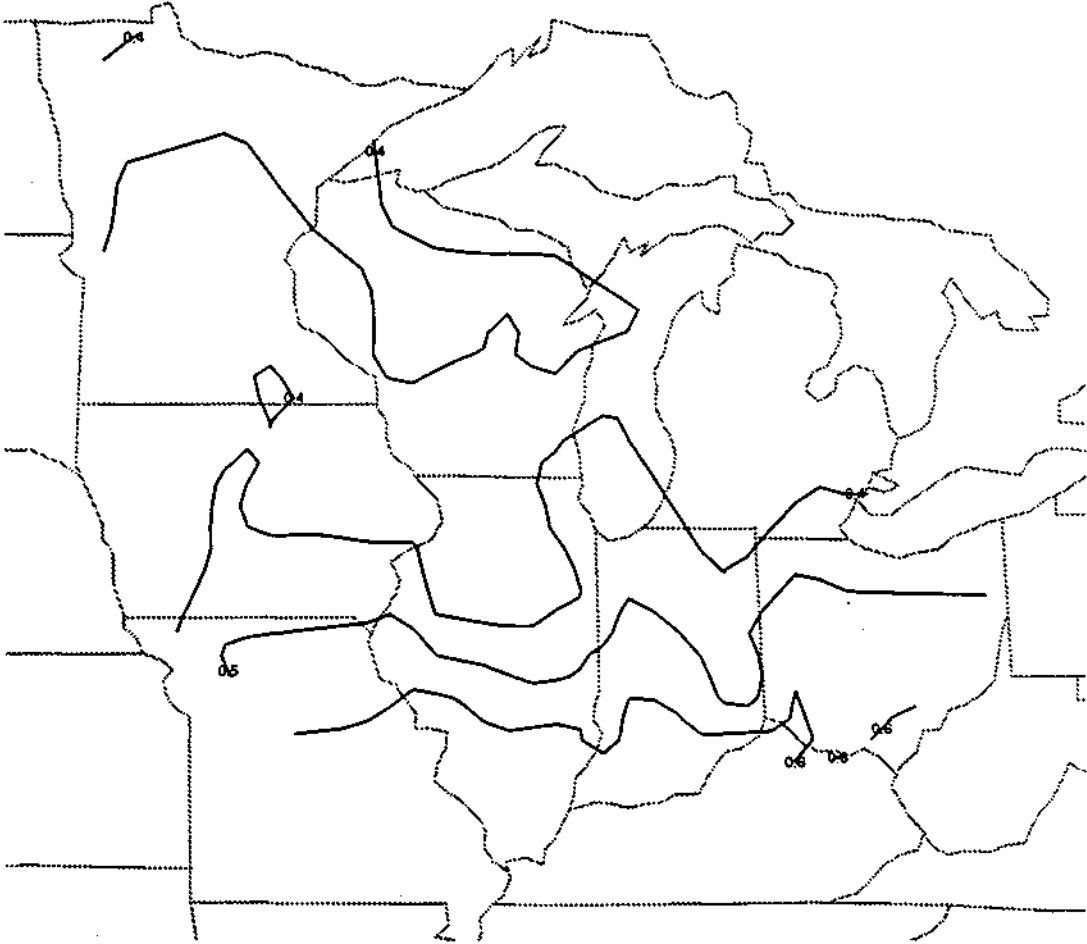


Figure 26b. Computer-generated contour analysis of the association values in Figure 26a.

Cold season Flood recurrence = 1 year Precip recurrence = 1 year



Proportion of floods with preceding extreme precipitation event

Figure 27b. Computer-generated contour analysis of the association values in Figure 27a.

Cold season Flood recurrence = 1 year Precip recurrence = .5 years

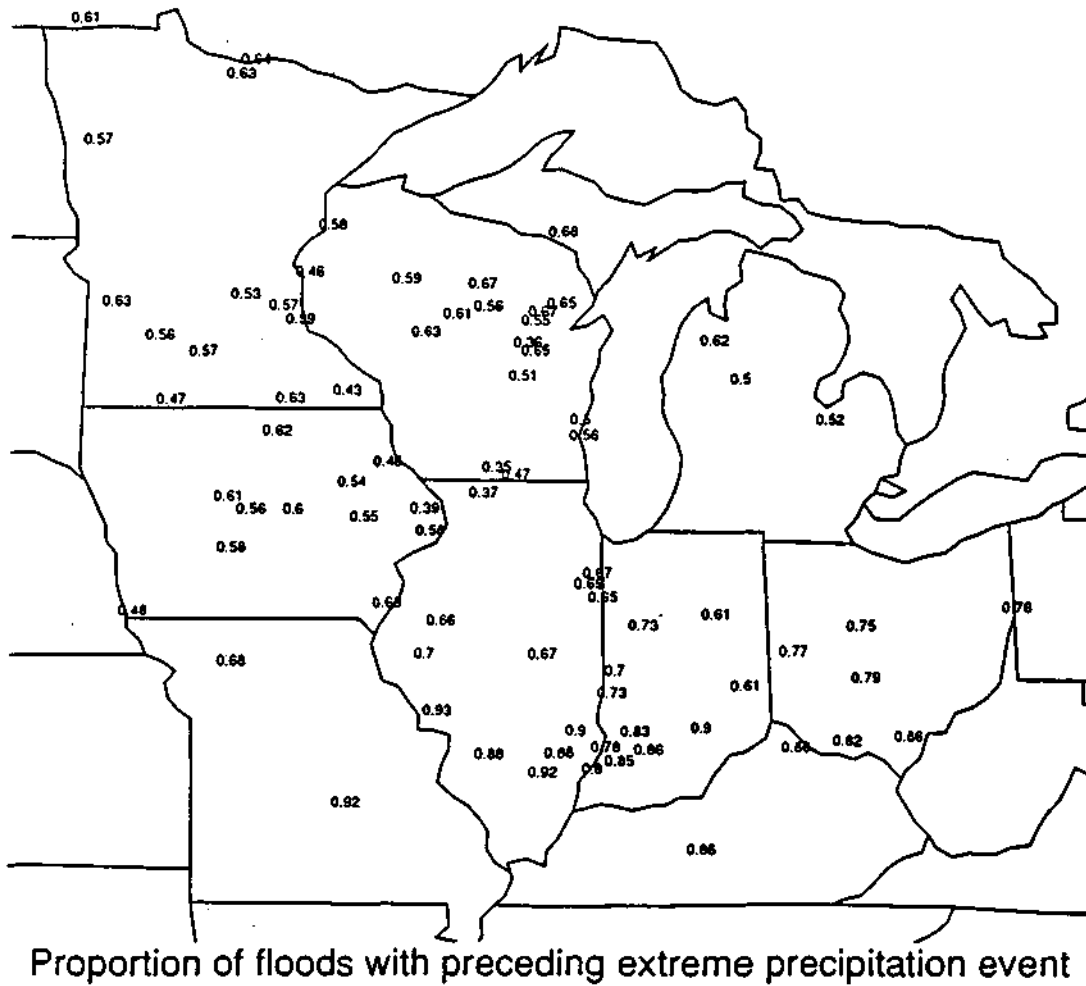


Figure 28a. Values of the temporal associations between flood events and precipitation events for the warm season for 0.5-year precipitation event and 1-year flood recurrences.

Cold season Flood recurrence = 1 year Precip recurrence = .5 years

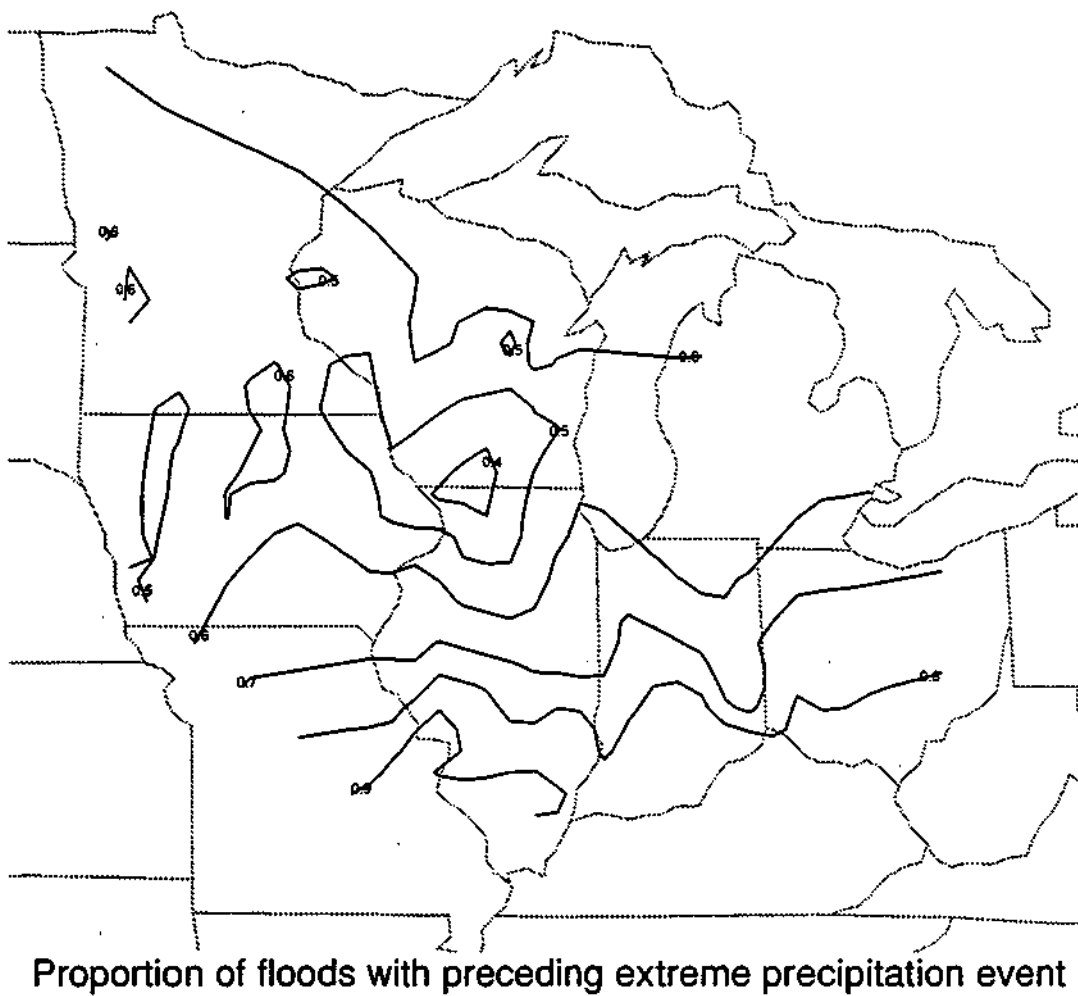


Figure 28b. Computer-generated contour analysis of the association values in Figure 28a.

amounts of precipitation are usually not locked up in snow or ice for an extended length of time.

The association levels observed here may have a significant impact on the comparative analysis of precipitation and flood time series. In particular, the interpentadal variability in the frequency of occurrence of flood and precipitation events is typically less than 50% of the mean value of 5 for a 1-year recurrence. Since this value is less than the association between the two time series at a typical station, it is quite possible to observe trends at a streamgaging station, which are not seen in the precipitation event time series.

Appendix G and H provide graphs of the pentadal frequencies of flood events for each basin for the warm and cold seasons, respectively. In addition, the pentadal frequencies of precipitation events are shown for a composite precipitation series calculated from the average of all associated precipitation stations.

B. Temporal Fluctuations

In prior sections, precipitation and flood data were analyzed separately with respect to temporal fluctuations and trends. In this section we discuss the relationships between the two, which can be seen by comparing Figures 10 and 11 with Figures 14 and 15.

For the warm season, Figures 10 and 14 reveal some general similarities between areas of significant trends in precipitation and flood event frequencies. For instance, the flood frequency analysis indicates an area of upward trends covering Minnesota, northwest Wisconsin, Iowa, and northern Illinois into northern Michigan. Precipitation event frequency analysis indicates that many of these areas also experienced upward trends in the frequency of extreme precipitation events. This is particularly true of northern and central Minnesota, western Iowa, and in the vicinity of Lake Michigan. The association is not perfect with some of the areas of higher flood frequencies showing little or no trends in the precipitation event frequencies. An area of little or no trends in flood frequencies from Missouri across southern Illinois, central Indiana, and into southern Michigan corresponds generally to an area of little or no trends in the precipitation event frequencies.

For the cold season, Figures 11 and 15 suggest the general similarity in the trends for flood and precipitation event frequencies. For instance, an area of Iowa and southern Minnesota shows upward trends in both flood and precipitation frequencies. Also, down-ward trends in flood and precipitation frequencies are found in central and southern Ohio. There are some differences, i.e., upward trends from central Illinois into southern Michigan are generally areas of little or no trends in flood frequencies. However, spatial patterns are much less coherent in this region, and these differences may simply reflect statistical sampling uncertainties. Other areas of similarity include much of Wisconsin and north-eastern Minnesota, with little or no trends in both flood and precipitation event frequencies.

To summarize, we find a general similarity in the patterns of trends for both flood and precipitation event frequencies. The agreement is not perfect, but this may stem from a number of reasons. The previous discussion has indicated that the associations between flood events and extreme precipitation events is not perfect. This imperfect association adds a considerable noise component to the comparative analysis of the flood and precipitation time series. Other possibilities include land use changes and river basin silting (caused by soil erosion), which may change the response of streamflow to precipitation events; however these possibilities are difficult to quantify.

6. SUMMARY AND CONCLUSIONS

This study focused on a nine-state region in the central United States and on the temporal/spatial relationships found in floods and related extreme precipitation conditions. Considerable effort was devoted to five broad areas of assessment: 1) data quality and means of defining floods and related precipitation events, 2) characteristics of extreme precipitation events and their relationship to total rainfall and the outputs of GCMs, 3) temporal/spatial trends in precipitation events and in floods (including three conditions of floods: frequency, intensity, and duration), 4) small-scale variations in flood events, and 5) relationships between floods and precipitation events. A variety of statistical tests were employed and tested against the various data. The research emphasis was not on a physical interpretation of the outcomes, but rather on a statistical, descriptive interpretation.

Various definitions relating to flood events and extreme precipitation events were established. Efforts to obtain quality data adequate to the study were extensive.

Many limitations were found in both the streamflow and precipitation data including breaks in the records, lack of precipitation data inside quality streamgauge basins, and inability of some USGS personnel to identify quality streamflow records from the various states.

The data were analyzed for various categories. First, seasonal analyses were employed due to major differences in causes of flooding. The cold season was defined as December-April, based on midwestern floods due to snowmelt and/or multi-day heavy precipitation conditions. The warm season was defined as May-November, a period when floods are related to convective rainstorms. Basically, flood conditions were analyzed for their frequency, duration, and intensity, and flood-related precipitation conditions were analyzed for their frequency and intensity. After various tests, partial duration series were selected to define floods and precipitation events. The period 1921-1985 was used for study because of widely available streamgauge data. Precipitation data utilized were widely available daily values, not the limited hourly data.

Three ways to aggregate the multi-station precipitation data from each individual basin were tested. Results indicated that the average value of the daily precipitation values was the best in its relationship to flooding events.

Various analyses of streamgauge data in the nine-state area indicated that 79 basins had quality data for most of the 1921-1985 period. The spatial density of stations was wide, ranging from a high of 17 streamgauge stations in Wisconsin to only 2 stations in Missouri and 2 in Kentucky. In the analysis, it was discovered that flood events derived from peak flow partial duration series were essentially coincident with those derived from water surplus partial duration series; thus, the study was based on the peak flow partial duration series.

One of the major analyses was to discern the most appropriate multi-day (1- to 10-day), precipitation period associated with floods. There was little difference between the 5-, 7-, and 10-day precipitation periods, which were periods best related to floods. Thus, 7-day duration precipitation events were chosen for subsequent studies.

Further analysis of the precipitation derived from the 1-year recurrent 7-day events revealed that, in general, the precipitation they produced related strongly to the occurrence of wet or dry pentads; e.g., more events in 5-year periods correlated

well (+0.7) to more total precipitation in the period. However, when the precipitation from these few extreme events was deleted from the pentad totals, there was no correlation between their incidence and pentad precipitation. Also, the temporal variability of these extreme precipitation events explained much of the pentadal variance in total precipitation. These events contributed nearly one-half of the interpentadal precipitation variance. Thus, the frequency of occurrence of extreme precipitation events appears to be random and not tied to any particular long-term circulation anomalies that create wet or dry periods. This has major implications for global climate change assessment. The results suggest that GCM estimates of precipitation changes for months or seasons are not adequate for estimating hydrologic (flooding) impacts if they do not adequately model the frequency of occurrence of these few extreme precipitation events.

A third major area of investigation related to the temporal distribution of heavy precipitation events and floods. The investigation of the temporal variability in warm-season precipitation events revealed no coherent regional patterns in the Midwest. However, a similar analysis of cold-season events revealed statistically significant temporal variability across a broad southwest-northeast oriented area including Iowa, southern Minnesota, northern Illinois, and lower Michigan.

Investigation of long-term variability in precipitation events provided similar results, particularly in relation to the cold season. The warm season trends of heavy-precipitation events revealed an upward trend in frequency from 1920 to 1985 across Minnesota, Iowa, and northern Illinois. This agrees with Changnon's (1983) findings. Cold-season trends in heavy precipitation events revealed that Iowa, southwestern Illinois, and Ohio had upward trends. Few areas had downward trends, and most (~75%) of the Midwest had no significant upward or downward trends in flood-producing precipitation events during 1921-1985.

Trends in flood frequencies, flood durations, and flood magnitudes were assessed. In general, much of the nine-state area was found to have slight to moderate upward trends during the warm season in flood frequencies. Trends in heavy precipitation events were also up-wards but only across the western region (Minnesota, Iowa, and Missouri), plus lower Michigan, Kentucky, and Ohio. Comparison of this outcome for warm-season trends with those for flood frequencies indicated general similarity, although some areas indicated increases in flood incidences without increases in precipitation events. Flood frequencies showed increases across Minnesota, Iowa, northern Illinois, lower Michigan, and southern

Indiana. However, flood durations and flood intensities in the warm season showed no large areas of either upward or downward trends.

The frequency of precipitation events in the cold season has increased over time across a zone from Iowa through lower Michigan. Examination of trends in cold-season flood events revealed increases across Minnesota, Iowa, Missouri, western Illinois, and lower Michigan. Durations of cold-season floods also increased in Minnesota and Iowa, as did cold-season flood intensities.

Analysis of the 5-year periods of maximum flood occurrences supported the findings from the trends of floods. Basins in Illinois, Iowa, Kentucky, northern Indiana, southern Wisconsin, and Minnesota experienced their peak in flood frequencies during 1981-1985, with 25% of all 79 basins peaking during this one period. A second group of basins across lower Michigan and upper Wisconsin had their peak in flood frequencies during 1941-1945. Basins in Missouri and Ohio showed an early peak in floods during 1926-1930.

The small-scale variability in flood events was analyzed as an aid to interpreting the nine-state patterns and as a check on data quality. Floods in Wisconsin, an area with the largest number of streamgauge stations, were analyzed. Results revealed considerable small-scale variability in trends of flood incidences over short distances. The frequency of floods increased over most of Wisconsin from 1921 to 1985, but the trends of incidence were not well related to those of flood duration or flood intensity.

An ongoing and yet-to-be completed analysis of the relationship between extreme precipitation events and floods indicated that 50% of the 1-year recurrence interval floods were associated with 1-year precipitation events. Furthermore, 70% of the 1-year recurrence interval floods were associated with 0.5-year precipitation events. The differences between these flood and precipitation events results largely from inadequate sampling of precipitation events within basins. Typically, anywhere between 1 and 4 precipitation stations were found within the basins under investigation with the largest basins (e.g., Wabash River at Mt. Carmel, Illinois) having as many as 20.

ACKNOWLEDGMENTS

This work was partially supported by the U.S. Geological Survey under award number 14-08-0001-G1731. We thank James Zandlo, Fred Nurnberger, Kenneth Scheeringa, and Pam Naber Knox for providing precipitation data. We also thank Melvin Lew, Richard Novitzky, and the USGS District Offices in Illinois (Wayne Curtis), Indiana (Ronald Thompson), Iowa (Phil Soenksen), Michigan (Stephen Blumer), Minnesota (George Carlson), Ohio (Harold Shindel), and Wisconsin (William Krug and Dianne Maertz) for providing information on streamflow stations. We thank Arthur Scott and Ken Wahl for their assistance in our interactions with the USGS District Offices. Finally, we thank Jean Dennison for her professional preparation of the manuscript, Eva Kingston for editing the report, and John Brother and Linda Hascall for preparing the figures.

REFERENCES

- Bickel, P., and K. Doksum, 1977: Mathematical Statistics: Basic Ideas and Selected Topics. Holden-Day: San Francisco, CA.
- Birnbaum, Z., 1952: Numerical tabulation of the distribution of Kolmogorov's statistic for finite sample size. J. Amer. Statist. Assoc., 47, 425-441.
- Changnon, S.A., 1983: Trends in floods and related climate conditions in Illinois. Climatic Change, 5, 341-363.
- Changnon, S.A., and F.A. Huff, 1971: Evaluation of Potential Benefits of Weather Modification on Agriculture: Description of Individual Studies. Final Report, Illinois State Water Survey, Champaign.
- Giorgi, F., G.T. Bates, R.M. Errico, and R.E. Dickinson, 1989: Modeling the climate of the western U.S. with a limited area model coupled to a General Circulation Model. Proceedings of the Sixth Conference on Applied Climatology, American Meteorological Society, Boston, MA, pp. 201-208.
- Hampel, F., E. Ronchetti, P. Rousseeuw, and W. Stahel, 1986: Robust Statistics: The Approach Based on Influence Functions. Wiley: New York.

- Kunkel, K.E., S.A. Changnon, C.G. Lonquist, and J.R. Angel, 1990: A real-time climate information system for the midwestern United States. Bull. Amer. Meteor. Soc., 71, 1601-1609.
- Pitman, A.J., A. Henderson-Sellers, and Z.-L. Yang, 1990: Sensitivity of regional climates to localized precipitation in global models. Nature, **346**, 734-737.
- Rind, D., R. Goldberg, and R. Ruedy, 1989: Change in climate variability in the 21st Century. Climatic Change, 14, 5-37.
- U.S. Water Resources Council, 1981: Guidelines for Determining Flood Flow Frequency. Bulletin #17B, 2120 L Street, N.W., Washington, D.C.

PUBLICATIONS

- Kunkel, K.E., S.A. Changnon, and R.T. Shealy, 1991: Extreme precipitation variability: The link to temporal variability in seasonal precipitation. Proceedings of the Fifth Conference on Climate Variations, American Meteorological Society, Boston, MA, pp. 90-91.
- Kunkel, K.E., S.A. Changnon, and R.T. Shealy, 1991: Extreme precipitation variability: The link to temporal variability in seasonal precipitation. Proceedings of the Seventh Conference on Applied Climatology, American Meteorological Society, Boston, MA, pp. 123-126.

APPENDIX A

STREAMGAGING STATIONS

A list of the streamgaging stations used in this analyses follows. The information included is the station identification number, the name of the station, the latitude (degrees), the longitude (degrees), the drainage area upstream of the station (square miles), the starting and ending dates and the percentage of missing data for that period.

STATION ID	NAME	LAT	LONG	DRAIN	STRT	END	%MS
03109500	L BEAVER C NR EAST LIVERPOOL OH	40.68	80.54	496	1915	1987	0
03202000	RACCOON C AT ADAMSVILLE OH	38.87	82.36	585	1915	1986	4
03219500	SCIOTO R NR PROSPECT OH	40.42	83.20	567	1925	1987	11
03230500	BIG DARBY C AT DARBYVILLE OH	39.70	83.11	534	1921	1987	5
03237500	OHIO BRUSH C NR WEST UNION OH	38.80	83.42	387	1926	1987	8
03253500	LICKING RIVER AT CATAWBA, KY.	38.71	84.31	3300	1915	1986	16
03265000	STILLWATER R AT PLEASANT HILL OH	40.06	84.36	503	1916	1987	9
03275000	WHITEWATER RIVER NEAR ALPINE, IND	39.58	85.16	522	1928	1987	0
03308500	GREEN RIVER AT MUNFORDVILLE, KY.	37.27	85.89	1673	1914	1987	15
03326500	MISSISSINEWA RIVER AT MARION, IND.	40.58	85.66	682	1923	1987	0
03335500	WABASH RIVER AT LAFAYETTE IND	40.42	86.90	7267	1923	1987	0
03340500	WABASH RIVER AT MONTEZUMA, IND.	39.79	87.37	11118	1927	1987	0
03341500	WABASH RIVER AT TERRE HAUTE, IND.	39.47	87.42	12265	1927	1987	0
03343000	WABASH RIVER AT VINCENNES, IND.	38.71	87.52	13706	1929	1987	0
03345500	EMBARRAS RIVER AT STE. MARIE, IL	38.94	88.02	1516	1909	1987	3
03360500	WHITE RIVER AT NEWBERRY, IND.	38.93	87.02	4688	1928	1987	0
03365500	EAST FORK WHITE RIVER AT SEYMOUR IND	38.98	85.90	2341	1927	1987	0
03373500	EAST FORK WHITE RIVER AT SHOALS, IND.	38.67	86.79	4927	1903	1987	11
03374000	WHITE RIVER AT PETERSBURG IND	38.51	87.29	11125	1927	1987	0
03377500	WABASH RIVER AT MT. CARMEL, ILL.	38.40	87.75	28635	1927	1987	0
03379500	LITTLE WABASH RIVER BELOW CLAY CITY, IL	38.63	88.30	1131	1914	1987	0
03380500	SKILLET FORK AT WAYNE CITY, IL	38.36	88.58	464	1908	1987	11
04 61000	BRULE RIVER NEAR FLORENCE, WI	45.96	88.27	389	1913	1988	36
04 71000	OCONTO RIVER NEAR GILLETT, WI	44.86	88.30	705	1905	1988	5
04 73500	FOX RIVER AT BERLIN, WI	43.95	88.95	1340	1897	1988	0
04 77400	WOLF RIVER NEAR SHAWANO, WI	44.84	88.62	816	1906	1988	1
04 78500	EMBARRASS RIVER NEAR EMBARRASS, WI	44.72	88.74	384	1918	1988	1
04 79000	WOLF RIVER AT NEW LONDON, WI	44.39	88.74	2260	1913	1988	0
04 80000	LITTLE WOLF RIVER AT ROYALTON, WI	44.41	88.87	507	1913	1985	14

STATION ID	NAME	LAT	LONG	DRAIN	STRT	END	%MS
04 86500	CEDAR CREEK NEAR CEDARBURG, WI	43.32	87.98	120	1929	1988	3
04 87000	MILWAUKEE RIVER AT MILWAUKEE, WI	43.10	87.91	696	1913	1988	0
04121500	MUSKEGON RIVER AT EVART.MICH.	43.90	85.26	1450	1930	1988	3
04124000	MANISTEE RIVER NEAR SHERMAN, MI	44.44	85.70	857	1902	1987	19
04151500	CASS RIVER AT FRANKENMUTH, MICH.	43.33	83.75	841	1907	1988	33
05 62500	WILD RICE RIVER AT TWIN VALLEY, MN	47.27	96.24	888	1908	1984	16
05112000	ROSEAU RIVER BELOW STATE DITCH 51 NR CARIBOU, MN	48.98	96.46	1570	1916	1987	6
05131500	LITTLE FORK RIVER AT LITTLEFORK, MN	48.40	93.57	1730	1908	1987	14
05132000	BIG FORK RIVER AT BIG FALLS, MN	48.20	93.81	1460	1908	1987	24
05280000	CROW RIVER AT ROCKFORD, MN	45.09	93.73	2520	1905	1987	16
05300000	LAC QUI PARLE RIVER NEAR LAC QUI PARLE, MN	44.99	95.92	983	1909	1987	21
05316500	REDWOOD RIVER NEAR REDWOOD FALLS, MN	44.52	95.17	697	1908	1987	20
05317000	COTTONWOOD RIVER NEAR NEW ULM, MN	44.29	94.44	1280	1908	1987	22
05331000	MISSISSIPPI RIVER AT ST. PAUL, MN	44.94	93.09	36800	1891	1987	1
05333500	ST. CROIX RIVER NEAR DANBURY, WI	46.07	92.25	1580	1913	1988	4
05340500	ST. CROIX RIVER AT ST. CROIX FALLS, WI	45.41	92.65	6240	1901	1988	5
05344500	MISSISSIPPI RIVER AT PRESCOTT, WI	44.75	92.80	44800	1927	1987	0
05362000	JUMP RIVER AT SHELDON, WI	45.31	90.96	576	1914	1988	0
05381000	BLACK RIVER AT NEILLSVILLE, WI	44.56	90.61	749	1904	1988	5
05384000	ROOT RIVER NEAR LANESBORO, MN	43.75	91.98	615	1909	1987	30
05394500	PRAIRIE RIVER NEAR MERRILL, WI	45.24	89.65	184	1913	1988	9
05397500	EAU CLAIRE RIVER AT KELLY, WI	44.92	89.55	375	1913	1988	15
05399500	BIG EAU PLEINE RIVER NEAR STRATFORD, WI	44.82	90.08	224	1913	1988	13
05412500	TURKEY RIVER AT GARBER, IOWA	42.74	91.26	1545	1912	1987	5
05418500	MAQUOKETA RIVER NEAR MAQUOKETA, IOWA	42.08	90.63	1553	1913	1987	0
05421000	WAPSIPINICON R AT INDEPENDENCE, IOWA	42.46	91.89	1048	1933	1987	0
05422000	WAPSIPINICON RIVER NEAR DE WITT, IOWA	41.77	90.53	2330	1933	1987	0
05430500	ROCK RIVER AT AFTON, WI	42.61	89.07	3340	1913	1988	0
05435500	PECATONICA RIVER AT FREEPORT, IL	42.30	89.62	1326	1914	1987	0
05436500	SUGAR RIVER NEAR BRODHEAD, WI	42.61	89.40	523	1913	1988	0
05451500	IOWA RIVER AT MARSHALLTOWN, IOWA	42.07	92.91	1564	1902	1987	19

STATION ID	NAME	LAT	LONG	DRAIN	STRT	END	%MS
05457000	CEDAR RIVER NEAR AUSTIN, MN	43.64	92.97	425	1908	1987	39
05459500	WINNEBAGO RIVER AT MASON CITY, IOWA	43.17	93.19	526	1932	1987	0
05464500	CEDAR RIVER AT CEDAR RAPIDS, IOWA	41.97	91.67	6510	1902	1987	0
05470000	SOUTH SKUNK RIVER NEAR AMES, IOWA	42.07	93.62	315	1920	1987	8
05474000	SKUNK RIVER AT AUGUSTA, IOWA	40.75	91.28	4303	1913	1987	0
05476000	DES MOINES RIVER AT JACKSON, MN	43.62	94.99	1220	1908	1987	20
05481300	DES MOINES RIVER NR STRATFORD, IOWA	42.25	94.00	5452	1919	1987	0
05484500	RACCOON RIVER AT VAN METER, IOWA	41.53	93.95	3441	1914	1987	0
05520500	KANKAKEE RIVER AT MOMENCE, IL	41.16	87.67	2294	1904	1987	11
05525000	IROQUOIS RIVER AT IROQUOIS, IL	40.82	87.58	686	1944	1987	0
05526000	IROQUOIS RIVER NEAR CHEBANSE, IL	41.01	87.82	2091	1923	1987	0
05570000	SPOON RIVER AT SEVILLE, IL	40.49	90.34	1636	1914	1987	0
05572000	SANGAMON RIVER AT MONTICELLO, IL	40.03	88.59	550	1907	1987	3
05585000	LA MOINE RIVER AT RIPLEY, IL	40.03	90.63	1293	1920	1987	0
05587000	MACOUPIN CREEK NEAR KANE, IL	39.23	90.39	868	1920	1987	10
05594000	SHOAL CREEK NEAR BREESE, IL	38.61	89.49	735	1909	1987	42
06810000	NISHNABOTNA RIVER ABOVE HAMBURG, IOWA	40.63	95.63	2806	1921	1987	8
06897500	GRAND RIVER NEAR GALLATIN MO	39.93	93.94	2250	1920	1986	0
06933500	GASCONADE RIVER AT JEROME MO	37.93	91.98	2840	1902	1986	19

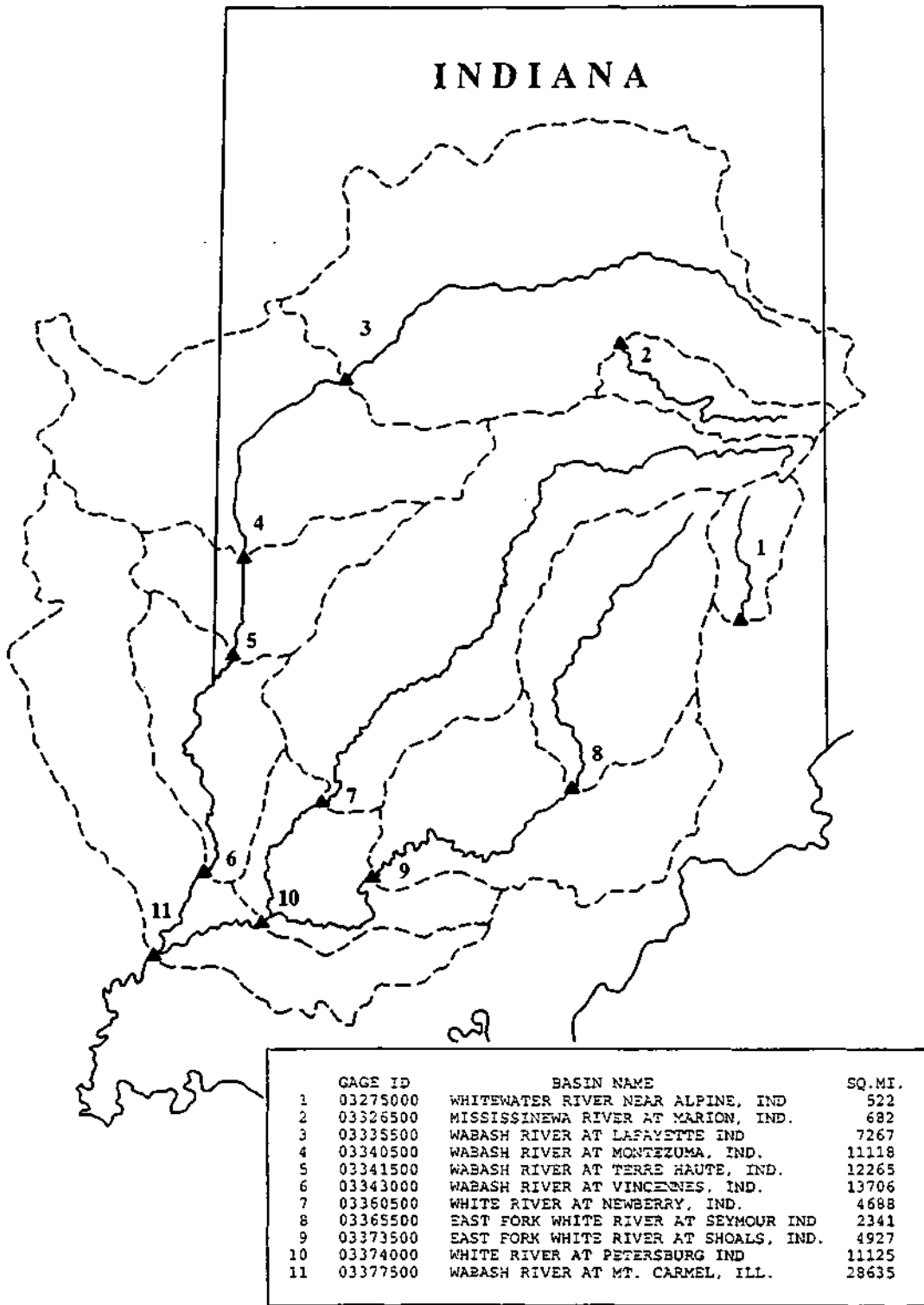
APPENDIX B

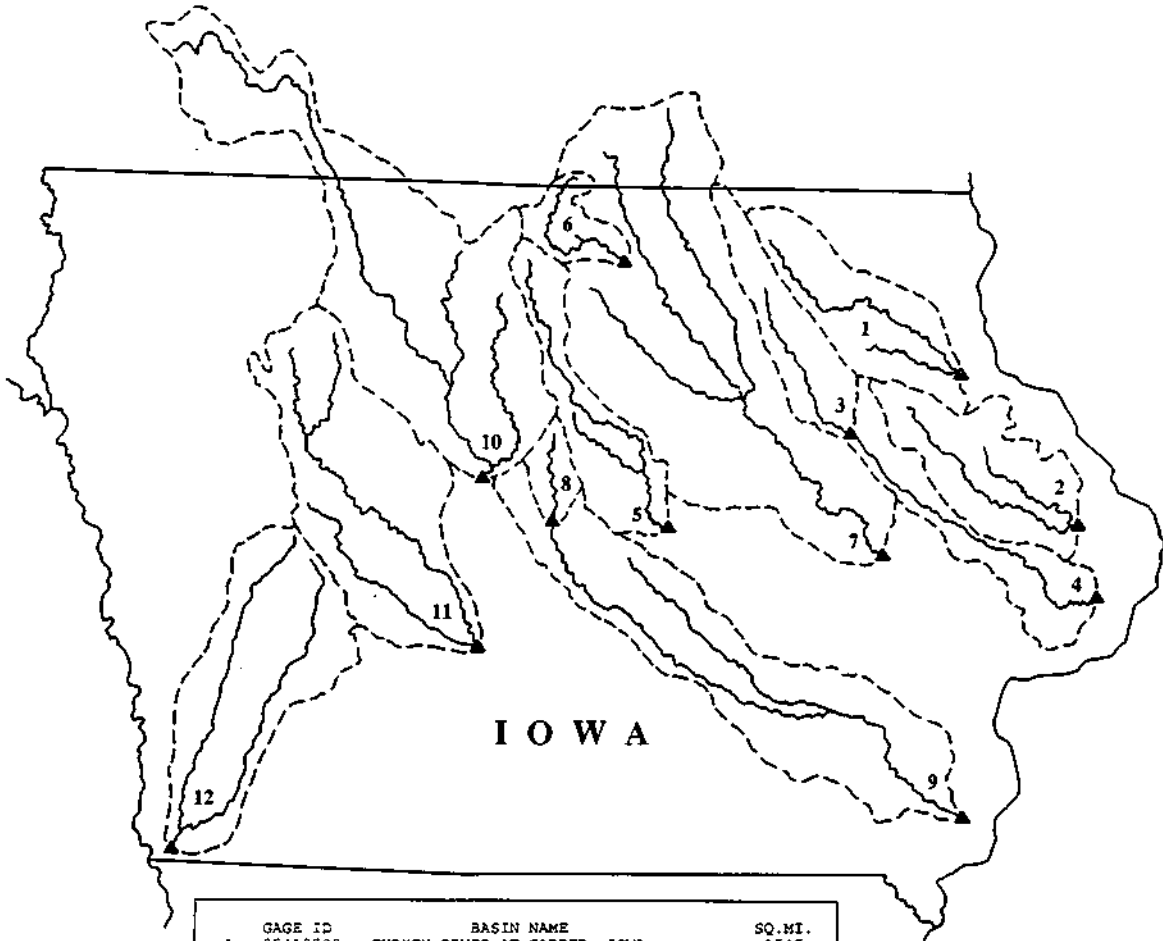
STREAM BASINS

The following maps show the boundaries of each basin. The map inset gives the names of the basins. In some cases, basins wholly contain other smaller basins. The Wabash River in Indiana and Illinois is a representative example. Careful inspection of the maps will allow the exact boundaries of each basin to be identified.



GAGE ID	BASIN NAME	SQ. MI.
1	03345500 EMBARRAS RIVER AT STE. MARIE, IL	1515
2	03379500 LITTLE WABASH RIVER BELOW CLAY CITY, IL	1131
3	03380500 SKILLET FORK AT WAYNE CITY, IL	464
4	05435500 PECATONICA RIVER AT FREEPORT, IL	1326
5	05520500 KANKAKEE RIVER AT MOMENCE, IL	2294
6	05525000 IROQUOIS RIVER AT IROQUOIS, IL	686
7	05526000 IROQUOIS RIVER NEAR CHEBANSE, IL	2091
8	05570000 SPOON RIVER AT SEVILLE, IL	1636
9	05572000 SANGAMON RIVER AT MONTICELLO, IL	550
10	05585000 LA MOINE RIVER AT RIPLEY, IL	1293
11	05587000 MACOUPIN CREEK NEAR KANE, IL	868
12	05594000 SHOAL CREEK NEAR BREESE, IL	735

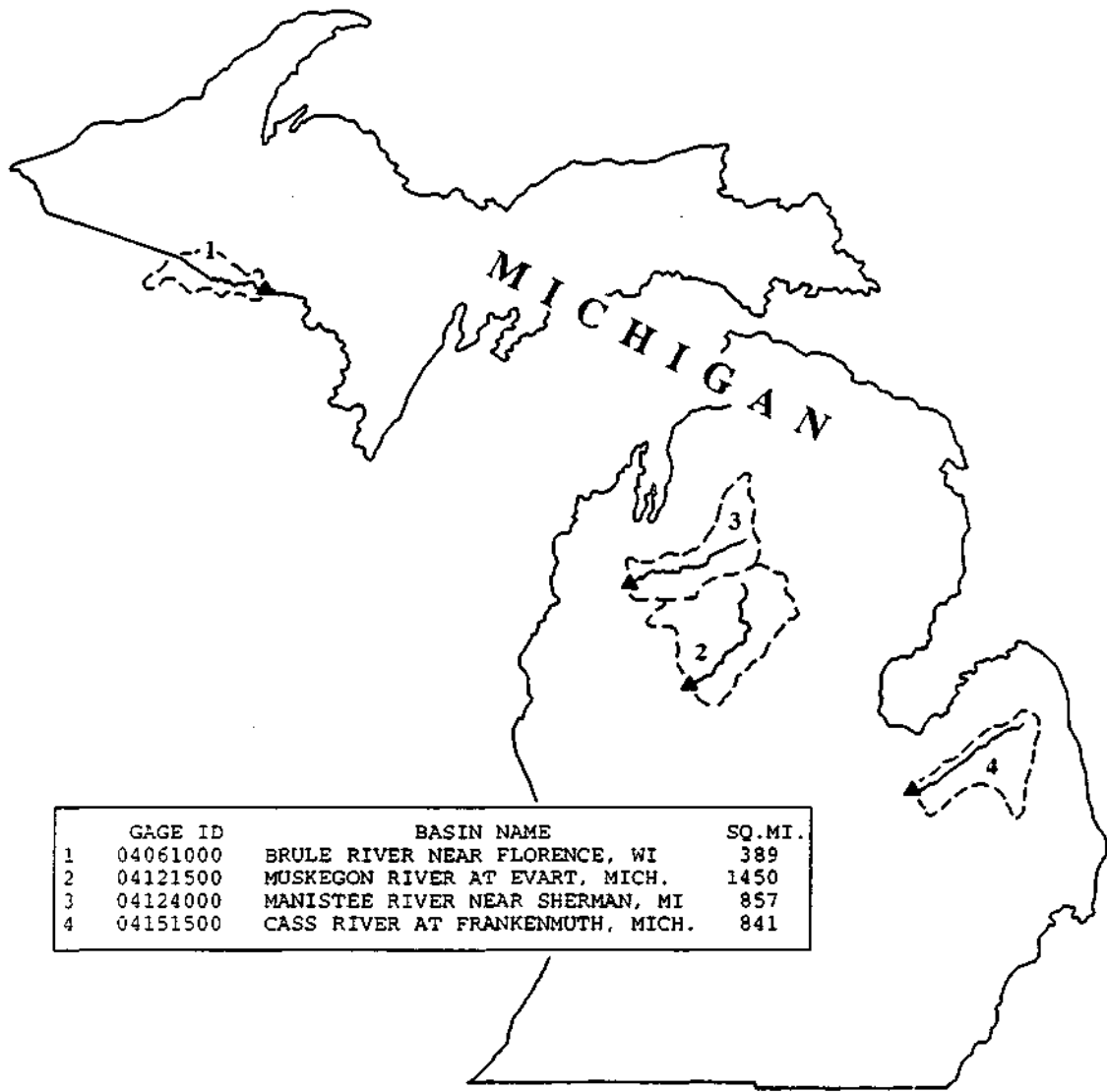




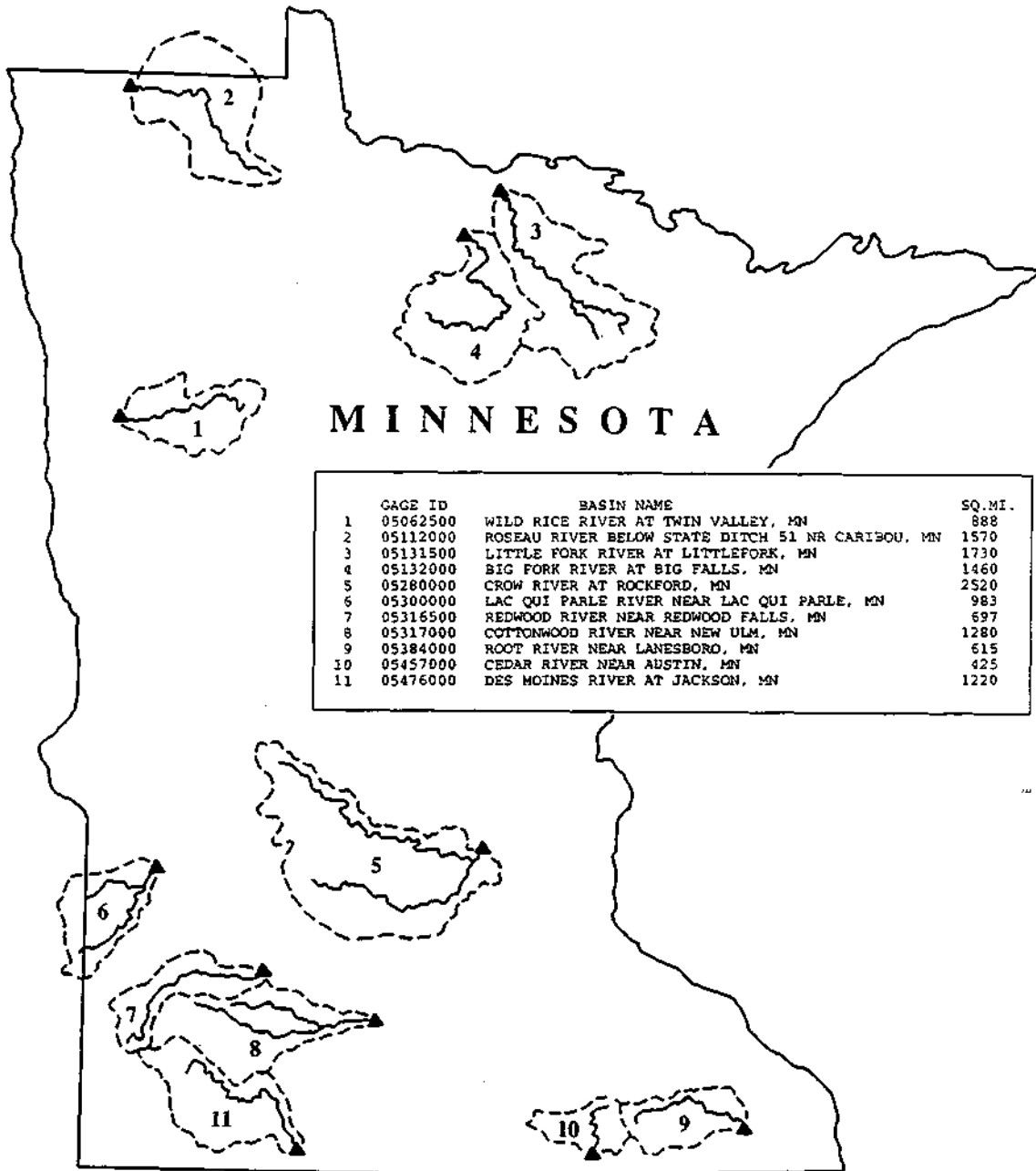
GAGE ID	BASIN NAME	SQ. MI.
1	05412500 TURKEY RIVER AT GARBER, IOWA	1545
2	05418500 MAQUOKETA RIVER NEAR MAQUOKETA, IOWA	1553
3	05421000 WAPSIPINICON R AT INDEPENDENCE, IOWA	1048
4	05422000 WAPSIPINICON RIVER NEAR DE WITT, IOWA	2330
5	05451500 IOWA RIVER AT MARSHALLTOWN, IOWA	1564
6	05459500 WINNEBAGO RIVER AT MASON CITY, IOWA	526
7	05464500 CEDAR RIVER AT CEDAR RAPIDS, IOWA	6516
8	05470000 SOUTH SKUNK RIVER NEAR AMES, IOWA	315
9	05474000 SKUNK RIVER AT AUGUSTA, IOWA	4303
10	05481300 DES MOINES RIVER NR STRATFORD, IOWA	5452
11	05484500 FACCOON RIVER AT VAN METER, IOWA	3441
12	06610000 WAPAHOSETA RIVER ABOVE HAMBURG, IOWA	2806



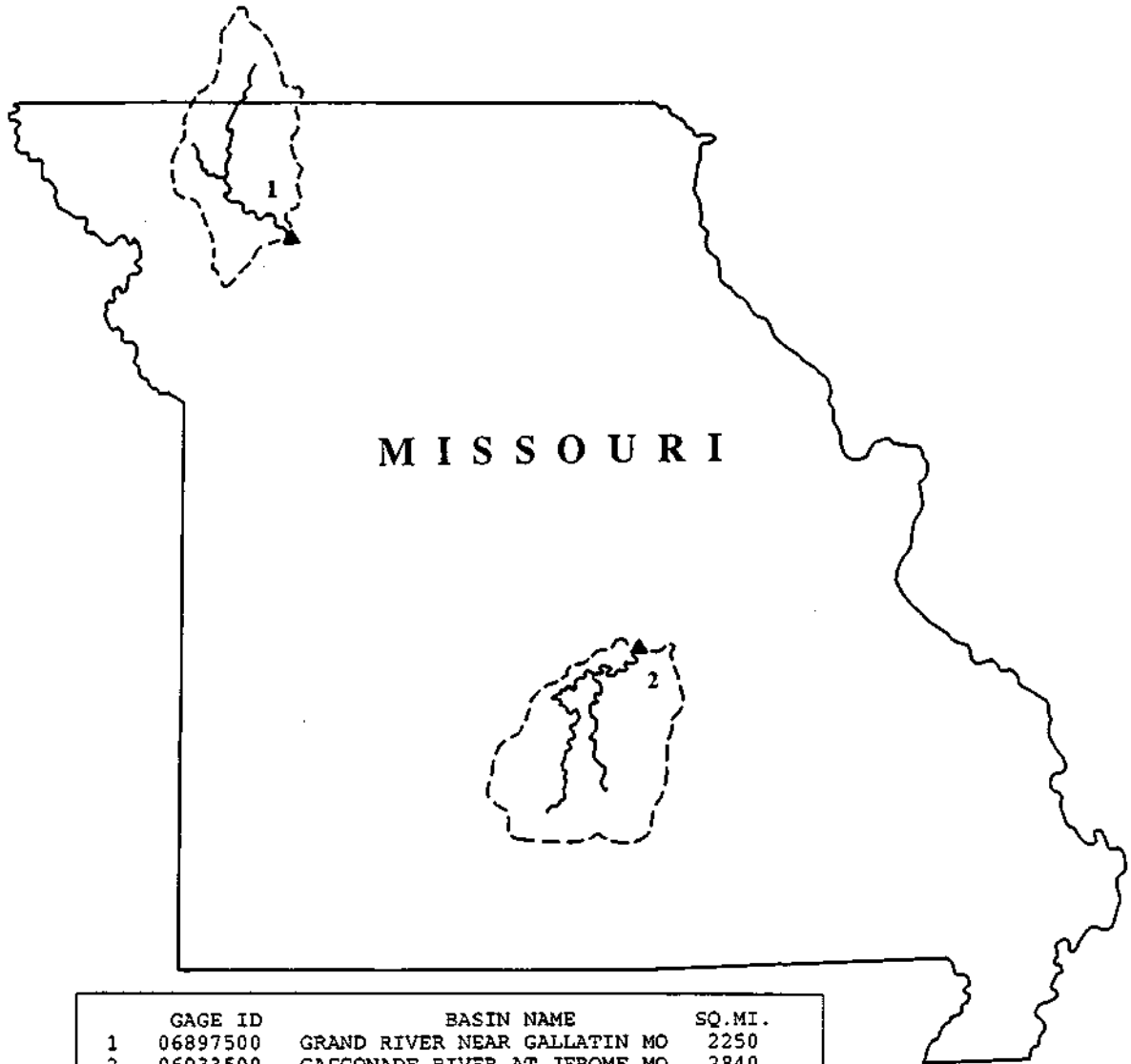
	GAGE ID	BASIN NAME	SQ.MI.
1	03253500	LICKING RIVER AT CATAWBA, KY.	3300
2	03308500	GREEN RIVER AT MUNFORDVILLE, KY.	1673



	GAGE ID	BASIN NAME	SQ.MI.
1	04061000	BRULE RIVER NEAR FLORENCE, WI	389
2	04121500	MUSKEGON RIVER AT EVART, MICH.	1450
3	04124000	MANISTEE RIVER NEAR SHERMAN, MI	857
4	04151500	CASS RIVER AT FRANKENMUTH, MICH.	841





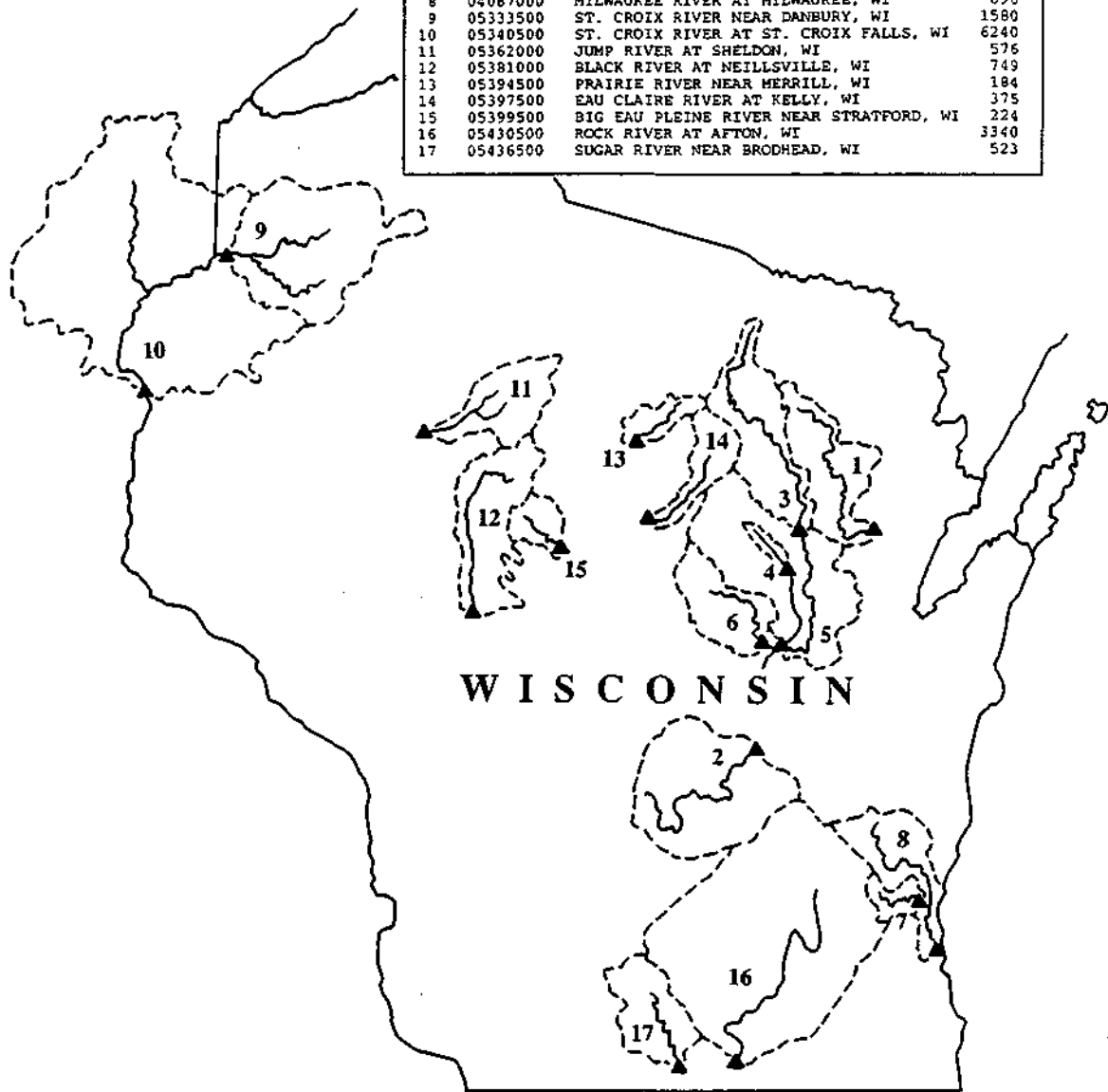


	GAGE ID	BASIN NAME	SQ.MI.
1	06897500	GRAND RIVER NEAR GALLATIN MO	2250
2	06933500	GASCONADE RIVER AT JEROME MO	2840

	GAGE ID	BASIN NAME	SQ. MI.
1	03109500	L BEAVER C NR EAST LIVERPOOL OH	496
2	03202000	RACCOON C AT ADAMSVILLE OH	585
3	03219500	SCIOTO R NR PROSPECT OH	567
4	03230500	BIG DARBY C AT DARBYVILLE OH	534
5	03237500	OHIO BRUSH C NR WEST UNION OH	387
6	03265000	STILLWATER R AT PLEASANT HILL OH	503



	GAGE ID	BASIN NAME	SQ. MI.
1	04071000	OCONTO RIVER NEAR GILLETT, WI	705
2	04073500	FOX RIVER AT BERLIN, WI	1340
3	04077400	WOLF RIVER NEAR SHAWANO, WI	816
4	04078500	EMBARRASS RIVER NEAR EMBARRASS, WI	384
5	04079000	WOLF RIVER AT NEW LONDON, WI	2260
6	04080000	LITTLE WOLF RIVER AT ROYALTON, WI	507
7	04086500	CEDAR CREEK NEAR CEDARBURG, WI	120
8	04087000	MILWAUKEE RIVER AT MILWAUKEE, WI	696
9	05333500	ST. CROIX RIVER NEAR DANBURY, WI	1580
10	05340500	ST. CROIX RIVER AT ST. CROIX FALLS, WI	6240
11	05362000	JUMP RIVER AT SHELDON, WI	576
12	05381000	BLACK RIVER AT NEILLSVILLE, WI	749
13	05394500	PRAIRIE RIVER NEAR MERRILL, WI	184
14	05397500	EAU CLAIRE RIVER AT KELLY, WI	375
15	05399500	BIG EAU PLEINE RIVER NEAR STRATFORD, WI	224
16	05430500	ROCK RIVER AT AFTON, WI	3340
17	05436500	SUGAR RIVER NEAR BRODHEAD, WI	523



APPENDIX C

PRECIPITATION STATIONS

A list of the precipitation stations used in this analysis follows. This list includes the state, the name of the station, the identification number, the latitude, (degrees), the longitude, (degrees), the beginning year of data for available for this study, and the percentage of available data for the period 1921-1985.

STATE	NAME	ID NO.	LAT.	LONG.	STRT	%MSG
IL	Aledo	110072	41.23	90.73	1921	0
IL	Anna 1 E	110187	37.47	89.23	1921	0
IL	Aurora	110338	41.75	88.35	1921	1
IL	Carbondale	111265	37.72	89.19	1921	2
IL	Carlinville	111280	39.28	89.87	1921	1
IL	Charleston	111436	39.48	88.17	1921	3
IL	Danville	112140	40.13	87.65	1921	1
IL	Decatur	112193	39.82	89.01	1921	0
IL	Dixon 1 NW	112348	41.83	89.52	1921	0
IL	Du Quoin 4 SE	112483	38.00	89.25	1921	1
IL	Effingham	112687	39.12	88.34	1921	1
IL	Fairfield	112931	38.37	88.31	1921	1
IL	Flora	113109	38.67	88.56	1921	3
IL	Galva	113335	41.16	90.04	1921	0
IL	Greenville 1 E	113693	38.88	89.40	1921	3
IL	Griggsville	113717	39.71	90.72	1921	2
IL	Harrisburg	113879	37.75	88.55	1921	0
IL	Hillsboro	114108	39.15	89.48	1921	1
IL	Hoopeston	114198	40.46	87.66	1921	0
IL	Jacksonville	114442	39.72	90.19	1921	0
IL	La Harpe	114823	40.58	90.97	1921	0
IL	Lincoln	115079	40.14	89.37	1921	1
IL	Marengo	115326	42.25	88.60	1921	2
IL	Mc Leansboro	115515	38.09	88.54	1921	0
IL	Minonk	115712	40.89	89.04	1921	6
IL	Monmouth	115768	40.92	90.63	1921	0
IL	Morrison	115833	41.82	89.97	1921	1
IL	Mount Carroll	115901	42.08	89.98	1921	1
IL	Mt Vernon	115943	38.34	88.86	1921	1
IL	Olney	116446	38.71	88.17	1921	3
IL	Ottawa 4 SW	116526	41.33	88.92	1921	1
IL	Palestine	116558	39.00	87.61	1921	0
IL	Pana	116579	39.37	89.07	1921	0
IL	Paris Waterworks	116610	39.63	87.70	1921	1
IL	Pontiac	116910	40.87	88.62	1921	1
IL	Rushville	117551	40.11	90.57	1921	1
IL	Sparta	118147	38.13	89.72	1921	0
IL	Urbana	118740	40.07	88.21	1921	0
IL	Walnut	118916	41.54	89.59	1921	1
IL	White Hall 1 E	119241	39.43	90.38	1921	0
IL	Windsor	119354	39.42	88.59	1921	0
IN	Angola	120200	41.62	84.97	1921	6
IN	Berne	120676	40.66	84.94	1921	0
IN	Bloomington	120784	39.16	86.51	1921	3
IN	Columbus	121747	39.19	85.91	1921	0

STATE	NAME	ID NO.	LAT.	LONG.	STRT	%MSG
IN	Delphi 3 NNE	122149	40.62	86.67	1921	2
IN	Farmland	122825	40.25	85.14	1921	11
IN	Kokomo 7 SE	124662	40.42	86.05	1921	18
IN	La Porte	124837	41.59	86.71	1921	1
IN	Madison	125237	38.72	85.39	1921	5
IN	Marion	125337	40.56	85.66	1921	0
IN	Mount Vernon	126001	37.94	87.87	1921	0
IN	Bedford	126580	38.87	86.54	1921	0
IN	Paoli	126705	38.55	86.48	1921	2
IN	Plymouth	127028	41.32	86.31	1921	0
IN	Princeton	127125	38.34	87.57	1921	1
IN	Rockville	127522	39.77	87.23	1921	2
IN	Rushville	127646	39.59	85.44	1921	3
IN	Scottsburg	127875	38.70	85.77	1921	0
IN	Seymour	127935	38.97	85.89	1921	0
IN	Valparaiso	128999	41.51	87.02	1921	0
IN	Vevay	129080	38.75	85.07	1921	2
IN	Washington	129253	38.65	87.17	1921	1
IN	W Laf Agron	129430	40.46	87.00	1921	2
IN	Wheatfield 2 NNW	129511	41.23	87.07	1921	2
IN	Whitestown	129557	40.00	86.32	1921	0
IA	Algona	130133	43.06	94.29	1921	2
IA	Atlantic	130364	41.41	95.00	1921	2
IA	Cedar Rapids No 1	131319	42.03	91.58	1921	2
IA	Clarinda	131533	40.72	95.02	1921	1
IA	Corning	131833	41.00	94.75	1921	2
IA	Denison	132171	42.02	95.32	1921	1
IA	Fairfield	132789	41.02	91.94	1921	0
IA	Fayette	132864	42.82	91.79	1921	1
IA	Glenwood 3sw	133290	41.00	95.77	1921	2
IA	Grinnell	133473	41.71	92.72	1921	24
IA	Guthrie Center	133509	41.68	94.52	1921	7
IA	Hampton	133584	42.75	93.20	1924	10
IA	Indianola	134063	41.37	93.55	1921	0
IA	Keosauqua	134389	40.73	91.97	1921	2
IA	Le Mars	134735	42.80	96.17	1921	0
IA	Logan	134894	41.63	95.82	1921	0
IA	Maquoketa 2 W	135131	42.07	90.70	1925	11
IA	Marshalltown	135198	42.07	92.93	1921	0
IA	Mason City	135230	43.15	93.20	1921	2
IA	Mount Ayr	135769	40.64	94.29	1921	5
IA	New Hampton	135952	43.04	92.31	1921	4
IA	Onawa	136243	42.02	96.10	1921	3
IA	Oskaloosa	136327	41.31	92.64	1921	2
IA	Rock Rapids	137147	43.42	96.16	1921	1
IA	Rockwell City	137161	42.40	94.62	1921	3
IA	Spencer 1 N	137844	43.17	95.15	1921	5
IA	Storm Lake	137979	42.62	95.17	1921	1
IA	Tipton	138266	41.77	91.11	1921	1

STATE	NAME	ID NO.	LAT.	LONG.	STRT	%MSG
IA	Washington	138688	41.28	91.68	1921	0
IA	Webster City	138806	42.47	93.80	1921	1
KY	Ashland	150254	38.45	82.62	1921	1
KY	Bowling Green FAA AP	150909	36.97	86.42	1921	0
KY	Carrollton Lock 1	151345	38.65	85.15	1921	1
KY	Cynthiana	151998	38.37	84.29	1921	5
KY	Farmers 2S(Cave Runl)	152791	38.12	83.55	1921	1
KY	Franklin	153036	36.71	86.56	1921	19
KY	Greensburg	153430	37.25	85.50	1921	1
KY	Greenville 2 W	153451	37.18	87.22	1921	8
KY	Henderson	153762	37.75	87.62	1921	12
KY	Hopkinsville	153994	36.83	87.50	1921	0
KY	Lexington WSO AP	154746	38.03	84.60	1921	1
KY	Middlesboro	155389	36.60	83.73	1921	5
KY	Paducah Sewage Plant	156117	37.10	88.60	1921	30
KY	Shelbyville	157324	38.19	85.19	1921	1
MI	Adrian 2 NNE	200032	41.92	84.02	1921	2
MI	Allegan	200128	42.51	85.82	1921	3
MI	Alma	200146	43.37	84.66	1921	1
MI	Alpena WSO AP	200164	45.07	83.57	1921	1
MI	Ann Arbor U Of Mich	200230	42.30	83.72	1921	1
MI	Battle Creek	200552	42.33	85.18	1921	1
MI	Benton Harbor Airport	200710	42.13	86.43	1921	2
MI	Bergland Dam	200718	46.58	89.55	1921	23
MI	Big Rapids Waterworks	200779	43.70	85.48	1921	0
MI	Cadillac	201176	44.27	85.40	1921	1
MI	Chatham	201484	46.34	86.92	1926	8
MI	Cheboygan	201492	45.65	84.47	1921	2
MI	Coldwater	201675	41.94	85.00	1921	1
MI	Hart	203632	43.69	86.36	1921	0
MI	Houghton FAA Airport	203908	47.17	88.50	1921	7
MI	Iron Mtn.-Kingsford Wwtp	204090	45.78	88.08	1921	0
MI	Ironwood	204104	46.46	90.17	1921	1
MI	Jackson FAA AP	204150	42.26	84.45	1921	1
MI	Ludington 4 SE	204954	43.90	86.40	1921	3
MI	Manistee	205065	44.22	86.28	1921	2
MI	Newberry State Hosp	205816	46.33	85.50	1921	0
MI	Saginaw FAA Airport	207227	43.53	84.08	1921	0
MI	Traverse City FAA AP	208251	44.73	85.58	1921	0
MN	Ada	210018	47.30	96.52	1921	5
MN	Albert Lea	210075	43.61	93.41	1921	1
MN	Argyle	210252	48.32	96.72	1921	10
MN	Baudette	210515	48.72	94.62	1921	4
MN	Bemidji	210643	47.50	94.92	1921	5
MN	Canby	211263	44.72	96.28	1921	10
MN	Cloquet	211630	46.70	92.52	1921	0
MN	Collegeville St John	211691	45.58	94.40	1921	9

STATE	NAME	ID NO.	LAT.	LONG.	STRT	%MSG
MN	Crookston NW Exp Sta	211891	47.80	96.62	1921	0
MN	Detroit Lakes	212142	46.81	95.69	1921	2
MN	Fosston	212916	47.57	95.72	1921	6
MN	Grand Marias	213282	47.72	90.34	1921	4
MN	Grand Meadow	213290	43.70	92.57	1921	0
MN	Grand Rapids	213303	47.22	93.50	1921	0
MN	Hallock	213455	48.77	96.95	1921	2
MN	Itasca Univ Of Minn	214106	47.22	95.20	1921	0
MN	Litchfield	214778	45.11	94.52	1941	35
MN	Little Falls 1 N	214793	45.98	94.35	1921	2
MN	Minneapolis RFC	215435	44.88	93.22	1921	0
MN	Montevideo	215563	44.92	95.75	1921	1
MN	Mora	215615	45.88	93.30	1921	1
MN	Morris	215638	45.57	95.87	1921	0
MN	New London	215842	45.30	94.93	1921	11
MN	New Ulm	215887	44.29	94.44	1921	0
MN	Pine River Dam	216547	46.67	94.12	1921	0
MN	Pipestone	216565	44.02	96.32	1921	4
MN	Pokegama Dam	216612	47.25	93.58	1921	0
MN	Red Lake Indian Agcy	216795	47.87	95.03	1921	30
MN	Redwood Falls FAA AP	216835	44.55	95.08	1921	0
MN	Rochester WSO AP	217004	43.92	92.50	1928	16
MN	Roseau 1 E	217087	48.85	95.77	1921	9
MN	St Cloud WSO AP	217294	45.55	94.07	1921	4
MN	Tracy	218323	44.23	95.62	1921	4
MN	Virginia	218543	47.50	92.55	1921	1
MN	Wadena	218579	46.39	95.14	1921	7
MN	Warroad	218679	48.92	95.32	1921	4
MN	Waseca	218692	44.06	93.51	1921	0
MN	Willmar State Hospital	219004	45.13	95.02	1921	0
MN	Windom	219033	43.87	95.10	1941	36
MN	Winnebago	219046	43.77	94.17	1921	0
MN	Winnibigoshish Dam	219059	47.43	94.05	1921	1
MN	Winona	219067	44.05	91.63	1921	4
MN	Zumbrota	219249	44.29	92.66	1921	2
MO	Arcadia	230224	37.58	90.62	1921	1
MO	Bethany	230608	40.25	94.04	1921	5
MO	Bolivar	230789	37.59	93.41	1921	16
MO	Brunswick	231037	39.42	93.12	1921	3
MO	Caruthersville	231364	36.19	89.66	1921	2
MO	Clinton	231711	38.39	93.76	1921	3
MO	Farmington	232809	37.69	90.37	1921	2
MO	Fulton	233079	38.84	91.94	1921	3
MO	Jefferson City	234271	38.57	92.14	1921	3
MO	Kirksville Radio KIRX	234544	40.22	92.58	1921	3

STATE	NAME	ID NO.	LAT.	LONG.	STRT	%MSG
MO	Lebanon 2 W	234825	37.67	92.65	1921	1
MO	Lexington	234904	39.20	93.87	1921	4
MO	Lockwood	235027	37.37	93.94	1921	0
MO	Maryville 2 E	235340	40.35	94.83	1921	1
MO	Mountain Grove	235834	37.14	92.26	1921	0
MO	Neosho	235976	36.86	94.36	1921	0
MO	Nevada	235987	37.84	94.39	1921	1
MO	Poplar Bluff	236791	36.76	90.41	1921	2
MO	Rolla	237263	37.94	91.76	1921	4
MO	St Charles	237397	38.78	90.50	1921	3
MO	Salem	237506	37.62	91.52	1921	3
MO	Seligman	237645	36.52	93.93	1921	7
MO	Steffenville	238051	39.96	91.87	1921	1
MO	Tarkio	238289	40.41	95.39	1921	7
MO	Trenton	238444	40.08	93.63	1921	2
MO	Unionville	238523	40.48	93.00	1921	3
MO	Warrensburg	238712	38.72	93.71	1921	4
MO	Warrenton 1 N	238725	38.82	91.13	1921	12
OH	Cadiz	331152	40.27	81.00	1921	2
OH	Canfield 1 S	331245	41.02	80.77	1921	2
OH	Greenville Water Plant	333375	40.10	84.65	1921	1
OH	Hillsboro	333758	39.20	83.62	1921	0
OH	Hiram	333780	41.30	81.15	1921	2
OH	Jackson 2 NW	334004	39.07	82.65	1921	0
OH	Kenton	334189	40.65	83.60	1921	2
OH	Marysville	334979	40.23	83.37	1921	0
OH	Mc Connellsville Lk 7	335041	39.65	81.85	1921	1
OH	Millport 2 NW	335315	40.72	80.90	1921	1
OH	Norwalk Wwtp	336118	41.27	82.62	1921	1
OH	Wooster Exp Station	339312	40.78	81.92	1921	0
OH	Youngstown WSO AP	339406	41.25	80.67	1921	1
WI	Antigo	470239	45.12	89.14	1921	0
WI	Ashland	470349	46.56	90.96	1921	1
WI	Beloit	470696	42.50	89.03	1921	3
WI	Darlington	472001	42.67	90.11	1921	1
WI	Fond Du Lac	472839	43.80	88.45	1921	1
WI	Hancock	473405	44.11	89.52	1921	1
WI	Long Lake Dam	474829	45.90	89.13	1921	0
WI	Manitowoc	475017	44.10	87.68	1921	0
WI	Marshfield Exp Farm	475120	44.65	90.13	1921	0
WI	Medford	475255	45.13	90.35	1921	1
WI	Merrill	475364	45.18	89.68	1921	3
WI	Minocqua Dam	475516	45.88	89.73	1921	0
WI	Neillsville	475808	44.52	90.62	1921	1
WI	New London	475932	44.37	88.72	1921	1
WI	Oconto 4 W	476208	44.90	87.95	1921	2
WI	Park Falls	476398	45.93	90.45	1921	3

STATE	NAME	ID NO.	LAT.	LONG.	STRT	%MSG
WI	Plymouth	476678	43.75	87.98	1921	3
WI	Prentice No. 2	476859	45.52	90.28	1921	1
WI	Sheboygan	477725	43.75	87.72	1921	1
WI	Spooner Exp Farm	478027	45.82	91.88	1921	0
WI	Stanley	478110	44.97	90.93	1921	5
WI	Sturgeon Bay	478267	44.86	87.32	1921	0
WI	Viroqua	478827	43.56	90.89	1921	3
WI	Watertown	478919	43.17	88.72	1921	1
WI	Wausau FAA Airport	478968	44.92	89.62	1921	0

APPENDIX D

STREAMGAGING-PRECIPIATION STATION ASSOCIATIONS

The following table lists the precipitation stations located within or near the drainage basin for each streamgaging station. The name of the streamgaging station is followed by a list of identification numbers for the precipitation stations.

STREAMGAUGING STATION	CLIMATE STATION ID
L BEAVER C NR EAST LIVERPOOL OH	331245 335315 339406
RACCOON C AT ADAMSVILLE OH	334004
SCIOTO R NR PROSPECT OH	334189 334979
BIG DARBY C AT DARBYVILLE OH	334979
OHIO BRUSH C NR WEST UNION OH	333758
LICKING RIVER AT CATAWBA, KY.	151998 152791
STILLWATER R AT PLEASANT HILL OH	333375
WHITewater RIVER NEAR ALPINE, IND	122825
GREEN RIVER AT MUNFORDVILLE, KY.	153430
MISSISSINEWA RIVER AT MARION, IND.	122825
WABASH RIVER AT LAFAYETTE IND	120334 120676 122149 122825 124181 124662 125337 127028 129430 129511
WABASH RIVER AT MONTEZUMA, IND.	120676 122149 122825 124181 124662 125337 127028 127522 129430 129511 129557
WABASH RIVER AT TERRE HAUTE, IND.	112140 114198 116610 118740 120676 122149 122825 124181 124662 125337 127028 127522 129430 129511 129557
WABASH RIVER AT VINCENNES, IND.	111436 112140 114198 116558 116610 118740 120676 120784 122149 122825 124181 124662 125337 127028 127522 129430 129511 129557
EMBARRAS RIVER AT STE. MARIE, IL	111436 112140 112687 114198 116610 118740

WHITE RIVER AT NEWBERRY, IND.	120784	121747	122825
	124662	127522	127646
	129557		
EAST FORK WHITE RIVER AT SEYMOUR IND	121747	125237	127646
	127875	127935	
EAST FORK WHITE RIVER AT SHOALS, IND	120784	121747	126580
	126705	127646	127875
	127935		
WHITE RIVER AT PETERSBURG IND	120784	121747	122825
	124662	126580	126705
	127522	127646	127875
	127935	129253	129557
WABASH RIVER AT MT. CARMEL, ILL.	111436	112140	112687
	114198	116446	116558
	116610	118740	120334
	120676	120784	122149
	122825	124181	124662
	125337	126580	127028
	127125	127522	129253
	129430	129511	129557
LITTLE WABASH RIVER BELOW CLAY CITY,	111436	112687	113109
	116446	116579	119354
SKILLET FORK AT WAYNE CITY, IL	112931	113109	115943
	116446		
BRULE RIVER NEAR FLORENCE, WI	204090	474829	475516
OCONTO RIVER NEAR GILLETT, WI	470239	474829	476208
FOX RIVER AT BERLIN, WI	472839	473405	475017
	476678	477725	
WOLF RIVER NEAR SHAWANO, WI	470239	474829	475516
EMBARRASS RIVER NEAR EMBARRASS, WI	470239	475120	475255
	475364	475932	478968

WOLF RIVER AT NEW LONDON, WI	470239	474829	475120
	475364	475516	475932
	478968		
LITTLE WOLF RIVER AT ROYALTON, WI	475120	478968	
CEDAR CREEK NEAR CEDARBURG, WI	479050		
MILWAUKEE RIVER AT MILWAUKEE, WI	472839	476678	477725
MUSKEGON RIVER AT EVART.MICH.	200779		
MANISTEE RIVER NEAR SHERMAN, MI	201176	208251	
CASS RIVER AT FRANKENMUTH, MICH.	207227		
WILD RICE RIVER AT TWIN VALLEY, MN	210018	212142	212916
	213206	214106	
ROSEAU RIVER BELOW STATE DITCH 51 NR	210252	210515	210643
	213206	213455	216795
	217087	218679	
LITTLE FORK RIVER AT LITTLEFORK, MN	213303	216612	219059
BIG FORK RIVER AT BIG FALLS, MN	213303	216612	219059
CROW RIVER AT ROCKFORD, MN	211465	211691	214778
	215842	217294	219004
LAC QUI PARLE RIVER NEAR LAC QUI PAR	211263	215563	218429
REDWOOD RIVER NEAR REDWOOD FALLS, MN	216565	216835	218323
	218429		
COTTONWOOD RIVER NEAR NEW ULM, MN	216835	218323	219033

MISSISSIPPI RIVER AT ST. PAUL, MN	130133	210075	210643
	210939	211263	211374
	211465	211630	211691
	212142	212916	213206
	213303	213411	214106
	214778	214793	215435
	215563	215615	215638
	215842	215887	216547
	216565	216612	216795
	216835	217294	218323
	218429	218543	218579
	218692	219004	219033
	219046	219059	
ST. CROIX RIVER NEAR DANBURY, WI	470349	477892	478027
ST. CROIX RIVER AT ST. CROIX FALLS,	120676	122149	122825
	124181	124662	125337
	127028	127522	129430
	129511	129557	
MISSISSIPPI RIVER AT PRESCOTT, WI	130133	210018	210075
	210252	210515	210643
	211630	211691	211891
	212142	212916	213303
	213455	214106	214778
	214793	215012	215204
	215435	215563	215615
	215638	215887	216547
	216565	216612	216795
	216835	217087	217294
	218323	218429	218579
	218679	218692	219004
	219033	219046	219059
	219249	470349	477892
	478027		
JUMP RIVER AT SHELDON, WI	475255	476398	476859
BLACK RIVER AT NEILLSVILLE, WI	475255	475808	478110
ROOT RIVER NEAR LANESBORO, MN	213290	217004	219067
PRAIRIE RIVER NEAR MERRILL, WI	470239	475364	

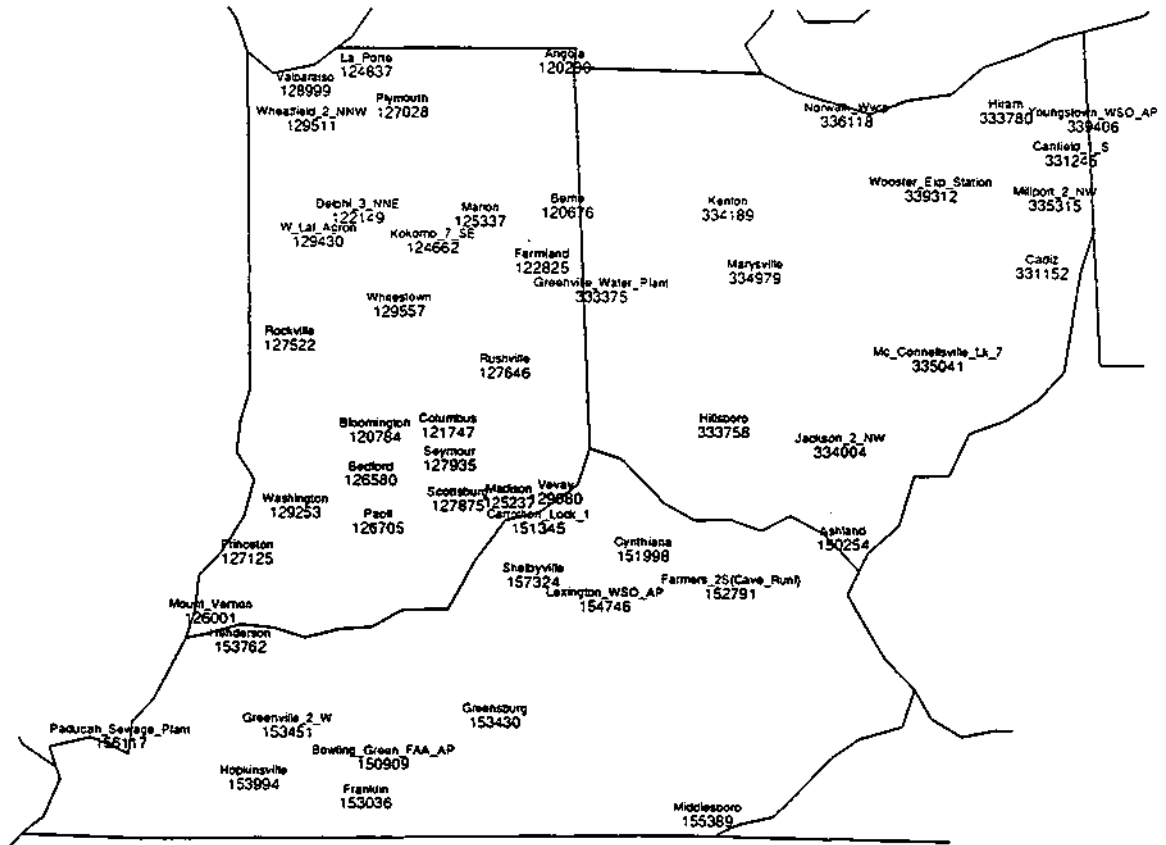
EAU CLAIRE RIVER AT KELLY, WI	470239	475120	475364
	478968		
BIG EAU PLEINE RIVER NEAR STRATFORD,	475120	475255	475364
	475808	478110	478968
TURKEY RIVER AT GARBER, IOWA	132864	135952	
MAQUOKETA RIVER NEAR MAQUOKETA, IOWA	132864	135131	
WAPSIPINICON R AT INDEPENDENCE, IOWA	132864	135952	
WAPSIPINICON RIVER NEAR DE WITT, IOW	131319	132864	135131
	135952	138266	
ROCK RIVER AT AFTON, WI	470696	472839	478919
PECATONICA RIVER AT FREEPORT, IL	472001		
SUGAR RIVER NEAR BRODHEAD, WI	470696		
IOWA RIVER AT MARSHALLTOWN, IOWA	133473	133584	134063
	135198	136327	138806
CEDAR RIVER NEAR AUSTIN, MN	210075	213290	
WINNEBAGO RIVER AT MASON CITY, IOWA	135230	210075	
CEDAR RIVER AT CEDAR RAPIDS, IOWA	131319	132864	133584
	135198	135230	135952
	210075	213290	217004
SOUTH SKUNK RIVER NEAR AMES, IOWA	138806		
SKUNK RIVER AT AUGUSTA, IOWA	132789	133473	134063
	134389	135198	136327
	138688	138806	
DES MOINES RIVER AT JACKSON, MN	219033	219170	
DES MOINES RIVER NR STRATFORD, IOWA	130133	137161	137844
	138806	218323	219033
	219046		

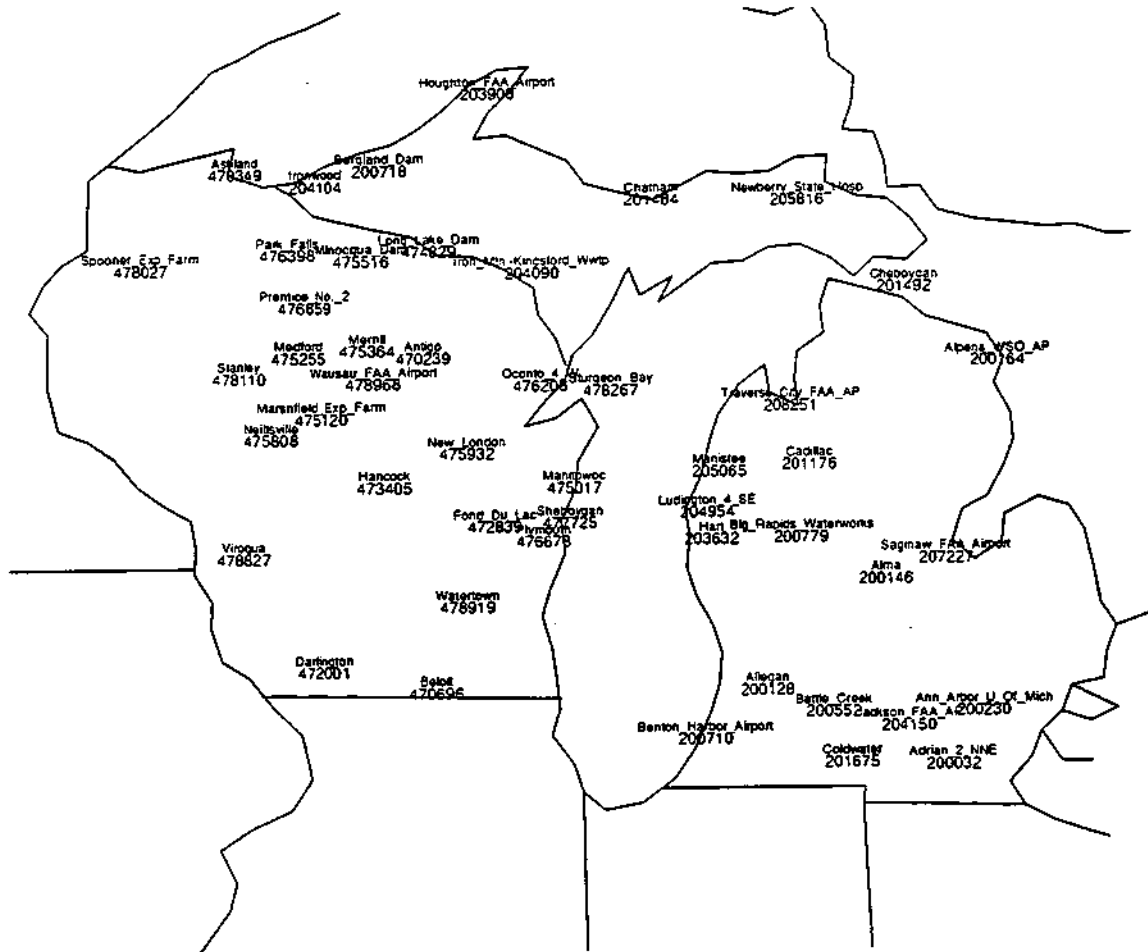
RACCOON RIVER AT VAN METER, IOWA	133509	137161	137979
KANKAKEE RIVER AT MOMENCE, IL	124837	127028	128999
	129511		
IROQUOIS RIVER AT IROQUOIS, IL	12	9511	
IROQUOIS RIVER NEAR CHEBANSE, IL	112140	114198	129430
	129511		
SPOON RIVER AT SEVILLE, IL	113335	115768	118916
SANGAMON RIVER AT MONTICELLO, IL	115712	116910	118740
LA MOINE RIVER AT RIPLEY, IL	114823	115768	117551
MACOUPIN CREEK NEAR KANE, IL	111280	114108	119241
SHOAL CREEK NEAR BREESE, IL	113693	114108	
NISHNABOTNA RIVER ABOVE HAMBURG, IOW	130364	131533	131833
	132171	133290	133509
	134894		
GRAND RIVER NEAR GALLATIN MO	131533	135769	230608
	235340		
GASCONADE RIVER AT JEROME MO	234825	235834	237263
	237506		

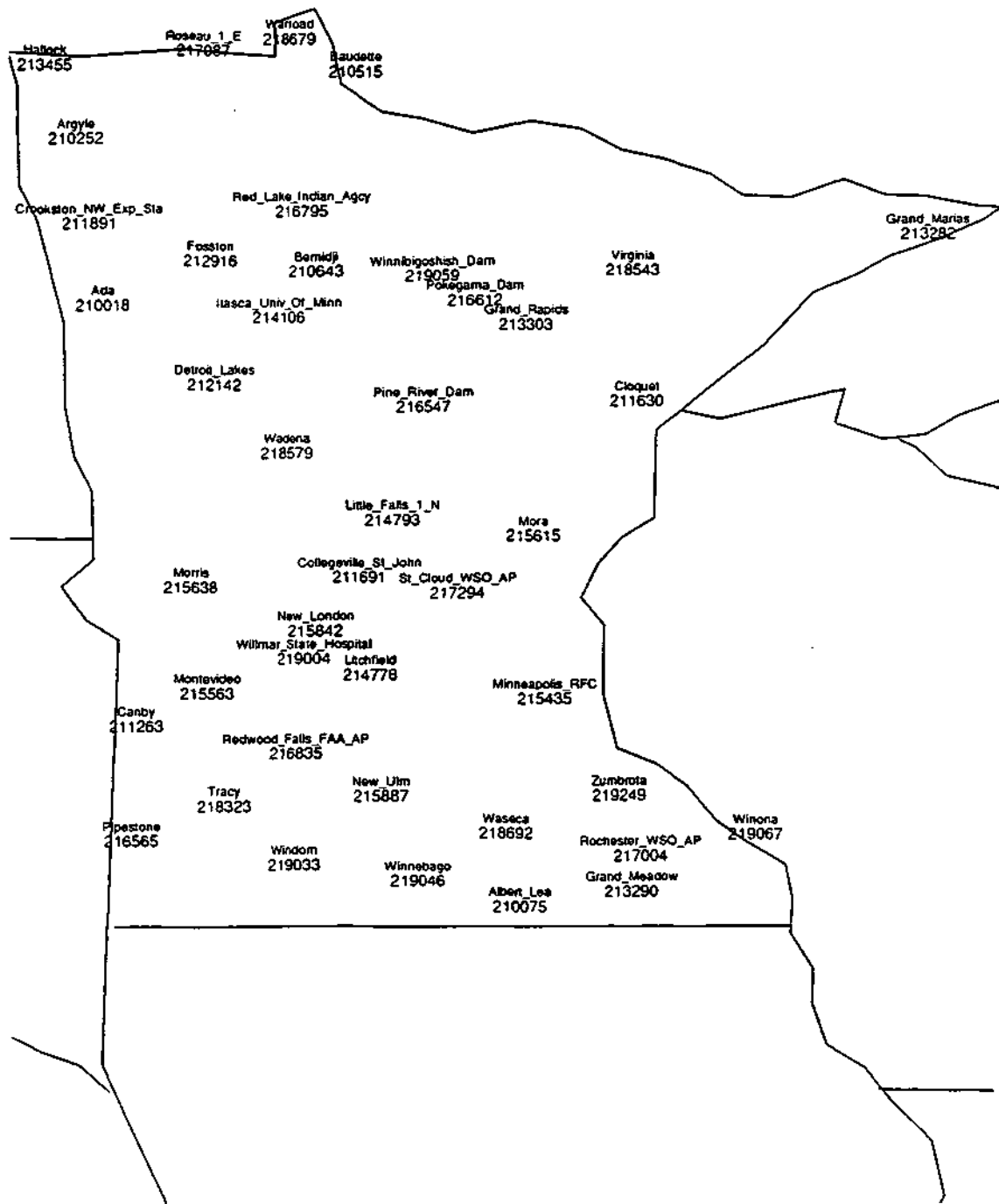
APPENDIX E

LOCATIONS OF PRECIPITATION STATIONS

The following maps show the names and station identification numbers of each precipitation station.



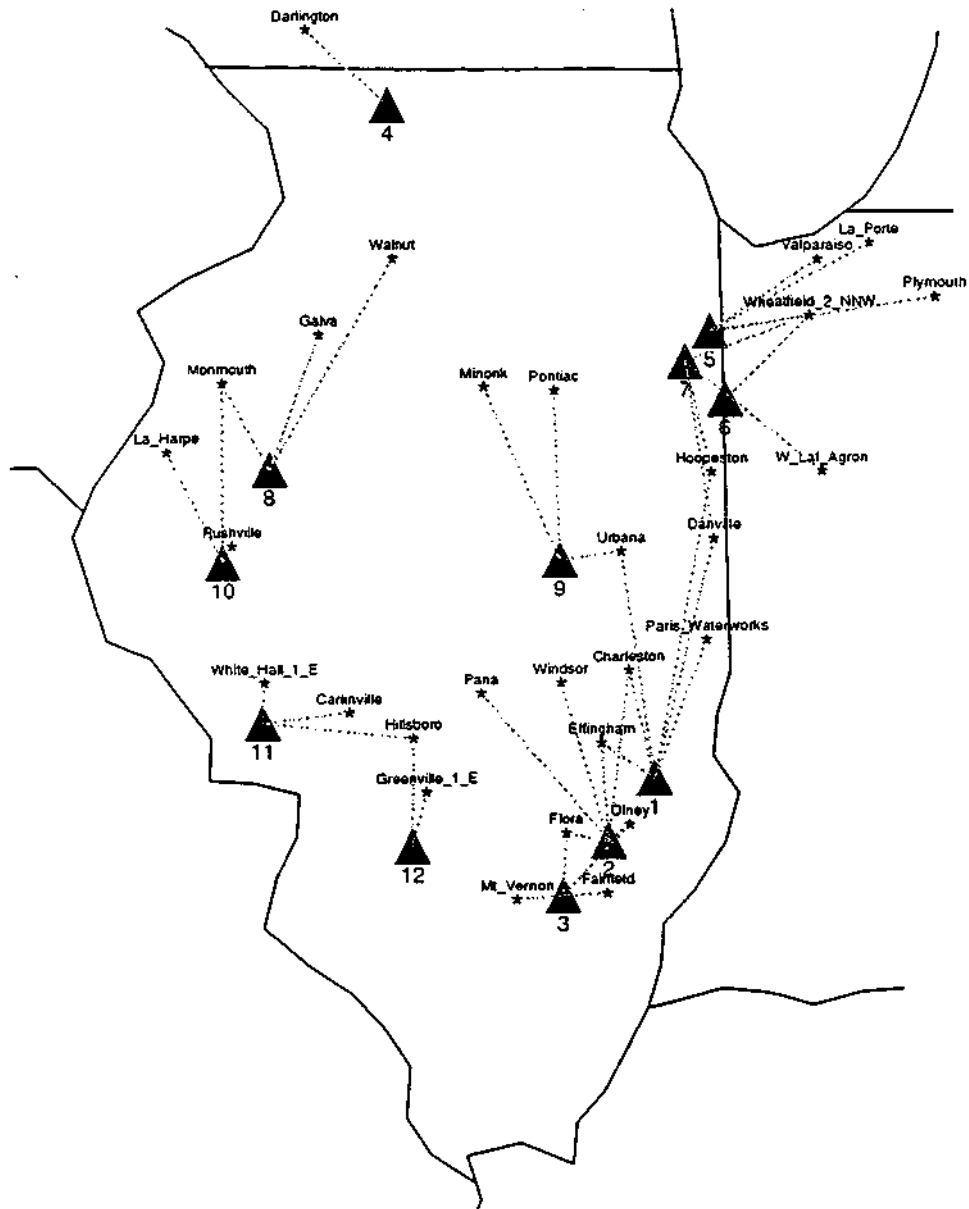




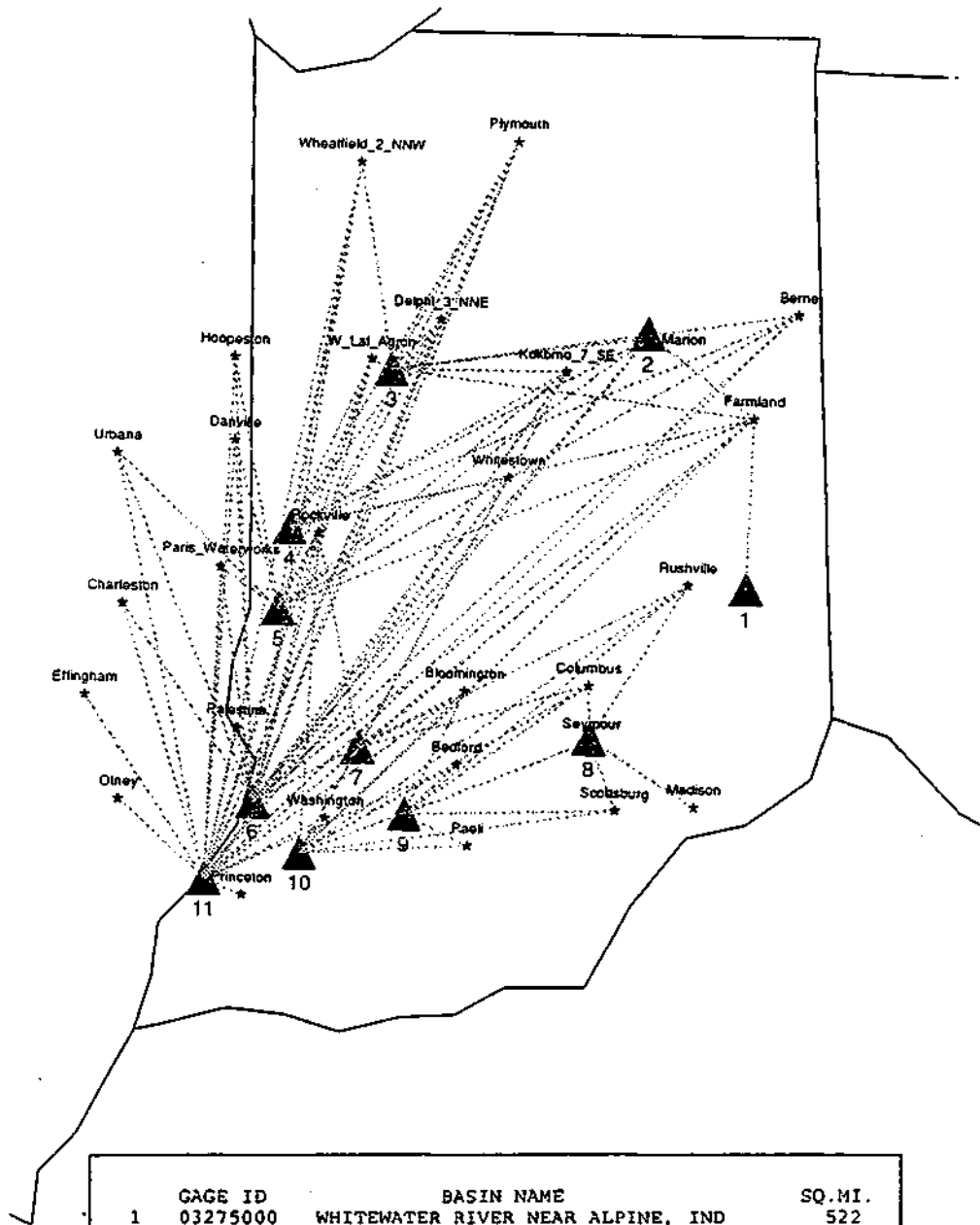
APPENDIX F

LOCATIONS OF ASSOCIATED PRECIPITATION STATIONS

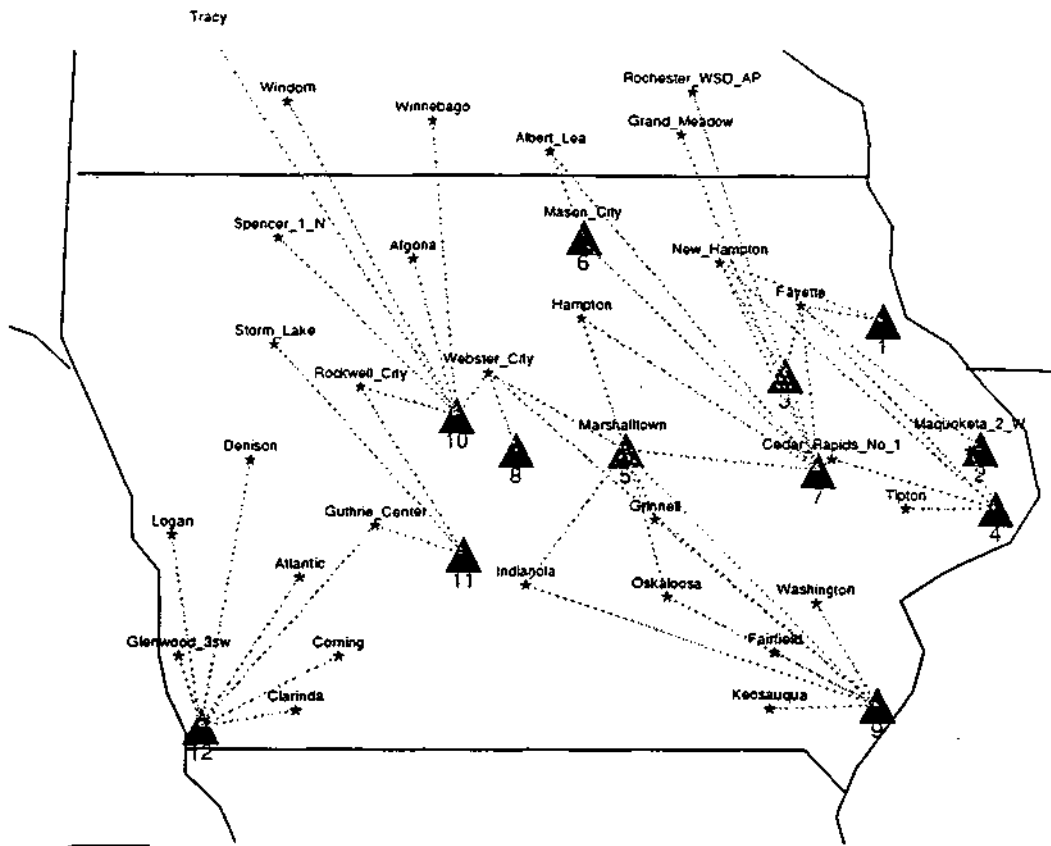
The following state maps indicate the locations of the precipitation stations associated with each basin in the study. The basins are indicated by their numbers in the accompanying table. Dotted lines indicate association. In some cases, a precipitation station is co-located with a streamgage and so may be covered by the triangular gage symbol. These precipitation stations correspond to the list given in Appendix C.



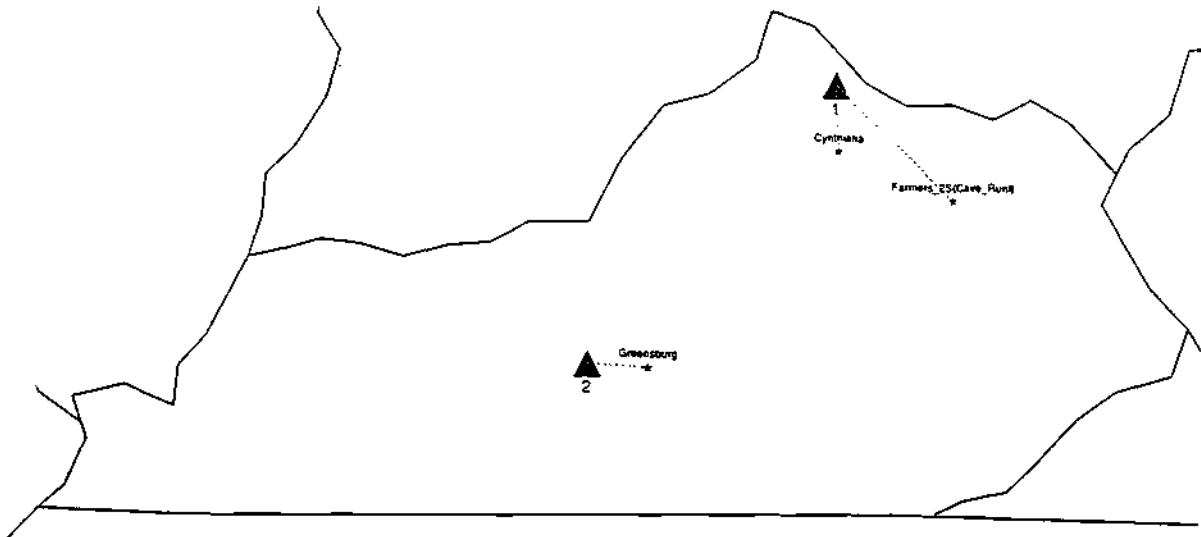
	GAGE ID	BASIN NAME	SQ. MI.
1	03345500	EMBARRAS RIVER AT STE. MARIE, IL	1516
2	03379500	LITTLE WABASH RIVER BELOW CLAY CITY, IL	1131
3	03380500	SKILLET FORK AT WAYNE CITY, IL	464
4	05435500	PECATONICA RIVER AT FREEPORT, IL	1326
5	05520500	KANKAKEE RIVER AT MOMENCE, IL	2294
6	05525000	IROQUOIS RIVER AT IROQUOIS, IL	686
7	05526000	IROQUOIS RIVER NEAR CHEBANSE, IL	2091
8	05570000	SPOON RIVER AT SEVILLE, IL	1636
9	05572000	SANGAMON RIVER AT MONTICELLO, IL	550
10	05585000	LA MOINE RIVER AT RIPLEY, IL	1293
11	05587000	MACOUPIN CREEK NEAR KANE, IL	868
12	05594000	SHOAL CREEK NEAR BREESE, IL	735



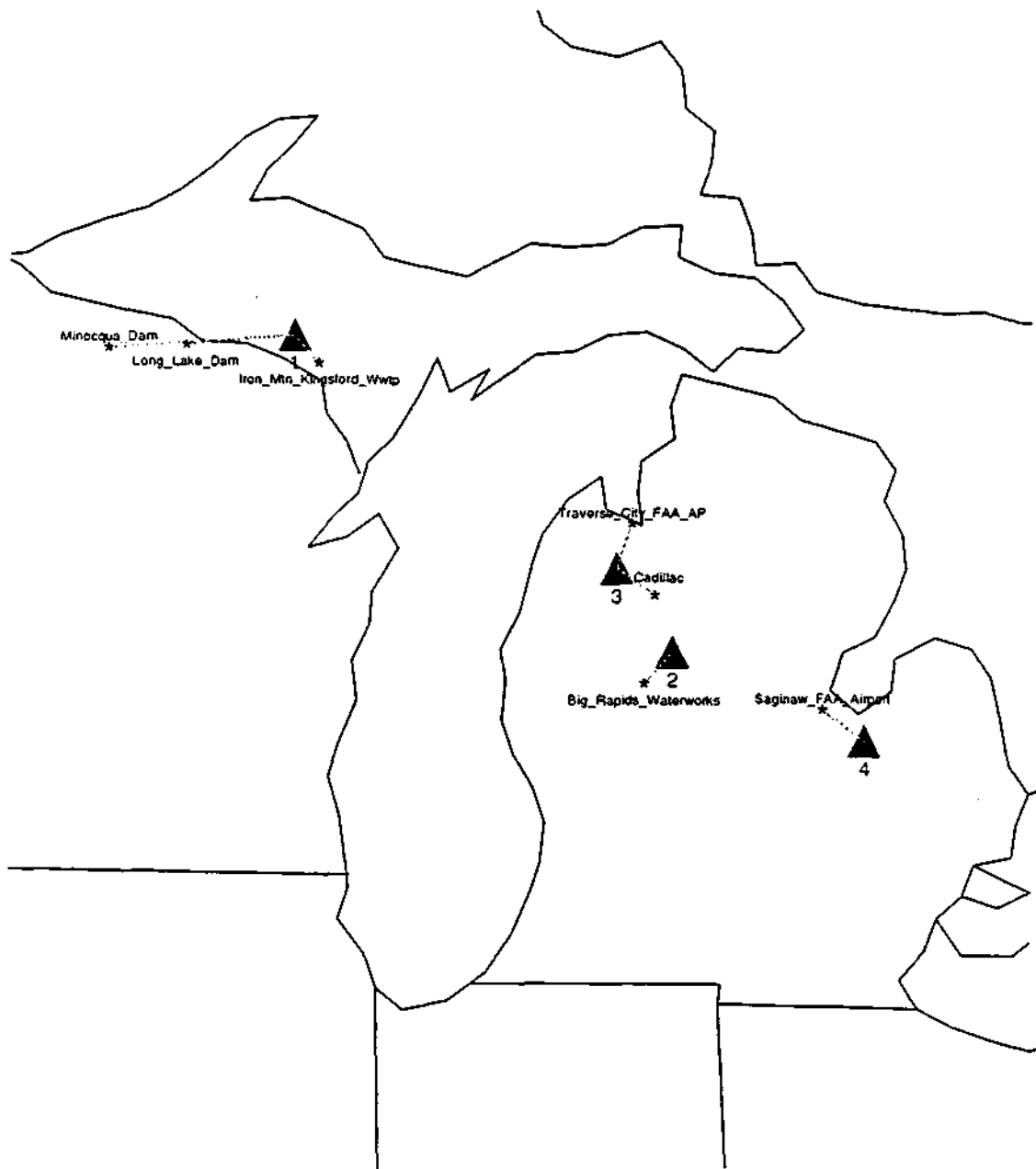
GAGE ID	BASIN NAME	SQ. MI.
1	03275000 WHITWATER RIVER NEAR ALPINE, IND	522
2	03326500 MISSISSINAWA RIVER AT MARION, IND.	682
3	03335500 WABASH RIVER AT LAFAYETTE IND	7267
4	03340500 WABASH RIVER AT MONTEZUMA, IND.	11118
5	03341500 WABASH RIVER AT TERRE HAUTE, IND.	12265
6	03343000 WABASH RIVER AT VINCENNES, IND.	13706
7	03360500 WHITE RIVER AT NEWBERRY, IND.	4688
8	03365500 EAST FORK WHITE RIVER AT SEYMOUR IND	2341
9	03375500 EAST FORK WHITE RIVER AT SHOALS, IND.	4927
10	03374000 WHITE RIVER AT PETERSBURG IND	11125
11	03377500 WABASH RIVER AT MT. CARMEL, ILL.	28635



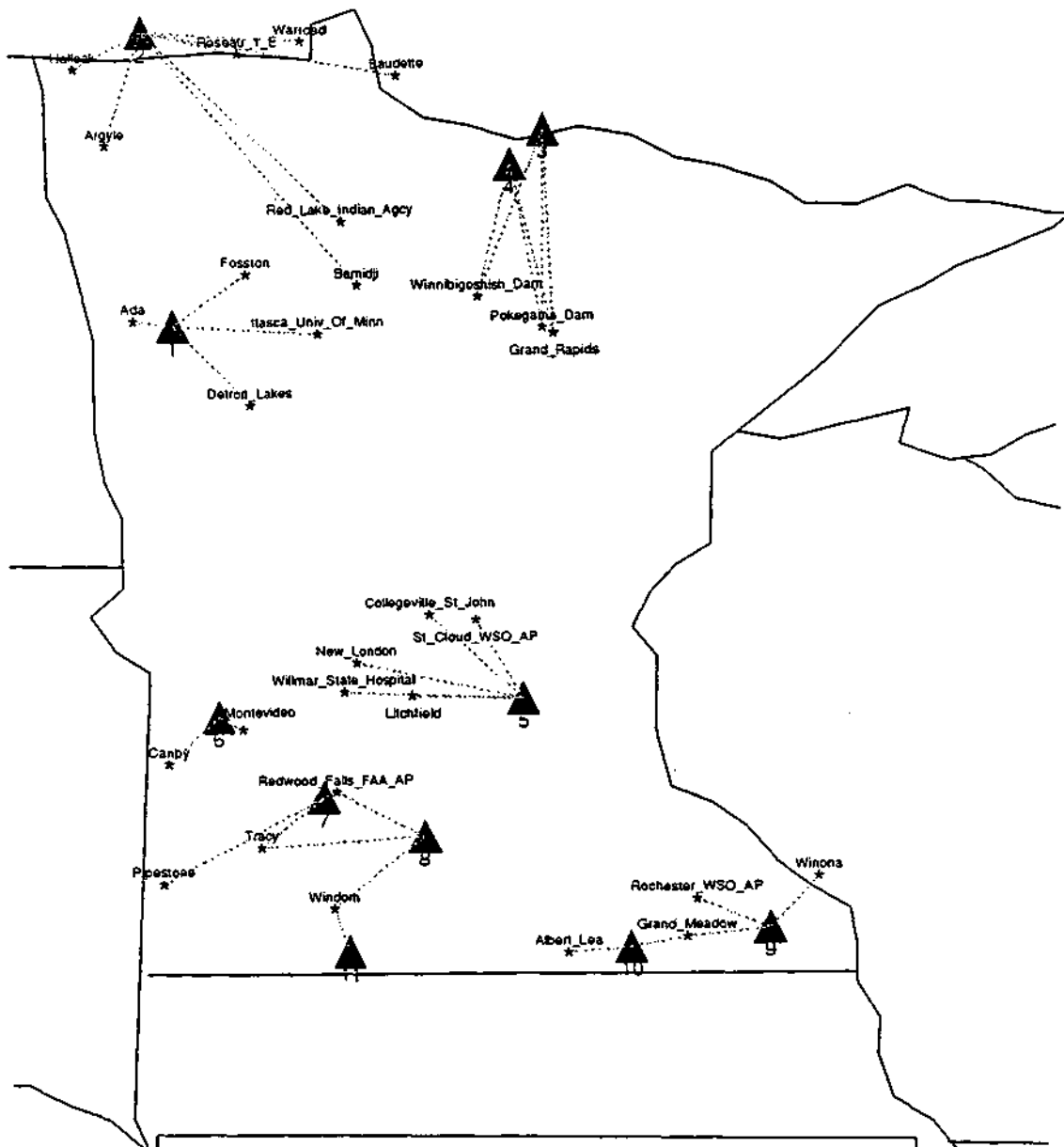
GAGE ID	BASIN NAME	SQ. MI.
1	TURKEY RIVER AT GARBER, IOWA	1545
2	MAQUOKETA RIVER NEAR MAQUOKETA, IOWA	1553
3	WAPSIPINICON R AT INDEPENDENCE, IOWA	1048
4	WAPSIPINICON RIVER NEAR DE WITT, IOWA	2330
5	IOWA RIVER AT MARSHALLTOWN, IOWA	1564
6	WINNEBAGO RIVER AT MASON CITY, IOWA	526
7	CEDAR RIVER AT CEDAR RAPIDS, IOWA	6510
8	SOUTH SKUNK RIVER NEAR AMES, IOWA	315
9	SKUNK RIVER AT AUGUSTA, IOWA	4303
10	DES MOINES RIVER NR STRATFORD, IOWA	5452
11	RACCOON RIVER AT VAN METER, IOWA	3441
12	NISHNABOTNA RIVER ABOVE HAMBURG, IOWA	2906



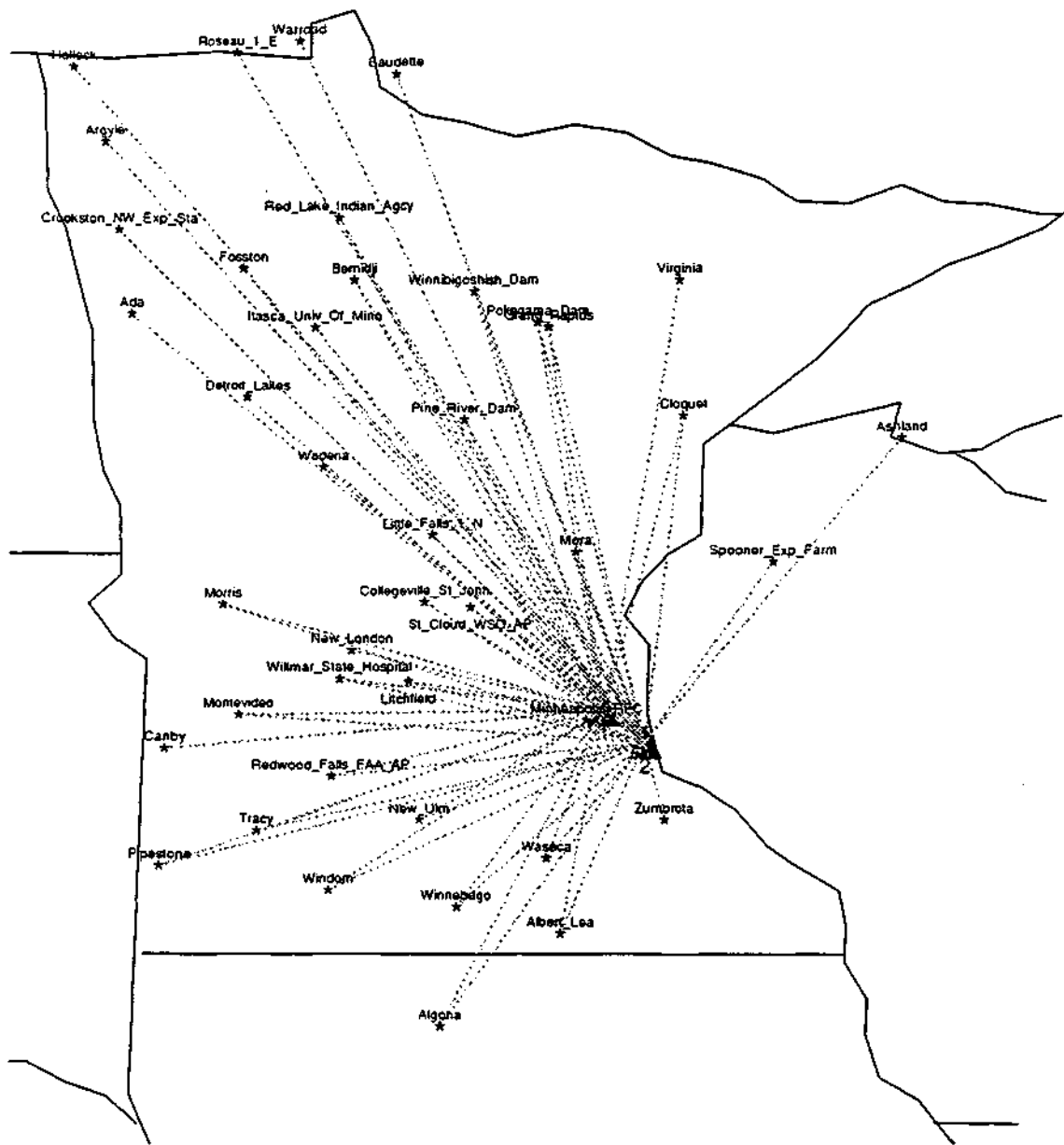
	GAGE ID	BASIN NAME	SQ. MI.
1	03253900	LICKING RIVER AT CATAMBA, KY.	3100
2	03308500	GREEN RIVER AT HUNFORDVILLE, KY.	1673



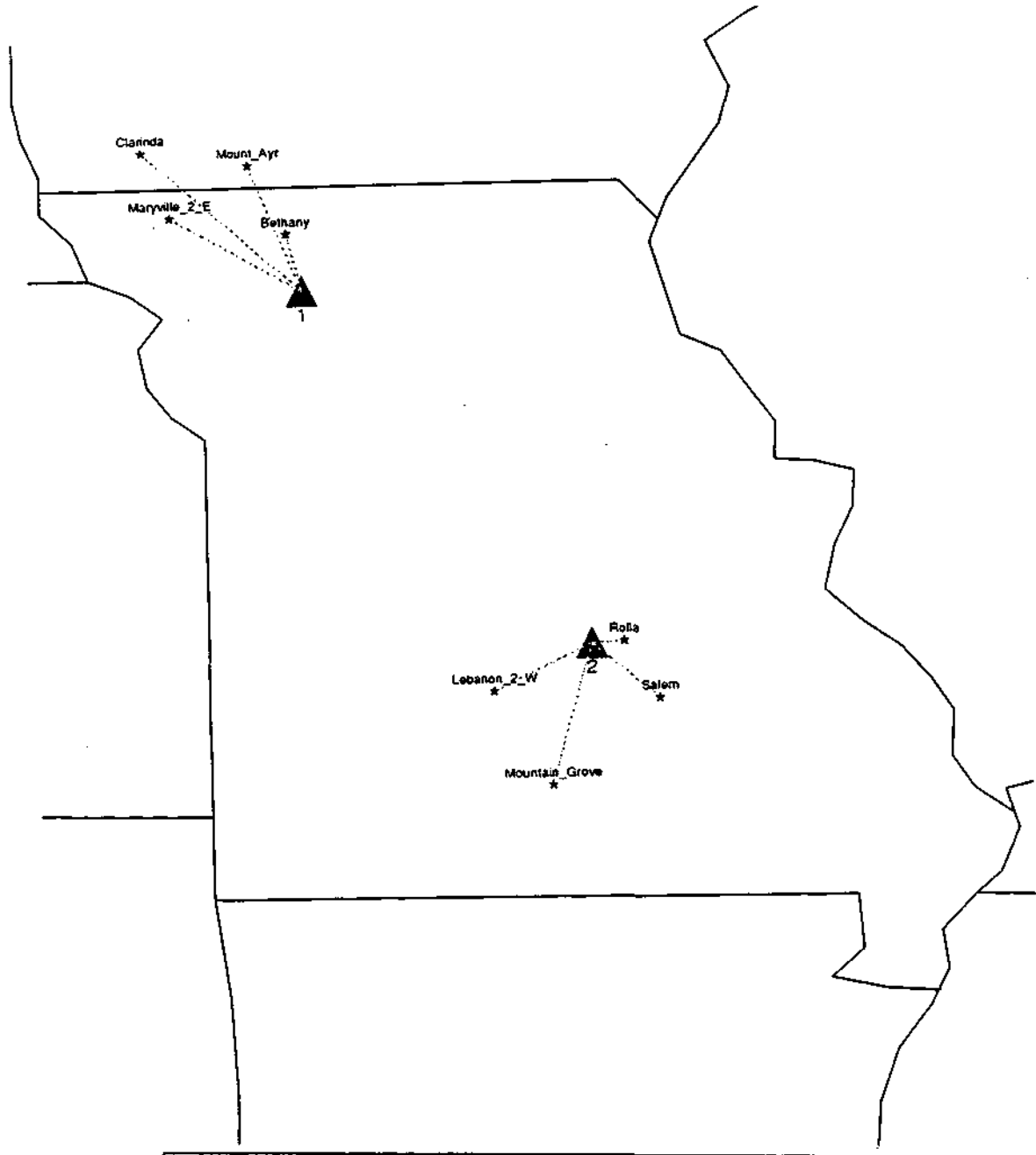
	GAGE ID	BASIN NAME	SQ.MI.
1	04061000	BRULE RIVER NEAR FLORENCE, WI	389
2	04121500	MUSKEGON RIVER AT EVART, MICH.	1450
3	04124000	MANISTEE RIVER NEAR SHERMAN, MI	857
4	04151500	CASS RIVER AT FRANKENMUTH, MICH.	841



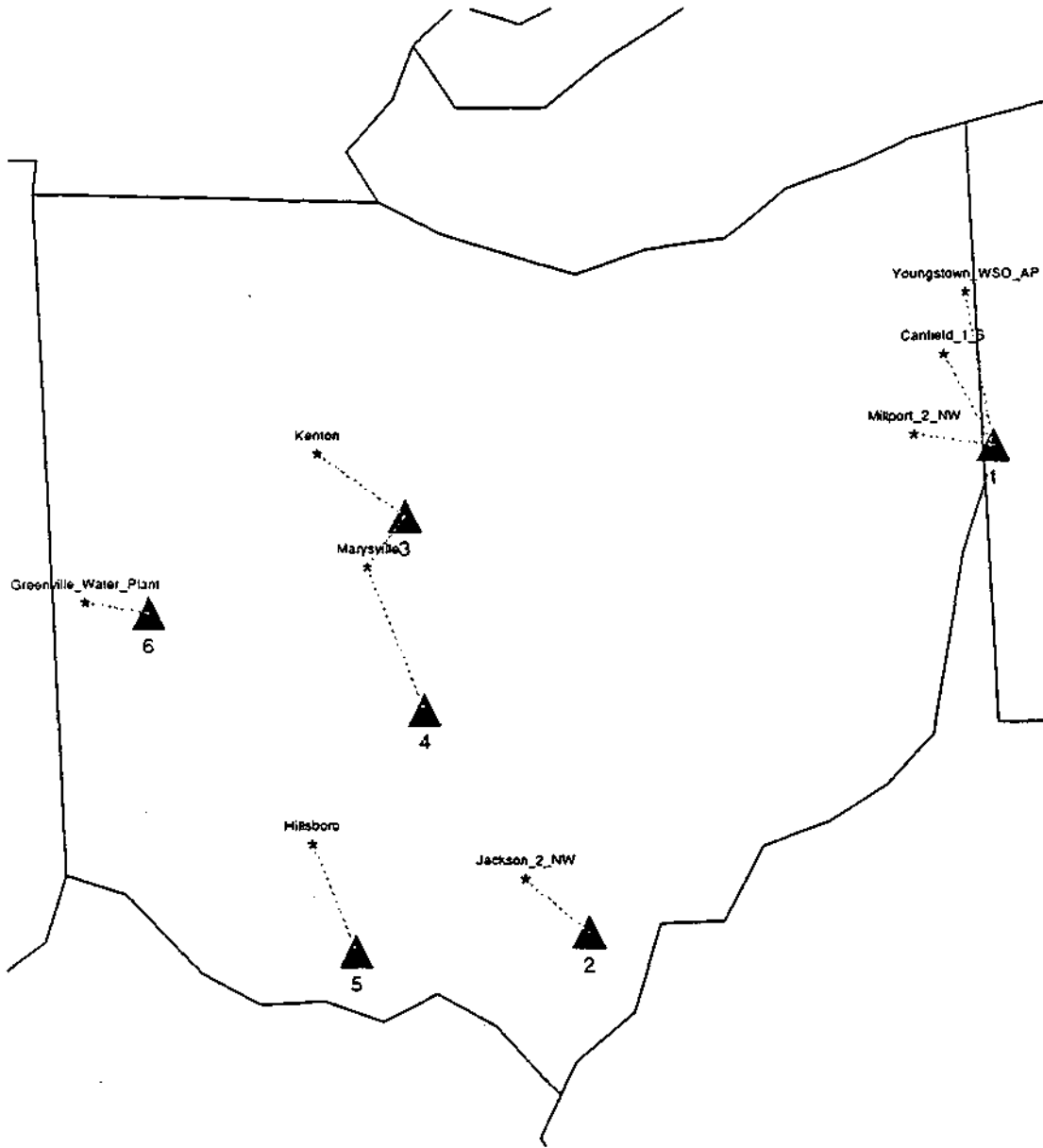
	GAGE ID	BASIN NAME	SQ. MI.
1	05062500	WILD RICE RIVER AT TWIN VALLEY, MN	888
2	05112000	ROSEAU RIVER BELOW STATE DITCH 51 NR CARIBOU, MN	1570
3	05131500	LITTLE FORK RIVER AT LITTLEFORK, MN	1730
4	05132000	BIG FORK RIVER AT BIG FALLS, MN	1460
5	05280000	CROW RIVER AT ROCKFORD, MN	2520
6	05300000	LAC QUI PARLE RIVER NEAR LAC QUI PARLE, MN	983
7	05316500	REDWOOD RIVER NEAR REDWOOD FALLS, MN	697
8	05317000	COTTONWOOD RIVER NEAR NEW ULM, MN	1280
9	05384000	ROOT RIVER NEAR LANESBORO, MN	615
10	05457000	CEDAR RIVER NEAR AUSTIN, MN	425
11	05476000	DES MOINES RIVER AT JACKSON, MN	1220



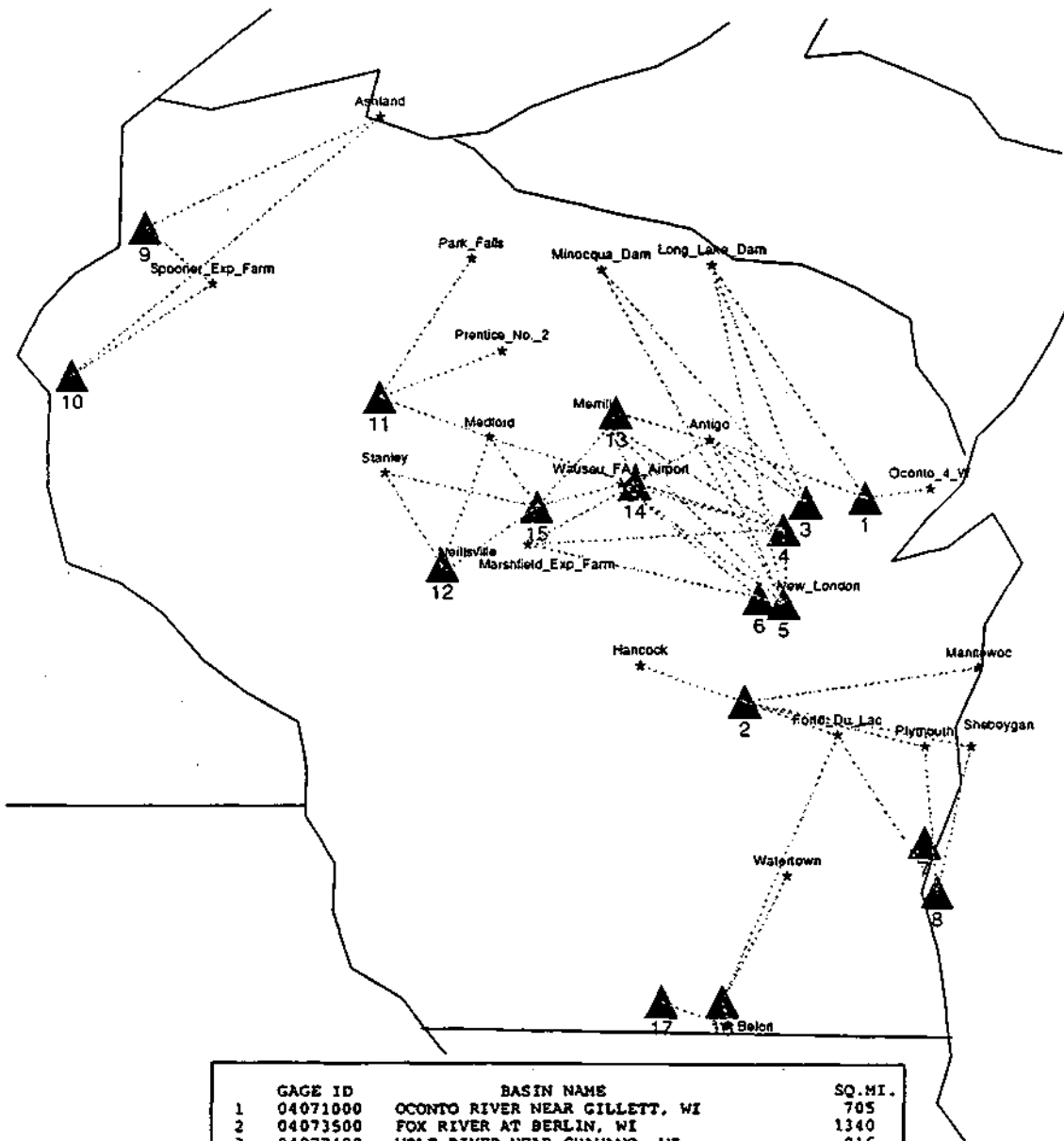
	GAGE ID	BASIN NAME	SQ.MI.
1	05331000	MISSISSIPPI RIVER AT ST. PAUL, MN	36800
2	05344500	MISSISSIPPI RIVER AT PRESCOTT, WI	44800



	GAGE ID	BASIN NAME	SQ.MI.
1	06897500	GRAND RIVER NEAR GALLATIN MO	2250
2	06933500	GASCONADE RIVER AT JEROME MO	2840



	GAGE ID	BASIN NAME	SQ.MI.
1	03109500	L BEAVER C NR EAST LIVERPOOL OH	496
2	03202000	RACCOON C AT ADAMSVILLE OH	585
3	03219500	SCIOTO R NR PROSPECT OH	567
4	03230500	BIG DARBY C AT DARBYVILLE OH	534
5	03237500	OHIO BRUSH C NR WEST UNION OH	387
6	03265000	STILLWATER R AT PLEASANT HILL OH	503



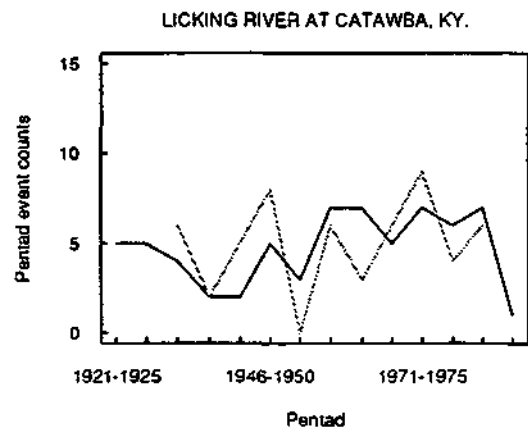
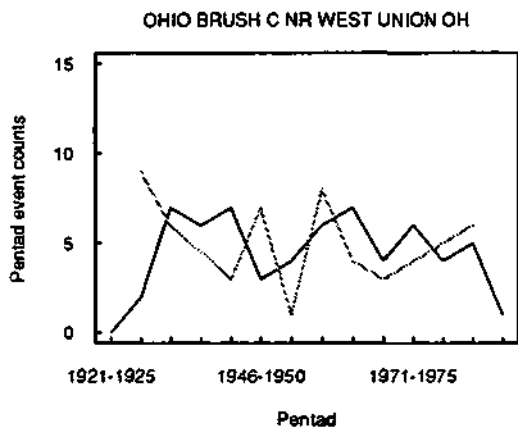
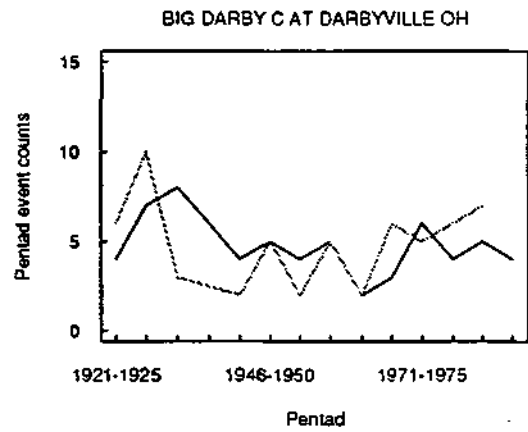
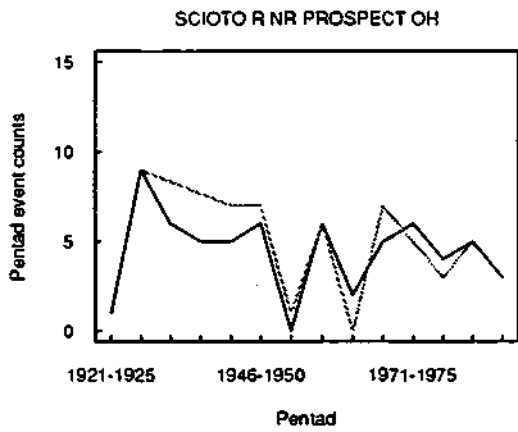
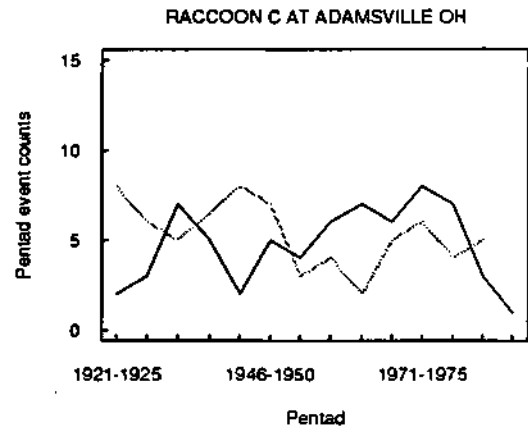
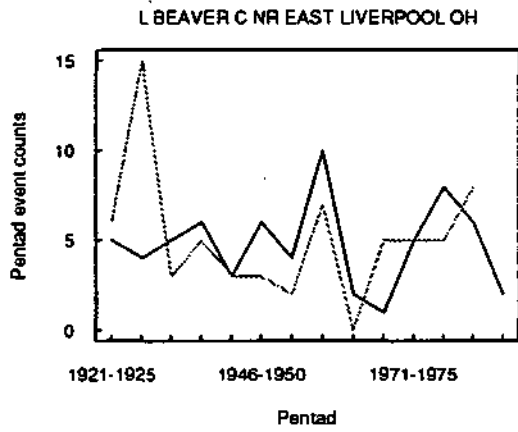
GAGE ID	BASIN NAME	SQ. MI.
1	OCONTO RIVER NEAR GILLETT, WI	705
2	FOX RIVER AT BERLIN, WI	1340
3	WOLF RIVER NEAR SHAWANO, WI	816
4	EMBARRASS RIVER NEAR EMBARRASS, WI	384
5	WOLF RIVER AT NEW LONDON, WI	2260
6	LITTLE WOLF RIVER AT ROYALTON, WI	507
7	CEDAR CREEK NEAR CEDARBURG, WI	120
8	MILWAUKEE RIVER AT MILWAUKEE, WI	696
9	ST. CROIX RIVER NEAR DANBURY, WI	1580
10	ST. CROIX RIVER AT ST. CROIX FALLS, WI	6240
11	JUMP RIVER AT SHELDON, WI	576
12	BLACK RIVER AT NEILLSVILLE, WI	749
13	PRAIRIE RIVER NEAR MERRILL, WI	184
14	EAU CLAIRE RIVER AT KELLY, WI	375
15	BIG EAU PLEINE RIVER NEAR STRATFORD, WI	224
16	ROCK RIVER AT APTON, WI	3340
17	SUGAR RIVER NEAR BRODHEAD, WI	523

APPENDIX G

PENTADAL FREQUENCIES OF FLOOD AND PRECIPITATION EVENTS (WARM SEASON)

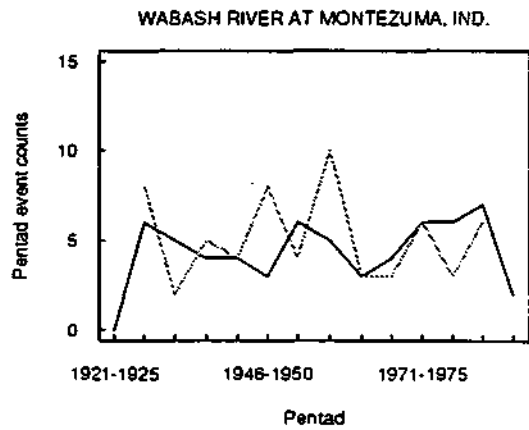
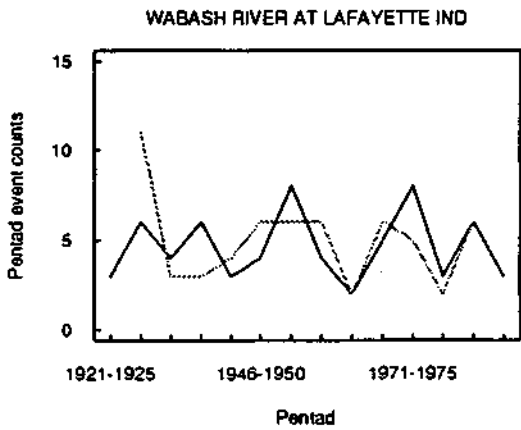
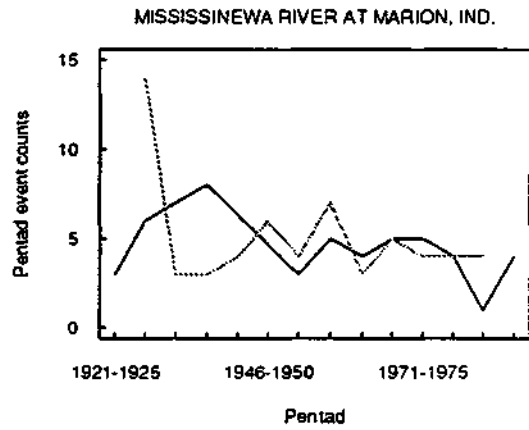
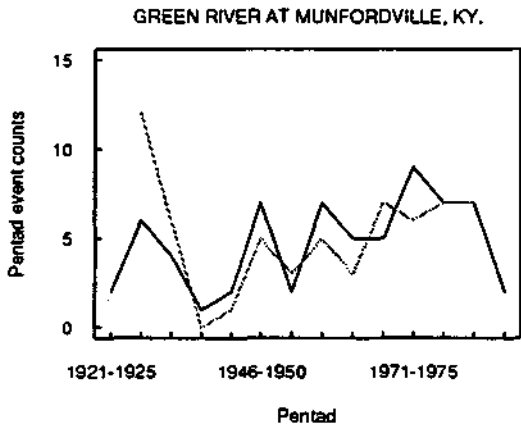
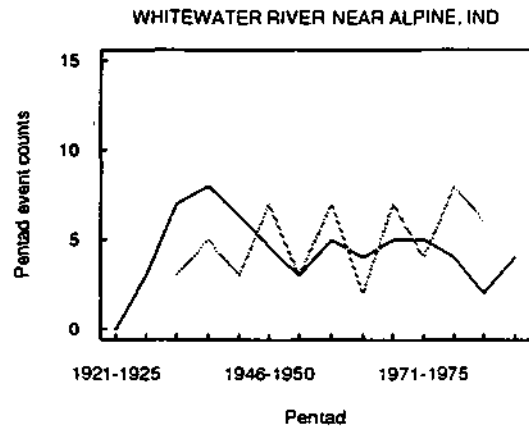
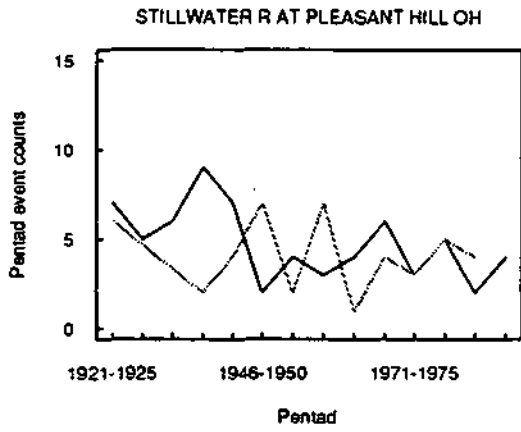
The following graphs give the pentadal frequencies of flood events for each of the 79 stream basins for the warm season. Both the flood and precipitation values displayed are for a 1-year recurrence interval.

Warm season



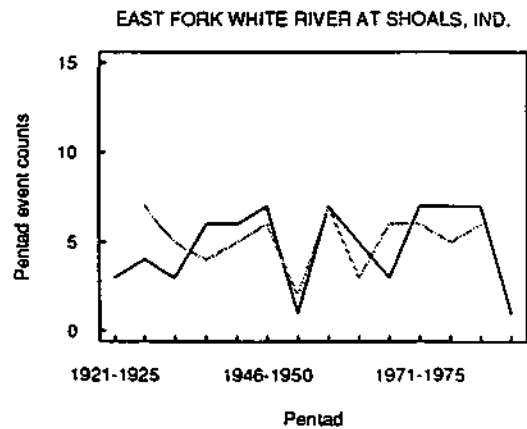
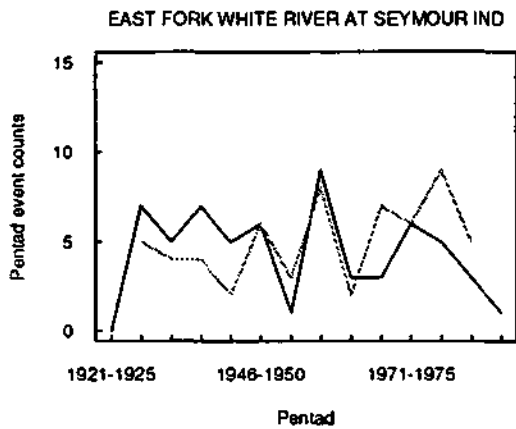
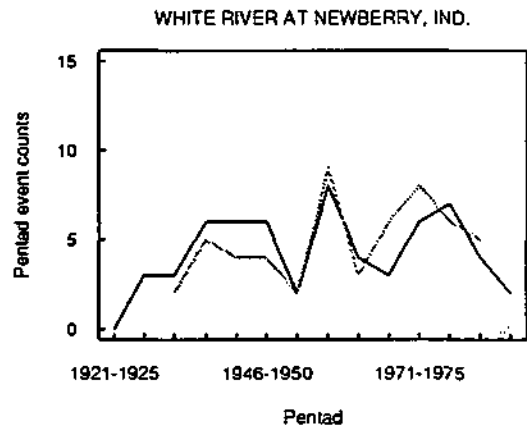
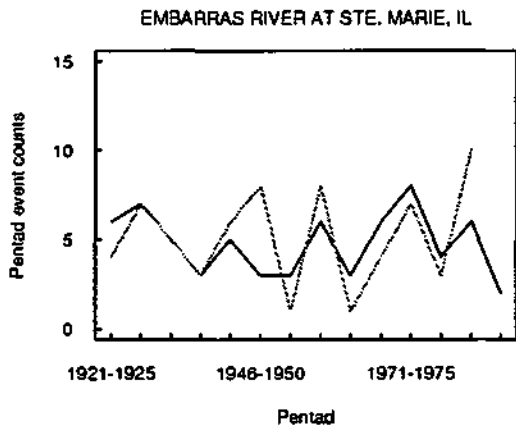
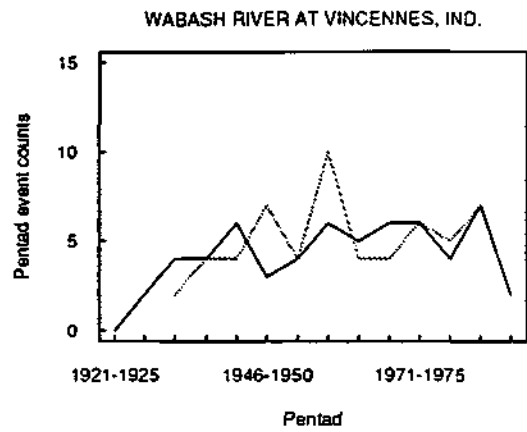
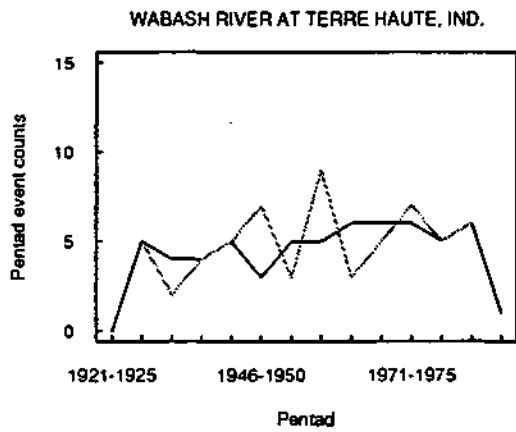
Solid: precip event count Dashed: flood event count

Warm season



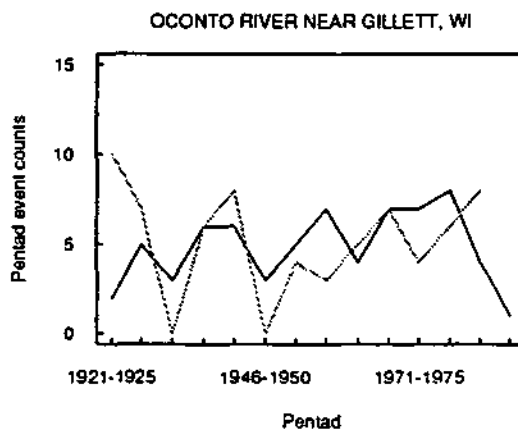
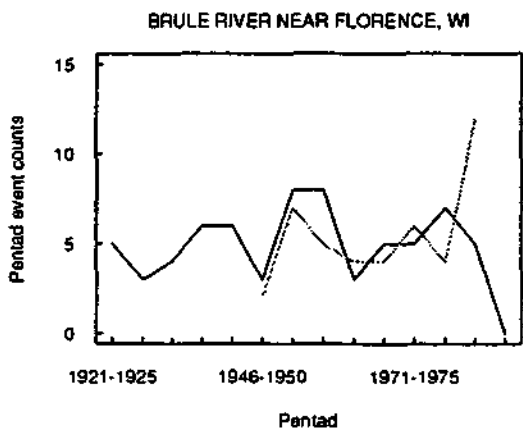
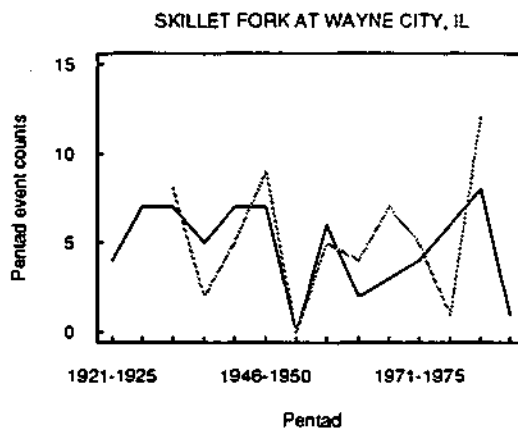
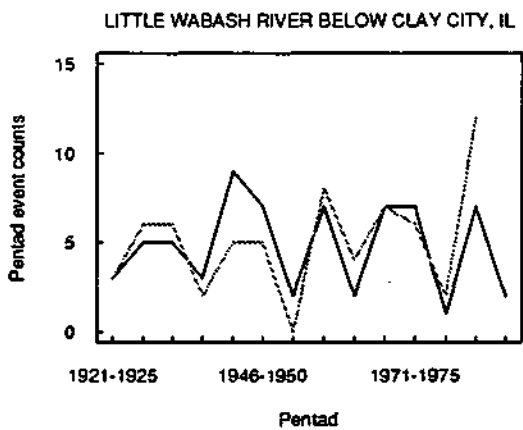
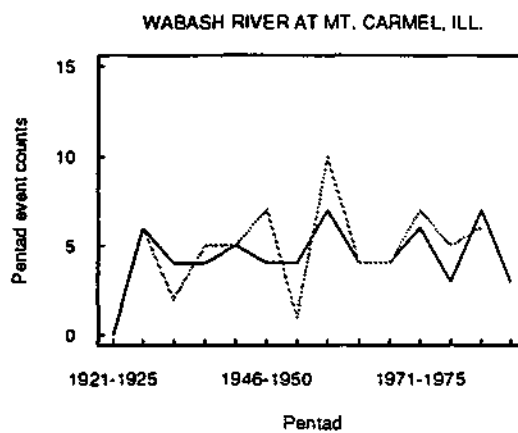
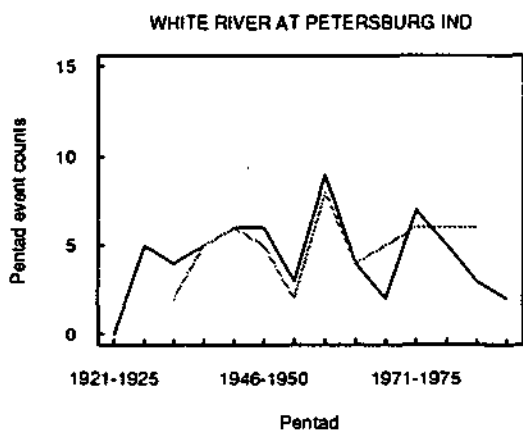
Solid: precip event count Dashed: flood event count

Warm season



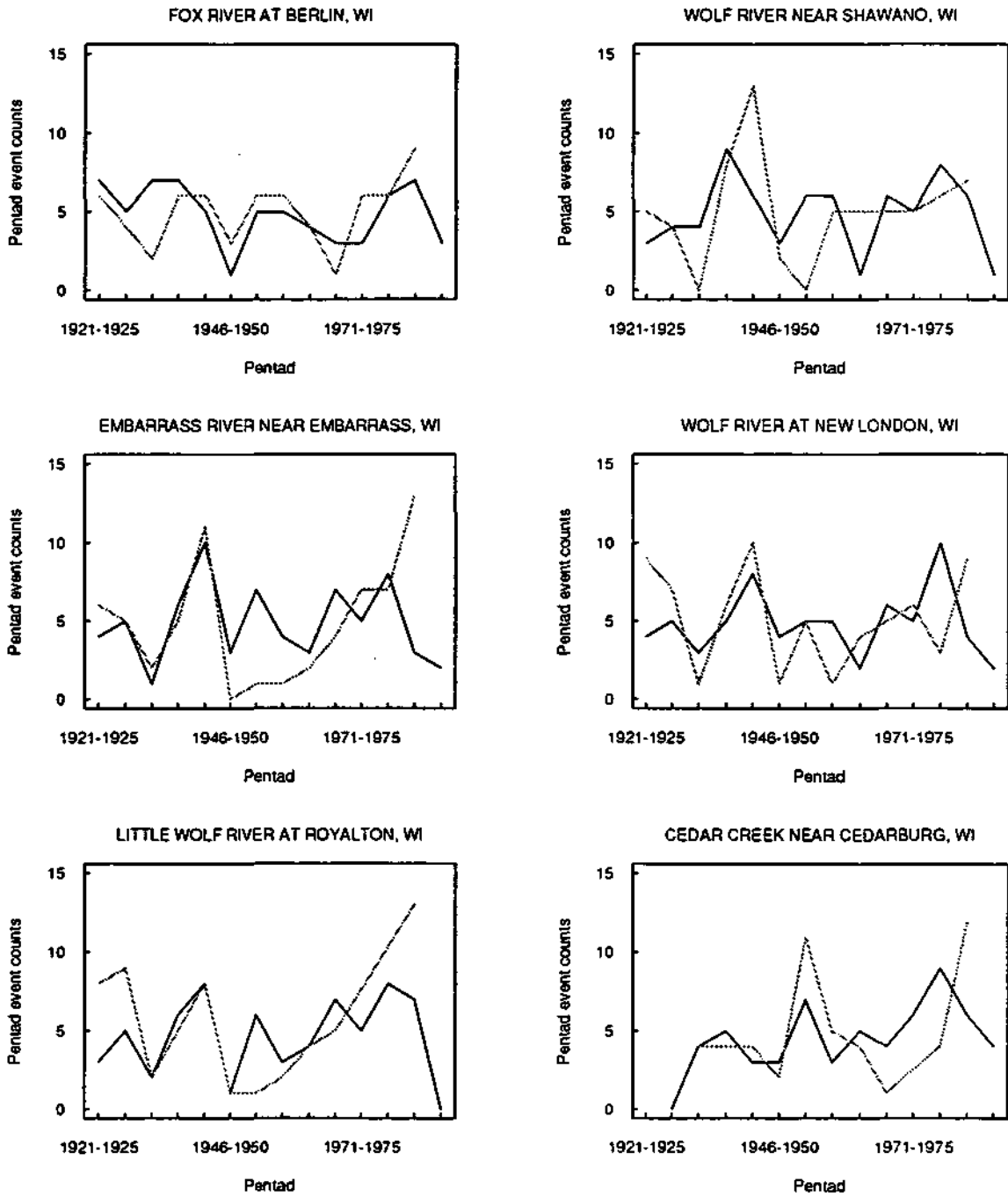
Solid: precip event count Dashed: flood event count

Warm season



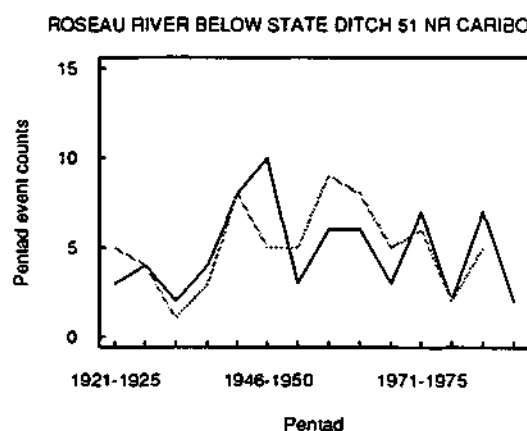
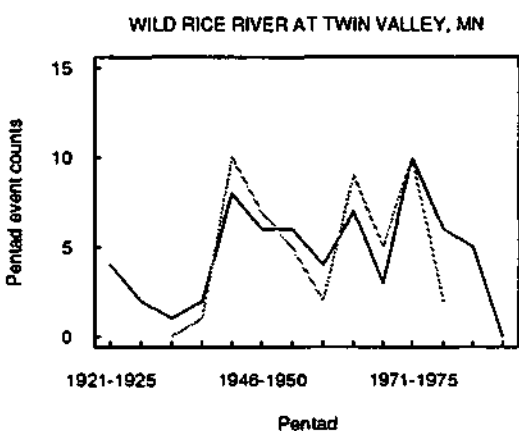
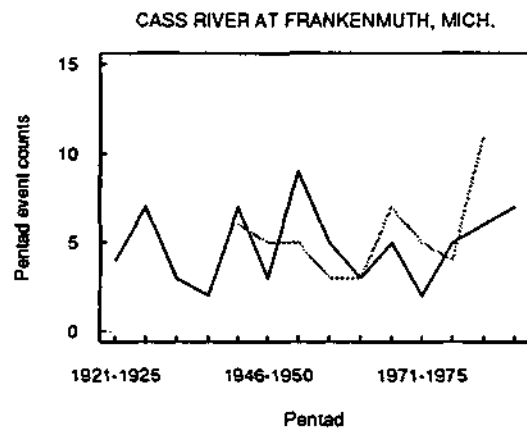
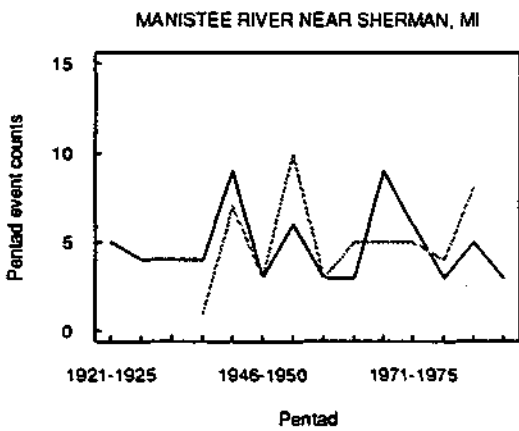
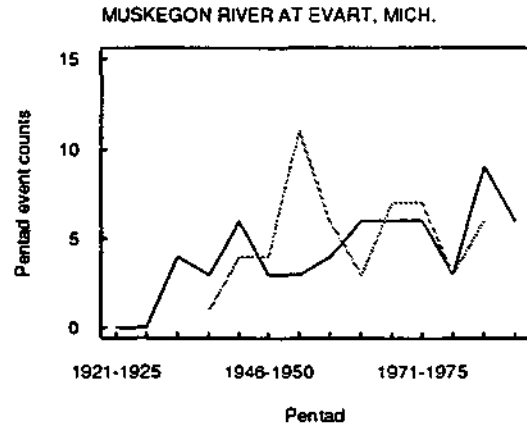
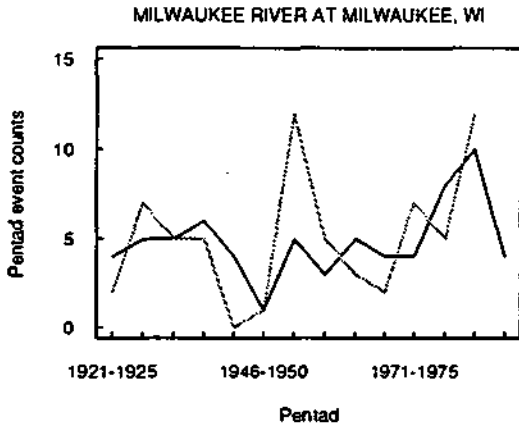
Solid: precip event count Dashed: flood event count

Warm season



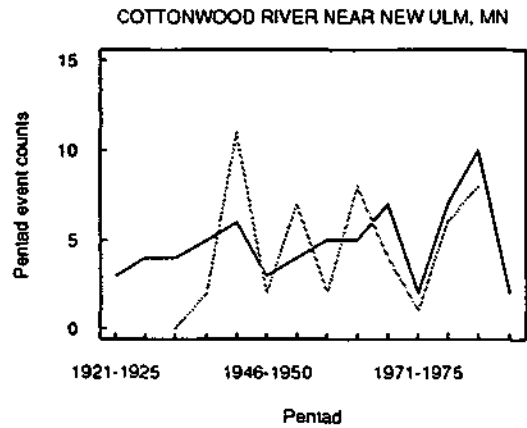
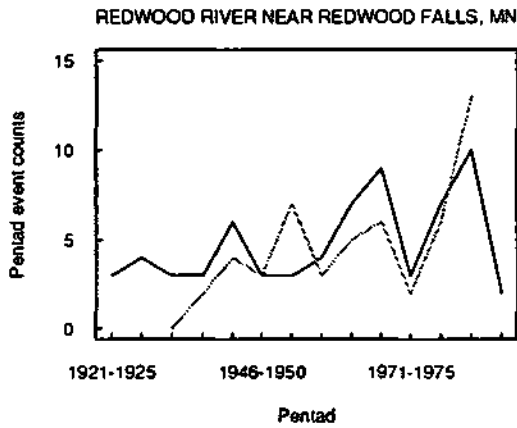
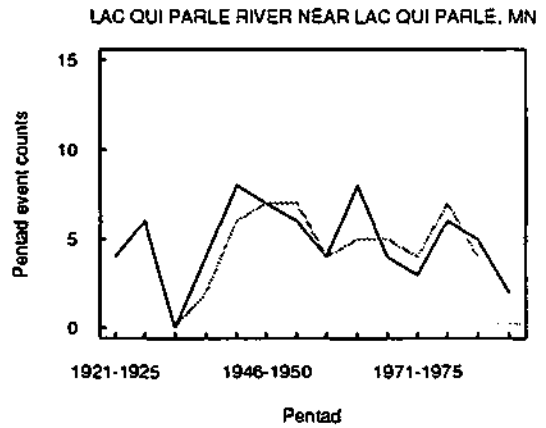
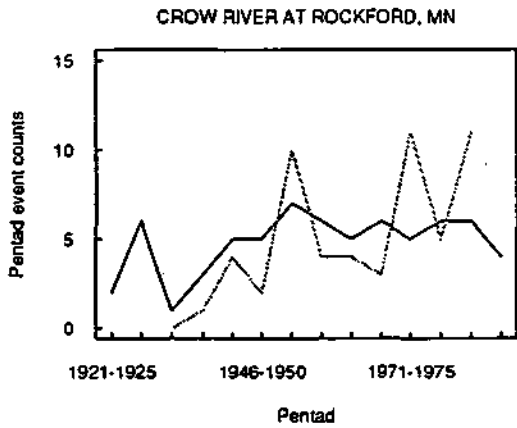
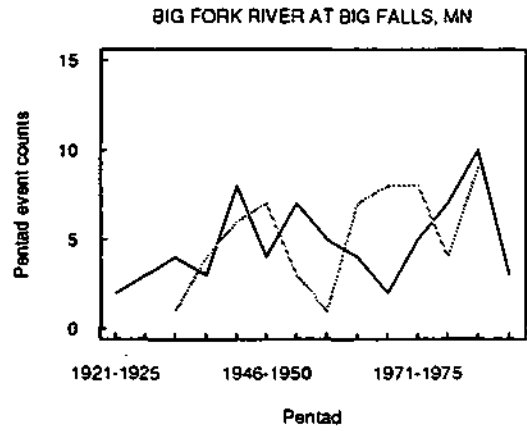
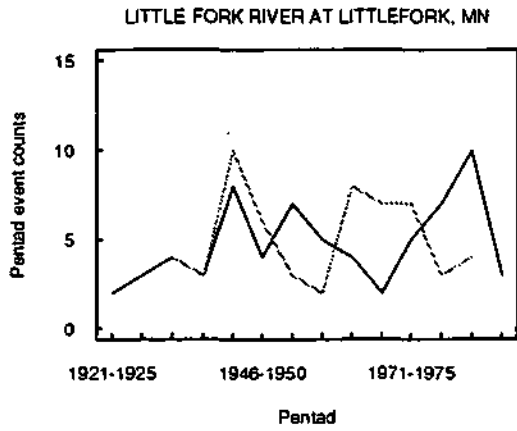
Solid: precip event count Dashed: flood event count

Warm season



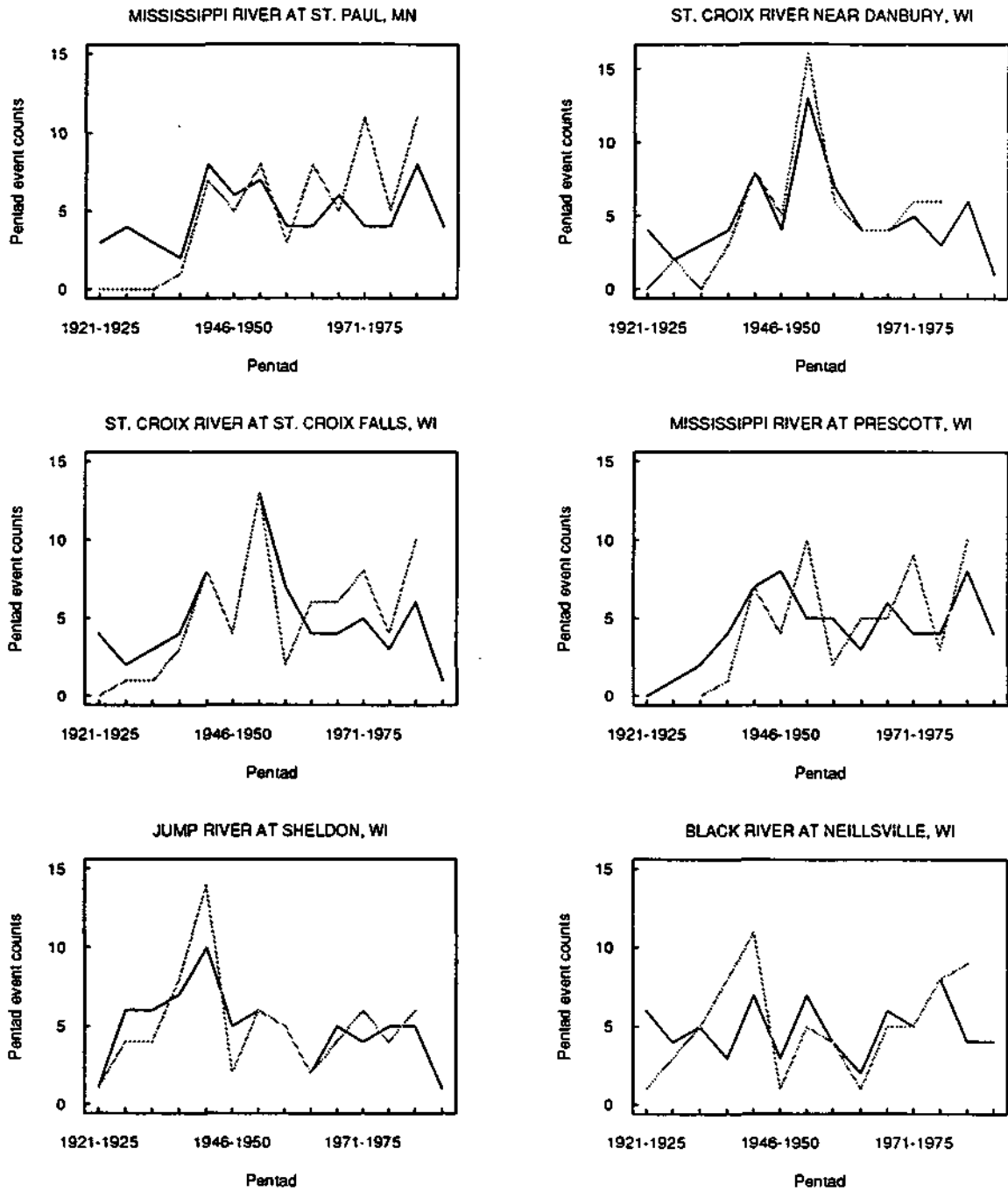
Solid: precip event count Dashed: flood event count

Warm season



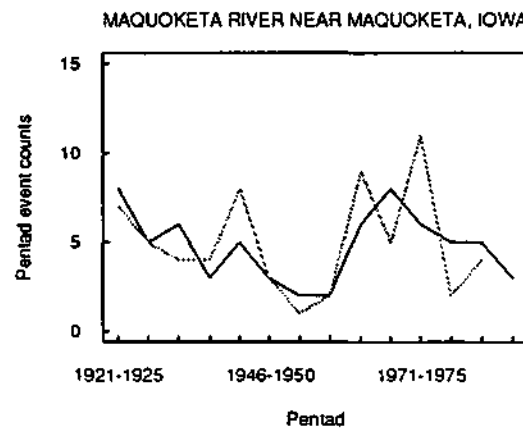
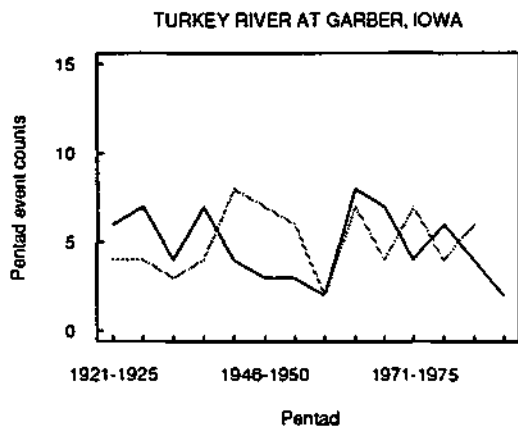
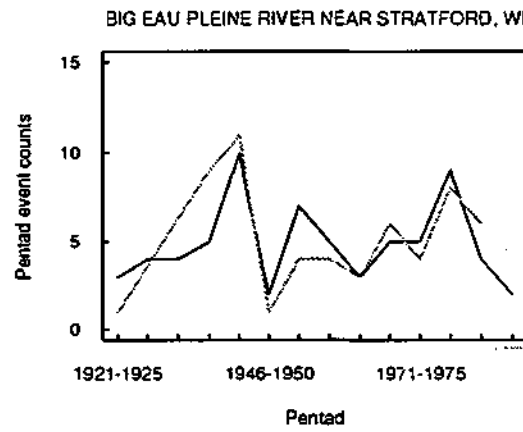
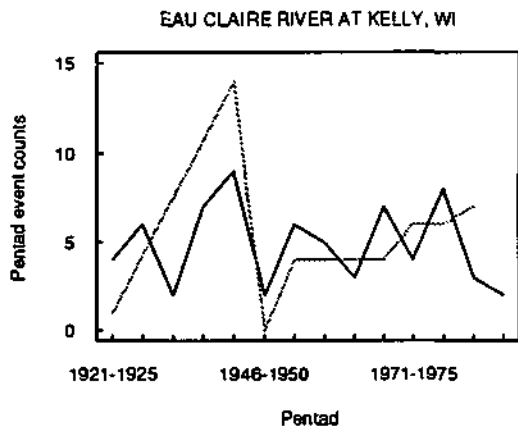
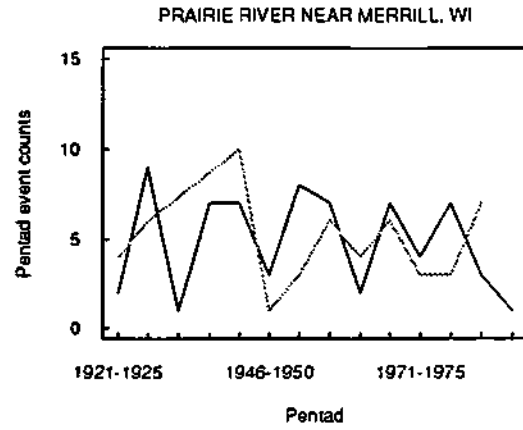
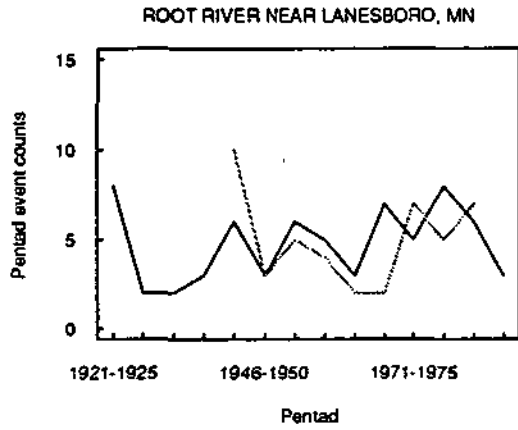
Solid: precip event count Dashed: flood event count

Warm season



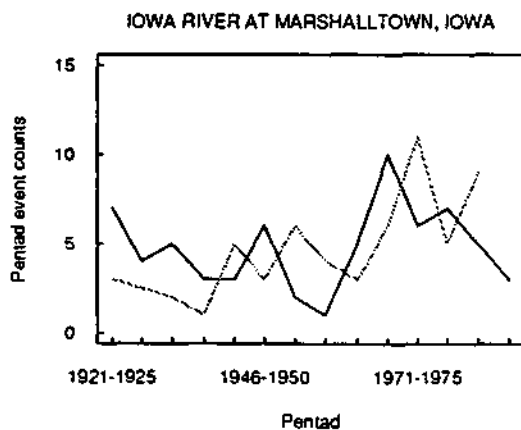
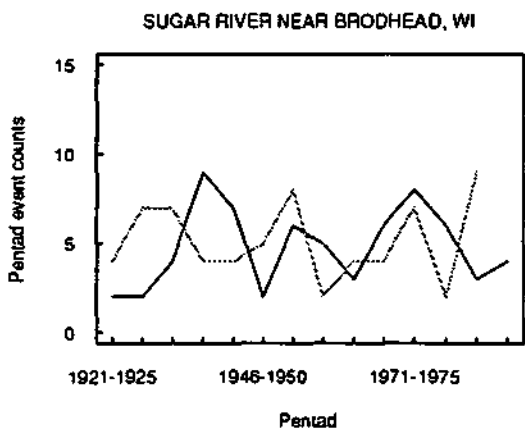
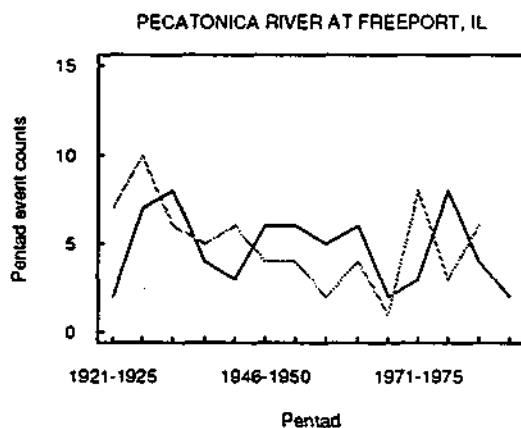
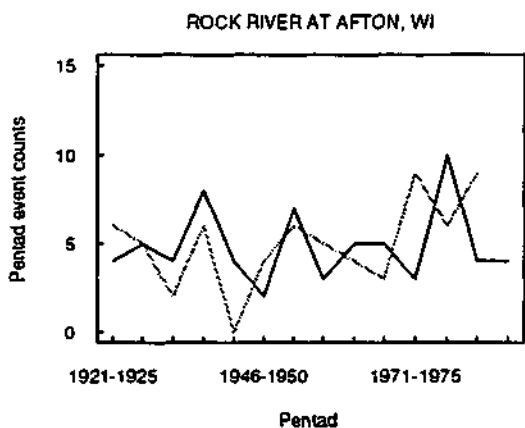
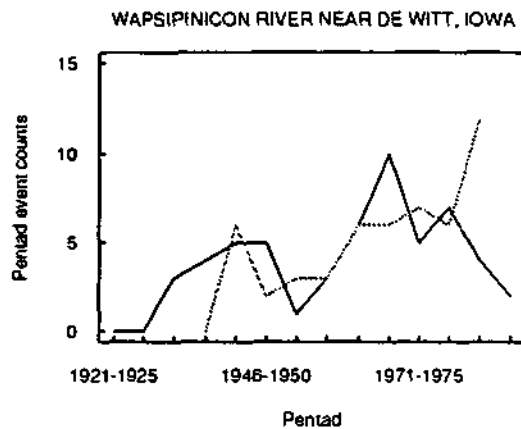
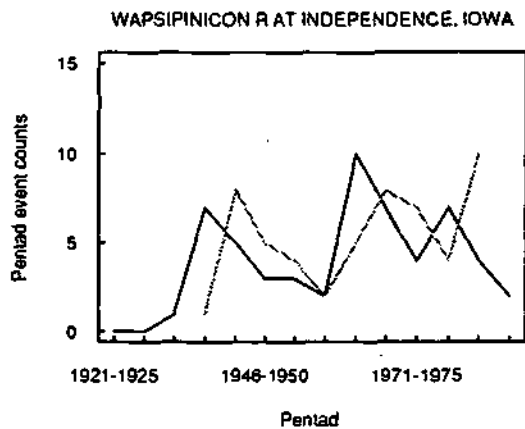
Solid: precip event count Dashed: flood event count

Warm season



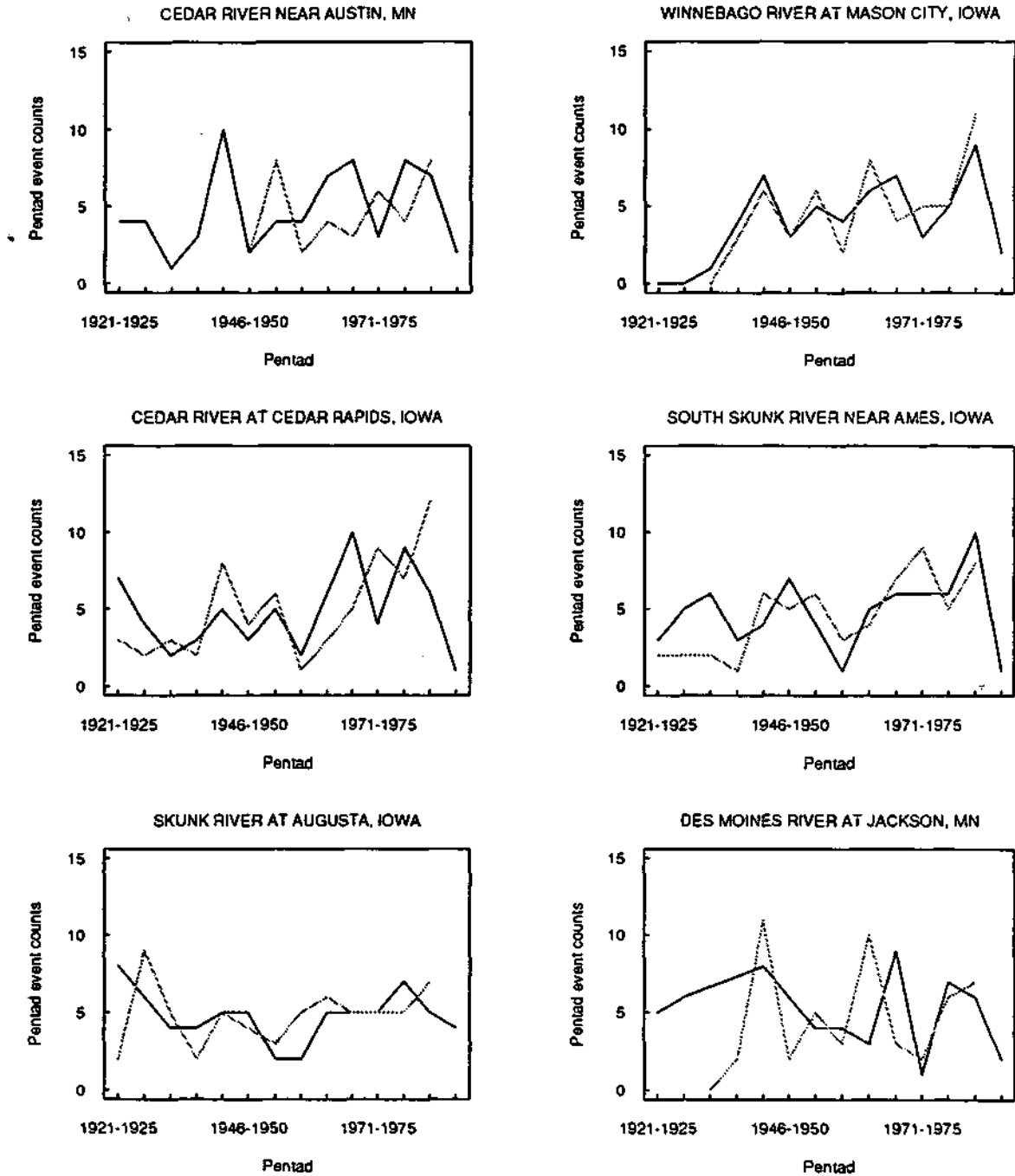
Solid: precip event count Dashed: flood event count

Warm season



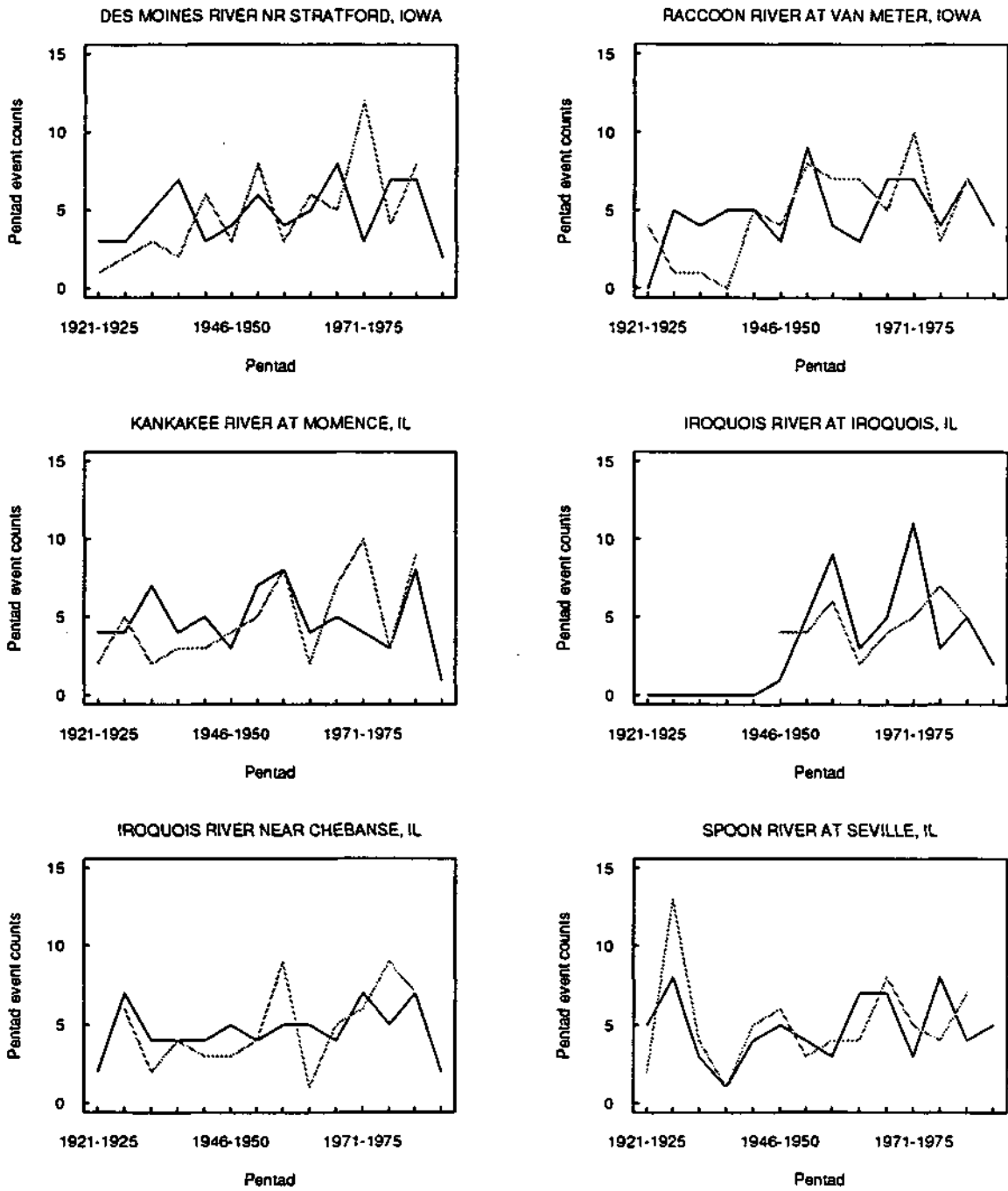
Solid: precip event count Dashed: flood event count

Warm season



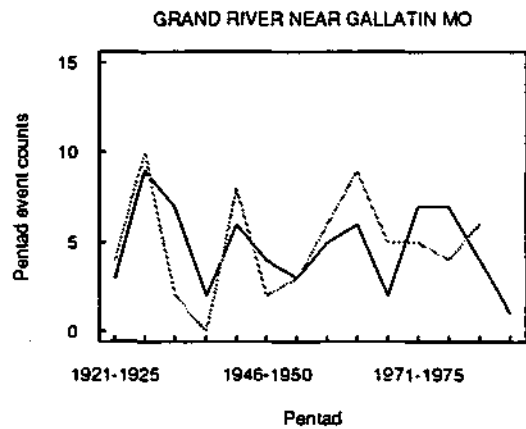
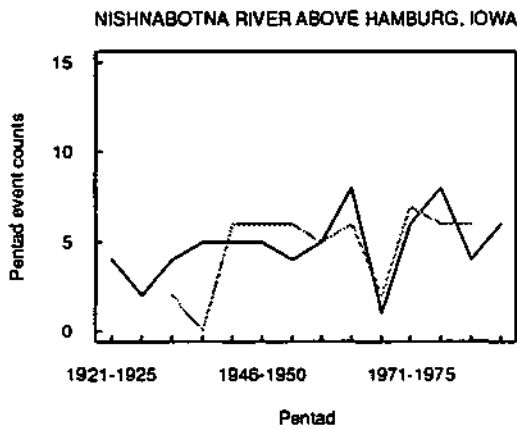
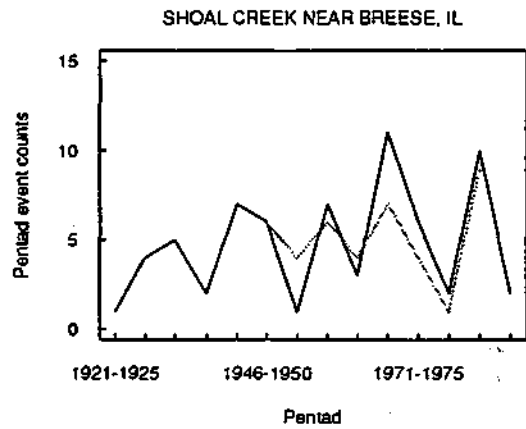
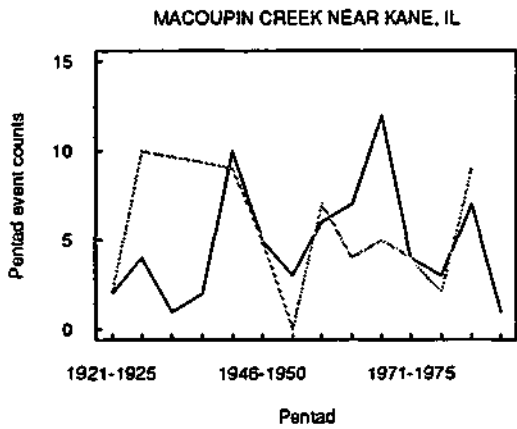
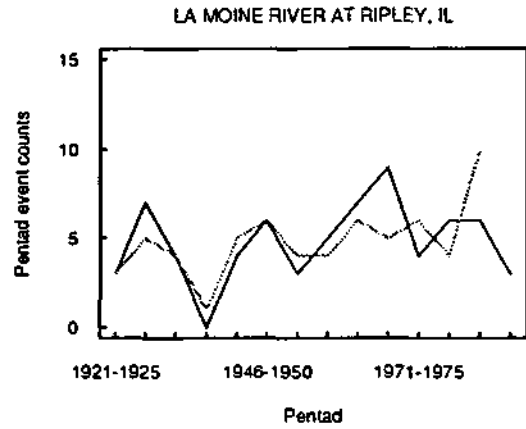
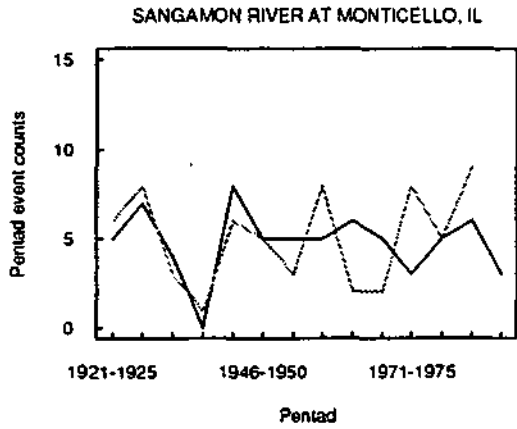
Solid: precip event count Dashed: flood event count

Warm season

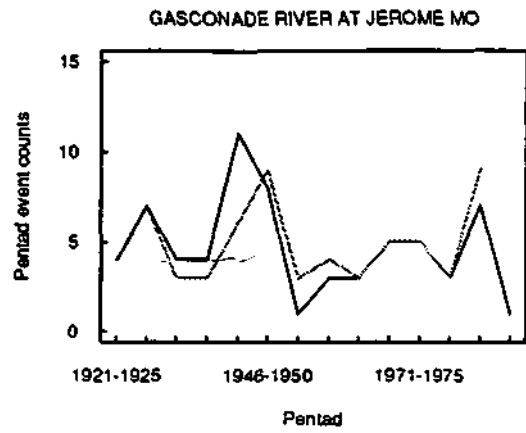


Solid: precip event count Dashed: flood event count

Warm season



Solid: precip event count Dashed: flood event count

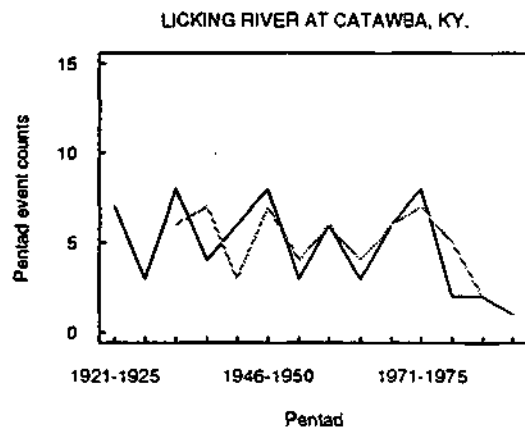
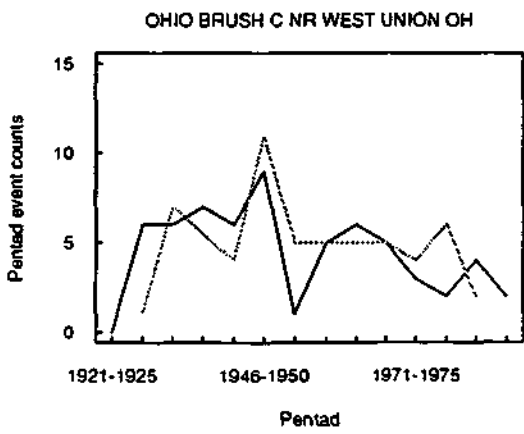
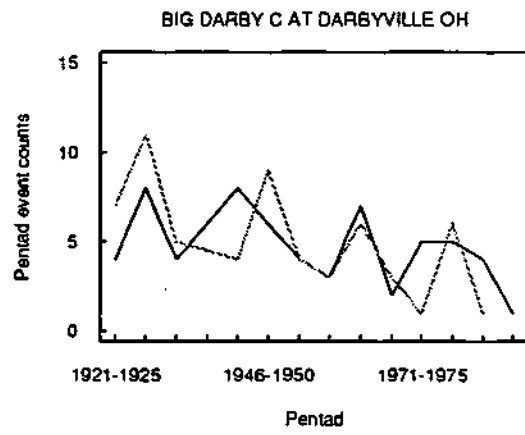
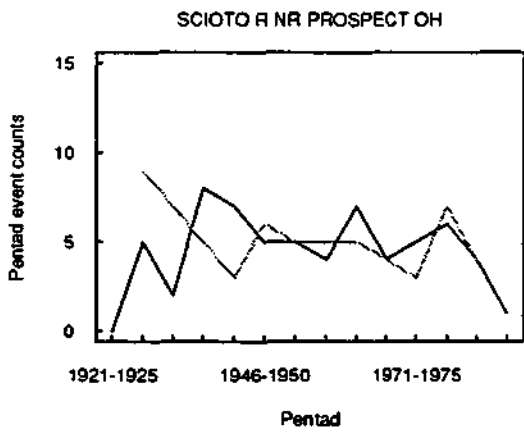
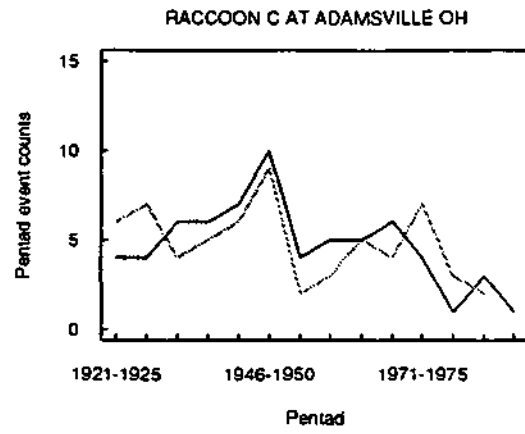
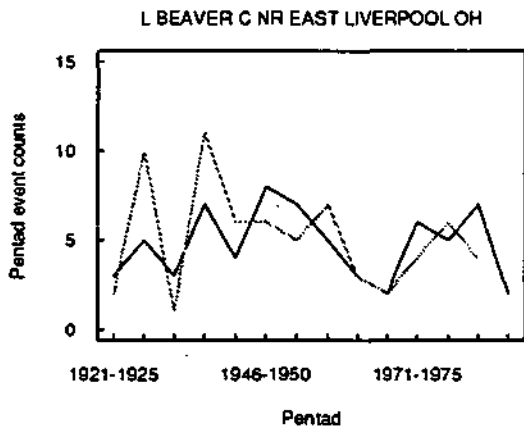


APPENDIX H

PENTADAL FREQUENCIES OF FLOOD AND PRECIPITATION EVENTS (COLD SEASON)

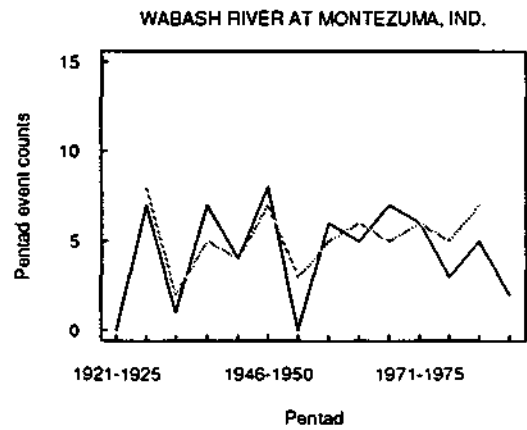
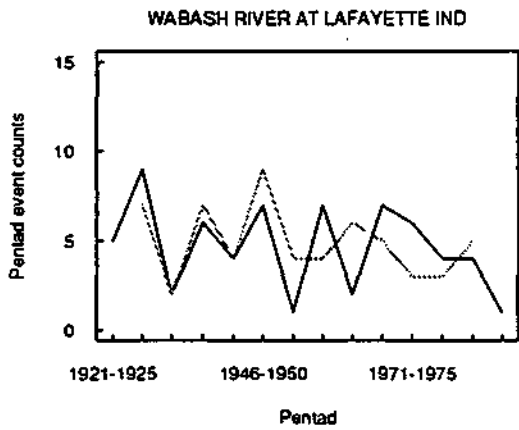
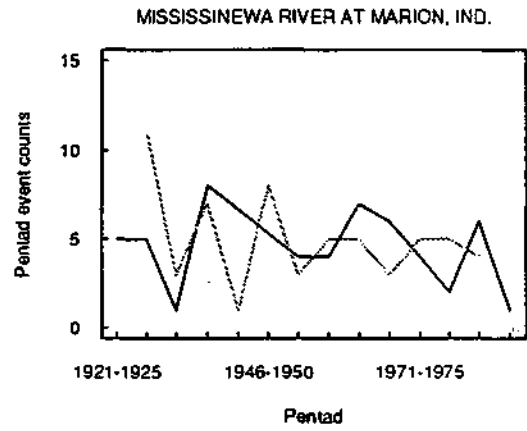
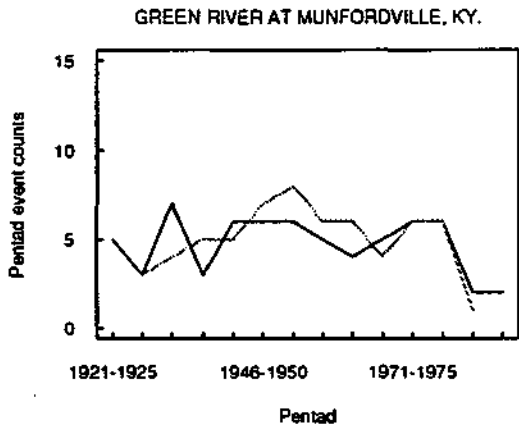
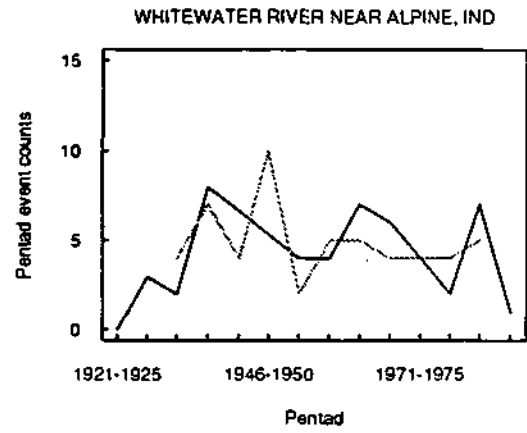
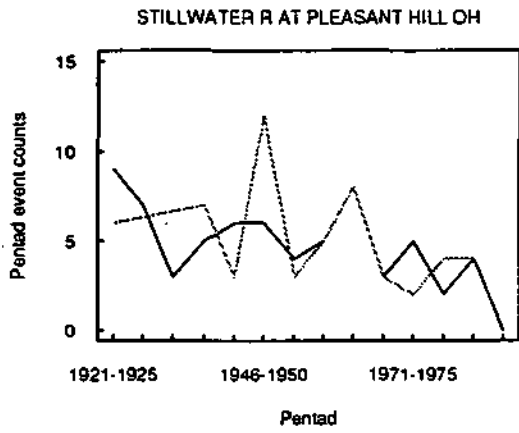
The following graphs give the pentadal frequencies of flood events for each of the 79 stream basins for the cold season. Both the flood and precipitation values displayed are for a 1-year recurrence interval.

Cold season



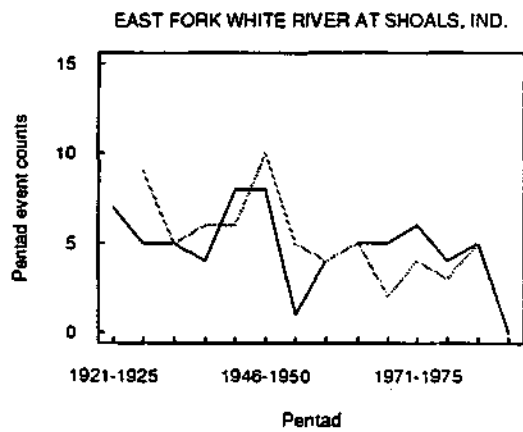
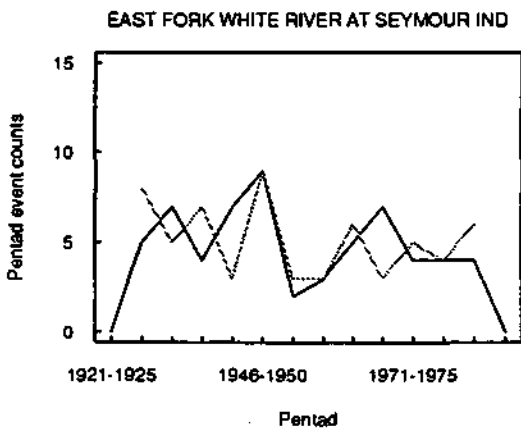
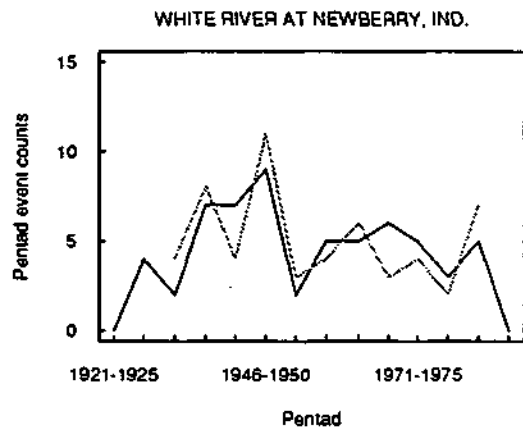
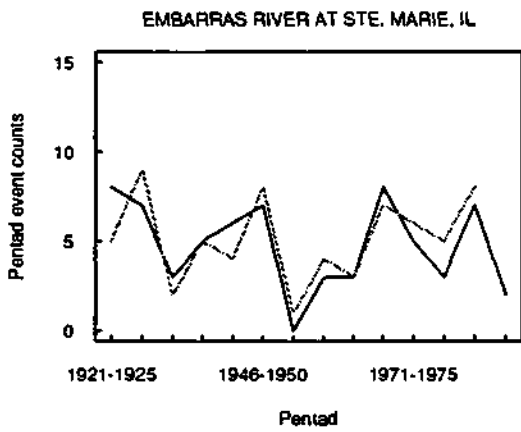
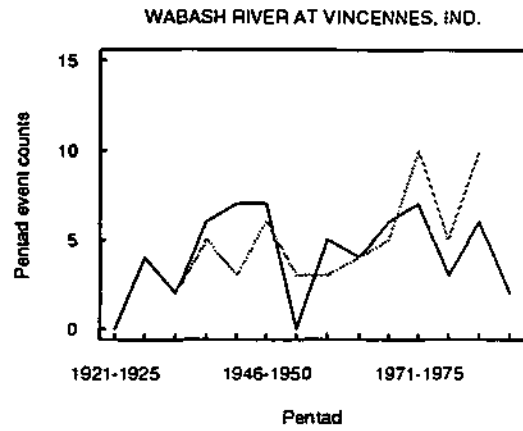
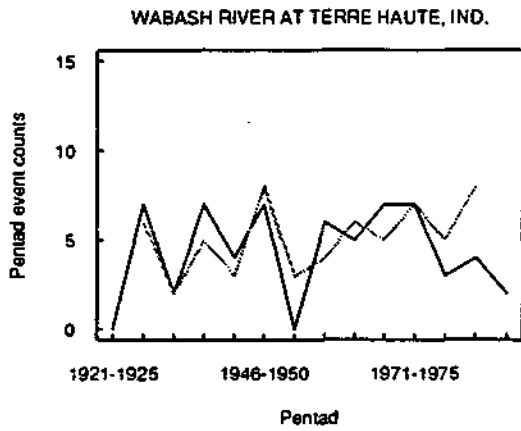
Solid: precip event count Dashed: flood event count

Cold season



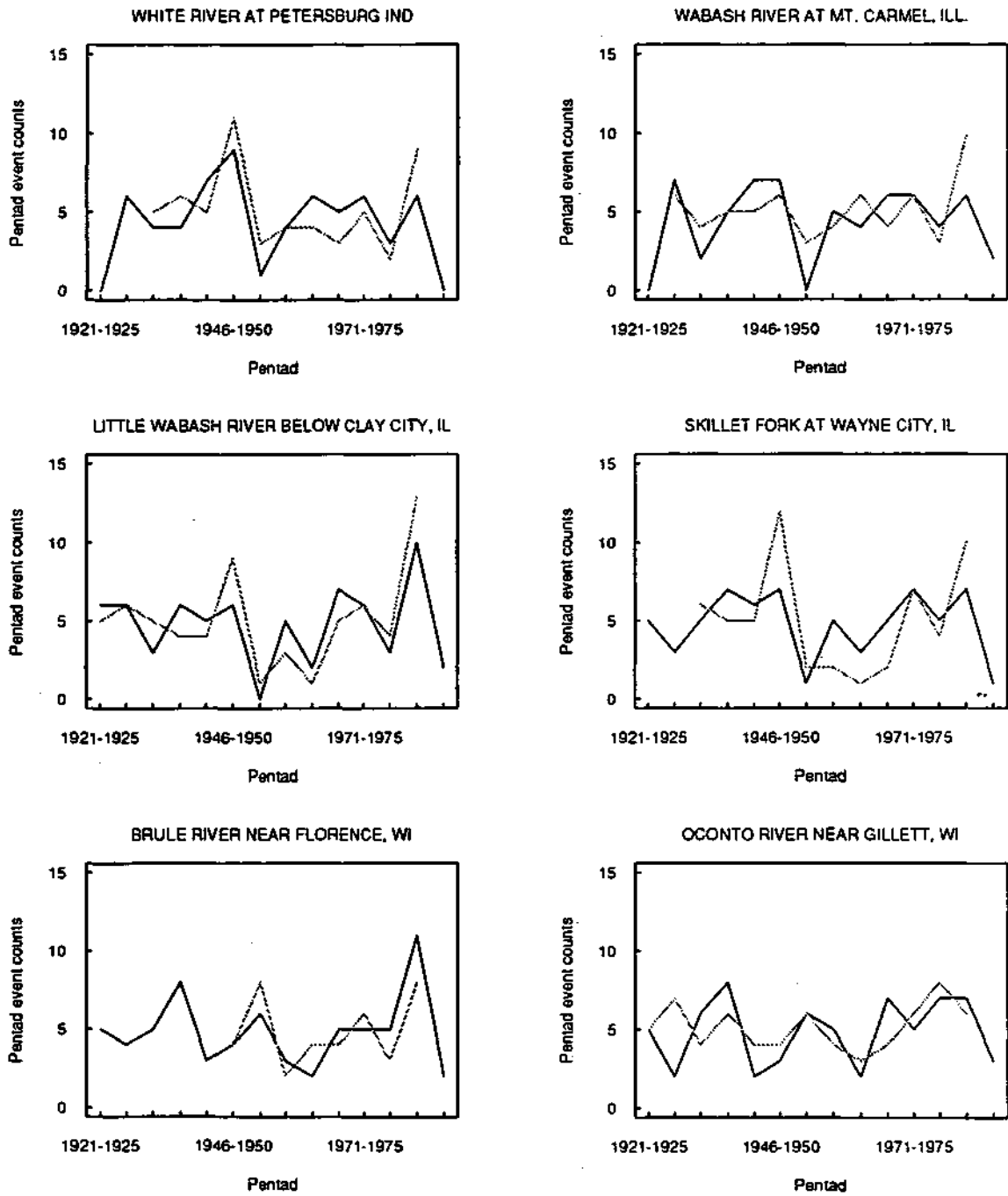
Solid: precip event count Dashed: flood event count

Cold season



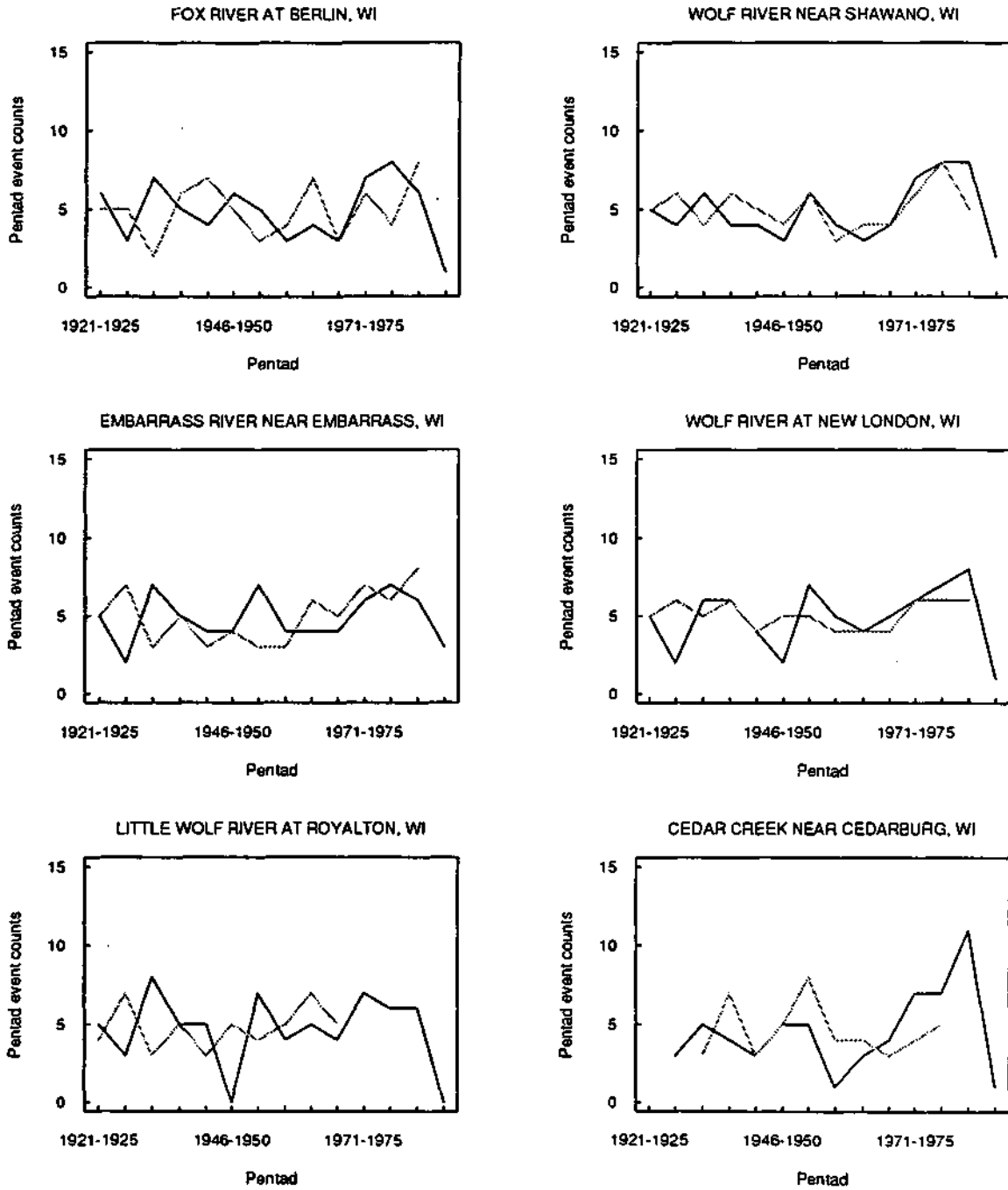
Solid: precip event count Dashed: flood event count

Cold season



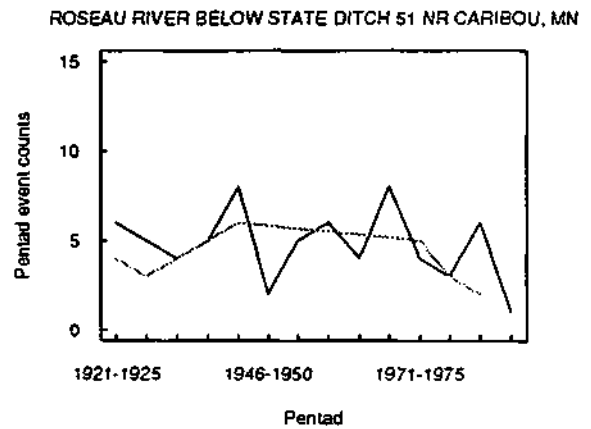
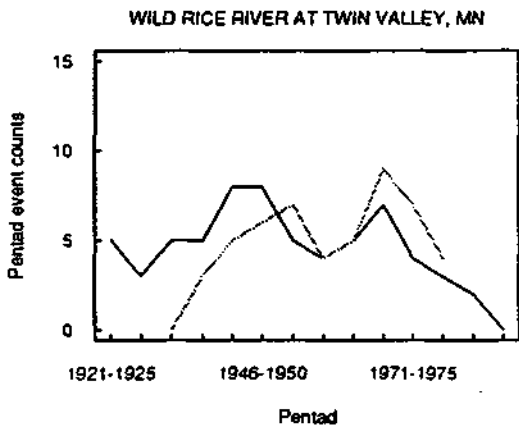
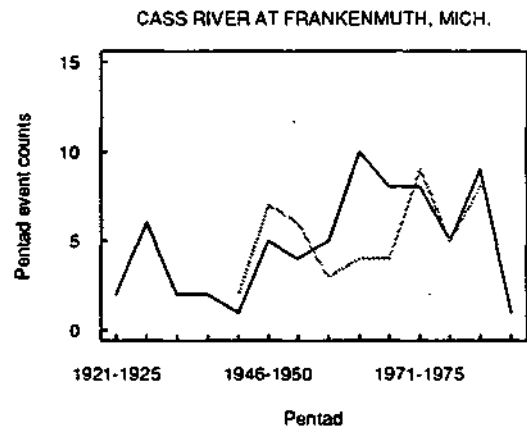
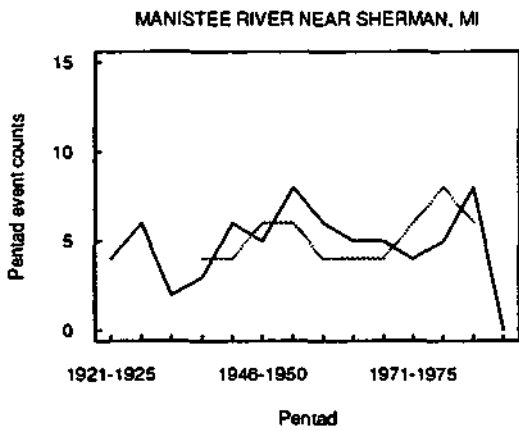
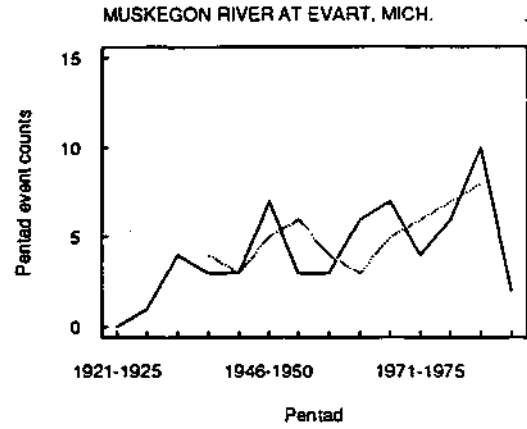
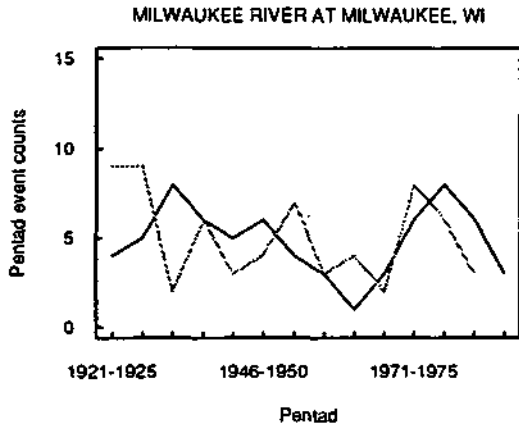
Solid: precip event count Dashed: flood event count

Cold season



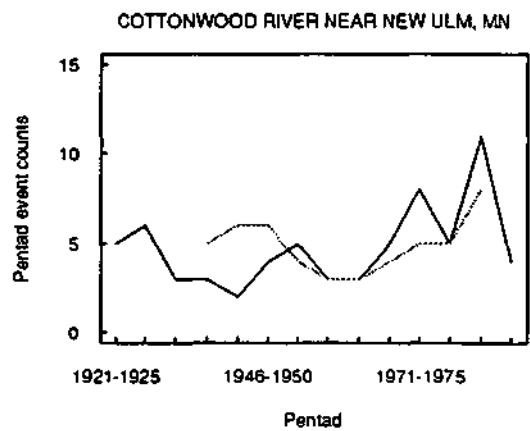
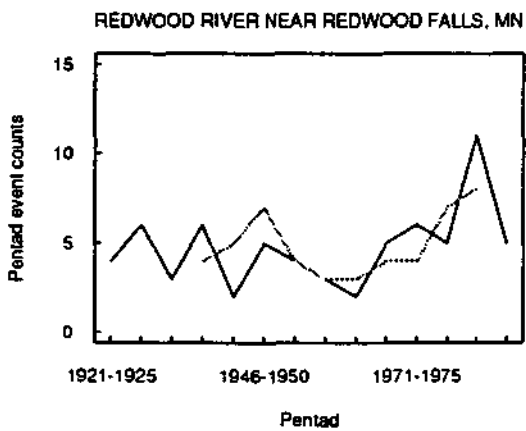
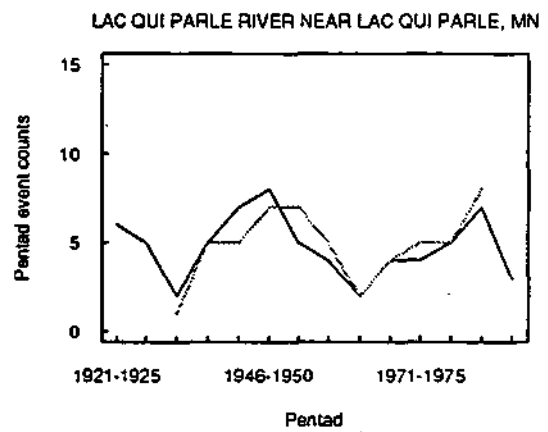
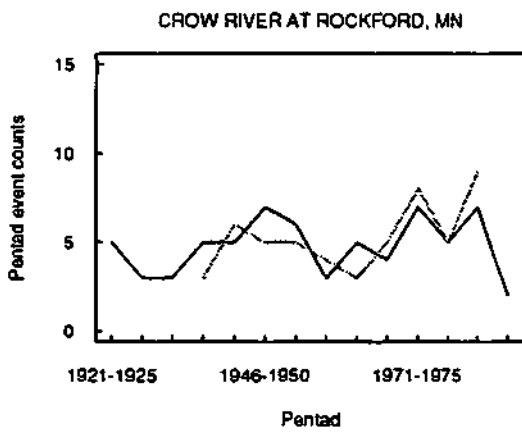
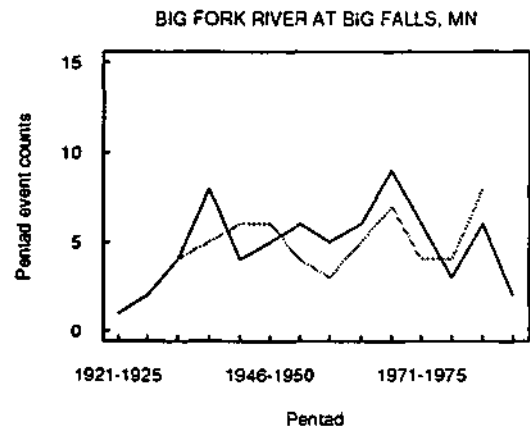
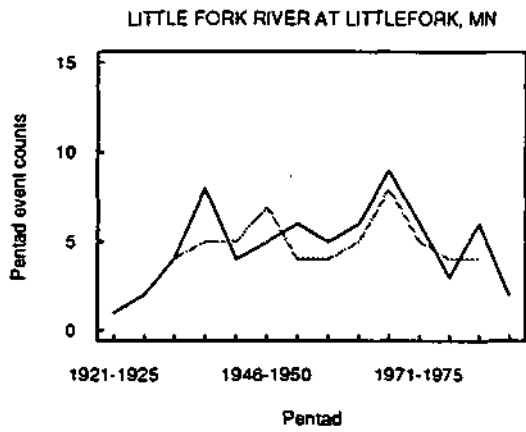
Solid: precip event count Dashed: flood event count

Cold season



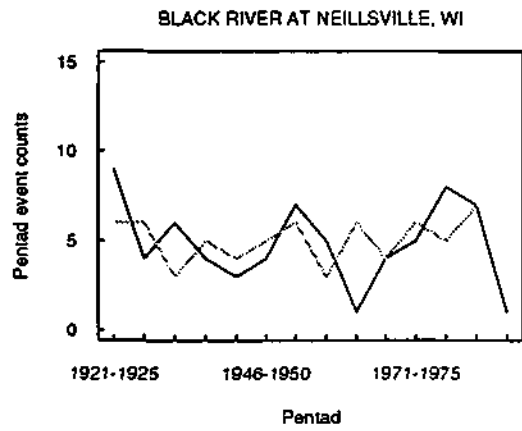
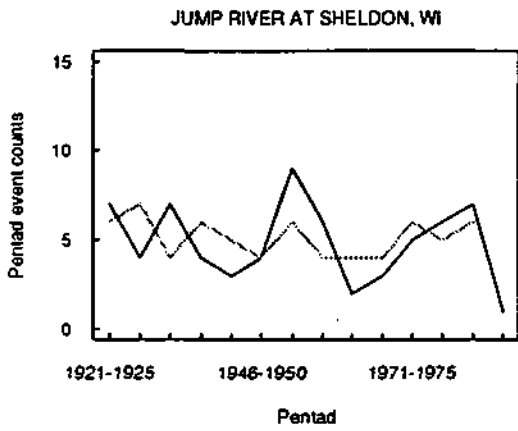
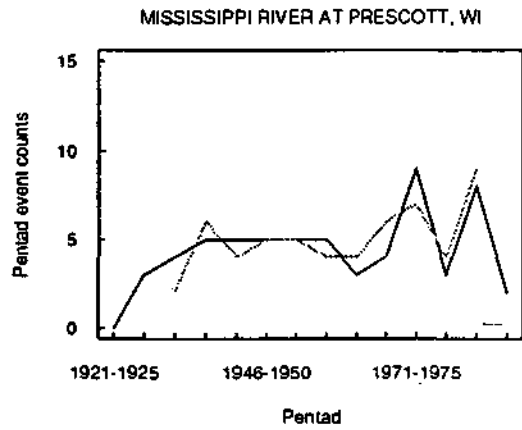
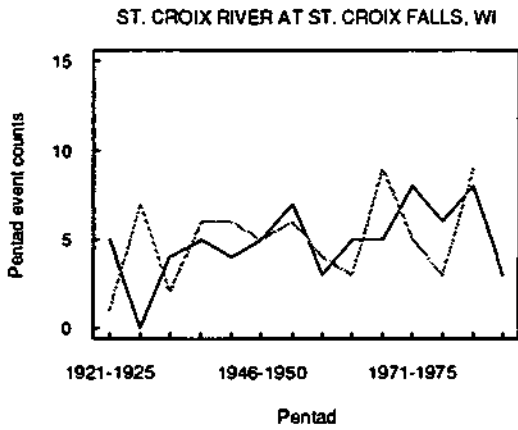
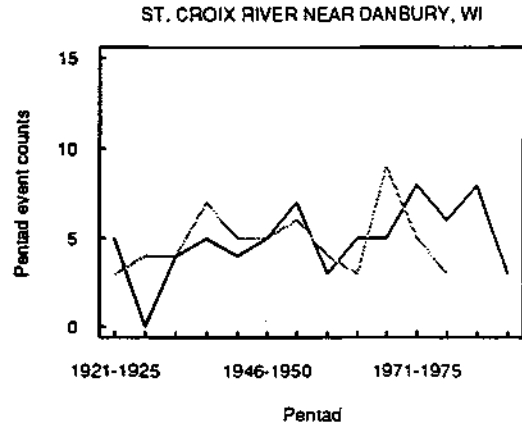
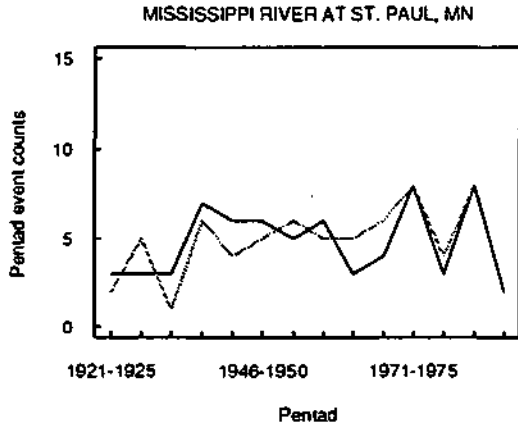
Solid: precip event count Dashed: flood event count

Cold season



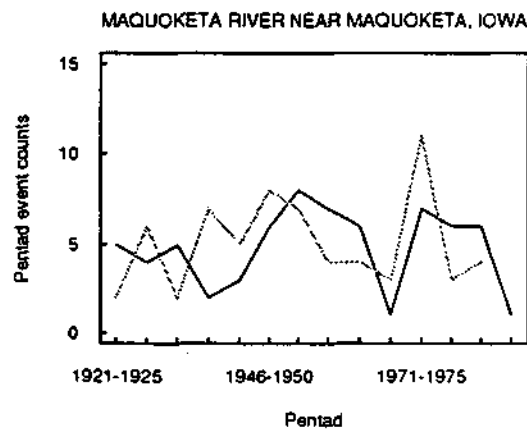
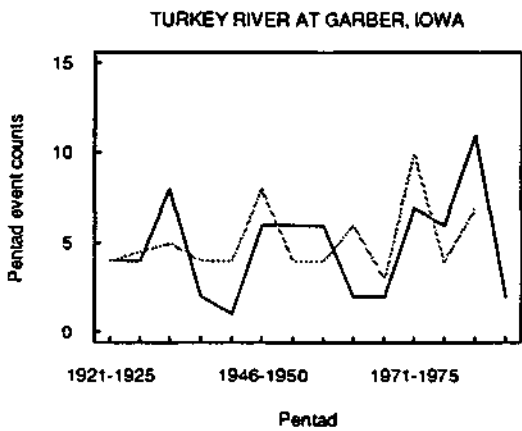
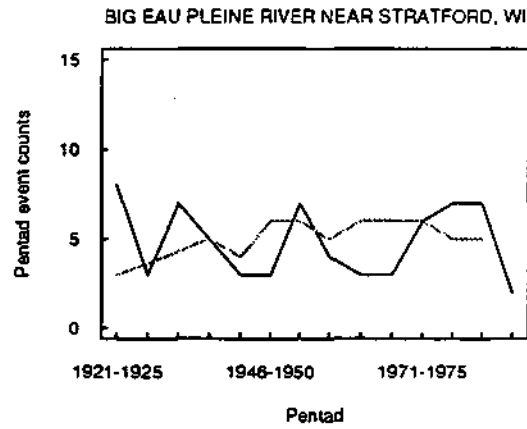
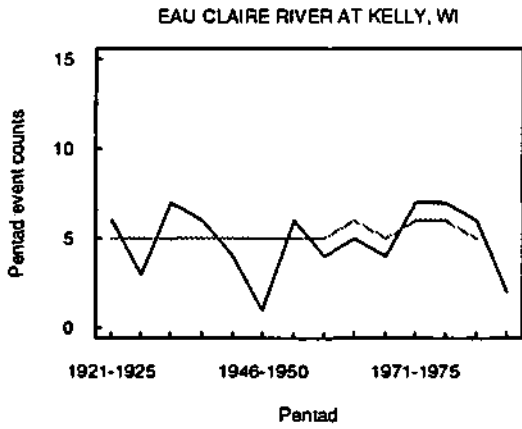
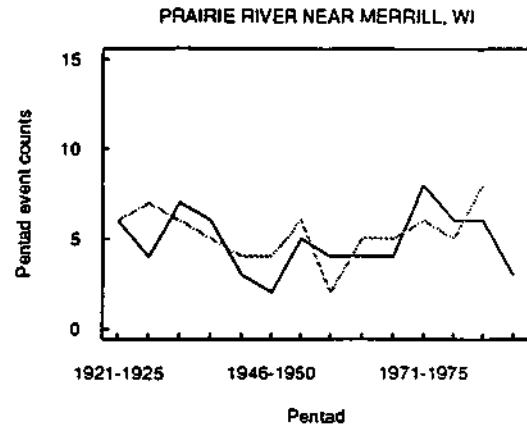
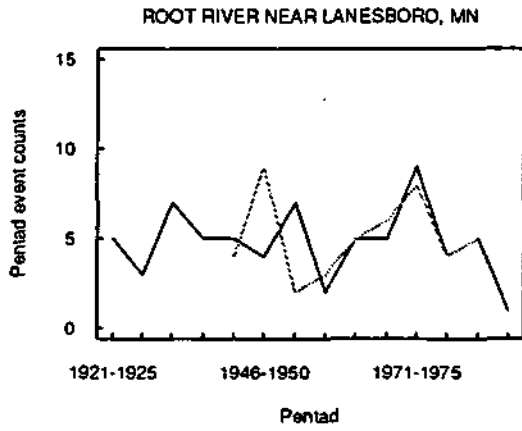
Solid: precip event count Dashed: flood event count

Cold season



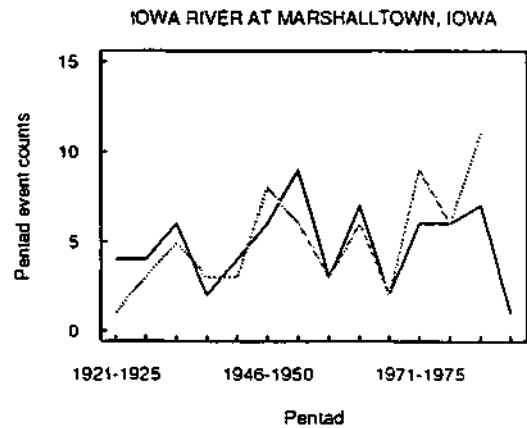
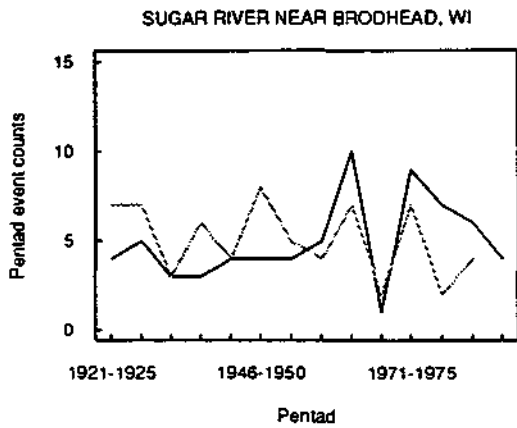
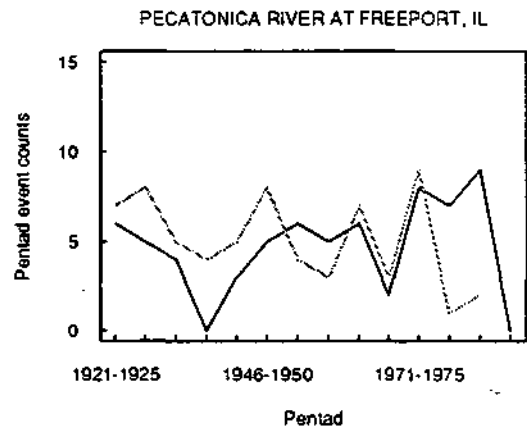
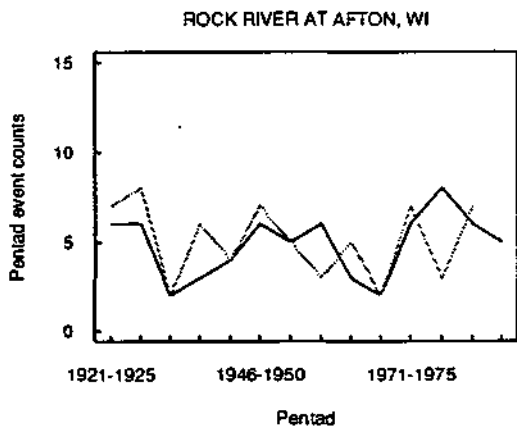
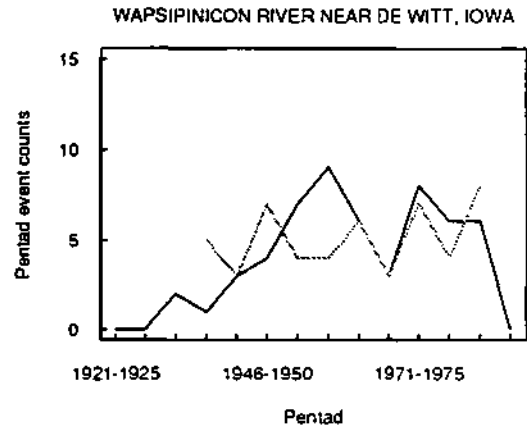
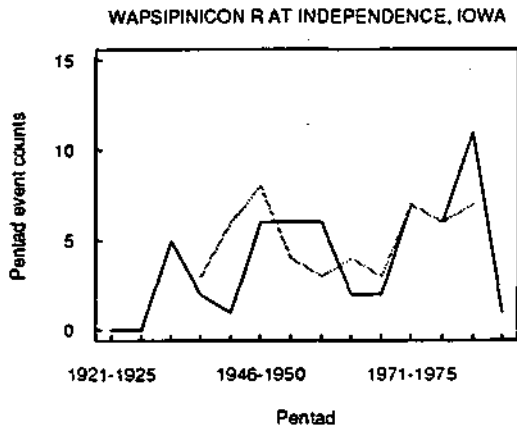
Solid: precip event count Dashed: flood event count

Cold season



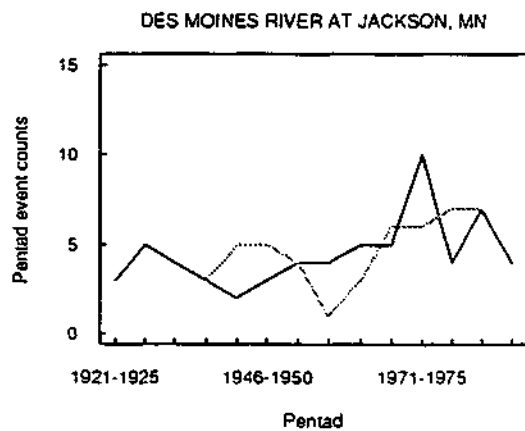
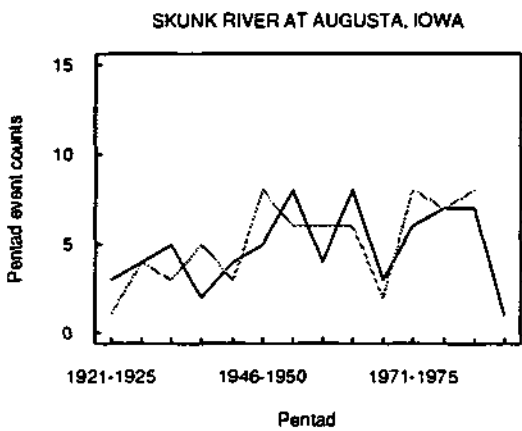
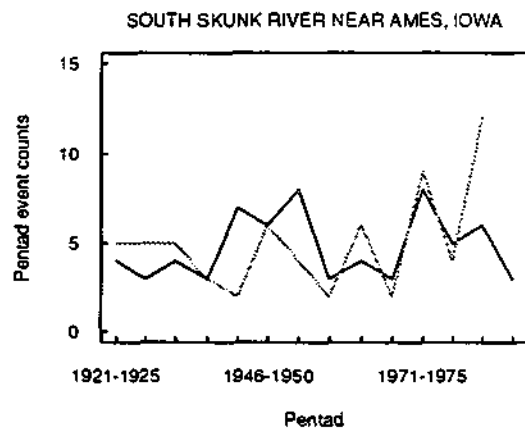
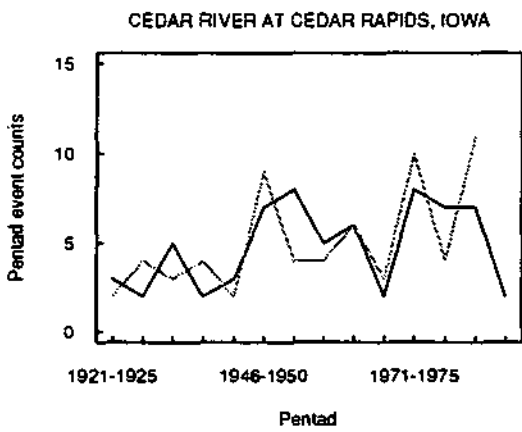
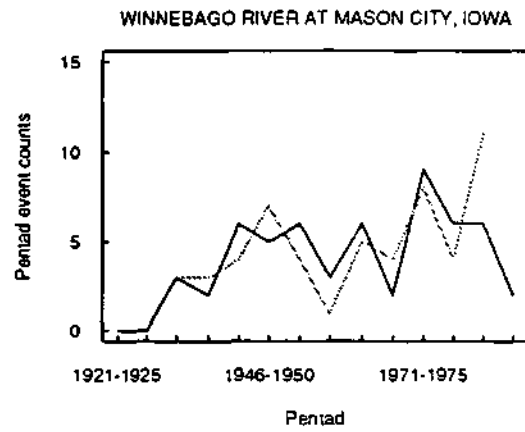
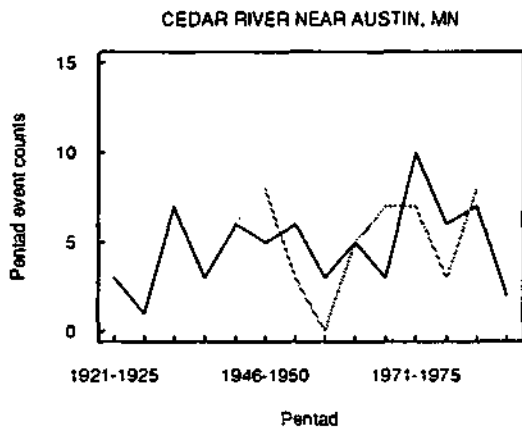
Solid: precip event count Dashed: flood event count

Cold season



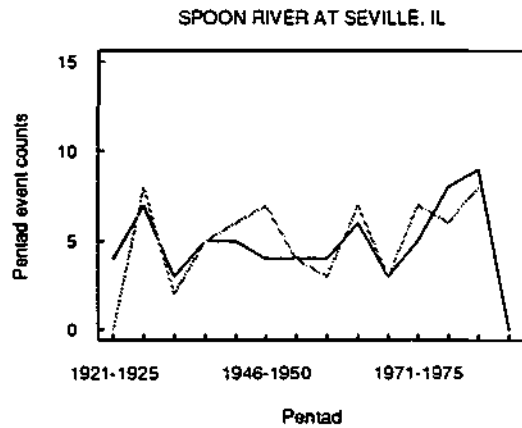
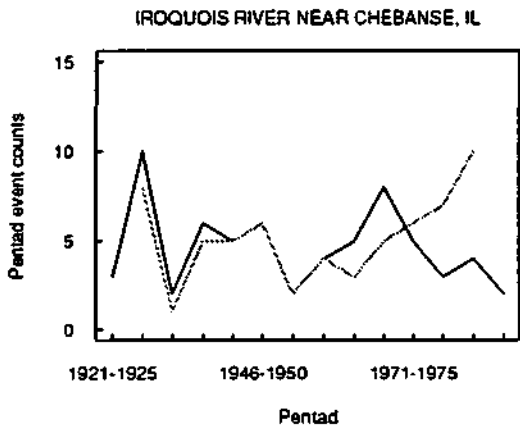
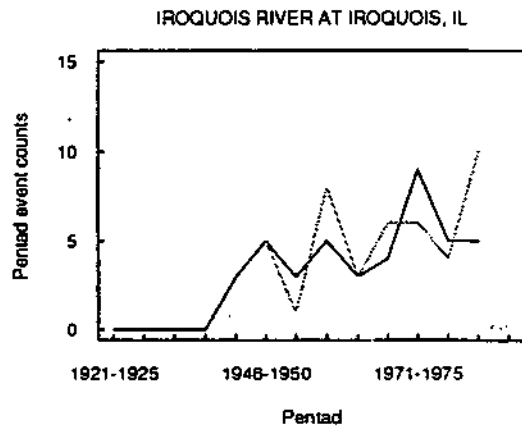
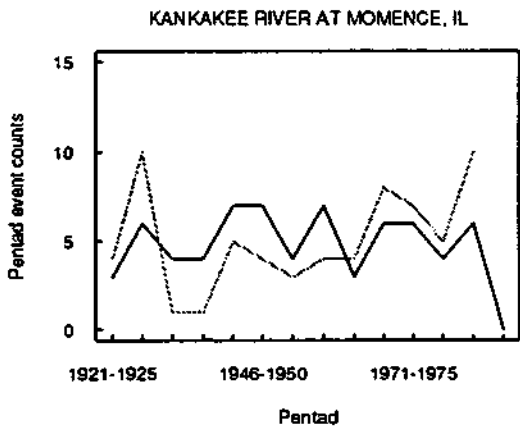
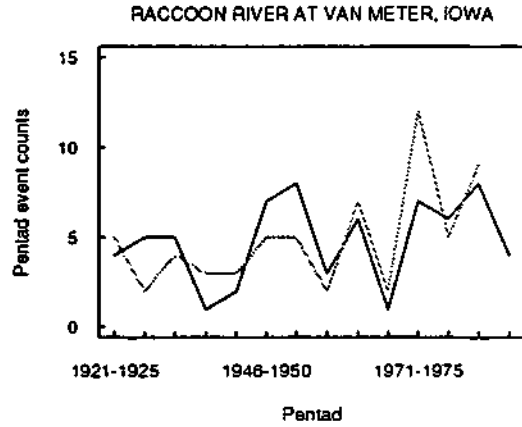
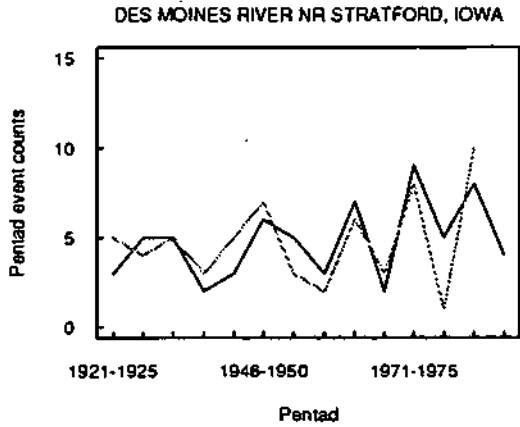
Solid: precip event count Dashed: flood event count

Cold season



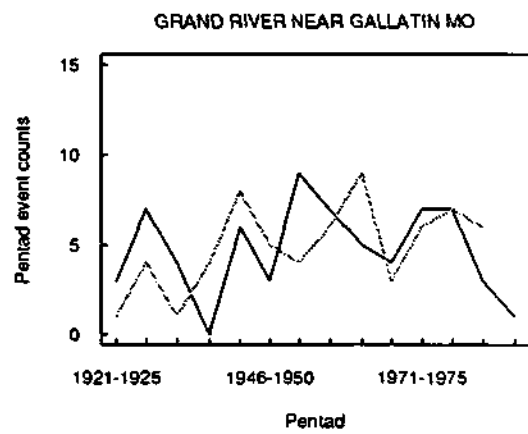
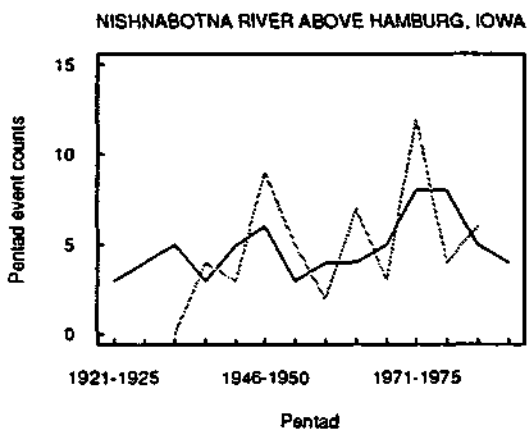
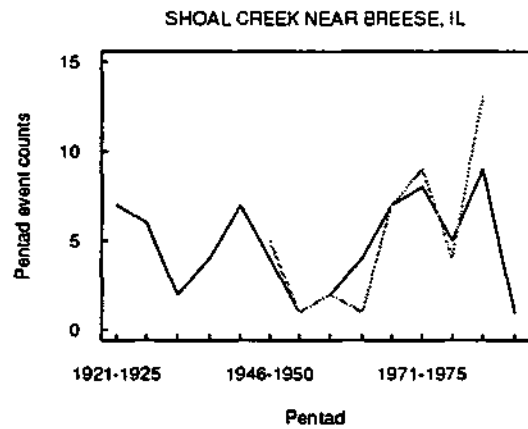
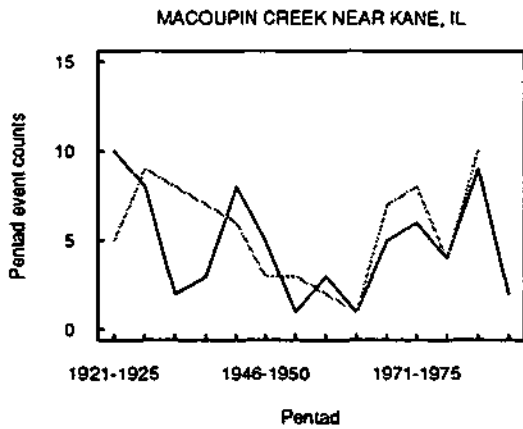
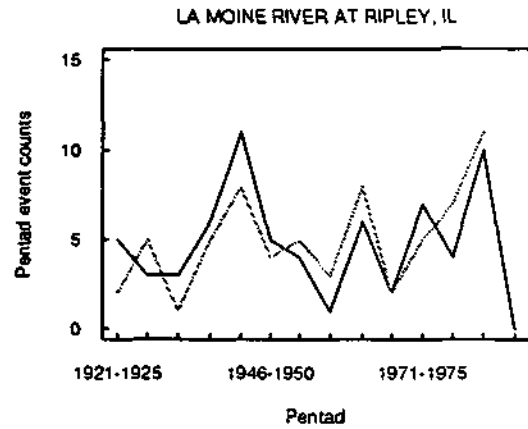
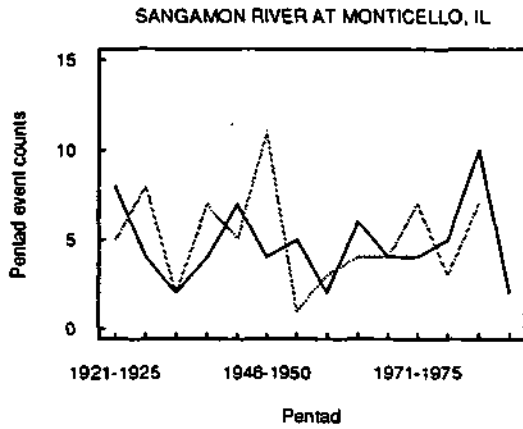
Solid: precip event count Dashed: flood event count

Cold season



Solid: precip event count Dashed: flood event count

Cold season



Solid: precip event count Dashed: flood event count

GASCONADE RIVER AT JEROME MO

